STUDIES ON THE TRANSPORT BEHAVIOR OF ACTINIDES AND LANTHANIDES ACROSS SUPPORTED LIQUID MEMBRANES CONTAINING DI-GLYCOLAMIDE CARRIERS

By

Surajit Panja

Bhabha Atomic Research Centre, Mumbai-85

A

Thesis submitted to the

Board of Studies in Chemical

Sciences

In partial fulfillment of requirements

For the Degree of

DOCTOR OF PHILOSOPHY

of

HOMI BHABHA NATIONAL INSTITUTE

AUGUST 2011

Homi Bhabha National Institute

Recommendations of the Viva Voce Board

As members of the Viva Voce Board, we certify that we have read the dissertation prepared by Mr. Surajit Panja entitled "*Studies on the transport behavior of actinides and lanthanides across supported liquid membranes containing di-glycolamide carriers*" and recommend that it may be accepted as fulfilling the dissertation requirement for the Degree of Doctor of Philosophy.

Chairman - Prof. A.Goswami *Date:* 30.4.12

Guide / Convener - Prof. P.K.Mohapatra *Date:* 30.4.2012

A K Singh
External Examiner – Prof. A.K.Singh *Date:* 30.4.2012

Member 1 - Prof. B.S.Tomar *Date:* 30.4.2012

Member 2 – Prof. A.V.R.Reddy *Date:*

Final approval and acceptance of this dissertation is contingent upon the candidate's submission of the final copies of the dissertation to HBNI.

I hereby certify that I have read this dissertation prepared under my direction and recommend that it may be accepted as fulfilling the dissertation requirement.

Date: 30.4.12

Place:BARC, Mumbai

STATEMENT BY AUTHOR

This dissertation has been submitted in partial fulfillment of requirements for an advanced degree at Homi Bhabha National Institute (HBNI) and is deposited in the Library to be made available to borrowers under rules of the HBNI.

Brief quotations from this dissertation are allowable without special permission, provided that accurate acknowledgement of source is made. Requests for permission for extended quotation from or reproduction of this manuscript in whole or in part may be granted by the Competent Authority of HBNI when in his or her judgment the proposed use of the material is in the interests of scholarship. In all other instances, however, permission must be obtained from the author.

(Surajit Panja)

DECLARATION

I, hereby declare that the investigation presented in the thesis has been carried out byme. The work is original and has not been submitted earlier as a whole or in part for a degree / diploma at this or any other Institution / University.

(Surajit Panja)

DEDICATIONS

TO My Wife
Saswati

ACKNOWLEDGEMENTS

I am deeply indebted to Prof. P.K.Mohapatra, Head, Actinide Chemistry Section, Radiochemistry Division, Bhabha Atomic Research Centre, Mumbai for his invaluable guidance, critical comments and constant encouragement during the entire course of this study. I take this opportunity to state that his keen interest and valuable suggestions were of immense help in improving the quality of work as well as enriching my knowledge. It is also my pleasure to express my sincere thanks to him for his constant help and support during planning, execution of the work and interpretation of the results.

It gives me great pleasure to thank Dr. S.C.Tripathi, Dr. A.Dakshinamoorthy, Dr. P.S.Dhami, Dr. S.K.Misra for their active help and continuous support at all stages of this work. I wish to express my sincere gratitude to Mr. P.K.Dey, former Head, FRD, Mr. P.M.Gandhi, CS(RF), Reprocessing facilities, Trombay, Mr. P.Janardan, Head, Fuel Reprocessing Division for allowing me to pursue the research work. My special thanks are due to all the respected Doctoral committee members including respected chairman Prof. V.K.Manchanda for their constructive and critical evaluation of my work during the course of the studies. I also wish to sincerely thank Dr. P.N.Pathak, Dr. S.A.Ansari, Dr. A.Bhattacharya,Mr. D.R.Rout, Mr. P.Kandwal for their co-operation during the course of this study. My batch mates from 48th batch OCES chemistry discipline have been like real friends supporting me during all the difficult periods and I wish to thank all of them.

Nothing is going to be complete without saying thank you to my parents, my brother, my grand mother, and my in-laws without whose support I would not have completed the research work.

Last but not least, my family- my son and wife have been like pillars of strength for me and I take this opportunity to express my profound gratitude to my beloved family.

B. A. R. C., Mumbai **Surajit Panja**
August 2011

Synopsis

"Studies on the transport behavior of actinides and lanthanides across supported liquid membranes containing di-glycolamide as carriers"

In the ever growing demand of energy with minimal impact on environment, 'nuclear power' has been projected as one of the potential alternatives to fossil fuel. The basis of nuclear energy is the neutron induced controlled fission of various fissile materials like, ^{235}U, ^{239}Pu, ^{233}U etc. However due to limited resources of naturally occurring fissile element (^{235}U), closed nuclear fuel cycle is the option to sustain the nuclear power programme. Closed fuel cycle has been adopted by various countries like India, and emphasizes on the reprocessing of the spent fuel. During reprocessing of spent nuclear fuel, the recyclable fissile elements (Plutonium and Uranium) are recovered using solvent extraction process leaving behind very highly radioactive liquid waste solution which is subsequently concentrated to yield the High Level Waste (HLW). The HLW solution consists of long lived alpha emitting radio-nuclides such as ^{241}Am, ^{243}Am, ^{245}Cm and ^{237}Np (referred to as minor actinides) apart from small amount of un-recovered plutonium and uranium as well as beta / gamma emitting fission products and significant concentrations of structural materials and process chemicals. HLW poses a long term radiological risk to the environment due to very long half lives of the minor actinides [1]. Efficient management of the HLW for minimizing the long term radiotoxic effect is essential for sustainability of nuclear power.

Minor actinides having half lives of several million years are the major concern for the safe disposal of HLW. The most accepted strategy for the safe management of HLW is to vitrify it in glass matrix. However due to the long half lives of the minor actinides, surveillance of the vitrified matrix is required which makes it economically as well as environmentally a daunting task. Partitioning and Transmutation (P&T) is an alternative / complimentary concept for the management of HLW [2]. This process

involves selective removal of minor actinides from HLW by a process called ‘actinide partitioning’ followed by their subsequent and burning in reactors as mixed oxide fuels.Apart from with alleviating the need for long term surveillance of the geological repositories, the P&T process would also lead to the generation of extra energy. After partitioning of the actinides along with the long lived fission products, the residual waste can be vitrified and buried in subsurface repositories at a much reduced risk and cost. Concerted efforts are being made by separation scientists to develop efficient and environmentally benign processes for the separation of long-lived radionuclides from HLW solution.

Various ‘actinide partitioning’ processes have been proposed by different laboratories viz. TRUEX, DIAMEX, DIDPA and TRPO which employ octyl(phenyl)-N,N-diisobutyl carbamoyl methyl phosphine oxide (CMPO), N,N′-dimethyl-N,N′-dibutyl tetradecyl malonamide (DMDBTDMA), diisodecyl phosphoric acid (DIDPA) and trialkyl phosphine oxide (TRPO) as the extractants, respectively [3]. All these reagents have their advantages and draw backs. This led to the search for alternative and efficient reagents for actinide partitioning purpose. It has been observed that the introduction of etherial oxygen atom between the two amide groups of diamides (diglycolamide) causes significant enhancement in the extraction of trivalent actinides / lanthanides. Amongst the several derivatives of diglycolamide studied, N,N,N′,N′-tetraoctyl diglycolamide (TODGA) has been identified as one of the most promising extractants for the partitioning of trivalent actinides and lanthanides from HLW solutions [4]. Some of the salient features of TODGA include; (i) high distribution co-efficient values of trivalent actinides from moderate acidic aqueous solutions, (ii) possibility of complete incineration as the constituent elements are C, H, N and O, (iii) good radiolytic and hydrolytic stability, and (iv) the ease of synthesis. In view of these favorable properties TODGA was evaluated for the partitioning of actinides from HLW solution by a series of mixer-settler runs [5]. Recently, a branched chain homolog of TODGA has also been synthesized and evaluated for actinide partitioning [6]. This reagent has been reported to have similar extraction properties as TODGA though somewhat reduced extraction of fission products due to stereo chemical hindrance from branched chain.

The main objective of the present work is to evaluate TODGA and TEHDGA as the carrier molecule and to study the transport behavior of actinides, lanthanides and fission products across supported liquid membranes. The present research work includes transport behavior of actinides in various oxidation states using TODGA and TEHDGA as carrier extractants. Effect of diluents and irradiation dose on the extraction and transport behavior of actinides was also carried out. Effect of structure variation of diglycolamides on the extraction and transport of actinides and lanthanides have also been evaluated in the present study.

CHAPTER 1: GENERAL INTRODUCTION

This Chapter gives an introduction to the research problem dealt with in this thesis. The importance of separation of minor actinides and long-lived fission products from radioactive waste is discussed in detail. It describes the source and type of radioactive waste along with the environmental impact of the radionuclides present in those wastes. Major aim of radioactive waste management is to separate long lived, alpha emitting elements which belong to the actinide series of the periodic table. Chemistry of the actinides which is important for separation of the elements has been discussed in brief. A brief description of the separation techniques which are used for actinide separation like solvent extraction, membrane technique etc. is also given in this Chapter. Literature reports on actinide separation using different class of extractants have also been summarized. A brief background of the development of diglycolamide extractants has been included in this chapter.

Membranes are barriers that separate two fluid phases and allow the mass transfer from one side of the barrier to the other. Advantages of membrane based separation techniques are low energy requirements, low capital and operating costs, the possibility of achieving high separation factors and simple modular design [7]. One of the important features of liquid membrane separations is simultaneous extraction and stripping unlike solvent extraction process.

This Chapter gives a brief description of the principles of various liquid membranes and theory of facilitated transport of metal ion across supported liquid membranes. Equations to calculate flux and permeability co-efficient of the transported species have been derived. A brief description of mathematical modeling of transport using MATLB-6.5 software has also been presented in this Chapter. Finally the aims and objectives of the present work are entitled.

CHAPTER-2: EXPERIMENTAL

A general outline of different experimental techniques and instrumentation used in the present work is given in this Chapter. The synthesis, purification and characterization of TODGA and other synthesized DGA's have been described. A brief mention about the various analytical techniques followed is also made in this Chapter. Liquid scintillation counter was employed for radiometric assay of alpha emitting radio nuclides such as Pu, and 233U while gamma counting using NaI(Tl) scintillator counter was followed for the assaying of ^{85,89}Sr, ^{152,154} Eu, ^{234}Th and ^{241}Am. The basic principles of these detectors are also described. Preparation and purification of various radiotracers are included in this Chapter. The UV-visible absorption spectrophotometry was followed for the analysis of Nd. Methods to adjust the oxidation state of Pu is described in this Chapter. Purity of the different oxidation states of Pu was checked by spectrophotometry. The complexometric titrations carried out for the analysis of various elements such as thorium and uranium is also described in this chapter.

CHAPTER-3: TRANSPORT OF ACTINIDES ACROSS SLM's USING N,N,N′,N′-TETRAOCTYL DIGLYCOLAMIDE (TODGA) AS CARRIER.

N,N,N′,N′-tetraoctyl diglycolamide (TODGA) has been proposed as a promising reagent for 'Actinide Partitioning' [8]. This Chapter deals with solvent extraction as well as supported liquid membrane transport studies of various actinides in different oxidation states using TODGA as the carrier extractant. The actinide ions studied in this work are Pu(III),Pu(IV),Pu(VI),U(VI) and Th(IV) and the oxidation states of Pu were confirmed by spectrophotometry as well as by TTA extraction.

Solvent extraction studies of Pu(III) with TODGA suggested extraction of a tetra-solvate species which was similar to the species reported with Am(III). Membrane transport properties of Pu(III) using varying reductants, varying feed acidity, varying TODGA concentration, different types of strippant are described in detail in the present Chapter. Flux of Pu(III) transport with varying concentration of Pu and stability of the membrane is also discussed in the Chapter. Striking similarities between Am(III) and Pu(III) transport behavior is the highlight of this work

Present Chapter also describes the extraction and transport behavior of Pu in its tetravalent oxidation state with TODGA as the extractant/carrier. Nature of the extracted species formed with TODGA was different than that of Pu(III). Role of feed acidity, TODGA concentration, membrane thickness on the transport of Pu(IV) is discussed in the Chapter. The membrane stability was limited up to 5 days as compared to 20 days of continuous operation reported earlier for Am^{3+} transport. Transport studies are also carried out using irradiated TODGA upto a maximum absorbed dose of 15 MRad.

Uranium is a major constituent of HLW and due to its presence in the +6 oxidation state, it is expected to behave differently than that of Pu or Am. Present Chapter gives a detailed description on the solvent extraction and transport properties of U(VI) using TODGA as the extractant/carrier. It was observed that the nature of species formed for U(VI) varied depending on the aqueous phase acidity. At 1 M HNO_3, it formed a di-solvate whereas at 3 M HNO_3 a mono-solvate was found to be formed. Membrane transport was described in detail with respect to variation of different parameters like feed acidity, carrier concentration, membrane pore size, feed U concentration etc.

In view of the importance of Th fuel cycle in Indian nuclear energy programme, separation of Th^{4+} from acidic feed is also studied using TODGA using both SX as well as SLM methods. Conditions for quantitative Th^{4+} transport has been arrived at by carrying out analogous transport studies.

Diluents play a major role in the extraction of metal ions for organic carriers. Solubility of the carriers in the diluents, polarity of the diluent, ability to form H-bonding, Hildebrand's solubility parameter, Schmidt's diluent parameter of the diluent are some of the parameters that determines the extraction performance and nature of species of the metal ion [9]. Present Chapter describes the role of diluents on the extractability and nature of species of Am(III) from nitric acid medium using TODGA as extractant. A series of diluents like kerosene, toluene, chloroform, methyl *iso*-butyl ketone, carbon tetra chloride, 1-octanol, *tert* butyl benzene etc. having widely different diluent properties have been used for Am(III) extraction in this study. Present Chapter also describes the transport property of Am(III) using TODGA in different diluents as the carrier solvents. Percentage transport of Am(III) with these diluents have been calculated and the effect of membrane pore size in these diluents have been investigated. Present Chapter also deals with the calculation of membrane diffusion parameters for different diluents.

Application of TODGA for actual process solution will lead to irradiation of the extractant by gamma radiation from the radio nuclides present in the HLLW solution. Gamma radiation leads to the degradation of TODGA with subsequent generation of degradation products which can affect the extraction/transport properties. Effect of radiolytic degradation on the solvent extraction of actinides and fission products have been reported [10]. But its effect on the membrane transport properties of various radio nuclides and fission products have not been reported in the literature. Present chapter describes the transport properties of actinides (+3,+4,+6 oxidation states) along with fission product (+2 oxidation state) using three chosen carrier concentrations with varying irradiation dose. The transport rate variation for all the radio nuclides and its effect on the decontamination factor of the actinides with respect to fission product have also been discussed in detail in the Chapter.

CHAPTER-4: TRANSPORT OF ACTINIDES AND LANTHANIDES USING N,N,N’,N’-TETRA (2-ETHYL HEXYL) DIGLYCOLAMIDE (T2EHDGA)

N,N,N’,N’-tetra (2-ethyl hexyl) diglycolamide (T2EHDGA) is a branched chain homolog of TODGA and has been evaluated for actinide partitioning purpose [6]. It is reported to favourably extract trivalent actinides similar to TODGA though higher decontamination factor values (with respect to the fission products) are expected due to stereo-chemical hindrance.

Present Chapter deals with the solvent extraction and the transport behavior of actinides in the trivalent (Am^{3+}) and hexavalent (UO_2^{2+}) state along with a trivalent lanthanide (Eu^{3+}) from nitric acid medium using TEHDGA as extractant/ carrier. Various parameters which effect the solvent extraction and transport behavior like feed nitric acid concentration/ nitrate concentration, carrier concentration, membrane pore size, nature of strippant, effect of phase modifier etc are described in this Chapter.

The Chapter gives a detailed description of the transport properties of trivalent actinide, Am(III) using T2EHDGA as carrier across a SLM. In contrary to TODGA which forms a tetra-solvate with Am(III), T2EHDGA was found to form a tri-solvate extractable complex. Membrane transport behavior was found to be comparable with that of TODGA. Effect of parameters such as feed acidity, T2EHDGA concentration, membrane pore size, nature of strippant etc on Am(III) transport have been investigated in detail in the present Chapter. Selectivity of Am(III) over other fission products was found to be quite high. Stability of the membrane was found to be quite satisfactory over a period of 15 days.

Along with minor actinides, HLW consists of large concentrations of trivalent lanthanides whose behavior is similar to that of trivalent actinides. So it was necessary to understand the transport properties of trivalent lanthanides from nitric acid medium. This Chapter also describes the transport properties of a representative trivalent lanthanide (Eu(III)) with T2EHDGA as the carrier extractant. Similar to Am(III), Eu(III) was found to form a tri-solvate with T2EHDGA. In this Chapter, Eu(III) transport using T2EHDGA as the carrier has been described in detail with elaborate description on various factors which effect the transport rate. Role of phase modifier in solvent extraction and transport of Eu(III) has also been described in this current Chapter.

Uranium is a major constituent of HLW. In order to assess the suitability of T2EHDGA as a carrier solvent, it was imperative to investigate the SX and SLM transport behavior of U(VI) using T2EHDGA as the extractant/carrier. The solvent extraction studies showed formation of mono-solvate of U(VI) with T2EHDGA at 3M HNO_3. The extraction was found to increase with increasing nitrate ion concentration in the feed and decrease with increasing phase modifier concentration in the extractant concentration. This Chapter also describes detailed membrane transport studies which were carried out to get the optimum transport rate as well as to understand the mechanism of transport. Some of the parameters described in the Chapter are: effect of phase modifier concentration, effect of feed acid concentration, effect of different acids and their corresponding salts, concentration of T2EHDGA, membrane pore size, concentration of U in the feed, effect of temperature etc.

CHAPTER-5: SOLVENT EXTRACTION AND MEMBRANE TRANSPORT BEHAVIOR OF TRIVALENT ACTINIDES AND LANTHANIDES USING SUBSTITUTED DI-GLYCOL AMIDES

Diglycolamide $(RR\text{-}NCO\text{-}CH_2)_2\text{-}O$, which is a kind of diamide derivative having two carbamoyl groups connected by the alkyl chain including an etherial oxygen, was introduced initially by Stephan et al [11,12]. Diglycolamides contain three oxygen atoms that can form strong complexes with the metal ions, and act as tridentate ligands. Present Chapter describes the effect of alkyl chain length of the substituents in the diglycolamides on the extraction and transport behavior of trivalent actinides, lanthanides and fission products. Different di-glycolamides studied in this Chapter are N,N,N′,N′-tetraoctyl diglycolamide (TODGA), N,N,N’,N’-tetra (2-ethyl hexyl) diglycolamides (T2EHDGA), N,N,N’,N’-tetrahexyl diglycolamide (THDGA), N,N,N’,N’-tetrapentyl diglycolamide (TPDGA), N,N,N’,N’-tetradecyl diglycolamide (TDDGA).

A detailed description on the solvent extraction properties of the actinides, lanthanides and fission product elements such as Sr using the substituted diglycolamides from nitric acid medium form the first part of the present Chapter. Various parameters which affect the extraction properties of the radio nuclides like kinetics of extraction, effect of feed acidity, composition of phase modifier, effect of phase modifier on the extraction, LOC value of Nd, extraction from synthetic high level waste (SHLW) for different diglycolamides have also been described in detail.

In the second part of the Chapter SLM transport behavior of the radio-nuclides using the substituted DGA’s as the carrier have been described. Effects of feed nitric acid concentration, phase modifier concentration, membrane pore sizes etc have been described for the actinides, lanthanides and fission product elements

CHAPTER-6: SUMMARY AND CONCLUSIONS

In conclusion, the present thesis demonstrates the possible application of membrane based separation of actinides and lanthanides from nitric acid feeds using TODGA, T2EHDGA and several other substituted diglycolamides as the carriers. Transport properties of actinides were found to be dependent on their oxidation states for TODGA with the trend of transport rate being An(III)>An(IV)>AnO_2^{2+}. Various factors that affect the transport properties were evaluated in detail to get the optimum transport condition. Stability of the supported liquid membranes was found to be satisfactory over a period of 20 days making them promising alternatives to solvent extraction for actinide recovery from wastes. Diluents were found to play a major role in the extraction and transport of actinides for TODGA. Irradiation stability of TODGA with respect to transport of actinides and fission products was also evaluated. It was observed that the transport rate decreased with increasing irradiation dose for all the actinides and fission products. But the decontamination factor of the actinides with respect to fission product increased with increasing irradiation dose. T2EHDGA based supported liquid membrane was also found to be effective for the transport of actinides and lanthanides from nitric acid medium. The transport properties of the radio nuclides were described in terms of various diffusional parameters. Structural effects of diglycolamides with respect to solvent extraction and membrane transport were also evaluated. Large scale application of the technique needs further studies using Hollow Fiber Contactors.

REFERENCES

1. Status and Trends of Spent Fuel reprocessing, IAEA TECDOC-1103, **1999**.
2. L.H. Baestle. Burning of Actinides: A complementary waste management option? IAEA Bulletin, 34(3) (**1992**), 32.
3. J.N. Mathur, M.S. Murali and K.L. Nash, Solv. Extr. Ion Exch., 19 (**2001**) 357.
4. Y. Sasaki, Y. Sugo, S. Suzuki and S. Tachimori, Solv. Extr. Ion Exch., 19 (**2001**) 91.
5. S.A. Ansari, D.R. Prabhu, R.B. Gujar, A.S. Kanekar, B. Rajeswari, M.J. Kulkarni, M.S. Murali, Y. Babu, V. Natarajan, S. Rajeswari, A. Suresh, R. Manivannan, M.P. Antony, T.G. Srinivasan and V.K. Manchanda, Separation and Purification Technology,66(1) (**2009**), 118.
6. S. Manohar, J.N. Sharma, B.V. Shah, P.K. Wattal; Nucl. Sci. Eng. 156 (**2007**) 96.
7. Ho WSW and Sirkar KK, Membrane Handbook. Chapman & Hall, New York (**1992**).

8. S.A.Ansari ; P.N.Pathak ; V.K.Manchanda; M.Husain; A.K.Prasad; V.S.Parmar; Solv. Extr. Ion Exch., 23 **(2005)** 463.
9. Y.Marcus; Chem. Soc. Rev. (**1993**) 409.
10. Y. Sugo, Y. Sasaki und S. Tachimori; Radiochimica Acta, 90(3) (**2002**), 161.
11. H. Stephan, K. Gloe, J. Bager and P. Muhl, Solv. Extr. Ion Exch., 9 (**1991**) 435.
12. H. Stephan, K. Gloe, J. Bager and P. Muhl, Solv. Extr. Ion Exch., 9 (**1991**) 459.

CONTENTS

3.8. REFERENCES

LIST OF FIGURES

LIST OF TABLES

Chapter I

GENERAL INTRODUCTION

1.1. Nuclear Energy and Nuclear Reactor

In this world of ever-growing demand for energy with less impact on the environment, ‘Nuclear Energy’ has been proposed as a viable alternative to fossil fuels. Nuclear energy produces large amount of energy using neutron induced fission of various fissile materials, viz. ^{235}U, ^{239}Pu, ^{233}U etc. In nuclear reactors, the fission reaction is used in a controlled manner to produce energy which in turn is used for the production of electricity. Currently, there are about 450 nuclear reactors in 16 countries all over the world. These reactors contribute to ~16% of the total energy demand of the world. In the near future, nuclear energy is going to be more important for meeting the ever-increasing energy demand of the world due to the limited resources of the conventional fossil fuels. It is also going to be more important due to less emission of green house gases from nuclear reactors. However, due to the limited resources of naturally occurring fissile element ^{235}U, the sustainability of Nuclear Power program depends on the availability of the man made fissile elements like ^{239}Pu, ^{233}U etc. Therefore it is imperative that the ‘closed fuel cycle’ program is followed to sustain the nuclear energy program beyond the naturally available fissile ^{235}U. Many countries like India, due to insufficient resources of ^{235}U have adopted the closed fuel cycle option which involves reprocessing of the spent fuel generated in the nuclear reactor. During the reprocessing of spent nuclear fuel, the valuables, Plutonium and Uranium, are recovered using solvent extraction process leaving behind the highly radioactive liquid waste solution which is subsequently concentrated to be known as High Level Waste (HLW). The HLW solution consists of long lived alpha emitting radionuclides such as ^{241}Am, ^{243}Am, ^{245}Cm and ^{237}Np (referred to as minor actinides) apart from the small amount of unrecovered plutonium and uranium as well as β- / γ- emitting fission products and significant concentrations of structural materials and process chemicals [1,2]. The safe management of HLW is of utmost importance for the acceptance of nuclear power to common man. This is due to the fact that the minor actinides which have very long half lives (few hundreds to millions of years) pose long term radiological risk to the human health and ecology [3]. Efficient management of radioactive waste requires knowledge of the source and composition of various wastes generated in nuclear reactors and reprocessing of spent fuel.

1.2 Radioactive Waste

Production of nuclear energy from nuclear reactors is associated with the generation of radioactive waste during various operations of the nuclear fuel cycle starting from the mining to the waste management. During the mining operation of uranium, decay products of ^{238}U / ^{233}U exist in the form of radioactive dust. The wastes from the milling operation include the radioactive radium which is reverted back to the mine and covered with rock and clay. The uranium oxide produced from the mining and milling of the ore is accompanied by only a fraction of total concentration of decay products as most of them are diverted to the tailings. The major concentration of waste generation starts during burning of the fissile elements in nuclear reactors which includes significant quantities of fission and activation products. The radioactivity which is produced in nuclear reactors is contained in the fuel rod (> 99.99%) and only a very small percent (<0.01%) is distributed in other systems of reactor. These include ion-exchangers used for the water purification in PHT / coolant channels, chemical sludge, reactor components, etc. The major source of radioactive waste in nuclear fuel cycle is nuclear fuel reprocessing. The spent fuel from nuclear reactors is processed for separation of useful fissile elements like ^{239}Pu,^{233}U etc. leaving behind the beta/gamma emitting fission products, alpha emitting long lived actinides and lanthanides which are responsible for most of the dose [2] associated with spent fuel solution. The major contributors to the fission product activity after a cooling period of 50 days are listed in Table 1.1. The spent fuel is often allowed to cool for a few years to allow the short lived radio nuclides to decay. After cooling the spent fuel for about one year, only ^{106}Ru, ^{106}Rh, ^{90}Sr, ^{90}Y, ^{144}Ce, ^{144}Pr, ^{134}Cs, ^{137}Cs and ^{147}Pm contribute significantly to the activity [2].

1.2.1 Classification of Radioactive Waste

Depending on the level of radioactivity, radioactive wastes are classified as low level, intermediate level and high level waste. The radioactivity associated with the wastes can vary from curies per liter to micro curies per liter.

1.2.1.1. Low Level Waste

When the total radioactivity of the waste is less than millicurie / liter, it is referred to as low level waste (LLW). It is generated as the liquid from the decontamination of equipments, radioactive laboratories and hospitals using radiopharmaceuticals as well as from the nuclear fuel cycle. The level of radioactivity and half-lives of radioactive isotopes present in LLW are relatively small. Storing the waste for a period of few months allows most of the radioactive isotopes to decay, the point at which the wastes can be disposed off safely. The LLW comprises about 90% of the total volume of the radioactive wastes generated, but only < 1% radioactivity of all the wastes. To reduce the volume of solid LLW, it is often incinerated and compressed before disposal. Usually, it is buried in shallow landfill sites.

1.2.1.2. Intermediate Level Waste

When the radioactivity of the waste ranges from millicurie to curie / litre, the waste is referred as intermediate level waste (ILW). The ILW contains higher amount of radioactivity as compared to the LLW and, therefore, may require special shielding. It typically comprises resins, chemical sludge, reactor components as well as reprocessing equipments. The ILW comprises about 7% of the total volume of the radioactive wastes, while it contains < 4% radioactivity of all the radioactive wastes.

1.2.1.3. High Level Waste

When the radioactivity of the waste is greater than curie / liter, the radioactive waste is

Table 1.1: Major contributors to the radioactivity in the spent fuel after a cooling period of 50 days

Nuclides	*Half life*	*Nuclides*	*Half life*
^{3}H	12.3 y	^{131}I	8.05 d
^{85}Kr	10.8 y	^{137}Cs	30.0 y
^{89}Sr	50.6 d	^{140}Ba	12.8 d
^{90}Sr	28.8 y	^{140}La	40.2 d
^{90}Y	64.4 h	^{141}Ce	32.4 d
^{91}Y	58.8 d	^{143}Pr	13.6 d
^{95}Zr	65 d	^{144}Ce	285 d
^{95}Nb	35 d	^{144}Pr	17.3 m
^{103}Ru	39.6 d	^{147}Nb	11.1 d
^{106}Ru	367 d	^{147}Pm	2.62 y
^{129m}Te	34 d	-	-

referred as high level waste (HLW). The HLW is the waste emanating from the reprocessing of spent fuel. While HLW comprises of only about 3% of the total volume of all the radioactive wastes, it contains more than 95% of the total radioactivity generated in the nuclear fuel cycle. This waste includes uranium, plutonium and other highly radioactive elements made up of fission products and alpha emitting minor actinides. The challenge for the final disposal of HLW is largely due to the radio toxicity associated with the minor actinides which have half lives ranging from few hundred to millions of years [4]. Efforts are being made by separation chemists to meet the challenges of radioactive waste management by developing efficient and environmentally benign processes for the separation of various radionuclides from HLW solution. This would minimize the volumes of radioactive wastes and costs of their final disposal.

1.3. Impact of Radionuclides on Environment

The long-lived radionuclides present in the raffinate of PUREX process after reprocessing of the spent nuclear fuel are of great environmental concern. The radioactive waste, whether natural or artificial, is a potential source of radiation exposure to the human being through different pathways. The raffinate from the PUREX process generally contains un-extracted U, Pu and bulk of minor actinides such as Am, Np, Cm and host of fission product elements like Tc, Pd, Zr, Cs, Sr and lanthanides as well as activation products. At present, the most accepted conceptual approach for the management of HLW is to vitrify it in the glass matrix followed by disposal in deep geological repositories [5,6]. Since the half lives of minor actinides concerned range between a few hundreds to millions of years, the surveillance of high active waste for such a long period is debatable from economical as well as environmental safety considerations. On the other hand, the vitrified mass of HLW will have to withstand the heat and radiation damages caused by the decay of beta/gamma

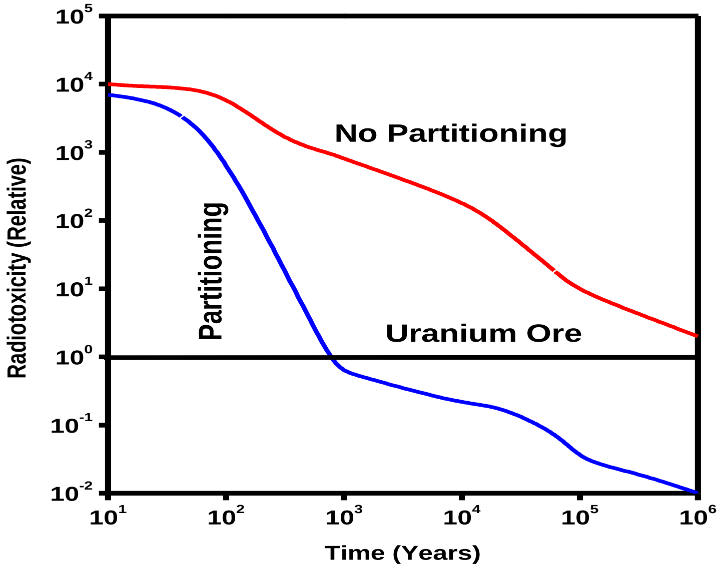

Fig. 1.1. Partitioning of minor actinides- Impact on waste management

emitting fission products such as ^{137}Cs and ^{90}Sr for about 100 years. Therefore, it may create the possible risk of the migration of long lived alpha emitting minor actinides from repository to the environment. The recommended activity level of 4000Bq per gram in terms of alpha activity is considered benign enough to be treated as LLW. As represented in Fig. 1.1, if actinides are not removed from the spent fuel, it will require millions of years to reduce its radio toxicity to this level. However, if one can remove U, Pu and minor actinides from the waste its radiotoxicity could reach an acceptable level after a few hundred years.

Therefore, the strategy of **P&T** (Partitioning of long-lived radionuclides followed by Transmutation) is being considered by several countries around the world [7,8]. The P&T process envisages the complete removal of minor actinides from radioactive waste and their subsequent burning in the reactors / accelerators as mixed oxide fuel. This process will lead to generation of extra energy and at the same time would alleviate the need for long term surveillance of geological repositories. After partitioning of the actinides along with the long lived fission products, the residual waste can be vitrified and buried in subsurface repositories at a much reduced risk and cost.

1.4. Chemistry of Actinides and Lanthanides

The work carried out in this thesis pertains to the separation chemistry of actinides and lanthanides from radioactive waste solutions. The actinides include uranium, plutonium, americium and thorium whereas europium was the lanthanide chosen for the separation studies. It is quite essential to understand the chemistry of actinides and lanthanides before their partitioning. A brief survey of the chemistry of actinide and lanthanide elements is, therefore, considered relevant.

1.4.1. History

The existence of rare earth like series in the seventh row of periodic table, which was suggested as early as 1926, gained wider acceptance with the discovery and study of transuranium elements [9]. In 1945, Seaborg proposed that actinium and transactinium elements form such a series in which the *5f* electron shell is being filled in a manner analogous to the filling of *4f* shell in lanthanides [10]. Except for uranium and thorium, which are well known actinide elements discovered in 1789 and 1828, respectively, all the other elements were discovered in the twentieth century. Among the actinide elements, uranium and thorium have isotopes with half-lives exceeding the estimated life of this planet and hence occur in nature. Actinium and protactinium owe their existence to the decay of long lived isotopes of uranium, thorium and their daughter products. The rest of the elements in this series are essentially “man made” with some evidence for the trace occurrence of neptunium and plutonium in the nature formed by nuclear reactions involving uranium [11,12]. Among the man made elements, plutonium and to a lesser extent, neptunium, americium and curium are produced in the nuclear power reactors and are recovered from the spent nuclear fuels. The elements beyond curium are generally produced through heavy ion reactions of transplutonium elements in accelerators. With increasing atomic number of actinides, the nuclei becomes rapidly less stable and only einsteinium has an isotope with a half-life long enough to offer any possibility for conventional chemical studies.

The lanthanides comprise a series of inner transition elements in which the number of *4f* electrons increases from 1 to 14. The main effect of increasing the number of electrons in the internal energy sublevel, as the nuclear charge increases is to gradually decrease the cationic radius of consecutive lanthanide ions, so that they range in size from that of La(III) to that of Sc(III). Due to the remarkable similarities in their cationic charge and radii, lanthanides form many isomorphic series of compounds and are always found as complex mixtures in rocks and minerals which comprise the earth’s crust. The primary exploited mineral sources are monazite, gadolinite, bastnasite and euxenite, but greater sophistication in chemical processes has made rare earth concentrates an exploitable by-product of other industries, e.g. the phosphate fertilizer industry [13].

1.4.2. Electronic Configuration

The fourteen *5f* electrons enter the actinide elements beginning formally with Th (Z=90) and ending with Lr (Z=103). These fourteen elements following Ac are placed in the 7th row of the periodic table separately analogous to lanthanides. Intensive chemical studies have revealed many similarities between the lanthanides and actinides. The ground state electronic configuration of lanthanides and actinides is shown in Table 1.2. Though there is over all similarity between the two groups of elements, some important differences also exist mainly because the *5f* and *6d* shells are of similar energy in actinides and *5f* electrons are not as well shielded as *4f* electrons in lanthanides [14]. The lighter actinides (Ac to Np) show greater tendency to retain *6d* electrons due to smaller energy differences between *6d* and *5f* orbitals relative to that between *5d* and *4f* orbitals of lanthanides. In case of transition series, the relative energy of orbitals undergoing the filling process becomes lower as the successive electrons are added. For actinides also, the *5f* orbitals of plutonium and subsequent elements are of lower energy than *6d* orbitals and, therefore, the subsequent electrons are filled in *5f* orbitals with no electrons in *6d* orbitals.

1.4.3. Solution Chemistry of Actinides

As the processes of separation and purification of actinides on large scale are essentially based on hydrometallurgical techniques, the study of solution chemistry of actinides has received considerable attention. The early actinide elements (upto Pu) exist in multiple oxidation states and most of their separation processes are based on the effective exploitation of these properties. It is, therefore, desirable to understand the various oxidation states of actinides in solution.

1.4.3.1. Oxidation States

The trivalent oxidation state is the most stable for all lanthanides. However, this is not so at least in the case of earlier members of actinide series. The *5f* electrons of actinides are subjected to a lesser attraction from the nuclear charge than the corresponding *4f* electrons of lanthanides. The greater stability of tetra positive ions of early actinides is attributed to the smaller values of fourth ionization potential for

5f electrons compared to *4f* electrons of lanthanides, an effect which has been observed experimentally in the case of Th and Ce [15]. Thus, thorium exists in aqueous phase only as Th(IV) while the oxidation state 3+ becomes dominant only for transplutonium elements. The actinides existing in different oxidation states are shown in Table 1.3, where the most stable oxidation states are underlined [14]. All the oxidation states are well known in acidic conditions except 7+ states for Np and Pu which exist in alkaline

Table 1.2: Electronic configuration of lanthanide and actinide elements

Lanthanides			*Actinides*		
Elements	*Atomic numbers*	*Electronic configurations*	*Elements*	*Atomic numbers*	*Electronic configurations*
La	57	$5d^1\ 6s^2$	Ac	89	$6d^1\ 7s^2$
Ce	58	$4f^1\ 5d^1\ 6s^2$	Th	90	$6d^2\ 7s^2$
Pr	59	$4f^3\ 6s^2$	Pa	91	$5f^2\ 6d^1\ 7s^2$
Nd	60	$4f^4\ 6s^2$	U	92	$5f^3\ 6d^1\ 7s^2$
Pm	61	$4f^5\ 6s^2$	Np	93	$5f^4\ 6d^1\ 7s^2$
Sm	62	$4f^6\ 6s^2$	Pu	94	$5f^6\ 7s^2$
Eu	63	$4f^7\ 6s^2$	Am	95	$5f^7\ 7s^2$
Gd	64	$4f^7\ 5d^1\ 6s^2$	Cm	96	$5f^7\ 6d^1\ 7s^2$
Tb	65	$4f^9\ 6s^2$	Bk	97	$5f^9\ 7s^2$
Dy	66	$4f^{10}\ 6s^2$	Cf	98	$5f^{10}\ 7s^2$
Ho	67	$4f^{11}\ 6s^2$	Es	99	$5f^{11}\ 7s^2$
Er	68	$4f^{12}\ 6s^2$	Fm	100	$5f^{12}\ 7s^2$
Tm	69	$4f^{13}\ 6s^2$	Md	101	$5f^{13}\ 7s^2$
Yb	70	$4f^{14}\ 6s^2$	No	102	$5f^{14}\ 7s^2$
Lu	71	$4f^{14}\ 5d^1\ 6s^2$	Lr	103	$5f^{14}\ 6d^1\ 7s^2$

Table 1.3: Oxidation states* of actinide elements

89	**90**	**91**	**92**	**93**	**94**	**95**	**96**	**97**	**98**	**99**	**100**	**101**	**102**	**103**
Ac	**Th**	**Pa**	**U**	**Np**	**Pu**	**Am**	**Cm**	**Bk**	**Cf**	**Es**	**Fm**	**Md**	**No**	**Lr**
						(2)		(2)				2	$\underline{2}$	
$\underline{3}$	(3)	(3)	3	3	3	$\underline{3}$	$\underline{3}$	$\underline{3}$	$\underline{3}$	$\underline{3}$	$\underline{3}$	$\underline{3}$	3	$\underline{3}$
	$\underline{4}$	4	4	4	$\underline{4}$	4	4	4						
		$\underline{5}$	5	$\underline{5}$	5	5								
			$\underline{6}$	6	6	6								
				7	7									

** Those underlined are the most stable oxidation states in aqueous solution; those in parentheses refer to oxidation states which are not known in solutions.*

medium [16]. Penta and hexavalent actinide ions exist in acid solution as oxygenated cations, viz. MO_2^+ and MO_2^{2+}.

1.4.3.2. Disproportionation

"Disproportionation" is referred to as simultaneous self oxidation-reduction reactions. For disproportionation to occur an element must have at least three oxidation states and M^{4+} and MO_2^{2+} ions, have pronounced effect on disproportionation reactions these ions must be able to co-exist in solutions, which depend on the closeness of the electrode potentials of redox couples involved. In case of Pu these values are so close that the

Table 1.4: Disproportionation reactions of actinides in aqueous solutions

Element	*Oxidation numbers*	*Reaction*	*Log K (25°C)*
U	V = IV + VI	$2UO_2^+ + 4H^+ \Leftrightarrow U^{4+} + UO_2^{2+} + 2H_2O$	9.30
Np	V = IV + VI	$2NpO_2^+ + 4H^+ \Leftrightarrow Np^{4+} + NpO_2^{2+} + 2H_2O$	-6.72
Pu	V = IV + VI	$2PuO_2^+ + 4H^+ \Leftrightarrow Pu^{4+} + PuO_2^{2+} + 2H_2O$	4.29
	V = III + VI	$3PuO_2^+ + 4H^+ \Leftrightarrow Pu^{3+} + 2PuO_2^{2+} + 2H_2O$	5.40
	IV + V = III + VI	$Pu^{4+} + PuO_2^+ \Leftrightarrow Pu^{3+} + PuO_2^{2+}$	1.11
	IV = III + VI	$3Pu^{4+} + 2H_2O \Leftrightarrow 2Pu^{3+} + PuO_2^{2+} + 4H^+$	-2.08
Am	IV + V = III + VI	$Am^{4+} + AmO_2^+ \Leftrightarrow Am^{3+} + AmO_2^{2+}$	12.5
	IV = III + VI	$3Am^{4+} + 2H_2O \Leftrightarrow 2Am^{3+} + AmO_2^{2+} + 4H^+$	32.5
	IV = III + V	$2Am^{4+} + 2H_2O \Leftrightarrow Am^{3+} + AmO_2^+ + 4H^+$	19.5

four oxidation states, viz. III, IV, V and VI are in equilibrium with each other. The disproportionation reactions of U, Pu, Np and Am have been well studied [14] and their equilibrium constant (log K) values are given in Table 1.4. In general, disproportionation reactions of MO_2^+ (M=U, Pu or Np) ions can be represented as follows,

$$2MO_2^+ + 4H^+ \Leftrightarrow M^{4+} + MO_2^{2+} + H_2O \tag{1.1}$$

It is clearly demonstrated from the equilibrium reaction (1.1) that the presence of hydrogen ion and complexing ions like F^- and SO_4^{2-}, which complex strongly with

1.4.3.3. Hydrolysis and Polymerization

In view of their large ionic potentials, the actinide ions in various oxidation states exist as hydrated ions in the absence of complexing ions. The actinide ions in divalent to tetravalent oxidation states are present as M^{2+}, M^{3+} and M^{4+}, respectively. The actinide ions in the penta and hexavalent oxidation states are prone to more hydrolysis as

compared to those in the lower oxidation states. These oxidation states exist as partially hydrolyzed actinyl ions, viz. MO_2^+ and MO_2^{2+} and can get further hydrolyzed under high pH conditions. The oxygen atoms of these ions are not basicin nature and thus, do not coordinate with protons. The degree of hydrolysis for actinide ions decreases in the order: $M^{4+} > MO_2^{2+} > M^{3+} > MO_2^+$ which is similar to their complex formation properties [17]. In general the hydrolysis of the actinide ions can be represented as follows,

$$M^{n+} + xH_2O \Leftrightarrow M(H_2O)_x^{n+} \Leftrightarrow M(OH)_x^{(n-x)+} + xH^+ \qquad (1.2)$$

The hydrolysis behaviour of Th(IV) is quite different from those of other tetravalent actinide ions [18]. For U(IV) and Pu(IV) the metal ion hydrolyses first in a simple monomeric reaction (Eq. 1.2) followed by a slow irreversible polymerization of the hydrolyzed products. For Th(IV), however, various polymeric species exist even in very dilute solutions. Whereas the polymer formation of Pu(IV) is irreversible, that of Th(IV) is reversible. The hydrolysis of some of the trivalent actinides such as Am(III), Cm(III) and Cf(III) is well studied which revealed the higher hydrolysis constant values for trivalent actinides as compared to their analogous lanthanides [14].

Though the polynuclear species of all actinide ions are of great interest, the polymers of Pu(IV) have attracted particular attention because of practical considerations. Pu(IV) polymers with varying molecular weights ranging from a few thousand to as high as 10^{10} have been observed [19]. In dilute HNO_3 or HCl solutions, Pu(IV) polymer appears in bright green colour with a characteristic spectrum different from that of monomeric Pu(IV) in these solutions. The rate of polymerization depends on acidity, temperature, Pu(IV) concentration as well as the nature of ions present in the solution [20,21]. Polymerization rate for Pu(IV) is higher when the ratio of acid to Pu(IV) concentration is low. Thus, Pu(IV) polymerization can occur even at higher acidities if Pu(IV) concentration is raised. Depolymerization of Pu(IV) is best accomplished by heating the Pu solution in 6–10 M HNO_3. Strong complexing agents such as fluoride and sulphate ions as well as oxidizing agents such as permanganate and dichromate also promote depolymerization of plutonium.

1.4.3.4. Complexation of Actinides

The actinide ions in the aqueous solutions exhibit strong tendency to form complexes. This property of actinides is widely exploited in devising methods for their separation and purification. One of the most important factors that determines the strength of the complex formed is the ionic potential (or charge density) of the metal ions, which is the ratio of ionic charge to ionic radius. Higher the ionic potential, greater the electrostatic attraction between cations and anions and hence stronger is the complex formed. The complexing strength of actinide ions in different oxidation states follows the order: $M^{4+} > MO_2^{2+} \geq M^{3+} > MO_2^{+}$. Similarly, for metal ions of the same oxidation state, the complexing ability increases with the atomic number due to increase in the ionic potential as a result of actinide contraction [14]. However, the above generalized statement may be valid when complexation is primarily ionic in nature. There are a large number of instances where hybridization involving *5f* orbitals, steric effects and hydration of metal ions affect the tendency of complexation. For anions, the tendency to form complex with a given actinide ion generally vary in the same manner as their abilities to bind with hydrogen ion [22]. For monovalent ligands the complexing tendency decreases in the order: $F^- > CH_3COO^- > SCN^- > NO_3^- > Cl^- > Br^- > I^- > ClO_4^-$. The divalent anions usually from stronger complexes than the monovalent anions and their complexing ability decreases in the order: $CO_3^{2-} > SO_3^{2-} > C_2O_4^{2-} > SO_4^{2-}$. The complexing ability of some of the organic ligands with Th(IV) varies as: EDTA > Citrate > Oxalate > α-HIBA > Lactate > Acetate.

While discussing the stability of complexes between metal ions and ligands, Pearson [23] proposed a scheme based on the concept of 'hard' and 'soft' acids and bases. Those metal ions are called hard which have a small radius and high charge and do not possess valence shell electrons that are easily distorted. The soft metal ions have the opposite characteristics. When similar classification is applied to the ligands it is observed that the hard metal ions form stronger complexes with hard ligands and soft metal ions with soft ligands. Actinide ions behave as “hard acids” and interact strongly with hard base ligands with donor atoms such as “O” or “F” rather than soft ligands with donor atoms such as “N”, “S” or “P”. However, as compared to lanthanides they show marked preference for the soft donors which is commonly referred to as covalent character due to the *f*-orbital participation. The complex formation reactions involving hard acids and bases are endothermic whereas the reverse is true for soft ions. This is because the complex formation between hard metal ions and hard ligands require the breaking of strong bonds between these metal ions and water molecules in the primary hydration sphere which require large energy. The process of removal of water molecules, however, results in large increase in entropy which contributes to the driving force of these reactions [14]. When the primary hydration shell is broken during the complex formation, the complex formed is referred to as “inner-sphere complex”. In contrast, “outer-sphere complexes” do not require breaking of the primary hydration shell. The actinide ions interact with soft bases in organic solvents of low solvating power, but not in aqueous solutions where the soft bases would have to replace inner sphere water molecule which is a hard base. Thus, depending upon the nature of the ligand and the medium, actinide cations form inner or outer sphere complexes.

1.4.3.5. Absorption Spectra

Similar to the transition metal ions, the actinide ions display a rich variety of colors in their aqueous solutions. The absorption spectra of actinides arise due to the electronic transitions and absorption bands appear mainly from three types of transitions, viz. i) *f*-*f*- transition, ii) *f-d* transition, and iii) charge transfer bands [14]. In the *f-f* transitions, the electronic transition occurs between the two *5f-5f* orbitals of different angular momentum. As the transitions occur between the orbitals of the same sub-shell they are generally Laporate forbidden. The probabilities of transitions are, therefore, low and the absorption bands are consequently low in intensity. However, the bands are sharp because the transitions take place in the inner shell and are, therefore, not affected much by the surrounding environment. The energy differences between the various energy levels are of such an order of magnitude that the bands due to the *5f-5f* transitions appear in the UV, visible and the near IR regions. The molar absorption coefficients are in the range of 10–50 $M^{-1}cm^{-1}$. On the other hand, in case of the *f-d* transitions the absorption bands are broad as these transitions are influenced by the surrounding environment. As transitions take place between the orbitals of different azimuthal quantum numbers they are 'Laporate allowed' and, therefore, these bands are relatively more intense. The molar absorption coefficienst are of the order of ~10,000 $M^{-1}cm^{-1}$. These bands appear invariably in the UV region due to large energy differences between the *d* and *f* orbitals. In case of charge transfer transitions, the absorption bands occur due to the transition between *5f* orbitals of actinide ions and ligand orbitals. Therefore, the nature of ligand plays an important role. These transitions are significantly affected by the surrounding environment. As a consequence, the charge transfer bands are broad. The absorption bands appear in the UV region and are generally less intense than those resulting from the *f-d* transitions.

The absorption spectra of actinide ions have been widely used in the analytical chemistry. The absorption spectra of actinide ions in different oxidation states differ widely, which have been successfully exploited for the quantitative analysis of their mixtures present in different oxidation states. The absorption bands of actinide ions have also been used for studying the redox reactions. Though the transitions in actinide ions take place in an inner shell resulting in sharp bands, complexing of metal ions can strongly affect the position as well as the intensities of the individual absorption bands. Therefore, change in the absorption spectra due to the presence of ligands have often been used to establish complex formation, and in some cases, even for the calculation of their stability constants. The complexes of some of the actinides formed with many organic and inorganic ligands have very high absorption in the visible region. This property has been conveniently utilized to develop sensitive analytical methods for the detection and estimation of actinide ions.

1.5. Methods for Separation of Metal Ions

The scientific principles that govern the separation of metal ions from solutions are chemical reaction equilibrium kinetics, fluid mechanics and mass transfer from one phase to another. The theory of separation utilizes these principles in different techniques including solvent extraction, extraction chromatography as well as liquid membranes. The principles behind these techniques are discussed in this Section. Amongst these techniques, solvent extraction is the most versatile technique and is extensively used for separation, preparation, purification, enrichment and analysis on micro scale to industrial scale.

1.5.1. Solvent Extraction

Solvent or liquid-liquid extraction is based on the principle that a solute can distribute itself in a certain ratio between the two immiscible solvents, one of which is usually water and the other is an organic solvent. In certain cases the solute can be more or less completely transferred into the organic phase. The liquid–liquid distribution systems can be thermodynamically explained with the help of phase rule [24] which is usually stated as,

$$P + V = C + 2 \tag{1.3}$$

where P, V and C denote the number of phases, variances and components, respectively. In general, a binary liquid-liquid distribution system has two phases ($P = 2$) and contains three or more components (two solvents and one or more solutes). When a system contains only one solute ($C = 3$), according to the phase rule the variance is three, which means that by keeping any two variables constant the system can be defined by the third variable. In other words, at a fixed temperature and pressure, the concentration of solute in the organic phase is dependent on its concentration in the aqueous phase. Thus, when molecular species of the solute is same in the two phases, its concentration in one phase is related to that in the other phase (the distribution law). Consider the following equilibrium reaction,

$$M_{(aq.)} \leftrightarrow M_{(org.)} \qquad (1.4)$$

where the subscripts (aq.) and (org.) represent aqueous and organic phases, respectively. According to the distribution law, the distribution coefficient (K_d) is represented as,

$$D_M = \frac{[M]_{org}}{[M]_{aq}} \qquad (1.5)$$

However, it has been observed that, in most cases, the molecular species of metal ions are not the same in both the phases. Therefore, the term “distribution ratio (D_M)” is used in the solvent extraction which is defined as the ratio of the total concentration of metal ions (in all forms) in the organic phase to that of in the aqueous phase.

The solubility of charged metal ions in the organic solvents are very less as they tend to remain in the aqueous phase due to ion-dipole interaction. For the extraction of metal ions in the organic phase, the charge on the metal ions must be neutralized so as to enhance the solubility in non-polar organic solvents. Therefore, a suitable extractant (ligand) molecule is generally added in the organic solvent which upon complexation with metal ions forms neutral hydrophobic species which is then extracted in the organic phase. In such cases, the extraction of metal ions may follow one of the four extraction mechanisms.

(i) ***Solvation****:* The extraction of metal ions by neutral ligands is followed by solvation mechanism. The extraction process proceeds via replacement of water molecules from the co-ordination sphere of metal ions by basic donor atoms such as 'O' or 'N' of the ligand molecules. The well known example is the extraction of U(VI) by tri-*n*-butyl phosphate (TBP) from nitric acid medium [25].

(ii) ***Chelation****:* The extraction of metal ions proceeds via the formation of metal chelates with chelating ligands. The example of this type is the extraction of Pu(IV) by 2-thenoyltrifluoroacetone (HTTA) in benzene [26]. As hydrogen ion is liberated due to complex formation the extraction is not favoured under acidic media.

(iii) ***Ion- pair extraction****:* This type of extraction proceeds with the formation of neutral ion-pair species between the metal ions and ionic organic ligands. Acidic ligands such as sulphonic acids, carboxylic acids and organophosphoric acids provide anions by liberating protons which then complexed with the metal cation to form ion-pair. On the other hand, basic ligands provide cations which complex with aqueous anion metal complex to form ion-pair. The best examples of basic extractants are quaternary ammonium salts.

(iv) ***Synergistic extraction****:* The phenomenon in which two extractants taken together to extract a metal ion result with a much higher efficiency as compared to the normal additive effect of these extractants (separately) is called synergism. The first careful study of this phenomenon in 1958 was carried out by Blake et al. [27]. The synergistic coefficient (S.C.) as described by Taube and Siekiereki [28] may be written as

$$S.C = \log \frac{D_1}{D_1 + D_2} \qquad (1.6)$$

Where D_1, D_2 and $D_{1,2}$ are the distribution ratios of the metal ions between the organic and aqueous phases with the two extractants taken independently and with the mixture of the two extractants, respectively. When S.C.>0, the extraction is termed synergistic [29]. In the extraction of trivalent actinides and lanthanides by various mixture of extractants, it has been observed that the synergistic enhancement is in many cases very high (of the order of 10^5, i.e. S.C. = 5). This is the main reason for the great interest shown in the synergistic extraction studies of this class of metal ions. In solvent extraction, the extractable metal complex is neutral, the charge of the metal ion being neutralized either by the anion from the aqueous medium employed for the extraction or the anion provided by the extractant itself. If the neutral species is coordinatively unsaturated, water can act as the auxiliary ligand to saturate its coordination to form hydrated neutral species which are relatively poorly extractable into organic diluents. Either the charge neutralizing ligand or the neutral coordinating ligand has to be hydrophobic for the resulting metal species to become extractable into the organic diluent. In synergism, the extracted complexes contain at least two types of ligands both of which are hydrophobic thus enhancing extraction [30]. Well known example of synergistic extraction is the extraction of U(VI) from nitric acid medium by a mixture of HTTA and tri-*n*-butyl phosphate (TBP) in cyclohexane [31].

1.5. 1.1. Criteria for selection of extractants

A number of factors are taken into consideration while selecting or designing a particular extractant for the separation of metal ions for industrial applications. Some of the important considerations are listed as follows,

i) High solubility in paraffinic solvents (non-polar solvents),
ii) Low solubility in the aqueous phase,
iii) Non-volatile, non-toxic and non-inflammable,
iv) High complexation ability with the metal ions of interest,
v) High solubility of the metal-ligand complex in the organic phase, i.e. high metal loading capacity in the organic phase,
vi) Ease of stripping of metal ions from the organic phase,
vii) Reasonably high selectivity for the metal ion of interest over the other metal ions present in the aqueous solution,
viii) Optimum viscosity for ease of flow and optimum inter facial tension (IFT) to enable a faster rate of phase disengagement,
ix) Ease of regeneration of the extractant for recycling,

x) High resistance to radiolytic and chemical degradation during operation, and

xi) Ease of synthesis / availability of the extractant at a reasonable cost.

1.5.2. Membrane Separations

Membranes are barriers that separate two liquid phases and allow the mass transfer from one side of the barrier to the other [32]. Solids are not the only materials that have been used as membranes and it is possible to use a liquid as a membrane. Liquid membranes are present in various forms in daily life; an oil layer on a water surface is a typical organic liquid membrane of an immiscible liquid phase, beer froth, foam on soap, detergent or surfactant solutions, oil films coated on a metal surface – popularly used in rust protection and lubrication are familiar liquid films separating two phases [33]. Advantages of membrane based separation techniques are low energy requirements, low capital and operating costs, the possibility of achieving high separation factors and simple modular design [34,35]. From a practical point of view, separation membranes find applications in the industrial [36-40], biomedical [41], and analytical fields [42-44] as well as in waste water treatment [45]. The use of liquid membranes containing a carrier has been proposed as an alternative to solvent extraction for selective separation and concentration of metal ions from dilute aqueous solutions [46-48]. One of the important features of liquid membrane based technique is that unlike solvent extraction, here the extraction and stripping of the metal ion as well as regeneration of the carrier are combined in a single stage. Liquid Membranes can be divided into different categories according to their configuration (Fig1.2).

1.5.2.1. Types of Liquid Membrane Configurations

1.5.2.1.1. Bulk Liquid Membranes (BLM)

BLMs usually consist of an aqueous feed and stripping phase separated by a bulk organic Liquid Membrane phase. In its simplest form, this technique can be carried out in a U-tube configuration in the laboratory (Fig. 1.3.A).

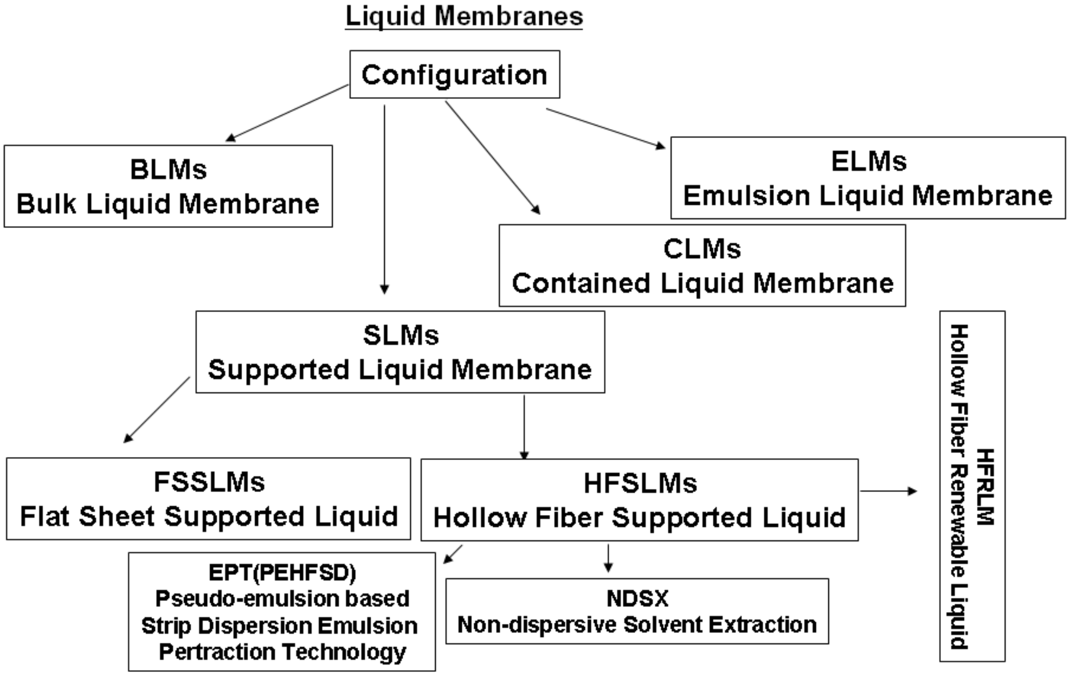

Fig. 1.2. Classification of Liquid Membrane Technologies

1.5.2.1.2. Emulsion Liquid Membrane (ELM)

ELMs may be in water-oil-water (W/O/W) or oil-water-oil (O/W/O) form, with the middle phase essentially the LM phase (Figure 1.3.B). This middle phase is a thin “shell” around the droplets where the continuous phase and the core of the droplet are the same phase (i.e., water with an organic shell). For membrane preparation, the first step commonly involves the formation of a stable emulsion of the stripping solution in the solvent phase, with the aid of a surfactant (normally 5-10%). The stable emulsion is then dispersed in a third continuous phase (the feed solution to be treated) to form a double emulsion. Extraction and separation take place by the transport of the solute(s) from the continuous outer feed phase through the LM phase to the inner stripping phase.

1.5.2.1.3. Supported Liquid Membrane (SLM)

SLMs offer a simpler configuration and process compared to ELMs. A microporous hydrophobic membrane is impregnated with an organic solvent (which is typically used in SX) and then sandwiched between an aqueous feed and strip solution (Figure 1.3.C). The microporous membrane for the SLM can be flat-sheet or hollow fibers (HFSLM). In the HFSLM the fiber wall is impregnated with the LM phase, the feed solution flows through the lumen of fibers, and the strip solution flows through the shell side of the fibers or vice versa.

1.5.2.1.4. Contained Liquid Membrane (CLM)

CLMs utilize two sets of membranes, between which the organic phase is contained (Figure 1.3.D). Similarly to the SLM, both flat-sheet and hollow fiber membranes can be used. When hollow fibers are used in a single module, the technique is known as the HFCLM. In the HFCLM, the strip and feed solutions are passed through the lumen of two separate sets of fibers, with the solvent membrane phase being stationary on the shell side; this uses the principle of the BLM.

1.5.2.2. Theory of Facilitated Transport of metal ion across SLM

The mechanism of coupled transport through SLMs is schematically described in Fig.1.4. The SLM consists of a solution, in a water-immiscible low dielectric constant organic diluent, of an extracting reagent-a metal carrier in membrane terminology-absorbed on to a micro porous polymeric film. The polymeric film, which acts as solid support of the liquid membrane, is generally made of polypropylene, polysulfone, poly tetra fluoro ethylene (PTFE) or other hydrophobic materials and has pore sizes ranging from 0.02 to 5 µm. The SLM is put between the two aqueous solutions. The aqueous solution, initially containing all the metal ions which can permeate the SLM, is referred to as the feed solution or source phase. The distribution ratio between the organic phase absorbed in the membrane pores and the aqueous feed solution of the metal species permeating the SLM, D should be high enough to favor metal extraction into the membrane phase. The aqueous solution present on the opposite side of the membrane,

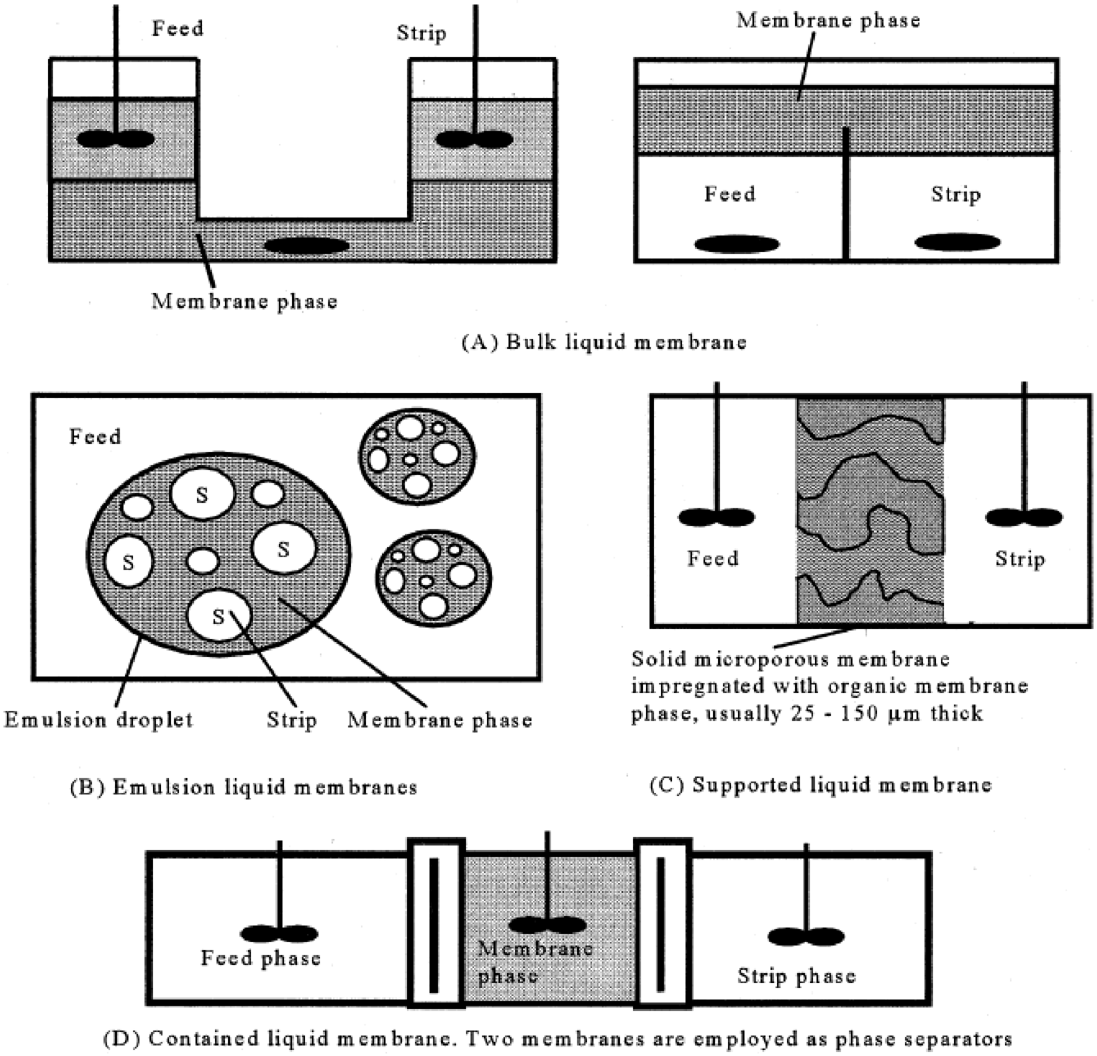

(A) Bulk liquid membrane

(B) Emulsion liquid membranes

(C) Supported liquid membrane

(D) Contained liquid membrane. Two membranes are employed as phase separators

Fig. 1.3. Schematics of A) a Bulk Liquid Membrane (BLM) B) an Emulsion Liquid Membrane (ELM) C) Supported Liquid Membrane (SLM) and D) Contained Liquid Membrane (CLM)

which is initially free from the permeable metal ions, is referred to as the strip solution or the receiver phase. In this case the distribution ratio D is made as low as possible in order to favor complete back extraction of the metal species from the liquid membrane. If the metal carrier is a neutral species (like diglycolamides studied in the present study), L, the difference in D between feed and strip is generally obtained by a concentration gradient of the counter ion, X^-, which is accompanying the metal cation into the membrane. In this case we deal with a co-transport phenomenon and the chemical reaction responsible for the coupled transport can be schematized as:

$$M^{n+}_{(aq)} + nX^-_{(aq)} + y\,L_{(org)} \leftrightarrows MX_n.yL_{(org)} \qquad (1.7)$$

From this schematic description of coupled transport it follows that the metal species can be transported across the membrane against their concentration gradient. This type of “uphill” transport will continue until all the metal species which can permeate the SLM have been transferred from the feed to the strip side, providing the driving force of the process is kept constant. This situation often occurs in practice when very dilute solutions of metal species are involved or when, in the case of more concentrated metal solutions, the concentration of the chemicals responsible for the driving force is continuously adjusted to keep it constant. It follows that in a SLM permeation process very high concentration factors can be obtained by using a volume of the strip solution which is much lower than that of the feed solutions. Moreover, by using carrier molecules, L, which is very selective for the given metal species, very clean separation processes can be performed. Since during the permeation the carrier acts as a shuttle, i.e., moving the metal-ligand complex species from the feed to the strip solution and then diffusing back (being continuously regenerated during the process), very small amounts of carrier are used in SLM separations. As a consequence, very expensive, highly selective, tailor-made carriers can be used economically. Other potential advantages of SLM separations over separations performed by traditional solvent extraction techniques are the lack of solvent entrainment phenomena (leading to high separation factors), the possibility of handling feed solutions containing suspended solids, the simplicity of the equipment involved, and the low energy consumption of the process. Moreover, with respect to separation processes performed with solid membranes, SLMs offer the additional advantage of higher fluxes since diffusion in liquids is much faster than in solids.

1.5.2.3. Flux Equations for Permeation

Various steps which characterize the transport of metal species through SLMs can be described with the help of Fig. 1.4.

Step 1: Diffusion of metal ion across the aqueous layer along with the counter ions (X^-) towards the feed membrane interface.

Step 2: Complexation of metal ion with carrier (L) (as per Eqn. (1.7)) incorporated in the membrane phase.

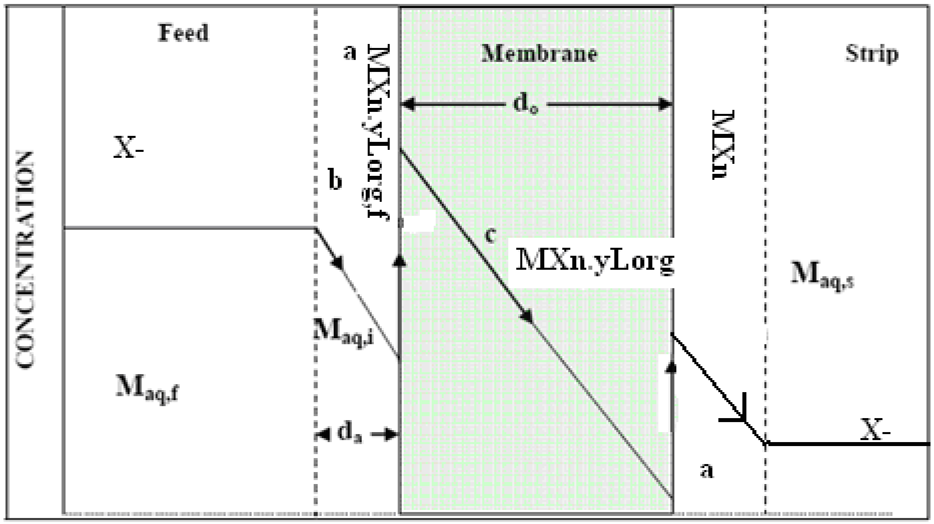

Fig. 1.4. Schematic description of the processes controlling the permeation rate through a SLM, a: Aqueous diffusion; b: Chemical reaction; c: Membrane diffusion

Step 3: Diffusion of the metal-carrier complex (MX_n.yL) through membrane phase towards the membrane–strip interface.

Step 4: De-complexation of metal ion at the membrane–strip interface and the release of metal ion in the strip solution due to favorable condition for de-complexation in the strip phase.

Step 5: Diffusion of metal ion from the membrane–strip interface towards the bulk strip solution due to concentration gradient.

Step 6: Diffusion of the free carrier to the feed-membrane interface.

The following assumptions [48-50] are made during the derivation of flux across the stagnant aqueous diffusion layer and membrane: (a) the composition of the strip solution is such that the metal-carrier complex is completely dissociated at the membrane-receiver interface, (b) The membrane polarity is low enough to neglect the presence of charged species in the membrane phase, and (c) there is no interaction of metal ions with pure diluent. If one includes the assumptions that the transport of metal ion occurs at the steady state, the concentration gradients are linear, and the feed concentration of X^- is constant, then the equations describing the aqueous diffusion film flux (J_a) and membrane flux (J_o) from Fick's law of diffusion are given as [48],

$$J_a = \frac{D_a}{d_a\{[M]_{aq,f} - [M]_{aq,i}\}} \tag{1.8}$$

$$J_o = \frac{D_o}{d_o\{[M.L]_{org,f} - [M.L]_{org,s}\}} \tag{1.9}$$

where D_a is the aqueous diffusion coefficient of the metal ions, d_a the thickness of the aqueous stagnant film, $[M]_{aq,f}$ and $[M]_{aq,i}$ the metal ion concentrations in the aqueous feed phase and at the aqueous feed-membrane interface, respectively, D_o the membrane diffusion coefficient of [M·L] and d_o the membrane thickness. The concentration of carrier-metal complex at the aqueous feed-membrane and at the membrane-aqueous strip interfaces are denoted by $[M\cdot L]_{org,f}$ and $[M\cdot L]_{org,s}$, respectively. The various parameters in Eqns. (1.8) and (1.9) are described in Fig. 1.4. The distribution ratio (D_M) of the given metal ion at the aqueous feed-membrane interface is reasonably high as equilibrium reaction (1.7) is shifted to the right due to favorable conditions. However, due to unfavorable conditions on the strip side, the equilibrium reaction (1.7) is shifted to the left as the D_M value of the given metal ion at the membrane-aqueous strip interface is much lower as compared to the aqueous feed-membrane interface, i.e. $[M.L]_{org,s} << [M.L]_{org,f}$. Therefore, Eq. (1.9) can be reduced to,

$$J_o = \frac{D_o}{d_o.[M.L]_{org,f}} \tag{1.10}$$

If we assume that the carrier in the liquid membrane is not saturated with the metal ions, then the concentration terms $[M{\cdot}L]_{org,f}$ and $[M]_{aq,i}$ are correlated to the D_M by the following equation,

$$D_M = \frac{[M.L]_{org,f}}{[M]_{aq,i}} \tag{1.11}$$

If the chemical reaction between ligand and the metal ion is assumed to be fast compared to the diffusion rate, a local equilibrium at the interface is reached. Thus, at steady state, $J_a = J_o = J$ and Eqs. (1.9), (1.10) and (1.11) can be solved to get the following expression,

$$J = \frac{D_M [M]_{aq,f}}{[D_M (d_a / D_a) + (d_o / D_O)]} \tag{1.12}$$

Here the value of membrane thickness (d_o) can be assumed to be equal to the nominal thickness of the membrane support. Substituting the permeability coefficient, P = J / $[M]_{aq,f}$ in the above equation, we get,

$$P = \frac{D_M}{[D_M(d_a / D_a) + (d_o / D_O)]} \tag{1.13}$$

Above equation can be used for predicting P from D_M values. In general, however, P is obtained experimentally using the following equation [48],

$$\ln([M]_t / [M]_o) = -\frac{P.Q}{V.t} \tag{1.14}$$

Where, $[M]_t$ and $[M]_o$ are the concentration of metal ion in the aqueous feed solution at time t and initial concentration (t = 0), respectively. Q is the effective membrane area obtained from the total exposed membrane surface area A and the porosity ε (Q = A·ε), V is the volume of the feed solution in cm^3, and t is the permeation time (seconds). A plot of $\ln([M]_t / [M]_o)$ versus time allows to calculate the P value from the slope of the linear fit. It should be noted that the above equation is valid only when the carrier is not saturated and the flux decreases linearly with time. In the present work, since all the experiments were carried out at tracer metal concentration, Eq. (1.14) was applied for the calculation of P.

The membrane diffusion coefficient (D_o) can be calculated from the knowledge of permeability coefficient (P) and the distribution ratio of the metal ions (D_M) as per the following equation [48],

$$P = \frac{D_M}{[D_M (d_a / D_a) + (d_o \tau / D_o)} \tag{1.15}$$

where τ is the tortuosity factor of the membrane. Assuming that the rate determining step is the diffusion of the bulky complex across the membrane, the first term in the denominator of Eqn. (1.15) (which refers to the transport of hydrated metal ions across aqueous diffusion layer) can be ignored. Therefore, Eqn. (1.15) can be rearranged as follows,

$$P = \frac{D_o . D_M}{\tau . d_o} \tag{1.16}$$

Thus, from the knowledge of P and D_M, the value of D_o of the metal-ligand complex in the membrane can be obtained by knowing the tortuosity factor of the membrane support used in the study. Alternatively, D_o can also be obtained experimentally by determining the P value of metal ions for varying thickness of the membrane (d_o). A plot of P vs $1/d_o$ would be a straight line and the value of D_o can be obtained from the slope of the linear fit.

1.5.2.4. Mathematical modeling of transport data

The carrier mass balance inside the membrane phase leads to the following equation:

$$\frac{nk_o^{-1} D_M C_t}{D_M k_a^{-1} + k_o^{-1}} + \frac{D_M^{1/n}}{\left[X_{fo} - 2\ C_o - C_t\right]^{2/n} K_{ex}^{1/n}} - E_T = 0 \qquad (1.17)$$

Where, k_a and k_o are the mass transfer coefficient of metal ion in feed solution phase and that of metal carrier complex in membrane phase, respectively while $X_{f,0}$ and E_T are the nitrate ion concentration in the feed at the starting of the experiment and the total concentration of the extractant, respectively. D_M is the distribution ratio of the metal ion at the feed-membrane interface while K_{ex} is the two-phase extraction constant. The equation giving the rate of change of metal ion concentration with time is as follows:

$$\frac{dC_t}{dt} = -\frac{A}{V}\left(\frac{D_M C_t}{D_M k_a^{-1} + k_o^{-1}}\right) \qquad (1.18)$$

The above two Eqn. (1.17) and (1.18) form the initial value problem (IVP) and are solved using a computer software. Solution of above equation gives the variation of D_M value and metal ion concentration with time. Relation between permeability coefficient and distribution ratio (D_M) is given as:

$$\frac{1}{P} = k_a^{-1} + \left(\frac{k_o^{-1}}{D_M}\right) \qquad (1.19)$$

The transport modeling was validated by comparing the experimentally obtained data points with the theoretically predicated profiles.

1.6. Reprocessing of Spent Nuclear Fuel

The fuel after use in the reactor is referred to as “spent fuel”. The spent fuel contains man made fissile materials such as ^{239}Pu along with minor actinides and fission products. Separation of major actinides containing fissile nuclides from the other elements is referred to as the reprocessing of the spent fuel. Reprocessing of the spent fuel is important for the recovery of valuable fissile materials to sustain the future nuclear energy programme. During reprocessing of the spent fuel the valuable uranium and plutonium are recovered in the hydrometallurgical process leaving behind highly radioactive liquid waste solution (HLW). Initially, different processes were tried for the reprocessing, viz. sodium bismuthate process, REDOX process, BUTEX process, etc [51]. However, Plutonium Uranium Reduction Extraction (PUREX) process based on tri *n*-butyl phosphate (TBP) as the extractant has been employed for the reprocessing of the spent nuclear fuel globally [52]. A brief mention about the reprocessing of the spent fuel by PUREX process is presented here.

1.6.1. The PUREX process

The PUREX process consists of the co-extraction of the hexavalent uranium and tetravalent plutonium (valency adjustment of plutonium is done using $NaNO_2$ or NO_2 gas) from moderately concentrated (~3 M) nitric acid solution leaving behind the minor actinides (trivalent and pentavalent), fission products and structural elements. The organic phase comprises of TBP in a hydrocarbon diluent such as odorless kerosene or *n*-dodecane. The mutual separation of uranium and plutonium is done by partitioning the plutonium from the organic to the aqueous phase after adjusting its valency to trivalent state employing U(IV) salt as the reducing agent. If the TBP solution of extracted actinides is subsequently contacted with dilute (~0.1 M) nitric acid, the U(VI) is easily back extracted (stripped) into the aqueous phase.

Np requires special attention because of the long half life of ^{237}Np (2.14 X 10^7 yrs). U, Pu and Np are separated by making use of the variable oxidation states of Pu and Np. Np exists mainly as Np(V), which is not extracted by TBP under the PUREX feed condition. At low HNO_2 concentration (10^{-4} – 10^{-3} M) in the dissolver solution, Np(V) is oxidized to Np(VI) and co-extracted with U and Pu. When HNO_2 concentration is >10^{-2} M, Np follows the raffinate along with the fission products. The raffinate of the PUREX process, containing long lived structural elements and process chemicals (at g/L scale), minor actinides (at mg/L scale) along with large quantities of fission products, which are either inactive or short lived, is referred to as high active waste (HAW). The HAW is concentrated by evaporation to obtain High Level Waste (HLW). Increase in acidity on evaporation is addressed by adding acid scavengers [52]. It is, therefore, very important to separate this small amount of the long lived minor actinides from the bulk of the waste of low radio toxicity for the safe management of the nuclear waste. This is called as ‘Actinide Partitioning’ and has been the focus of many R&D efforts at various international laboratories.

1.7. Actinide Partitioning: Co-extraction of Trivalent Actinides and Lanthanides

The selective extraction of trivalent actinides, namely Am(III) and Cm(III) present in the HLW resulting from the reprocessing of the spent fuel is influenced by the presence of trivalent lanthanides. The trivalent lanthanides have almost similar chemical properties to those of trivalent actinides and have several times higher concentration than the later, which represent about 1/3 of the total mass of the fission products. So owing to the complexity of the selective removal of trivalent actinides, the separation process can be split into two steps. The first step consists of co-extraction of An(III) and Ln(III) aiming to eliminate all the alpha activities and 1/3 of the fission products. The second step consists of the group separation of Ln(III) and An(III) by several processes including Selective Actinide Extraction (SANEX) process. During the last two decades, concerted research conducted around the world has identified a number of promising extractants for actinide partitioning. The performance and status of some of these extraction processes are briefed here.

1.7.1. Processes with Organo phosphorous Extractants

1.7.1.1. The TRUEX process

The Trans Uranium Extraction (TRUEX) process is a solvent extraction process designed to separate transuranic elements from various types of high level waste solutions. The key ingredient in this process is a phosphine oxide based extractant, viz.

octyl(phenyl)-N,N-diisobutyl carbamoyl methyl phosphine oxide (CMPO, Fig. 1.5(a)) [53]. The TRUEX extractant is usually 0.2 M CMPO + 1.2 M TBP (used as a phase modifier) in paraffinic hydrocarbon like *n*-dodecane [54]. In TRUEX solvent, TBP suppresses third phase formation, contributes to better acid dependencies for D_{Am}, improves phase compatibility, and reduces hydrolytic and radiolytic degradation of CMPO [55]. High distribution ratio of tri-, tetra- and hexavalent actinides from solutions of moderate acid concentration and good selectivity over fission products is the key feature of this extractant. Lanthanides such as Eu, Ce and Pr behave similar to the trivalent actinides, viz. Am(III). Other fission products, except Zr, show relatively small distribution values. Zirconium is also extractable with the TRUEX solvent; however, its extraction may be suppressed by the addition of oxalic acid. From the process perspective, the insensitivity of distribution values of actinides between 1 M and 6 M HNO_3 is important as it allows efficient extraction of these ions from waste with little or no adjustment of feed acidity. Due to high extraction of tetra- and hexavalent actinides such as Pu(IV) and U(VI) by CMPO in a wide range of acidity the stripping of these metal ions with dilute nitric acid is difficult. Therefore, stripping with powerful diphosphonate actinide extractant is required. Generally, 1-hydroxyethylene-1,1-diphosphonic acid (HEDPA) is used for stripping of Am, Pu and U from loaded organic phase [56]. The oxidation state specific stripping of actinide ions from loaded TRUEX solvent can be achieved in three steps: 0.04 M HNO_3 to remove trivalent actinides, dilute oxalic acid for selective stripping of tetravalent actinides, and finally

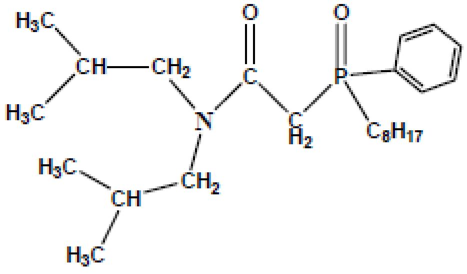

(a) CMPO

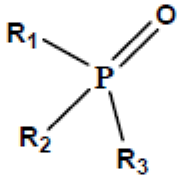

(b) TRPO
(R: *n*-octyl and *n*-hexyl)

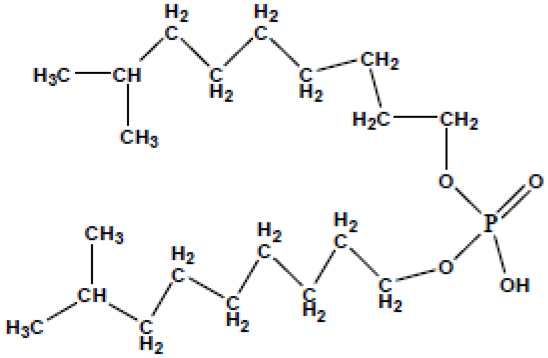

(c) DIDPA

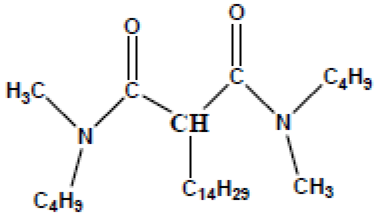

(d) DMDBTDMA

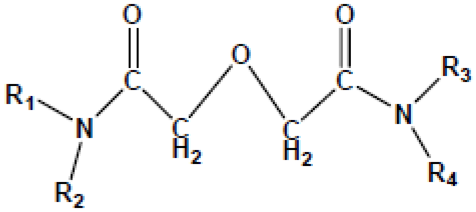

(e) Tetra alkyl diglycolamide

Fig. 1.5. Various extractants proposed for Actinide Partitioning

0.25 M Na_2CO_3 for uranium recovery. A mixture of formic acid, hydrazine hydrate and citric acid has shown promise for efficient stripping of Am and Pu from TRUEX solvent loaded with HLW in both batch as well as counter current modes [56,57].

Though CMPO shows high extraction efficiency and is a promising reagent for the separation of actinides, the TRUEX process exhibits certain limitations. Stripping of trivalent actinides is cumbersome and requires several stages of contact with 0.04 M HNO_3. Degradation products of CMPO can also inhibit the stripping of Pu and U. The presence of acidic degradation products can cause an increase in the D_{Am} values under stripping conditions. Such impurities must be removed from the used TRUEX solvent prior to their recycling. More stringent stripping condition of metal ions from the loaded organic phase is the major drawback of the TRUEX process.

1.7.1.2. TRPO Process

Trialkyl Phosphine Oxide (TRPO) process utilizes a mixture of four alkyl phosphine oxides (Fig. 1.5(b)) as the extractant. The TRPO solvent has been tested for the extraction of actinides, lanthanides and other fission products from HNO_3 and HLW solutions [58,59]. It was observed that >99% of U(VI), Np(IV), Np(VI) and Pu(IV) were extracted from 0.2–1 M HNO_3 through a single extraction with 30% (v/v) TRPO in kerosene [60]. Also >95% of Pu(III), Am(III) and Ln(III) could be extracted, while fission products such as Cs, Sr, Ru were not extracted. Trivalent lanthanides and actinides are generally stripped with 5 M HNO_3. On the other hand, tetravalent (Np and

Pu) and hexavalent (U) actinides are stripped with 0.5 M oxalic acid and 5% Na_2CO_3, respectively. Though TRPO, with its relatively low cost and its high extraction efficiency, is a promising extractant for actinide partitioning the process, however, it has, however, certain limitations. The TRPO process works only at relatively low acidity (0.1-1 M HNO_3) and, therefore, the HLW solution (acidity ~3 M HNO_3) has to be diluted several times to adjust the feed acidity. Poor stripping of actinide ions is also a disadvantage of the TRPO process.

1.7.1.3. The DIDPA Process

The extraction behavior of actinides and other fission products with di-isodecyl phosphoric acid (DIDPA, Fig. 1.5(c)) has been studied by Morita et al., at Japan Atomic Energy Research Institute (JAERI). It has been shown that DIDPA can simultaneously extract Am(III), Cm(III), U(VI), Pu(IV) and even Np(V) from a solution of low acidity such as 0.5 M HNO_3 [61,62]. The trivalent cations can be separated from their tetravalent counterparts by appropriate back-extraction procedures. The back extraction of trivalent actinides and lanthanides can be achieved by 4 M HNO_3. On the other hand, tetravalent Np and Pu and hexavalent uranium can be stripped by 0.8 M oxalic acid and 1.5 M Na_2CO_3 solution, respectively. For the partitioning of transuranic elements a mixture of 0.5 M DIDPA + 0.1 M TBP in *n*- dodecane has been proposed.

The major drawback of the DIDPA process is the re-adjustment of the acidity of HLW to about 0.5 M HNO_3 prior to the processing. In this process, the reduction of acidity and denitration is accomplished using formic acid. At such a low acidity, molybdenum and zirconium form precipitates which carries about 90% of plutonium.

1.7.2. Processes with Amide Extractants

1.7.2.1. The DIAMEX Process

The diamide extraction (DIAMEX) process was developed in France for the extraction of transuranic elements from the HLW solutions. One of the major drawbacks of using organophosphorus extractants is the solid residue that results upon their incineration at the end of their useful life. French researchers utilized the CHON (carbon, hydrogen, oxygen and nitrogen) principle for designing the extractants, which can be completely incinerated into gaseous products, thereby minimizing the generation of solid secondary wastes at the end of the process.

Among the numerous diamides synthesized and tested for the extraction of actinides, N,N′-dimethyl-N,N′-dibutyl tetradecyl malonamide (DMDBTDMA, Fig. 1.5(d)) has shown the greatest promise [63-68]. In France, this reagent is extensively evaluated for actinide partitioning from HLW solution. DMDBTDMA dissolved in *n*-dodecane does not give any third phase when contacted with 3-4 M HNO_3 and hence discount the use of any phase modifier. Generally, 1 M DMDBTDMA has been proposed for actinide partitioning which gives D_{Am} value of ~10 at 3 M HNO_3 [67]. Zirconium(IV) is strongly extracted by DMDBTDMA, however, its extraction can be suppressed to an acceptable level by complexing it with oxalic acid. Extraction of molybdenum can also be suppressed by complexation with hydrogen peroxide. Iron, which is almost always present in HLW from corrosion of the process equipments, also has high affinity for DMDBTDMA. However, the extraction kinetics for Fe(III) is slow and it may be separated from actinides and lanthanides by the judicial choice of contact time for their extraction [67].

Recently, a new diamide, viz. N,N′-dimethyl-N,N′-dioctyl-2-(2-hexylethoxy) malonamide (DMDOHEMA) has been reported as a substitute of DMDBTDMA for DIAMEX solvent [69]. Amongst several extractants described for actinide partitioning, diamides have been found to be particularly promising in view of their improved back extraction properties for Am(III) / Cm(III), their complete incinerability, and the innocuous nature of their radiolytic and hydrolytic products (mainly carboxylic acids and amines) that can be easily washed out. However, the major draw back of DMDBTDMA is that it shows only moderate extraction of trivalent actinides (Am and Cm) from HLW at acidity ≤ 3 M HNO_3 [67]. Therefore, it necessitates the structural modification of diamides so as to enhance the extraction efficiency of trivalent actinides in particular.

1.7.2.2. Digylycolamides: A Class of Promising Extractants for Actinide Partitioning

The performance of some of the extraction processes developed for actinide partitioning is briefly discussed in the earlier section. However, each of the described processes has certain limitations. The main drawbacks of the TRUEX process are; (a) the poor back extraction of Am(III) and Cm(III) at reduced acidity, and (b) interference due to solvent degradation products. On the other hand, the TRPO process works only at relatively low acidity (0.1-1 M HNO_3) and, therefore, can not be applied at 3-4 M HNO_3 conditions which is generally encountered in HLW. Similarly, DIDPA process can not be applied to the concentrated HLW solution without denitration which leads to the precipitation of actinides. In order to improve the efficiency of diamides towards the forward extraction of trivalent actinides, several structural modifications have been attempted. Recently, a series of diamide compounds have been synthesized by introducing different substituents on amide nitrogen or introducing ether oxygen into the bridging chain of malonamide [70]. It has been observed that the introduction of etheric oxygen between the two amide groups (diglycolamides, Fig. 1.5(e)) causes significant enhancement in the extraction of trivalent actinides / lanthanides. The work on diglycolamides was started after Stephan et al., reported the extraction of various metal ions with multidentate amido podands [71,72]. Sasaki and Choppin were probably the first to report the extraction of lanthanides and actinides with diglycolamides [73-77]. They used dimethyl dihexyl diglycolamide and its analogous compounds for the solvent extraction studies on lanthanides and actinides. These preliminary studies, however, were focused on the extraction of metal ions from aqueous solutions of pH ranging from 1 to 4. Narita et al., studied the extraction of lanthanides from acidic solutions employing N,N’-dimethyl N,N’-diphenyl diglycolamide [78]. They proved by XRD and EXAFS studies that the diglycolamide forms tridentate complex with lanthanides in solid complexes as well as in solution [79]. Sasaki et al. [80] synthesized a series of diglycolamides having the same central frame with different alkyl chains (ranging from *n*-propyl to *n*-dodecyl) attached to amidic nitrogen atoms (Fig. 1.5(e)). Various properties of the synthesized diglycolamide derivatives are represented in Table 1.5. They found that the diglycolamide derivatives with lower alkyl chain (*n*-propyl and *n*-butyl) werenot soluble in paraffinic solvents like *n*-dodecane due to the presence of three polar oxygen atoms. Though the higher homologues of diglycolamide were freely soluble in *n*-dodecane, the distribution values for Am(III) were found to decrease due to the steric hindrance during complexation of the bulky molecules. Amongst the different derivatives synthesized, N,N,N’,N’-tetraoctyl diglycolamide (TODGA) was demonstrated to be the best candidate with reference to its free solubility in *n*-dodecane and significantly high distribution values for trivalent actinides.

1.7.2.3. Main Features of TODGA and T2EHDGA

TODGA and T2EHDGA exhibit the excellent properties required for an extractant which can be exploited for the partitioning of radionuclides from HLW. Salient features of TODGA are listed as follows,

i) High extraction co-efficients of for minor actinides from moderate acidic aqueous solutions,

Table 1.5: Various properties of tetra- *n*-propyl, *n*-butyl, *n*-amyl, *n*-hexyl, *n*-octyl, *n*-decyl and *n*-dodecyl diglycolamide

Diglycolamide (DGA)	*Solubility in water [mM]*	*Solubility in n-dodecane*	*D_{Am} by 0.1M DGA in n-dodecane ($1M\ HNO_3$)*
TPDGA	57.0	Very poor	--
TBDGA	2.3	poor	--
TADGA	0.27	Soluble	100
THDGA	0.11	Soluble	40
TODGA	0.042	Freely soluble	30
TDDGA	0.042	Freely soluble	18
TDDDGA	0.040	Freely soluble	11

ii) Ease of stripping of minor actinides at lower acidity,

iii) Low extraction of fission products by T2EHDGA due to branching structure,

iv) High solubility in paraffinic solvents (freely soluble in *n*-dodecane),

v) Low concentration of TODGA/T2EHDGA to be used (~ 0.1 M / 0.2 M),

vi) Good radiolytic and hydrolytic stability,

vii) Possibilities of complete incineration as the constituent elements are C, H, N and O

viii) Ease of synthesis.

1.8. Scope of the present work

The performance of different types of liquid membranes, viz. BLM, ELM, FSSLM and HFSLM has been reviewed by Izatt, et al. [81]. A large number of publications are available on the facilitated transport of metal ions through SLM [82-86]. In such transport systems, the solute can be transported across the membrane against their concentration gradient, i.e. “uphill” transport. The driving force in such processes is provided by the chemical potential difference of the chemical species present on the two opposite sides of the membrane. The permeability of the transported species is influenced by the parameters like membrane thickness, aqueous diffusion coefficient of the solute, aqueous diffusion layer thickness, distribution and diffusion coefficients of the solute in the liquid membrane phase, etc.. While diffusion coefficient of the solute in the carrier solvent depends upon the chosen membrane and the aqueous diffusion coefficient of the solute depends on the stirring rate. Practically, the transport rates can be controlled through parameters, like feed acidity, soluteconcentration, carrier concentration, nature of diluent, strip phase composition etc.

Extensive work has been carried out by several laboratories to investigate N,N,N’,N;-tetraoctyl diglycolamide (TODGA) as carrier for the transport of actinides and few selected fission products from nitric acid solution across the SLM [87-88]. Membrane technology has gained world wide importance due to its ease of operation, simultaneous extraction and stripping, low ligand inventory etc,.

Present work describes the detailed transport properties of actinides in different oxidation states like U(VI),Pu(III),Pu(IV), Th(IV) using TODGA/ *n*-dodecane as the carrier across SLM. A detailed study was undertaken to optimize the metal transport process by investigating various parameters such as nature of strippant, carrier concentration, feed acidity etc. An attempt has also been made to elucidate the transport mechanism. The stability of the liquid membrane was also investigated.

- Efforts were also made to understand the role played by diluents in the transport properties of trivalent actinides for TODGA across SLM. Attempt was also made to investigate the role played by radiation on the degradation of TODGA and its effect on the transport of actinides having various oxidation states across SLM.
- The transport properties and transport mechanism of trivalent actinides and lanthanides along with hexavalent actinides using tetra(2-ethyl hexyl) diglycolamide (T2EHDGA)/ dodecane as the carrier extractant were also studied across SLM.
- Detailed solvent extraction and SLM transport experiments were also carried out for trivalent actinides and lanthanides along with fission products using a series of substituted diglycolamides. In this study, the effect of changing the substituent groups on acyl nitrogen atom on the extraction and transport of actinides was investigated in detail.

1.9. REFERENCES

1. J. F. Ahearne, Special issue: Radioactive wastes, Physics Today, 50 (1997) 22.
2. J.V. Holder, *Radiochim. Acta*, 25 (1978) 171.
3. W.E. Kastenberg and L.J. Gratton, Hazardous of managing and disposing of nuclear wastes, *Physics Today*, 50 (1997) 41.
4. K.D. Crowley, Nuclear waste disposal: The technical challenges, *Physics Today*, 50 (1997) 32.
5. Charles McCombie, Nuclear waste management world wide, *Physics Today*, 50 (1997) 56.
6. N.N. Egorov, M.A. Zakharov, C.N. Lazarev, R.I. Lyubtsev, A.S. Nikiforov, M.V. Strakhov and E.A. Filippov, “New approaches to solving the management problem of long lived radionuclides”, In proceedings of the third international conference on nuclear fuel reprocessing and waste management, RECOD-91, Vol. 1, P. 357.
7. Actinide and Fission Product Partitioning and Transmutation—Status and Assessment report, OECD/NEA, 1999.
8. L.H. Baestle, Burning of Actinides: A complementary waste management option? *IAEA Bulletin*, 34 (1992) 32.
9. J.C. McLean, A.B. McLay and H.G. Smith, *Proc. Roy. Soc. (London)*, 112 (1926) 76.
10. G.T. Seaborg, *Chem. Eng. News*, 23 (1945) 2190.
11. M.S. Milyukova, N.I. Gusev, I.G. Sentyurin and I.S. Skyarenko, “Analytical

Chemistry of Plutonium”, *Israel Prog. for Sci. Translation, Jerusalem* (1967), 5.

12. M. Taube, “Plutonium”, Pergamon Press, Oxford (1964), 5.
13. Handbook of Physics and Chemistry of Rare Earths, Eds, K. A. Gschneidner, Jr and L.R. Eyring, Vol. 3, Separation Chemistry by J. E. Powell, Chapter 22, 82.
14. S. Ahrland, J.O. Liljenzin and J. Rydberg, Solution Chemistry, In “Comprehensive Inorganic Chemistry”, J.C. Bailar Jr., H.J. Emeleus, R. Nyhlom and A.F.T. Dickenson (Eds.), Pergamon Press, Oxford (1973), Vol. 5, 465.
15. B.B. Cunningham, “*Proc. of XVII international congress of pure and applied chemistry*”, Butterworths, London. Vol. 1, 64.
16. V.I. Spitsyn, A.D. Gelman, N.N. Krot, M.P. Mefodiyeva, F.A. Zacharova, Y.A. Komokov, V.P. Shilov and I.V. Smirnovam, *J. Inorg. Nucl. Chem*., 31 **(**1969**)** 2733.
17. K.A. Kraus, *Proc. First U.N. Conference on Peaceful Uses of Atomic Energy*, 7 (1956) 245.
18. M. Haissinsky, “*Nuclear chemistry and its applications*” (English ed.), Addison-Wesley (1964), 233.
19. O.J. Wick, “*Plutonium Hand Book: A Guide to the Technology*”, Gordon and Breach, New York (1967), Vol. 1, 438.
20. R.H. Rainey, *USAEC Report* CF-59-12-95 (1959).
21. J.M. Cleveland, “*The chemistry of plutonium*”, Gordon and Breach, New York (1970), 84.
22. A.D. Janes and G.R. Choppin, *Actinides Rev*., 1 (1969) 311.

23. R.G. Pearson, *J. Am. Chem. Soc*., 85 (1963) 3533.

24. T. Sekine and Y. Hasegawa (Eds.), "*Solvent Extraction Chemistry: Fundamentals and Applications*", Marcel Dekker, New York (1977), 60.

25. S.V. Bagawade, P.R. Vasudeva Rao, V.V. Ramakrishna and S.K. Patil, *J. Inorg. Nucl. Chem.,* 40 (1978) 1913.

26. A. Ramanujam, M.N. Nadkarni, V.V. Ramakrishna and S.K. Patil, *J. Radioanal. Chem.*, 42 (1978) 349.

27. C. A. Blake, C. F. Baes, K. B. Brown, C. F. Coleman and J. C. White, Proc. Of the Second Int. Conf. on the Peaceful Uses of Atomic Energy, Geneva, 28, 289 (1958).(IAEA, Vienna, 1958).

28. M. Taube and S. Siekierski, *Nucleonika*, 6 (1961) 489.

29. J. N. Mathur, *Solv Extr. Ion Exch*., 1(2) (1983) 349.

30. V. V. Ramakrishna and S. K. Patil, Synergistic extraction of actinides, *Structure and Bonding*, vol 56, page 35.

31. H. Irving and D. N. Edgington, *J. Inorg. Nucl. Chem.*, 15 (1-2) (1960) 158.

32. Ho WSW and Sirkar KK, Membrane Handbook. Chapman & Hall, New York (1992).

33. Araki T and Tsukube H, Liquid Membranes: Chemical Applications. CRC Press, FL (1990).

34. H.J, Fendler, *J. Membr. Sci*., 30 (1987) 323.

35. R.D. Noble, *Sep. Sci. Technol*., 22 (1987) 731.

36. J.P. Shukla, A. Kumar and R.K. Singh, *Sep. Sci. Technol.*, 27 (1992) 447.

37. Y. Zhu, J. Chen, and R. Jiao; *Solv. Extr. Ion Exch.*, 14(4) (1996) 555.

38. I.J. Youri, P.J. Harrington, and G.W. Stevens, *Solv. Extr. Ion Exch.*, 18 (2000) 933.

39. N.S. Rathore, J.V. Sonawane, A. Kumar, A.K. Venugopalan, R.K. Singh, D.D. Bajpai and J.P. Shukla, *J. Membr. Sci.*, 189 (2001) 119.

40. A. Geist, M. Weigl U. Muellich and K. Gompper, *Memb. Technol.*, 5 (2003) 5.

41. A. Geist, M. Weigl and K. Gompper, *Sep. Sci. Technol.*, 37 (2002) 3369.

42. C. Fontas, V. Salvado and M. Hidalgo, *J. Membr. Sci.*, 223 (2003) 39.

43. A. Uheida, Y. Zhang and M. Muhammed, *J. Membr. Sci.*, 241 (2004) 289.

44. P.R. Danesi, *J. Membr. Sci.*, 20 (1984) 231.

45. P. R. Danesi, *Solv. Extr. Ion Exch.*, 2 (1984) 115.

46. E.L. Cussler and D.F. Evans, *Sep. Purif. Meth.*, 3 (1974) 399.

47. R. Marr and A. Kopp, *Int. Chem. Eng.*, 22 (1982) 44.

48. P.R. Danesi, E.P. Horwitz and P.G. Rickert, *J. Phys. Chem.*, 87 (1983) 4708.

49. M. Rovira and A.M. Sastre, *J. Membr. Sci.*, 149 (1998) 241.

50. K. Lee, D. F. Evans and E. L. Cussler, *AIChE J.* 24(5) (1978) 860.

51. C. MUSIKAS, W. W. SCHULZ, *Solvent Extraction in Nuclear Science and Technology, in: Principles and Practices of Solvent Extraction*, J. RYDBERG, C. MUSIKAS and G. R. CHOPPIN (Eds), Chapter 12, Marcel Dekker Inc., New York, (1992) 413.

52. H.A.C. McKay, J.H. Miles and J.L. Swanson, Applications of Tributyl Phosphate in

Nuclear Fuel Reprocessing, In "*Science and Technology of Tributyl Phosphate*", W.W. Schulz, L.L. Burger, J.D. Navratil and K.P. Bender (Eds.), CRC Press Inc., Boca Raton, Florida (1990), Vol. 3, P. 55.

53. B.M. Rapko, Synthesis, characterization and actinide extraction behaviour of bridge modified carbamoyl methyl phosphonates and phosphine oxides, In "*Separation of f-elements*", K.L. Nash and G.R. Choppin (eds.), Plenum Press, NY (1995), P. 99.

54. E.P. Horwitz, D.G. Kalina, G.F. Vandrift and W.W. Schulz, *Solv. Extr. Ion Exch*., 3 (1985) 75.

55. W.W. Schultz and E.P. Horwitz, *Sep. Sci. Technol*., 23 (1988) 1191.

56. R.R. Chitnis, P.K. Wattal, A. Ramanujam, P.S. Dhami, V. Goparkrishnan, A.K. Bauri and A. Banergy, *J. Radioanal. Nucl. Chem*., 240 (1999) 721.

57. R.R. Chitnis, P.K. Wattal, A. Ramanujam, P.S. Dhami, V. Goparkrishnan, A.K. Bauri and A. Banergy, *J. Radioanal. Nucl. Chem*., 240 (1999) 727.

58. Y. Zhu, R. Jio, S. Wang, S. Fan, B. Leu, H. Zheng, S. Zhou and S. Chen, An extractant (TRPO) for the removal and recovery of actinides from high level radioactive liquid waste, *ISEC-1983*, Denver, Colorado, USA.

59. Y. Zhu and R. Jiao, *Nucl. Technol.*, 108 (1994) 361.

60. R. Jiao, S. Wang, S. Fan, B. Liu and Y. Zhu, *J. Nucl. Radiochem*., 7 (1985) 65.

61. Y. Morita and M. Kubota, *J. Nucl. Sci. Technol*., 24 (1987) 227.

62.Y. Morita, I. Yamaguchi, Y. Kondo, K. Shirahashi, I. Yamagishi, T. Fujirawa and M. Kubota, Safety and environmental aspects of partitioning and transmutation of actinides and fission products, IAEA-TECDOC-783, IAEA ,Vienna (1995), P. 93.

63. C. Cuillerdier, C. Musikas, P. Hoel, L. Nigond and X. Vitart, *Sep. Sci. Technol*., 26 (1991) 1229.

64. C. Cuillerdier, C. Musikas and L. Nigond, *Sep. Sci. Technol*., 28 (1993) 155.

65. L. Nigond, C. Musikas and C. Cuillerdier, *Solv. Extr. Ion Exch*., 12 (1994) 261.

66. L. Nigond, C. Musikas and C. Cuillerdier, *Solv. Extr. Ion Exch*., 12 (1994) 297.

67. G.R. Mahajan, D.R. Prabhu, V.K. Manchanda and L.P. Badheka, *Waste Management*, 18 (1998) 125.

68. L.B. Kumbhare, D.R. Prabhu, G.R. Mahajan, S. Sriram and V.K. Manchanda, *Nucl. Technol*., 139 (2002) 253.

69. D.S. Purroy, P. Baron, B. Christiansen, J.P. Glatz, C. Madic, R. Malmbeck and G. Modolo, *Sep. Purif. Technol*., 45 (2005) 157.

70. L. Spjuth, J.O. Liljenzin, M.J. Hudson, M.G.B. Drew, B.P. Iveson and C. Madic, *Solv. Extr. Ion Exch*., 18 (2000) 1.

71. H. Stephan, K. Gloe, J. Bager and P. Muhl, *Solv. Extr. Ion Exch*., 9 (1991) 435.

72. H. Stephan, K. Gloe, J. Bager and P. Muhl, *Solv. Extr. Ion Exch*., 9 (1991) 459.

73. Y. Sasaki and G.R. Choppin, *Anal. Sci*., 12 (1996) 225.

74. Y. Sasaki and G.R. Choppin, *J. Radioanal. Nucl. Chem*., 207 (1997) 383.

75. Y. Sasaki, T. Adachi and G.R. Choppin, *J. Alloy comp*., 271-273 (1998) 799.

76. Y. Sasaki and G.R. Choppin, *Radiochim. Acta*, 80 (1998) 85.

77. Y. Sasaki and G.R. Choppin, *J. Radioanal. Nucl. Chem*., 246 (2000) 267.

78. H. Narita, T. Yaita, K. Tamura and S. Tachimori, *Radiochim. Acta*, 81 (1998) 223.

79. H. Narita, T. Yaita and S. Tachimori, Extraction Behavior for Trivalent Lanthanides with Amides and EXAFS Study of their Complexes. In Solvent Extraction for the 21st Century, Proceedings of ISEC'99, Barcelona, Spain, July, 1999; M. Cox, M. Hidalgo, and M. Valiente (Eds.), Society of Chemical Industry: London (2001), Vol. 1, P. 693.

80. Y. Sasaki, Y. Sugo, S. Suzuki and S. Tachimori, *Solv. Extr. Ion Exch.*,19 (2001) 91.

81. R.M. Izatt, J.D. Lamb and R.L. Bruening, *Sep. Sci. Technol.*, 23 (1988) 1645.

82. H.C. Visser, D.N. Reinhoudt and F. de Jong, *Chem. Soc. Rev.,* (1994) 75.

83. R.A. Bartsch, J.D. Way, L.A.J. Chrisstoffels, F. de Jong and D.N. Reinhoudt, "*Chemical Separations with Liquid Membranes*", R.A. Bartsch and J.D. Way (Eds.), ACS Symposium Series Number 642, ACS, Washington DC (1996), P. 1

84. L. Boyadzhiev and Z. Lazarova, "*Membrane Separations Technology. Principles and Applications*", R.D. Noble and S.A. Stern (Eds.), Elsevier Science B.V. 1995, 283.

85. G. Spach, Ed., "*Physical Chemistry of Transmembrane Ion Motions*", Elsevier: Amsterdam, 1983.

86. P.R. Danesi, *Sep. Sci. Technol.*, 19 (1985) 857.

87. S.A. Ansari, P.K. Mohapatra, D.R. Prabhu, V.K. Manchanda, *J. Membr. Sci.* 298 (2007) 174.

CHAPTER II

EXPERIMENTAL

In the present work, solvent extraction and supported liquid membrane transport of various actinides, lanthanides and fission products like U(VI), Am(III), Pu(III),Pu(IV), Pu(VI), Eu(III), Sr(II) have been investigated under different experimental conditions employing various di-glycolamides (N,N,N′,N′-tetraoctyl diglycolamide (TODGA), N,N,N’,N’-tetra (2-ethyl hexyl) diglycolamide (T2EHDGA), N,N,N’,N’-tetrapentyl diglycolamide (TPDGA), N,N,N’,N’-tetrahexyl diglycolamide (THDGA) and N,N,N’,N’-tetradecyl diglycolamide (TDDGA)) as extractant/carrier. This Chapter, therefore, deals with synthesis and characterization of different DGA’s and different separation techniques like solvent extraction and supported liquid membrane are described in brief. The details of various apparatus, materials, experimental techniques as well as analytical techniques used in the present work are also discussed in this Chapter.

2.1. Synthesis of different DGAs

Di-glycolamides (DGAs) were synthesized with slight modifications to the method reported elsewhere [1]. In a reaction flask containing 1 mol of diglycolic anhydride (dissolved in 600 mL of dichloromethane) connected with moisture and oxygen free nitrogen gas stream, 1 mol of di-pentyl/di-hexyl/di-octyl/di-2-ethyl hexyl/ di-decyl amine dissolved in ~300 mL of dichloromethane was added dropwise with constant stirring maintaining the temperature in the range of 0-5^o C. After complete addition of amine the

reaction mixture was stirred for 16 h at room temperature. Subsequently to the reaction mixture (at 0-5° C), 1.3 mol of N,N′-dicyclohexyl carbodiimide (DCC) dissolved in 100 mL dichloromethane was added dropwise with constant stirring. It should be noted that ~30% extra DCC was added (DCC was used as a dehydrating agent) as it is liable to decompose easily. After complete addition of DCC, the reaction mixture was stirred at the same temperature for 30 minutes followed by the addition of the next batch of the required amine (1 mol dissolved in dichloromethane) dropwise with constant stirring and maintaining the temperature in the range of 0- 5° C. After complete addition of the required amine, the reaction mixture was stirred for six days at room temperature. The white precipitate of N,N′-dicyclohexyl urea formed was discarded after filtering and washing with excess of dichloromethane. The dichloromethane was then removed from the filtrate by rotavaporator to get the crude product. The crude product, thus obtained, was purified by ethyl acetate when the insoluble impurities were discarded. The other soluble volatile impurities were removed by vacuum distillation (2.5 mm) at 120-140° C to get the product in the flask. The product was further purified by silica gel column. The final pure product of DGA was obtained as a pale yellow viscous liquid with about 70% yield. The synthesis scheme for DGA is represented in Scheme 2.1.

2.1.1. Characterization of N,N,N’,N’-tetraoctyl diglycolamide

The product was characterized by GC–MS, FTIR and elemental analyzer. GC– MS was performed on Thermo Finnigan Trace DSQ GC–MS instrument with a single quadrupole mass spectrometer at 112.15239×10−19 J (70 eV) using 15m×0.25mm DB5 fused silica capillary column. Helium was the carrier gas and temperature program was 100°C for 1min, increased to 280°C at 10°C rise per minute and held at 280°C for 20 min. The injector temperature was 300°C. The results are as follows:

GC–MS: 7.12 min, 1.59%, m/z 241 calculated for HN(C8H17)2; 22.00min, 98.01%, m/z 582 calculated for O[CH2C(O)N(C8H17)2]2. Similarly, the analytical data of synthesized TODGA are represented in Table 2.1. The appearance of characteristic vibrational frequency at 1640 cm^{-1} in FT-IR spectrum demonstrated the presence of carbonyl groups of diglycolamide. The CHN elemental analysis of the synthesized product yielded values close to the theoretical expected values. The CHN analyser used in the current study is shown in Fig. 2.1. The FT-IR and CHN analysis confirmed the formation of the product in good yield (70%). The other DGA’s were also characterized in a similar way.

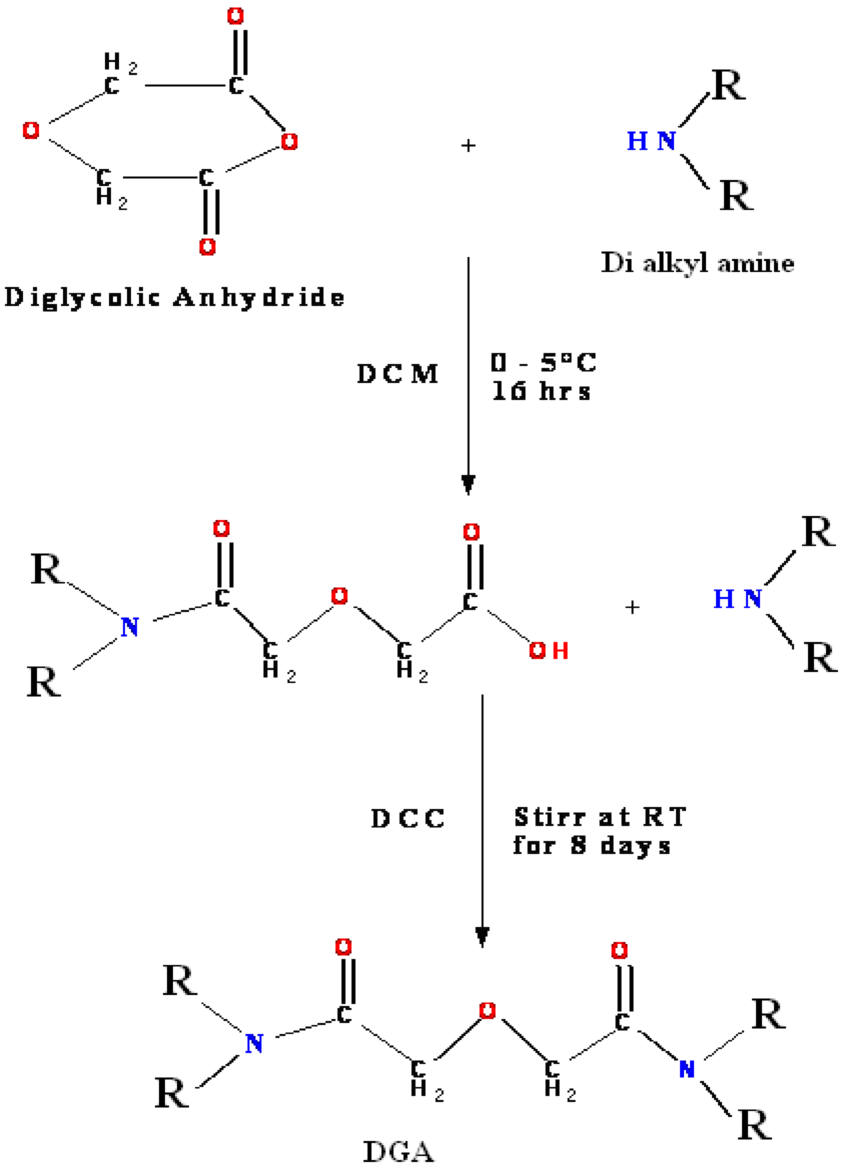

Scheme 2.1. Synthesis scheme of DGAs

2.2. RADIOTRACERS (Preparation and Purification)

The separation studies on metal ions reported in the present thesis were carried out with radiotracers. Procurement, preparation as well as purification of various radiotracers is given below:

Table 2.1: Analytical data of TODGA

Formula	$C_{36}H_{72}N_2O_3$
Product Yield	~ 70 %
C (%)	73.1 (74.5)$^{\#}$
H (%)	12.8 (12.4)$^{\#}$
N (%)	5.2 (4.8)$^{\#}$
$\nu_{>C=O}$	1640cm^{-1}

$^{\#}$ *Values in parentheses are the theoretical values*

Fig. 2.1.Elemental Analyzer

2.2.1. Uranium-233

^{233}U tracer ($t_{1/2}$ = 1.59x10^{5} years) was produced by the irradiation of ^{232}Th followed by its purification [2]. Purification of ^{233}U from its daughter products and Thorium was carried out from 6 M HCl using anion exchange procedure [3]. The uranium in 6 M HCl solution forms anionic complex which is held on the column, whereas thorium and daughter products are not retained on the column. The column was washed with excess of 6 M HCl to remove any adsorbed impurity. Finally, the loaded uranium was eluted with 0.01 M HNO_3 and used as stock solution (at 0.5 M HNO_3). The purity of ^{233}U tracer was ensured by alpha spectrometry.

2.2.2. Thorium-234

^{234}Th is a daughter product of ^{238}U and, therefore, it is separated from the natural uranium [4]. Uranium solution at 8 M HCl was extracted into a solution of 30% Aliquat 336 (tricapryl methyl ammonium chloride) dissolved in chloroform leaving behind the daughter product ^{234}Th in the aqueous phase which was subsequently purified from traces of U using a β-diketone based extraction method reported earlier [4]. This method involves the preferential extraction with 0.01 M HPBI (3-phenyl-4-benzoyl-5-isooxazolone) in xylene at 0.5 M HNO_3. ^{234}Th loaded organic phase was then scrubbed with 0.5 M HNO_3 to remove any trace of uranium. Finally, the pure ^{234}Th tracer was stripped with 8 M HNO_3 and used as stock. The purity of the purified product was confirmed by gamma spectrometry.

2.2.3. Plutonium-239

Plutonium (mainly Plutonium-239) is separated from spent fuel obtained from research reactors CIRUS and DHRUVA using PUREX process. Final purification of Pu is carried out by anion-exchange process [5]. In this method, plutonium is absorbed on the anion exchanger, DOWEX 1x4 (50-100 mesh) from 7.2 M nitric acid mainly as the hexa nitrato species $Pu(NO_3)_6^{2-}$. After adequate washing of the resin with 7.2 M nitric acid to remove residual uranium and fission products, the loaded plutonium from the resin is eluted with dilute nitric acid as pure and concentrated product. The resin is reused after conditioning once again with 7.2 M acid. Its radiochemical purity was ascertained by gamma spectrometry for the absence of ^{241}Am [5].

2.2.4. Other radiotracers

The radiochemical tracers such as $^{152-154}$Eu and ^{85,89}Sr were procured from BRIT, Mumbai and their radiochemical purity was ascertained by gamma spectrometry. Radiotracer ^{241}Am was purified by standard procedure [6]. The valency of Pu was adjusted to Pu(IV) with sodium nitrite and subsequently extracted by 0.5 M HTTA (2-thenoyltrifluoro acetone) in xylene at 1 M HNO_3 followed by stripping with 8 M HNO_3. The resulting plutonium solution was used as stock for Pu(IV). Further, plutonium valency in the aqueous phase was adjusted and maintained in tetravalent state by the addition of 0.05 M $NaNO_2$ + 0.005 M NH_4VO_3 (holding oxidants). On the other hand, Pu was reduced to Pu(III) by the addition of 0.1 M phenyl hydrazine (PH). 0.1 M PH was optimized as an efficient reductant for Pu [7].

2.2.5. PREPARATION OF SIMULATED HIGH LEVEL WASTE

The simulated high level waste (SHLW) solution was prepared by dissolving the metal ions salts in nitric acid solution. Salts in the nitrate form were preferred and in the cases where nitrate salts could not be arranged, metal powders were employed. Adequate care was taken to dissolve each of the salt separately in hot concentrated nitric acid before their addition to the mixture. Finally, the acidity of SHLW was adjusted as required with distilled water / HNO_3. The acidity of the SHLW was ascertained by acid-base titration in the presence of neutral saturated $K_2C_2O_4$ solution. The concentration of various metal ions in SHLW was ascertained by ICP-AES analysis. Composition of a typical simulated high level waste of pressurized heavy water reactor is mentioned in Table 2.3.

2.3. METHODS AND EQUIPMENTS

Different separation techniques for metal ions are known but in the present work solvent extraction and supported liquid membrane techniques have been used. Solvent extraction was used to study aqueous metal-ligand complexation in varying conditions. The basic understanding for the transport of metal ions through liquid membrane was developed using a transport cell. Various experimental setups and methodologies used in the present work are briefed below.

2.3.1. Solvent Extraction Studies

For metal ion distribution studies, suitable volume (0.5-2 mL) of aqueous phase at the desired acidity and containing the required radiotracer was equilibrated in Pyrex

glass stoppered equilibration tube with equal volume of the organic phase with desired concentration of the extractant in the chosen diluent. For all the studies, except stated otherwise, the organic phase was pre-equilibrated with the respective acid solutions. The agitation of the two phases was carried out in a thermostated water bath maintained at 25±0.1° C. For thermodynamic studies, however, the temperature of the water bath was maintained between 15-45° C within ±0.1° C. Adequate care was taken to maintain the required temperature of the equilibration tubes till the sample was removed for assaying. After equilibration, the two phases were centrifuged, separated and assayed by removing suitable aliquots (25-500 μL) from both the phases. The distribution ratio of the metal ions was calculated as the concentration of the metal ion (in terms of counts of radionuclides per unit time per unit volume) in the organic phase to that in the aqueous phase. The thermostated water bath used in the present study is shown in Fig. 2.2. During acid distribution studies the hydrogen ion concentrations in the two phases were obtained by titration with standard alkali solution using phenolphthalein as the indicator. The organic phase was titrated in aqueous ethanol medium previously neutralized to phenolphthalein end point. Each distribution ratio was obtained in duplicate or triplicate and the agreement between these values was within ± 2%. A good material balance (≥ 95%) was usually obtained in all the experiments.

Fig. 2.2. Thermostat water bath used for maintaining constant temperature

2.3.2. Membrane Studies

The supported liquid membrane (SLM) transport experiments were carried out by using a Pyrex glass cell consisting of two compartments, viz. the feed side and the strip side. As represented in Fig. 2.1, both the compartments of the glass cell were joined by glass flanges with the polymeric film containing the SLM placed in between. The two phases were stirred at an optimum speed using high speed magnetic stirrer equipped with precise speed control to ensure minimal thickness of the aqueous diffusion boundary layers without causing any damage to the membrane [8]. The volumes of aqueous feed and strip solutions were kept constant (16 ml/ 30 ml) in all the experiments. For the preparation of the SLM the microporous PTFE membranes were soaked in the carrier solution (DGA's in *n*-dodecane) for about 10 minutes prior to use.

Table 2.2: Composition of a typical Simulated High-Level Waste (SHLW) solution of Pressurised Heavy Water Reactor

Constituent	***Concentration (mg/L)***	***Constituent***	***Concentration (mg/L)***
Se^b	12.3	Rb^a	74.5
Sr^a	186.3	Y^d	99.0
Zr^a	771.3	Mo^b	731.3
Ru^d	463.8	$Co^{a,f}$	127.5
Pd^d	267.5	Ag^a	18.6
Cd^a	16.3	Sn^b	15.6
Sb^b	4.7	Te^b	102.8
Cs^a	543.8	Ba^a	308.8
$La^{d,e}$	263.8	Ce^a	532.5
Nd^c	862.5	Eu^c	22.6
Sm^c	163.8	Fe^b	500
Na^a	3000	Cr^a	100.0
Ni^a	100	$Mn^{a,g}$	181.3
U^a	20000	Tb^c	5.0
Pr^c	243.8	Dy^c	2.0
Gd^c	165.0		

[a]: Nitrate salt; [b]: Metal powder; [c]: Oxide; [d]: Chloride salt; [e]: Taken in place of Pm; [f]: Taken in place of Rh, and [g]: Taken in place of Tc.

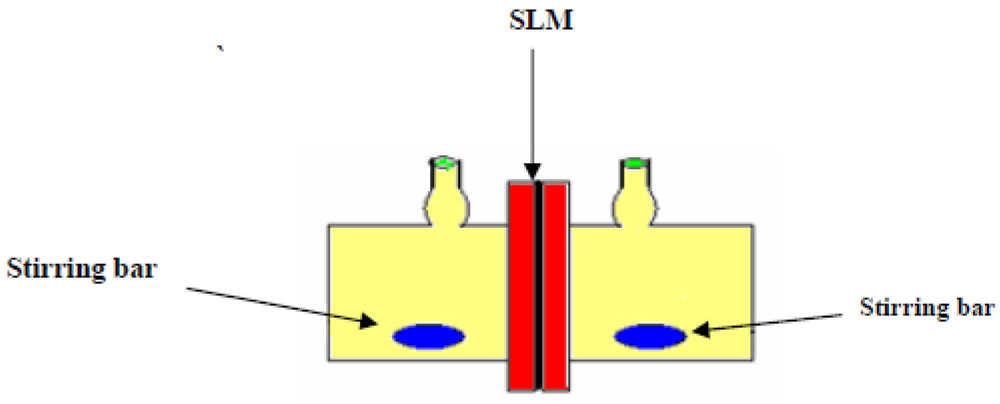

Fig. 2.3. A typical membrane transport cell used in the present studies

Subsequently, the submerged membranes were removed from the solution and wiped carefully with a tissue paper to clear it of the excess fluid at the outer surface of the support. This impregnation technique leads to SLMs which were reproducible within 5% with respect to their metal transport behaviour. The cumulative percentage transport (%T) of the metal ions at the given time was determined by the following equation,

$$\%T = \frac{100.([M]_o - [M]_t)}{[M]_o} \qquad (2.1)$$

where $[M]_t$ and $[M]_o$ are the concentration of the metal ions in the aqueous feed at the start of experiment (t =0) and at time t, respectively. The permeability coefficient, P is obtained experimentally using equation 1.14, P is related with the flux of the metal ions, J as follows:

$$P = \frac{J}{[M]_o} \tag{2.2}$$

where, $[M]_t$ and $[M]_o$ are the concentration of the metal ion in the aqueous feed solution at time t and its initial concentration (t = 0), respectively. Q is the effective membrane area obtained from the total exposed membrane surface area A and the porosity ε (Q = A·ε), V is the volume of the feed solution in cm^3. The exposed membrane surface area was measured from the number of square boxes of 1 mm × 1 mm size of a linear graph paper of the same surface area as that of the membrane. A plot of ln ($[M]_t$ / $[M]_o$) versus time allows calculating the P value from the slope of the linear fit. It should be noted that the above equation is valid only when the membrane is not saturated with the carrier. In the present work, since all the experiments were carried out at tracer metal concentration, Eq. (2.2) was applicable for the calculation of P.

2.3.3. Other equipments

Elemental (C, H, N) analysis was performed using an elemental analyzer EA 1110 from Carlo-Erba Instruments. The FT-IR spectra were recorded as thin film in IR spectrophotometer in the range 4000 – 400 cm^{-1}. The PMR spectra of the diglycolamide products were recorded in $CDCl_3$ medium using Bruker 200 MHz instrument employing TMS (tetramethyl silane) as an internal standard. Jasco V-530 UV-Spectrometer was employed for UV-Visible spectrophotometeric analysis.

Viscosity of the samples was determined using a digital viscometer from SVM 3000 Stabinger Viscometer (Antonpaar, Austria) at 25 ^{o}C.

2.4. Analytical Methods

The radio analytical techniques employed for the analysis of alpha emitting radionuclides were liquid scintillation counter, whereas NaI(Tl) scintillation counter and HPGe detector were used for the estimation of gamma emitting radionuclides. For the analysis U, Th and lanthanides, spectrophotometric as well as volumetric methods were followed.

2.4.1. Liquid Scintillation Counter

Liquid scintillation counter is the most widely used detector for the quantitative analysis of alpha emitters. Nearly 100% detection efficiency of this detector is of great advantage and even as low as few Bq of alpha activity can be assayed with good precision. A scintillator is a material that luminesces in a suitable wavelength region when ionizing radiation interacts with it. Interaction of the charged particles (alpha particles) with the scintillator results in emission of photons and the intensity of the emitted light is a quantitative measure of the incident radiation. The light emitted from scintillator is then collected by the photomultiplier tube (PMT) which produces signal representative of the primary radiation. In cases, where the scintillator emits photons in UV region, a wavelength shifter is added to the scintillator which has intermediate energy levels. In such cases the de-excitation takes place via these intermediate energy levels and hence the wavelength of the emitted photons is shifted from UV to visible region which is subsequently recorded in the PMT (as photo cathodes of most PMTs are compatible with visible light). The liquid scintillation counter is used to monitor gross alpha activity as it can not distinguish between alpha energies and thus can not be used for alpha spectrometry.

Many organic compounds are versatile scintillators for radiation measurements [9,10]. The liquid scintillation cocktail comprises of a solvent like dioxane or toluene, a scintillator like PPO (2,5-diphenyl oxazole) and a wavelength shifter such as POPOP (1,4-bis-2-(5-phenyl oxazolyl)-benzene). The solvent is the main stopping medium for radiation and must be chosen to give efficient energy transfer to the scintillating solute. In case of toluene based scintillator, a suitable extractant such as di(2-ethylhexyl) phosphoric acid (HD2EHP) is also added which facilitates the aqueous samples determinations by transferring the radionuclides from aqueous phase to the organic phase. In the present work, generally toluene based liquid scintillator was employed which consisted of 10 % (v/v) HD2EHP, 0.7 % (w/v) PPO and 0.03 % (w/v) POPOP. Suitable aliquots (25-100 μL) containing alpha activity were taken in glass vials containing liquid scintillator solution. When aqueous phase was added to the toluene scintillator, the two phases were mixed vigorously for ~2 min using an ultrasonic agitator to transfer the radionuclides into the organic phase. Each sample was counted for sufficient time so as to get more than 10,000 counts to restrict the statistical counting error to < ±1%.

2.4.2. NaI(Tl) Scintillation Counter

Sodium iodide activated with 0.1–0.2% of thallium, NaI(Tl), is by far the most widely used inorganic scintillator for the assay of gamma emitting radionuclides. Salient features of the detectors are the low cost, ease of operation and ruggedness [11,12]. The band gap in NaI crystal is of the order of 5-6 eV. When a charged particle (or gamma ray) falls on the detector its energy is used up either for excitation of electrons from the valence band to conduction band or for the ionization of atom. De-excitation of electrons from conduction band to valance band leads to the emission of photons in the UV region as the band gap is large. To shift the emitted photons in visible region, which is requisite of PMT, NaI crystal is doped with activator impurity like Tl which forms the intermediate level conduction band. The resolution of NaI(Tl) detector is about 7% at 662 keV.

In the present work, a 3” x 3” well type NaI(Tl) detector coupled with a multichannel analyzer has been used for gamma counting. Nearly 100 % detection efficiency for moderate energy photons in a well type NaI(Tl) detector offers great advantages for counting of low activity samples. A suitable aliquot (0.1 - 0.5 mL) of the desired analyte solution was taken in glass counting tubes which was then placed in the cavity of detector coupled with PMT and associated electronics. Each sample was counted for sufficient time so as to get more than 10,000 counts to restrict the statistical counting error within ±1%.

2.4.3. High Purity Germanium Detector

In the present work, high purity germanium (HPGe) detector coupled with multichannel analyzer was employed for gamma spectroscopy to check the radiochemical purity of the radionuclides. The HPGe detector is made up of exceptionally pure germanium in which the impurity level is around 10^{10} atoms/g. This is referred to as high purity germanium which approaches the theoretical pure semiconductor. HPGe is the most widely used semiconductor detector for gamma spectrometry and can be called as the workhorse of gamma ray spectroscopy. The high energy resolution (typically 1.9 keV at 1332 keV) is the key feature of this detector due to low energy band gap (0.7 eV). The great advantage of HPGe detector over Ge(Li) detector is that it can be stored at room temperature [13]. However, while operating it has to be cooled to liquid nitrogen temperature. The HPGe detectors are of two types, p-type and n-type. In case of p-type the outer surface of the germanium crystal is heavily doped with n-type impurity. As a result, the detection efficiency falls drastically below 100keV. On the other hand, n-type detectors are sensitive to wider range of photon energy. The n-type detector has added advantages in that it is more resistant to radiation damage in a neutron field as compared to a p-type detector.

2.4.4. Estimation of Uranium

2.4.4.1. Spectrophotometry

Uranium in the aqueous phase as well as in the organic phase could be determined by spectrophotometry using 2-(5-Bromo-2-pyridylazo)-5-(diethyl amino) phenol (Br-PADAP) as a chromogenic reagent [14]. Uranyl ion forms stable intense violet colored complex with Br-PADAP at pH 7-8 in the alcoholic medium buffered with triethanolamine (TEA) which shows absorption maxima at 575 nm with molar extinction coefficient of ~70,000. To a known volume of uranium solution in standard flask (10 mL), 1mL of complexing solution (1.25 g CDTA + 0.25 g NaF + 3.25 g sulphosalicylic acid dissolved in 100mL water adjusted to pH 7.8 with conc. NaOH), 1mL buffer solution (14 g TEA dissolved in 100 mL water adjusted to pH 7.8 with perchloric acid) and 0.8 mL Br-PADAP solution (50 mg Br-PADAP dissolve in 100 mL ethanol) were added, respectively. For organic samples the final volume (10 mL) was made up with ethanol. On the other hand, for aqueous samples the final volume (10 mL) was adjusted with distilled water after addition of 4mL of ethanol. The final absorption measurements were performed after 30min of colour development at 575 nm. This method was found to be very sensitive and no interference of Pu, Th, Al and Fe was observed. The calibration curve was plotted in the concentration range of $1x10^{-5}$ M to $1x10^{-6}$ M with standard uranium solution. The concentrations of unknown samples were determined from the calibration plot.

2.4.4.2. Davis- Gray Titration

Uranium in the concentration range 50-200 μg/mL was estimated volumetrically by the Davis-Gray method employing potentiometric end point detection [15,16]. The sample size was varied between 1-3 mL. This method involves the reduction of U(VI) to U(IV) by Fe(II) in the presence of concentrated phosphoric acid solution containing sulphamic acid. Then the excess Fe(II) is selectively oxidized by nitric acid in the presence of Mo(VI) which acts as a catalyst. The role of sulphamic acid is to destroy any trace of nitrous acid present in the solution which may oxidize Fe(II) and U(IV). The resulting U(IV) phosphate solution is then titrated with standard potassium dichromate solution to potentiometric end point. A small amount of vanadium(IV) sulphate is added in the solution which sharpens the end point. The concentration of uranium in the analyte solution is calculated from the volume of standard potassium dichromate solution consumed.

2.4.5. Estimation of Thorium

2.4.5.1. Spectrophotometry

Thorium in microgram quantities in aqueous samples could be determined by spectrophotometric method [17]. Thorium forms a red coloured complex with Arsenazo-III at 5-6 M acidity which shows absorption maxima at 665nm with a molar extinction coefficient of ~100,000. For sample preparation, a suitable aliquot of Th was taken in a standard flask (10 mL) followed by addition of 1 mL of 1 M sulphamic acid, 4 mL of concentrated nitric acid and 1 mL of 0.1% Arsenazo-III. The final volume was made up with distilled water and absorbance was recorded at 665 nm after waiting for 15 minutes after the colour development. The role of sulphamic acid is to remove any trace of nitrous acid which interferes in the method. The calibration plot was constructed by measuring the absorbance of standard solutions of thorium between the concentration ranges of 1x10^{-5} M to 1x10^{-6} M. The concentration of unknown analyte samples was determined from the calibration curve.

2.4.5.2. Complexometric Titration

When the concentration of thorium was in milligram quantities, the conventional complexometric titration was followed. A suitable aliquot of Th solution was titrated against standard EDTA (ethylenediamine tetra acetic acid) solution at pH 3 using xylenol orange as an indicator [18]. The end point of the reaction was the change in colour from deep purple to lemon yellow. The precision of these analyses was ± 2% (~5 mg Th). Similarly, the organic phase was also titrated with a precision of ± 5%. In the case of organic samples, the aliquot size was restricted to 0.5 mL.

2.5. REFERENCES

1. Y. Sasaki, Y. Sugo, S. Suzuki and S. Tachimori, *Solv. Extr. Ion Exch.*, 19 (2001) 91.
2. N. Srinivasan, M.N. Nadkarni, G.R. Balasubramanian, R.T. Chitnis and H.R. Siddiqui, BARC Report, Report-643, Bhabha Atomic Research Centre, Mumbai, India, (1972).
3. S.S. Rattan, A.V.R. Reddy, V.S. Mallapurkar, R.J. Singh and Satya Prakash, *J. Radioanal. Nucl. Chem.*, 67 (1981) 85.

4. P. Thakur, R. Veeraraghavan, P.K. Mohapatra, V.K. Manchanda and K.C. Dash, *Talanta*, 43 (1996) 1305.
5. D.E. Ryan and A.W. Wheelright, *Ind. Eng. Chem.,* 51 (1959) 60.
6. P.K. Mohapatra, *Ph. D. Thesis*, University of Bombay (1993).
7. G.Cousinou, M.Ganivet, Method of selective stripping of Plutonium from an organic solvent containing Plutonium and in some cases Uranium by reduction of said Plutonium, *US Patent*, 3980750 (1976).
8. P.R. Danesi, E.P. Horwitz and P.G. Rickert, *J. Phys. Chem.,* 87 (1983) 4708.
9. W.J. McDowell, "*Organic scintillators and liquid scintillation counting*", D.L. Horrocks, L.T. Peng (Eds.), Academic Press, Inc., New York (1971), 937.
10. H. Ihle, M. Karayannis and A. Murrenhoff, "*Organic scintillators and liquid scintillation counting*", D.L. Horrocks, L.T. Peng (Eds.), Academic Press, Inc., New York (1971), 879.
11. G.F. Knoll, *J. Radioanal. Nucl. Chem*., 243 (2000) 125.
12. D.D. Sood, A.V.R. Reddy and N. Ramamoorthy, "*Fundamentals of Radiochemistry*", 2nd ed., IANCAS publication, BARC, Mumbai (2004), 115.
13. G.F. Knoll, "*Radiation detection and measurement*", 3rd ed., John Willy and sons, New York (2000), 406.
14. W.J. Maeck, *Anal. Chem*., 31 (1955) 1130.
15. W. Davies and W. Gray, *Talanta*, 11 (1964) 1203.

16. F.P. Roberts, R. J. Brouns, K. R. Byers, J. E. Fager, B. W. Smith, K. L. Swinth (Eds.), NUREG/CR-3584, Method 3.0, 1984.
17. G.H. Jeffery, J. Bassett, J. Mendham and R. C. Denney (Eds.), "*Vogel's Textbook of Quantitative Analysis*", 5th ed., ELBS Longman Publishers, UK (1996), 329.
18. G.R. Balasubramanian, R.T. Chitnis, A. Ramanujam, M. Venkatesan, BARC Report, Report-940, Bhabha Atomic Research Centre, Mumbai, India, (1977).

Chapter III

TRANSPORT OF ACTINIDES ACROSS SUPPORTED LIQUID MEMBRANE CONTAINING N,N,N’,N’- TETRA OCTYL DIGLYCOLAMIDES (TODGA) AS THE CARRIER

3.1. Introduction

‘Actinide Partitioning’ involving separation of long lived minor actinides and lanthanides from the fission products and structural materials from High Level Liquid Waste (HLLW) has been proposed as a key step in the safe management of radioactive waste generated from the reprocessing of spent nuclear fuel [1-3]. It is not possible to use TBP, the work horse of fuel reprocessing, to carry out actinide partitioning without producing waste streams with high salt content. Thus, in recent years, it was needed to develop versatile reagents capable of extracting the actinides under the prevailing conditions of HLLW.

Completely incinerable substituted diamides have been the focus of numerous studies in the back end of the nuclear fuel cycle in recent years [4,5]. These extractants offer several advantages over organophosphorus compounds, especially with respect to (i) the innocuous nature of their degradation products, viz. carboxylic acids / amines; and (ii) the possibility of complete incineration of the spent solvent leading to reduced volume of the secondary waste volumes [6-8]. In addition, the physico-chemical properties of this class of ligands can be tuned by the judicious choice of alkyl groups. In the last decade, several investigations have been conducted on the modification of diamide structure in order to further improve its extracting properties. It has been observed that the introduction of etheric oxygen between the two amide groups of the malonamides (diglycolamide) causes significant enhancement in the extraction of trivalent actinides / lanthanides. Diglycolamide (DGA) was initially introduced by Stephan et al. [9,10] for the extraction of divalent and trivalent cations. Studies involving various DGA derivatives concerning fundamental as well as applied research have been reported extensively [11-15]. The physico-chemical properties of the DGAs can be changed by the attachment of different alkyl chains to N atoms. For example, DGA ligands with short alkyl groups ($-CH_3$, $-C_2H_5$) are water soluble and have been utilized as masking agent [16]. On the other hand, DGA molecules with long alkyl chains ($-C_8H_{17}$, $-C_{10}H_{21}$, $-C_{12}H_{25}$) can be dissolved in non-polar organic diluents and hence can be utilized in solvent extraction process for the separation of metal ions. Amongst several substituted diglycolamides studied for separation processes, recently developed *N*,*N*,*N′*,*N′*-tetraoctyl diglycolamide (TODGA, Fig. 3.1) has been identified as one of the most promising extractants for the partitioning of trivalent actinides and lanthanides from HLW solution [17-23].

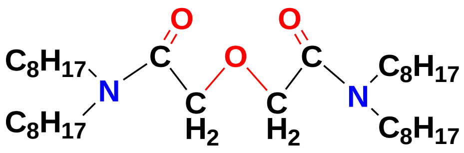

Fig. 3.1. N,N,N’,N’-Tetra octyl diglycolamide (TODGA)

Chapter III

Though solvent extraction processes using TODGA as the extractant have been proposed for ‘actinide partitioning’, they suffer from various drawbacks like (a) generation of large volume of secondary waste (b) third phase formation (c) large solvent inventory (d) phase disengagement difficulties, etc. Now-a-days, membrane technology has gained considerable importance worldwide due to various advantages [24,25]. Supported Liquid Membrane (SLM) based separation methods have gained considerable importance for various applications.

SLM transport of various metal ions [26-40] has been reviewed by various authors. TODGA based supported liquid membrane transport studies of actinides and lanthanides and fission products have been reported in various literature reports [41,42]. The present Chapter describes membrane transport properties of various actinides from nitric acid medium using TODGA as the carrier molecule.

3.2. Transport of Plutonium

3.2.1. Introduction

The HLLW solution contains significant amount of plutonium due to losses from the PUREX process. Due to its strategic nature, it is required to recover it quantitatively. In High Level Waste (HLW) solution Pu is expected around 10-15 mg/L along with the other actinides depending on the efficiency of PUREX process [52]. At the acidity generally encountered in HLW major concentration of Pu is expected to be in +4 oxidation state. However, in view of significantly higher extraction of trivalent actinide ions as compared to the tetravalent actinides ions [44] with TODGA, it was required to convert plutonium to the +3 oxidation state and investigate its extraction and transport behavior and compare with those of Am^{3+}.Zhu et al. [47] reported unusually high extraction, with TODGA, of metal ions with ionic radii close to 1.0 Å. Distribution coefficient values for trivalent actinides such as Am^{3+} (ionic radius: 1.06 Å) were reported to be much larger compared to those for Pu^{4+} (ionic radius: 0.96 Å) for comparable feed acidity [44,48]. Though the extraction behaviour of trivalent actinides was thoroughly investigated, using TODGA as the extractant [49-51], that of tetravalent actinides, other than Th^{4+}, is not well studied. Therefore, it is also required to understand the extraction behaviour of Pu^{4+} using TODGA under acidic feed conditions.

The present work deals with the transport behavior of Pu^{3+} and Pu^{4+} from HNO_3 feed solutions under varying experimental conditions. Solvent extraction studies were carried out to optimize the conditions for extraction as well as stripping while the transport studies were carried out at varying experimental conditions such as, feed nitric acid concentration, TODGA concentration, effect of nature of strippant, plutonium concentration, etc. Attempt was made to predict the mechanism of transport and diffusion coefficient for the permeating species was calculated.

3.2.2. Trivalent Plutonium

3.2.2.1. Solvent Extraction Studies

3.2.2.1.1. Effect of the Nature of the Reducing Agent on Pu(III) Extraction

Pu has the unique property of simultaneously existing in +3, +4, +5, and +6 oxidation states at the same time (43). Therefore, the chemistry of plutonium is challenging and requires special care such as finding appropriate conditions for stabilization of a particular oxidation state. It is important to note here that the extraction of trivalent actinides is much higher than the tetra- and hexa-valent actinide ions when TODGA is used as the extractant (44,45). This trend is entirely opposite of that observed with other extractants such as CMPO and tetra-alkyl malonamides such as DMDOHEMA or DMDBTDMA. Therefore, Pu can be more efficiently extracted by TODGA if present in the +3 state.

Various reducing agents like ascorbic acid (AA), hydroxyl ammonium nitrate (HAN), phenyl hydrazine (PH), and hydrazinium nitrate (HN) were evaluated for the conversion of Pu to Pu^{3+}. As indicated from the solvent extraction data (Table 3.1), ascorbic acid and phenyl hydrazine were more efficient reducing agent as the $D_{Pu(III)}$ value was the highest using this reducing agent (under no condition $D_{Pu(III)}$ value greater than 100 was obtained). It is also evident from Table 3.1 that the concentration of the reducing agents also played an important role in determining the extent of conversion of Pu to Pu^{3+} (as indicated by the $D_{Pu(III)}$ using 0.1 M TODGA/*n*-dodecane). This is due to the fact that the reduction of Pu is not stoichiometric due to the role of nitrous acid which plays a role of oxidizing agent (45). With increasing concentration of the reducing agent, quantitative reduction of Pu (from predominantly in the +4 state) to Pu^{3+} was possible which caused an increase in the $D_{Pu(III)}$ value with TODGA. The optimum concentration of the reducing agents, in the concentration range of Pu studied, was found to be 0.1 M, as further increase in the reducing agent concentration does not increase the distribution ratio further. Out of the four reducing agents used, phenyl hydrazine (PH) was found to be the most efficient and was used in the subsequent studies. Though AA was found to be marginally inferior to PH as a reductant, and is a more benign chemical that the latter, it was not subsequently used due to its instability in acidic medium. Complete conversion of Pu to its +3 state in the presence of 0.1 M PH was confirmed by spectrophotometry (Fig. 3.1) where the bands characteristic of Pu^{4+} are suppressed to a large extent and those belonging to Pu^{3+} appeared prominently. Earlier reports also indicate facile reduction of Pu^{4+} to Pu^{3+} using hydrazine as the reducing agent (45,53). The conversion was further checked by carrying out solvent extraction studies of the reduced Pu^{3+} species using 30% TBP/dodecane and comparing the $D_{Pu(III)}$ values with that reported in literature.

3.2.2.1.2. Nature of the extracted species

On the basis of the literature report on actinide extraction using TODGA, the extraction equilibrium involving Pu^{3+} can be conveniently written as:

$$Pu^{3+} + 3NO_3^- + n\,TODGA \rightleftharpoons Pu(NO_3)_3.nTODGA \qquad (3.1)$$

The value of n was determined by plotting log D vs log TODGA concentration at 3

Table 3.1. Solvent extraction data of Pu^{3+} using 0.1 M TODGA in n-dodecane in the presence of various reducing agents at 3 M HNO_3

Reducing agent	$D_{Pu(III)}$ at varying reducing agent concentration	
	0.01 M	0.1 M
Ascorbic acid	78	95
Hydroxyl ammonium nitrate	64	93
Hydrazinium nitrate	75	91
Phenyl hydrazine	79	96

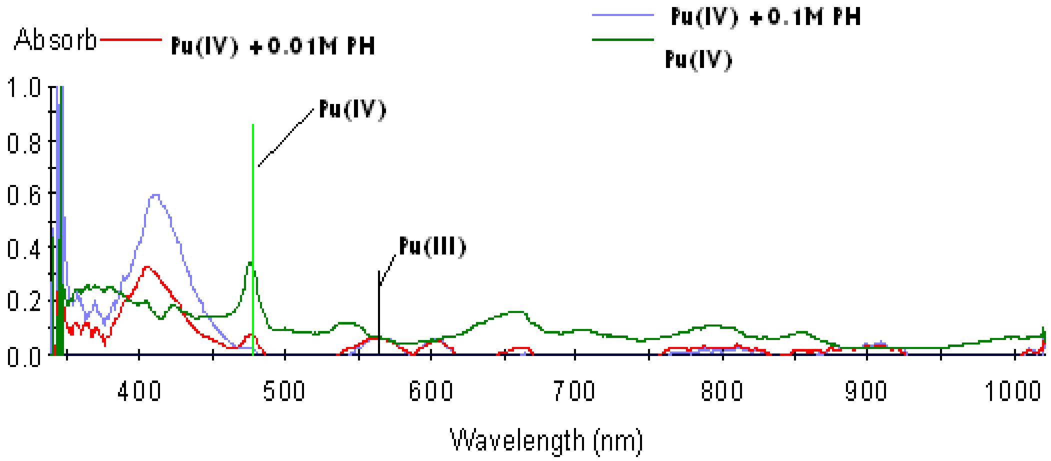

Fig. 3.2. UV-Visible spectra of Pu in the absence of reducing agent (green line), in the presence of 0.01 M phenyl hydrazine (red line) and in the presence of 0.1 M phenyl hydrazine (blue line)

M HNO_3 and the value was found to be ~4 (Fig. 3.3). To our knowledge, there is no data available in the literature on the extraction behaviour of Pu^{3+} using TODGA as the extractant. However, analogous extracted species was reported for Am^{3+} in an earlier report [44].

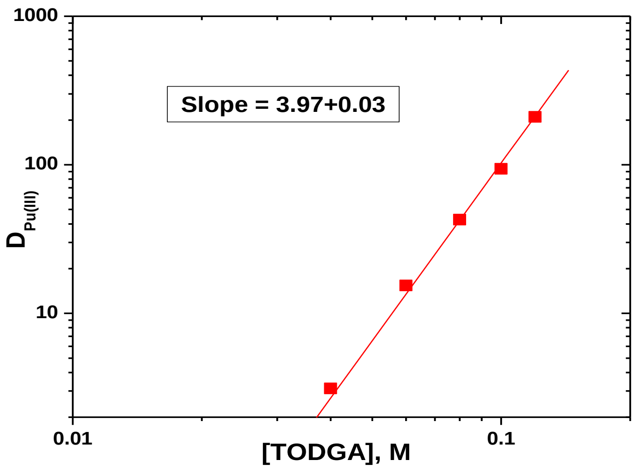

Fig. 3.3. Dependence of $D_{Pu(III)}$ on TODGA concentration. Aqueous phase acidity: 3 M HNO_3

3.2.2.2. Transport Studies

The transport studies were carried out using Pu which was previously reduced to the +3 state. Usually, 0.1 M HNO_3 was used as the strippant in the receiver phase in order to rule out the possibility of hydrolysis.

3.2.2.2.1. Effect of reducing agent on Pu(III) transport

As evident from the solvent extraction studies, choice of reducing agent should also play an important role in the transport of Pu^{3+}. Various reducing agents (at an effective concentration of 0.1 M) were used to study the transport of Pu^{3+} from 3 M HNO_3 into 0.1 M HNO_3 where 0.1 M TODGA/*n*-dodecane was chosen as the carrier extractant. Similar to the solvent extraction data presented above, Fig. 3.4 indicated that phenyl hydrazine (PH) facilitated quantitative transport of Pu(III) after about 180 minutes which was similar to that observed earlier for Am^{3+} [41]. Though ascorbic acid (AA) gave the comparable D value (Table 3.1), transport rate was found to be quite slow (~86% transport was observed in 6 h). This could be due to the poor stability of AA in the nitric acid medium. To improve its stability, *tert*-butyl hydroquinone (TBH), an organic reducing agent [43], was added in the carrier phase and the transport of Pu(III) was followed using AA as the reducing agent. Though the transport rate was found to increase it was slower than PH. Therefore, 0.1 M PH was chosen as the reducing agent in the subsequent transport studies involving Pu^{3+}. The permeability coefficients for different feed conditions (with different reducing agents) were calculated and are listed in Table 3.2.

The transport rate of Pu^{3+} was compared with those obtained for Am^{3+} (in the present study) and Th^{4+} (54). As shown in Table 3.3, the transport rates for Pu^{3+} were closer to those observed for Am^{3+} than those of Th^{4+}. This confirms near complete conversion of Pu to the +3 oxidation state. The relatively slow transport in case of Pu^{3+}

is due to lower $D_{Pu(III)}$ (96) as compared to $D_{Am(III)}$ (297 [44]) at 0.1 M TODGA for a feed acidity of 3 M HNO_3. As already mentioned, the presence of Pu^{3+} in the extracted species was further confirmed by UV-Visible Spectrophotometry (Fig.3.1) and solvent extraction studies.

Table 3.2: Permeability coefficient (P, cm/s) data of Pu^{3+} - TODGA transport system for various strippants and reducing agents

Extraction system		**Stripping system**	
Reducing agent[a]	$P_{Pu(III)}x10^3$	Strippant[b]	$P_{Pu(III)}x10^3$
Ascorbic acid	1.34±0.17	0.1 M HNO_3	3.26±0.04
Phenyl hydrazine	3.26±0.04	Distilled water	2.24±0.01
Hydrazinium nitrate	2.05±0.07	0.1 M oxalic acid	1.64±0.02
Hydroxyl ammonium nitrate	2.17±0.11	Buffer mixture	1.78±0.01
Ascorbic acid + *tert*-butyl hydroquinone	1.74±0.10	-	-

Note: [a]: Strippant: 0.1 M HNO_3; [b]: Reducing agent: Phenyl hydrazine

3.2.2.2.2. The effect of TODGA concentration:

The effect of TODGA concentration on the transport of Pu(III) was studied at four different extractant concentrations (0.05 – 0.2 M) using 0.1 M PH as the reducing agent in the feed phase (3 M HNO_3) while 0.1 M HNO_3 was used as the receiver phase. As

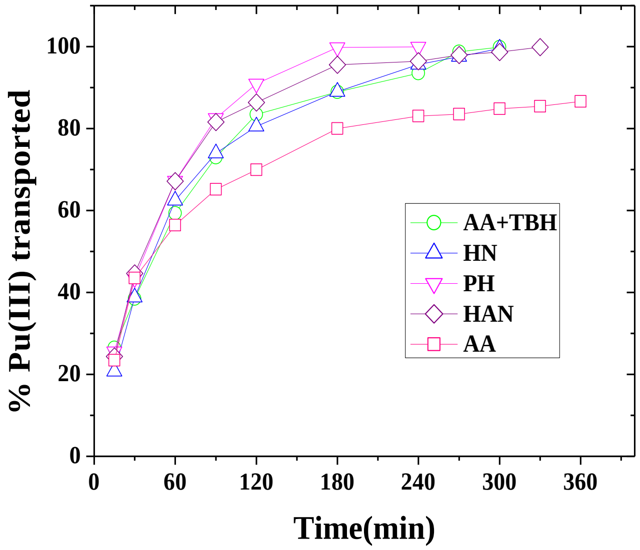

Fig. 3.4. Effect of the nature of the strippant on the transport of Pu^{3+}. Carrier: 0.1 M TODGA/ *n*-dodecane; Feed phase: 3.0 M HNO_3; Receiver phase: 0.1 M HNO_3

evident from Fig. 3.5, the transport rate increased up to 0.1 M and decreased thereafter. Using 0.1 M TODGA / *n*-dodecane as the carrier extractant, quantitative Pu^{3+}transport was observed at about 3 h which was comparable to that reported earlier for Am(III) [41]. Further increase in TODGA concentration was found to decrease the transport rate which was attributed to an increase in the viscosity of the carrier in the membrane phase. This increased viscosity of the carrier creates a hindrance to the diffusivity of the complex which causes a decrease in the transport rate. The viscosity effect can be explained by the Stokes-Einstein equation:

$$D_0 = \frac{\kappa T}{6\pi\eta R} \tag{3.2}$$

Table 3.3. Comparison of plutonium transport data with those reported with Am^{3+} and Th^{4+} with TODGA as the carrier extractant. Strippant: Distilled water

Time (minutes)	% Metal ion transported		
	Am (present work)	Th^{4+} [54]	Pu (present work)
15	34.5	8.53	27.3
30	57.0	18.1	45.5
60	81.8	31.8	64.2
120	93.6	53.1	83.5
180	99.3	66.6	94.2

Where D_o is the diffusion co-efficient of the extracted complex in the membrane phase, k, the Boltzman constant, T, absolute temperature, R, the radius of the diffusing species and η, the dynamic viscosity of the carrier solution. The dependence of the permeability coefficient (P) values on viscosity is shown in Table 3.4.

3.2.2.2.3. The Effect of the Feed Acidity

As indicated by eqn. (3.1), the extraction of Pu^{3+} is influenced not only by TODGA concentration, but also by the concentration of nitrate ion. We have reported earlier that

Table 3.4. Permeability coefficient (P, cm/s) data of Pu^{3+} - TODGA transport system at varying TODGA and nitric acid concentrations

$[HNO_3]$, M	**$P_{Pu(III)}x10^{3,a}$**	**[TODGA], M**	**$P_{Pu(III)}x10^{3,b}$**	**Viscosity (mPa.S)**
0.5	0.61±0.07	0.05	2.44±0.08	1.539
1.0	1.06±0.12	0.10	3.26±0.04	1.641
3.0	3.26±0.04	0.15	2.40±0.15	1.860
6.0	1.19±0.04 (1.38±0.06)[c]	0.20	2.54±0.08	2.012

Note: [a]: [TODGA] = 0.1 M; [b]: $[HNO_3]$ = 1.0 M; [c]: Values in parenthesis indicates data generated in the presence of *tert*-butyl hydroquinone

though increasing the nitrate ion concentration should increase the metal ion extraction at the feed-membrane interface, nitric acid facilitates higher mass transfer as compared to $NaNO_3$ [41]. Therefore, the feed nitric acid concentration was varied and the transport rates of Pu^{3+} were measured. We reported that the transport rate did not follow the same trend for all the actinides using TODGA as carrier with different feed acidity. For Am^{3+} [41] and Th^{4+} [54] the transport rate was found to increase up to 3 M HNO_3 and then decreased thereafter. On the other hand, UO_2^{2+} transport increased with increasing feed acidity up to 3 M and remained constant thereafter up to 6 M [55]. The transport of Pu^{3+} with different feed acidities using 0.1 M PH as the reducing agent was

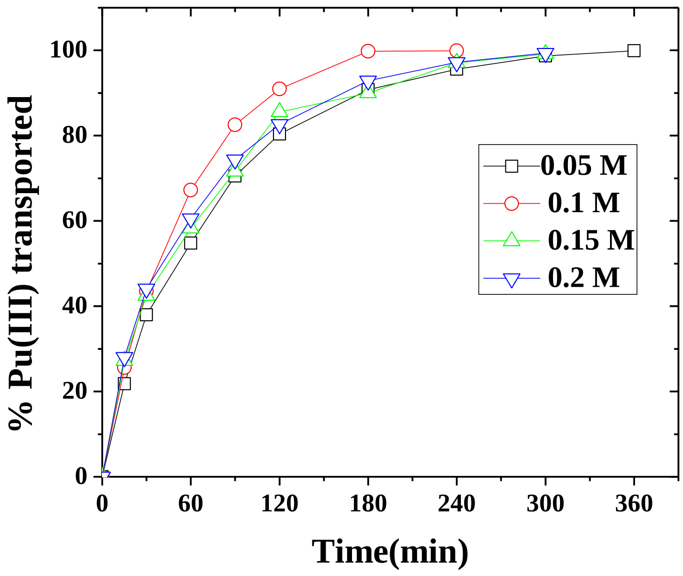

Fig. 3.5. Effect of TODGA concentration on the transport of Pu^{3+}. Feed: 3.0 M HNO_3; Receiver: 0.1 M HNO_3

monitored as a function of time. The results (Fig. 3.6) indicated that the transport rate of Pu^{3+} increased from 0.5 M HNO_3 up to 3 M HNO_3 and decreased thereafter up to 6 M HNO_3 which is similar to our observation with Am^{3+} and Th^{4+}. We also observed near quantitative transport (~99%) for Pu^{3+} at about 180 min for 3 M HNO_3 acidity. The permeability coefficients at various feed acidities are also listed in Table 3.4.

The receiver phase acidity was found to increase from 0.1 M to 0.4 M HNO_3 after 360 minutes of operation when 6 M nitric acid was used as the feed. It is well known that with increasing nitric acid concentration, the possibility of conversion of Pu^{3+} to Pu^{4+} increases due to the stabilization of the +4 state in higher complexing media provided by 6 M HNO_3 (43). These two effects are likely to decrease the transport rate of Pu from the feed at 6 M HNO_3. To check whether this decrease is due to oxidation of Pu^{3+} to Pu^{4+} at higher acidity, *tert*-butyl hydroquinone (TBH) was added to the organic phase to maintain Pu in the +3 state and the transport rate was followed for 6 M HNO_3. The trend was observed to be the same in the presence and in the absence of TBH which conclusively proved that the decrease in transport rate was due to increase in strip phase acidity and not due to oxidation of Pu^{3+} to Pu^{4+}.

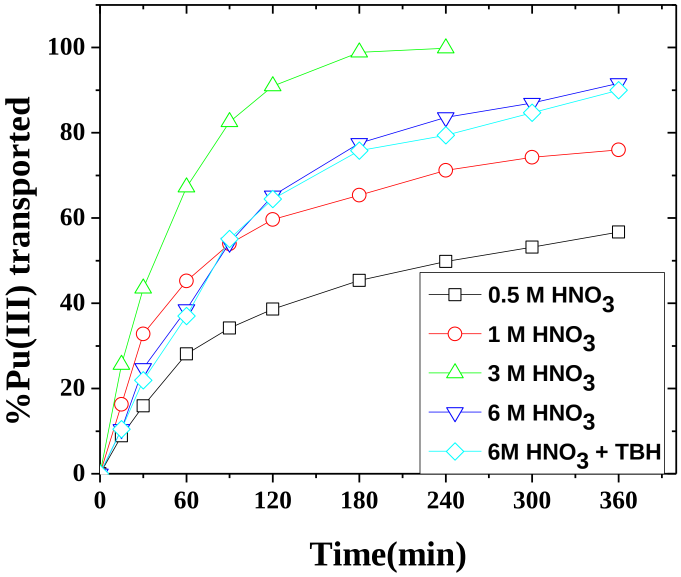

Fig.3.6. Effect of feed acid concentration on the transport of Pu^{3+}. Receiver: 0.1 M HNO_3; Carrier extractant: 0.1 M TODGA

3.2.2.2.4. Effect of the Nature of the Strippant

In SLM transport studies, effective transport means efficient extraction, rapid diffusion of the extracted complex, and efficient stripping. Therefore, the distribution co-efficient of the metal ion in the receiver compartment should be as low as possible to achieve efficient stripping. For this purpose, the strippant should be of low acidity (as per Eq. (3.1)) or should consist of metal complexing solution. Transport of Pu(III) was studied using various strippants such as 0.1 M HNO_3, distilled water, 0.1 M oxalic acid, and a buffer mixture (consisting of 0.4 M hydrazine hydrate, 0.4 M formic acid and 0.1 M citric acid) from 3 M HNO_3 which contained 0.1 M phenyl hydrazine as the reducing agent and the transport and permeability data are presented in Fig. 3.7 and Table 3.2, respectively. Among these strippants 0.1 M HNO_3 gave near quantitative transport after about 180 minutes which was about the same time taken for the quantitative transport of Am^{3+} in an earlier report (41).

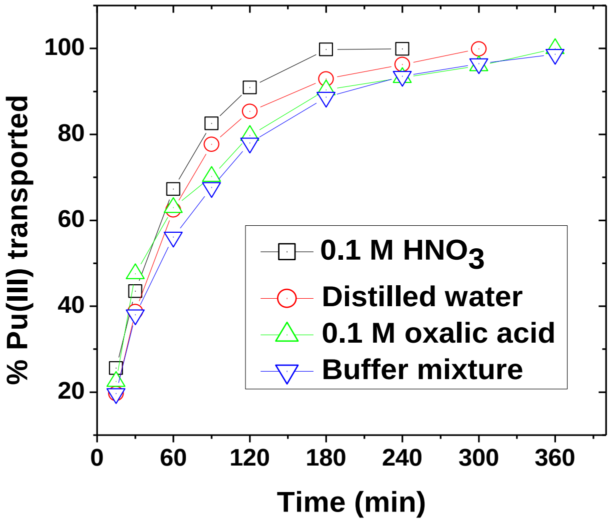

Fig. 3.7. Effect of nature of strippant on the transport of Pu^{3+}. Feed: 3.0 M HNO_3; Carrier extractant: 0.1 M TODGA

3.2.2.2.5. Effect of Pu Concentration in Feed

Increasing the concentration of Pu(III) would increase the flux of Pu as indicated by transport equation. But due to the limitation of amount of carrier in the membrane phase the transport rate as well as the permeability coefficient was found to decrease with increasing the metal ion concentration in the feed phase. Effect of increasing Pu(III) concentration on the transport as well as flux of Pu(III) was investigated in the concentration range of 5-50 mg/L. It was found that the transport rate decreased with increasing Pu concentration which is expected due to limited carrier concentration. Therefore, when the flux was plotted against Pu concentration (Fig. 3.8) it was found to increase initially which subsequently saturated. We found ~ 90 % transport in around 360 minutes even for 50 mg/L Pu. Therefore, effective transport of Pu can be achieved even for 50 mg/L concentration when the oxidation state can be adjusted to +3. The values of permeability coefficients for different Pu concentration are listed in Table 3.5

3.2.2.2.6. Membrane Stability

The stability is one of the major concerns of this membrane based technique which limits its application. Kemperman et al. (56) reported various factors that affected the stability of the liquid membrane. We, on the other hand, reported that the stability is mainly dependent on the diluent properties and were found to be reasonably good in cases where *n*-dodecane was used as the diluent (55). To corroborate, the membrane

Table 3.5. Permeability coefficients as a function of the Pu concentration in the feed

Pu Concentration (mg/L)	P x10^3 (cm/s)	Flux × 10^7(moles/cm^2/s)
Tracer	3.26±0.04	-
4	3.18±0.07	0.53
12	2.08±0.06	1.04
24	1.44±0.02	1.45
48	0.96±0.03	1.93

stability was investigated by continuously operating the same supported liquid membrane transport system using 0.2 micron PTFE filters for 20 days. Feed and strip solutions used in this studies were 3 M HNO_3 (containing 0.1 M PH as the holding reductant) and 0.1 M HNO_3, respectively. The data (Fig. 3.9) indicated slight decrease in the transport rate over the entire period of time which is probably due to partial oxidation of Pu(III) to Pu(IV). However, the mean value of P was 3.1×10^{-3} cm/s which indicated no significant decrease in the transport rates. These observations thus led us to the conclusion that the loss of liquid membrane phase (carrier and/or solvent) out of the membrane phase was insignificant under the experimental conditions. Thus SLM

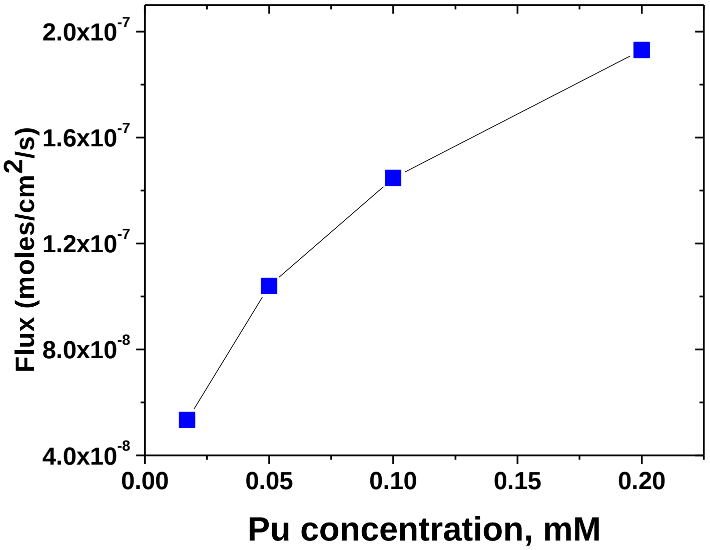

Fig. 3.8. Effect of Pu concentration on Pu^{3+} flux. Feed: 3.0 M HNO_3; Receiver: 0.1 M HNO_3; Carrier: 0.1 M TODGA

containing TODGA can be used for the recovery of Pu (preferably in the +3 oxidation state) from acidic waste solutions including HLW.

3.2.3. Tetravalent Plutonium

3.2.3.1. Solvent Extraction Studies

Major difficulty in the studies involving plutonium ions is maintaining the oxidation states. In the present study, Pu^{4+} was maintained using $NaNO_2$ as the holding oxidant. 0.03 M $NaNO_2$ was found to be the optimum concentration of the holding oxidant as indicated in Table 3.6. The complete conversion of plutonium to the +4

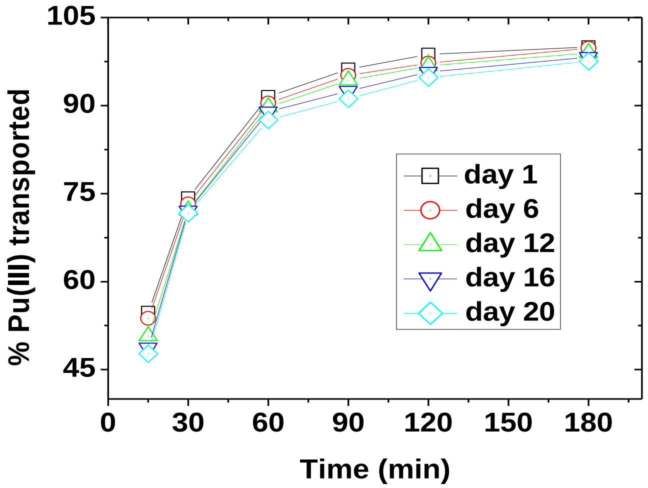

Fig. 3.9. Successive transport experiments for the stability evaluation of the SLM; Feed: 3.0 M HNO_3; Membrane: 0.2 µm PTFE; Carrier, 0.1 M TODGA in *n*-dodecane; Receiver phase: 0.1 M HNO_3

oxidation state was confirmed by spectrophotometry. As shown in Fig. 3.10, the prominent peak at 470 nm is indicative of the presence of Pu^{4+} while those characteristic of Pu^{3+} (550, 590 nm) are not seen. It was safe to assume that Pu did not exist as PuO_2^{2+} under the given experimental conditions [43,45]. It was also important that the oxidation state did not change with time in the presence of the holding oxidant. In order to distinguish the ionic species, the D_{Pu} values obtained with 0.1 M TODGA with different oxidation states are listed in Table 3.7. The effect of the holding oxidant / reductant is also indicated immediately after carrying out the extraction and determining the D_{Pu} values again after 24 hours. The efficiency of the holding oxidants is clearly

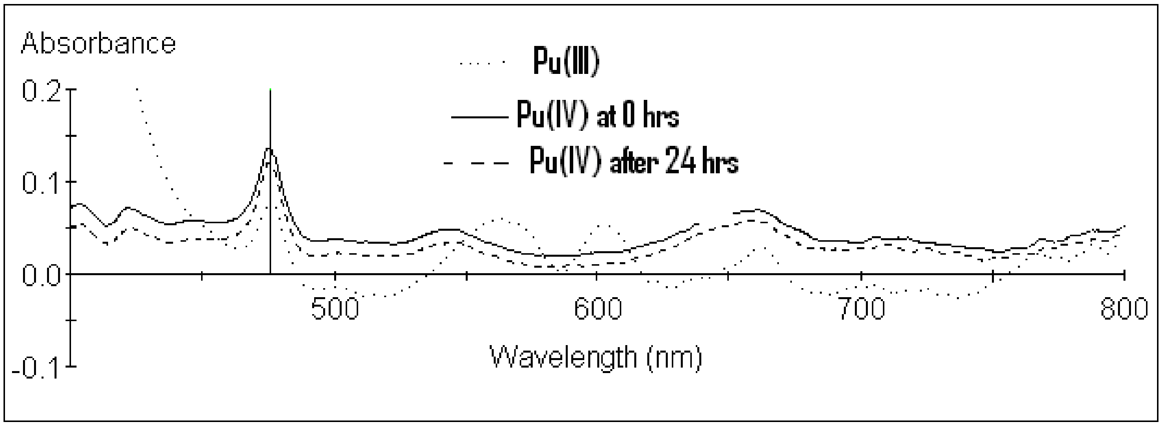

Fig. 3.10. UV-visible spectra of plutonium under varying redox conditions

Table 3.6. $D_{Pu(IV)}$ values in presence of varying concentration of holding oxidant ($NaNO_2$) using 0.1 M TODGA as extractant from 3 M HNO_3 medium

$[NaNO_2]$,M	$D_{Pu(IV)}$
0.01	21.34 ± 1.68
0.03	10.54 ± 1.35
0.06	10.58 ± 1.42

demonstrated in the table. The stripping data is also included in Table 3.7 and it is clear that quantitative stripping of Pu^{4+} was possible using 0.1 M oxalic acid. The extraction and stripping kinetics is presented in Fig. 3.11 and it is clear from the data that both the steps are fast and takes about 10 minutes to attain equilibrium.

The two phase extraction equilibrium involving Pu^{4+} can be represented by the following extraction equilibrium.

$$Pu^{4+} + 4\,NO_3^- + nTODGA_{(o)} \rightleftharpoons Pu(NO_3)_4\cdot nTODGA_{(o)} \qquad (3.3)$$

where, the subscript (o) represent species in the organic phase, while those without any subscript refer to species in the aqueous phase. The log-log plot of $D_{Pu(IV)}$ vs TODGA concentration at fixed acidity of 3 M HNO_3 (Fig. 3.12) suggested that the number of TODGA molecules associated with the extracted species of Pu^{4+} was 3 which is in agreement with the results reported in the literature [47]. However, this is in sharp contrast to the species of the type $Pu(NO_3)_3\cdot 4TODGA_{(o)}$ extracted with Pu^{3+}. This was, probably, the reason for the lower extraction of Pu^{4+} as compared to Pu^{3+} [57].

Table 3.7: Distribution data for Pu^{3+}, Pu^{4+} and PuO_2^{2+} with 0.1 M TODGA in *n*-dodecane with 3 M HNO_3 as the feed and 0.1 M HNO_3 as the strippant

Ionic species of Pu	D_{Pu} (extraction)		D_{Pu} (stripping)
	Immediate	After 24 h	
Pu^{3+}	95 ± 1.35	96 ± 1.54	0.01
Pu^{4+}	10.59 ± 1.02	10.61 ± 1.10	0.04
PuO_2^{2+}	1.64 ± 0.13	1.70 ± 0.18	0.04

Note: 0.1 M Phenyl Hydrazine was the holding reductant for Pu(III), 0.03 M $NaNO_2$ was holding oxidant for Pu(IV) and 0.1 M AgO was the oxidizing agent for Pu(VI)

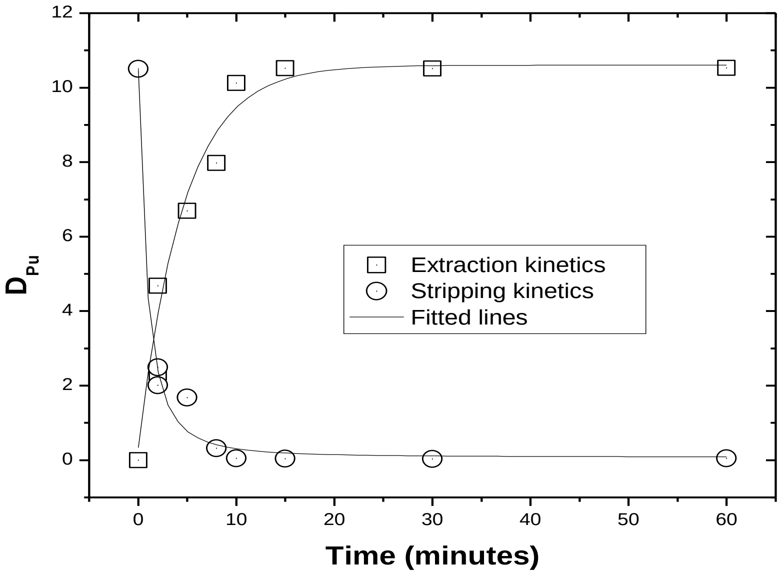

Fig. 3.11: Extraction and stripping kinetics studies for Pu^{4+}. Organic phase: 0.1 M TODGA in *n*-dodecane. Aqueous phase for extraction: 3 M HNO_3; Strippant: 0.1 M oxalic acid

3.2.3.2. Transport Studies

3.2.3.2.1. Effect of the feed acidity

The feed acidity can affect the transport rate in more than one ways. As indicated in eqn. (3.3), the extraction of Pu^{4+} is dependent on the acidity of the feed phase. The transport rate depends on the concentration of Pu^{4+} in the membrane-feed interface and hence any mechanism which enhances Pu^{4+} concentration (such as extraction) is bound to facilitate Pu^{4+} transport. The effect of nitric acid concentration on the Pu^{4+} transport rates is depicted in Fig. 3.13. It is clearly seen from the figure that the

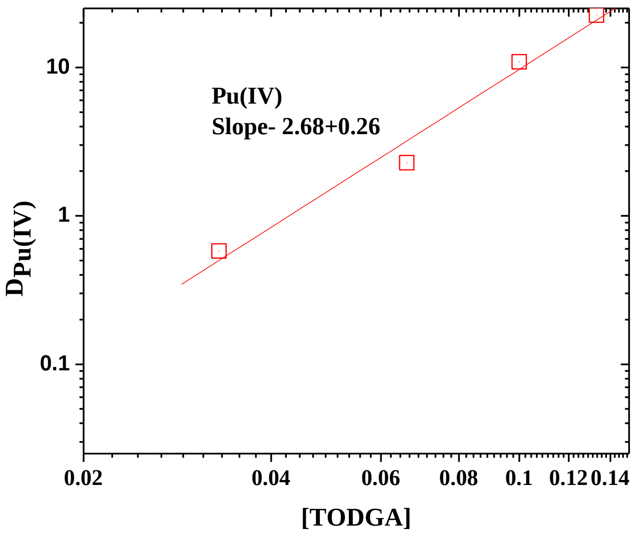

Fig. 3.12. Dependence of D_{Pu} on TODGA concentration. Aqueous phase acidity: 3 M HNO_3

transport rates increased with increasing feed acidity. Maximum transport of ~ 99.5% was observed for Pu^{4+} at feed acidity of 6 M in 6 h. During the same time period, the % T values are 91.7, 94.9 and 97.3 for 0.5 M, 1.0 M and 3.0 M nitric acid as the feed, respectively. These results are in variance with those reported with Th^{4+} and the trivalent actinides, viz. Pu^{3+} and Am^{3+} [54,57,58]. In general, though increase in the transport rates was expected with increasing acidities in the lower acidity range (up to 3-4 M HNO_3), at 6 M HNO_3 a decrease in transport rates was observed due to acid transport. The acid transport data for the present case is presented in Table 3.8 which clearly shows marginal difference in the acid co-transport with 6 M HNO_3 vis-à-vis 3 M

Table 3.8: Transport of nitric acid from the feed to the receiver phase as indicated by the feed phase acidity. [TODGA] = 0.1 M; Receiver: 0.1 M oxalic acid

Sampling time (minutes)	Feed phase HNO_3 concentration	
	3 M	**6 M**
30	3.0	6.0
60	3.0	6.0
90	3.0	6.0
120	3.0	5.92
180	2.95	5.90
240	2.86	5.84
300	2.80	5.74
360	2.75	5.65

HNO_3 as the feed solution. It appears that, the effect of acid co-transport, which retards the transport rates, is insignificant and is effectively countered by the higher distribution coefficients of Pu^{4+} as compared to Th^{4+}, thereby leading to an increase in the transport efficiency at 6 M HNO_3 for Pu^{4+} as compared to Th^{4+}. The permeability coefficient (P) values were also calculated and are listed in Table 3.9. The P values followed the same trend as shown in the transport profiles (Fig. 3.13) and also the D_{Pu} values.

Table 3.9: Permeability data of Pu^{4+} using TODGA as the carrier extractant

$[HNO_3]$, M[a]	P $\times 10^3$(cm/s)	[TODGA], M[b]	P $\times 10^3$(cm/s)
0.5	1.32±0.04	0.05	1.46±0.05
1.0	1.57±0.07	0.10	2.11±0.04
3.0	2.11±0.04	0.15	0.95±0.05
6.0	2.98±0.36	0.20	0.88±0.07

Note: [a]: [TODGA] = 0.1 M; [b]: $[HNO_3]$ = 3.0 M

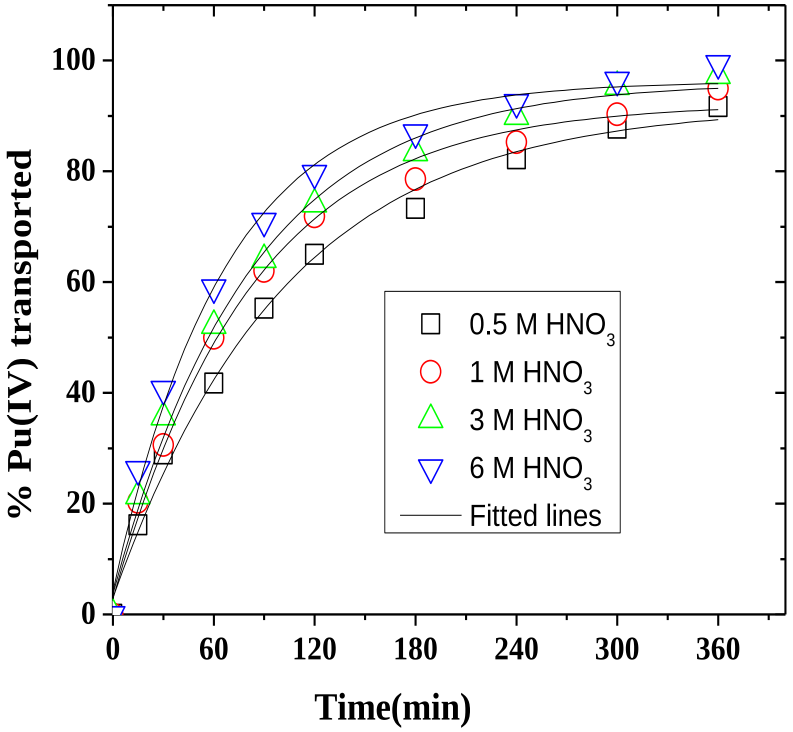

Fig. 3.13. Effect of feed phase acid concentration on the transport of Pu^{4+}. Receiver: 0.1 M oxalic acid; Carrier extractant: 0.1 M TODGA in *n*-dodecane

3.2.3.2.2. Effect of the carrier concentration

The role of the carrier extractant is extremely important in the transport of the metal ion in SLM studies. As indicated by the extraction equilibrium above (eqn. (3.3)), the transport rate is expected to increase with increasing carrier concentration. The effect of TODGA concentration on Pu^{4+} transport rates is presented in Fig. 3.14. It was observed that though the material balance was within $\pm$5% for 0.05 M and 0.1 M TODGA, deviations as high as -12% (in case of some data points) were seen for 0.15 M and 0.2 M TODGA. The permeability coefficients were calculated from the Pu concentration in the feed compartment and are listed in Table 3.9. An initial increase in the P value (at 0.1 M TODGA) followed by a sharp decrease is ascribed to the viscosity effect as per the Stoke's-Einstein equation (Eqn.3.2) A plot of P vs TODGA concentration is given in Fig. 3.15. The behavior is similar to that reported for Pu^{3+} transport with the exception that the peak value of P was obtained at 0.15 M in case of the latter transport system. For the tetravalent thorium also, maximum transport was observed at 0.15 M TODGA [54]. Though exact reason for this anomalous behaviour is not understood, reduction to the +3 oxidation state is ruled out as that would have led to higher transport rates [41,57].

3.2.3.2.3. Calculation of diffusion parameters

The permeability coefficient depends on the distribution coefficients (D_{Pu}) as per the following equation:

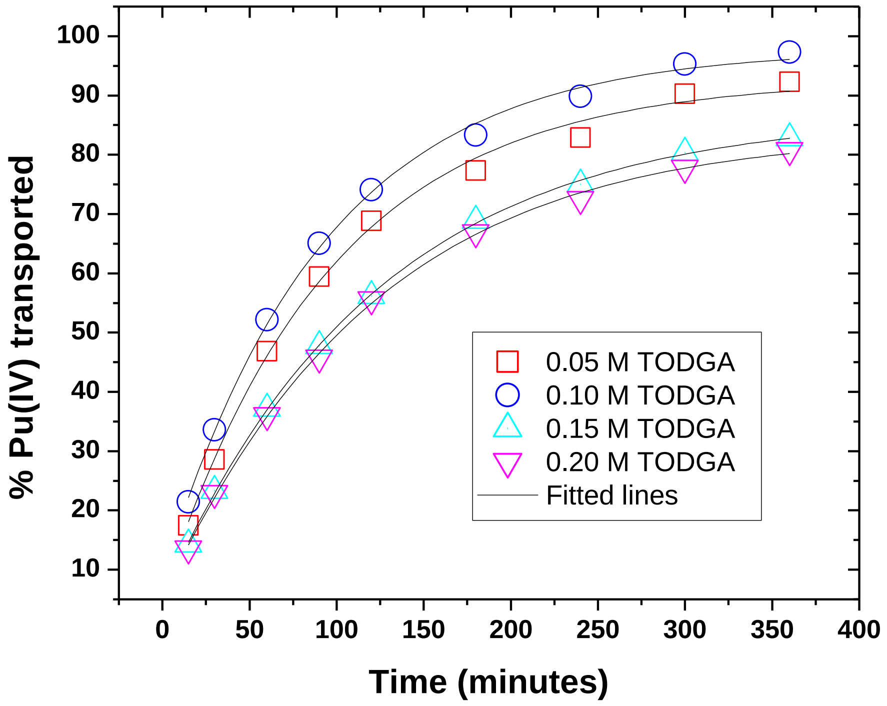

Fig. 3.14. Effect of TODGA concentration on the transport of Pu^{4+}. Feed: 3.0 M HNO_3; Receiver: 0.1 M oxalic acid

$$P = D_{Pu}/\{D_{Pu}(d_a/D_a) + (d_m / D_m)\} \tag{3.4}$$

where, d_a, D_a, d_m and D_m represent the thickness of the aqueous diffusion layer, aqueous diffusion coefficient, thickness of the membrane and membrane diffusion coefficient, respectively. In order to calculate the diffusion coefficients, it was required to carry out the transport studies at varying membrane thickness. The experiments were carried out by laminating the required number of membranes (0.2 µm thickness). As expected, the transport rates decreased with increasing membrane thickness. The plot of 1/P vs d_m is shown in Fig. 3.15. Assuming that the transport is diffusion controlled, the first term in

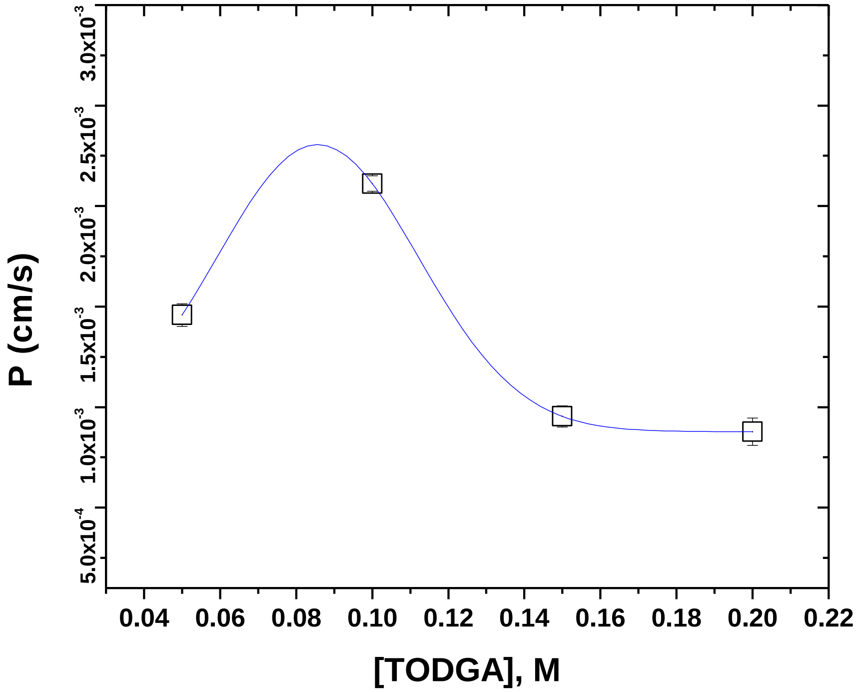

Fig. 3.15. Dependence of TODGA concentration on Pu^{4+} permeability coefficients. Feed: 3.0 M HNO_3; Receiver: 0.1 M oxalic acid

the denominator of eqn. (3.5) can be ignored and the intercept of the straight line plot can be close to the origin. For 3 M HNO_3 as the feed and 0.1 M TODGA as the carrier, the membrane diffusion coefficient was calculated to be 7.66×10^{-7} cm^2/s. The D_m value for Th^{4+} was calculated using the Wilke-Chang equation and was reported to be 2.13×10^{-7} cm^2/s in an earlier report [59]. Larger membrane diffusion coefficient for Pu^{4+} was due to the faster transport of the tri-solvate species (smaller molar volume) as compared to the tetra-solvate species in case of Th^{4+}.

3.2.3.2.4. Stability of the supported liquid membrane

As reported earlier, the stability of the SLM is a key factor in its applicability and it was reported that the nature of the diluent played a vital role in deciding the long term membrane stability [60-62]. For cases involving Pu^{4+}, the stability may also be affected by the disproportionation as well as autoradiolytic effects. In order to understand this, the transport studies were carried out as a function of number of days after loading the membrane with the organic carrier. The results, plotted in Fig. 3.17, indicated that the stability of the membrane was satisfactory up to 5 days and

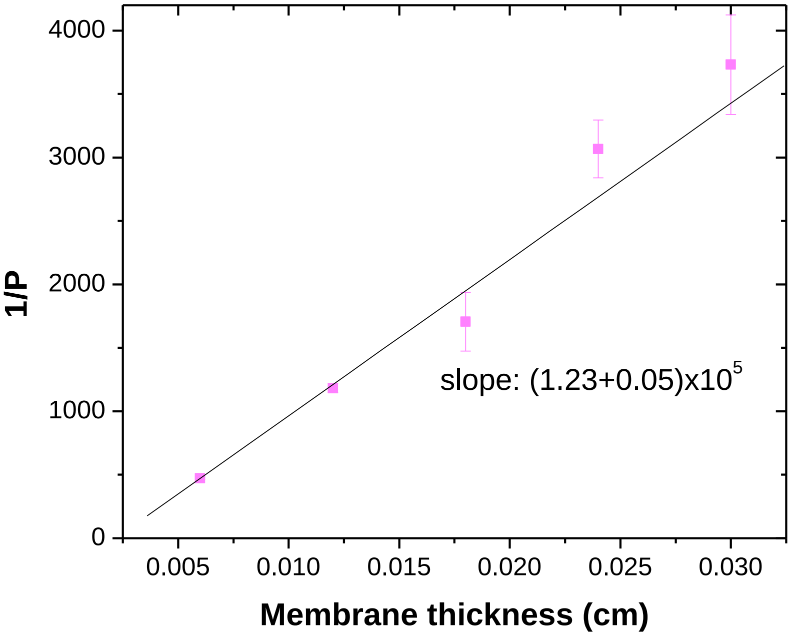

Fig. 3.16. Effect of membrane thickness on Pu^{4+} permeability coefficients. Feed: 3.0 M HNO_3; Receiver: 0.1 M oxalic acid

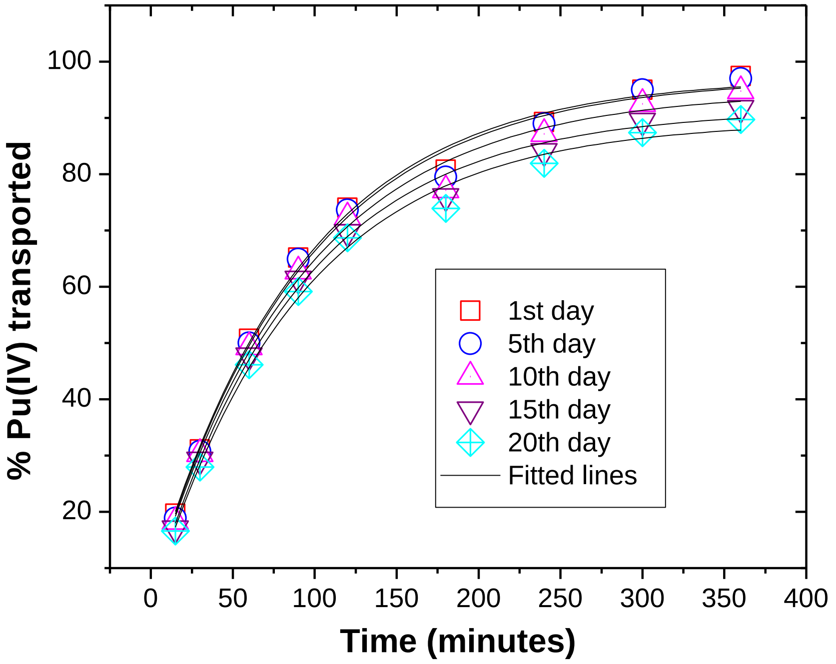

Fig. 3.17. Membrane stability as a function of days of continuous operation. Feed: 3.0 M HNO_3; Receiver: 0.1 M oxalic acid. Carrier: 0.1 M TODGA in *n*-dodecane

Table 3.10: Membrane stability data for Pu^{4+} transport using TODGA as the carrier extractant

Number of days	P x10^3(cm/s)	%T (6 h)	Comments
1	2.07±0.05	97.4	--
5	2.04±0.07	97.2	Stable
10	1.88±0.06	94.7	Deteriorating
15	1.47±0.06	91.4	Deteriorating
20	1.35±0.08	89.5	Deteriorating

decreased thereafter with time. The permeability coefficient values are listed in Table 3.10 and the %T values as indicated after 6 h suggested a decrease from 97.4 after 1 day to 89.5 after 20 days of continuous operation.

3.2.3.2.5. Irradiation Stability of TODGA

The use of SLM method for long term application in Pu recovery from acidic solutions under high loading conditions (for example, several mg/L of Pu is present in HLW), can also lead to the radiation damage of TODGA which will be reflected in a decrease in the transport rates. In order to quantify this effect, TODGA was exposed to varying radiation doses and the transport data was generated with 0.1 M TODGA + 0.5 M DHOA (di-*n*-hexyl octanamide) as the carrier and 3.0 M HNO_3 as the feed. It may be noted here that radiation effects become important under high loading conditions and a phase modifier may be required for this purpose. Though both DHOA and TBP have been suggested as the phase modifiers for TODGA, use of DHOA is preferred due to its complete incinerability similar to TODGA [63,64]. Transport studies were carried out with the carrier solution (mixture of 0.1 M TODGA and 0.5 M DHOA in *n*-dodecane) irradiated from 5 MRad to 100 MRad. Fig. 3.18 gives the transport profiles as a function of the absorbed irradiation dose. It is clearly seen that the transport efficiency decreased with increasing absorbed dose suggesting that the carrier solvent should be replenished after exposure to about 15 MRad dose. The irradiation stability of TODGA has also been studied in an earlier paper where the effect of diluent has been reported to

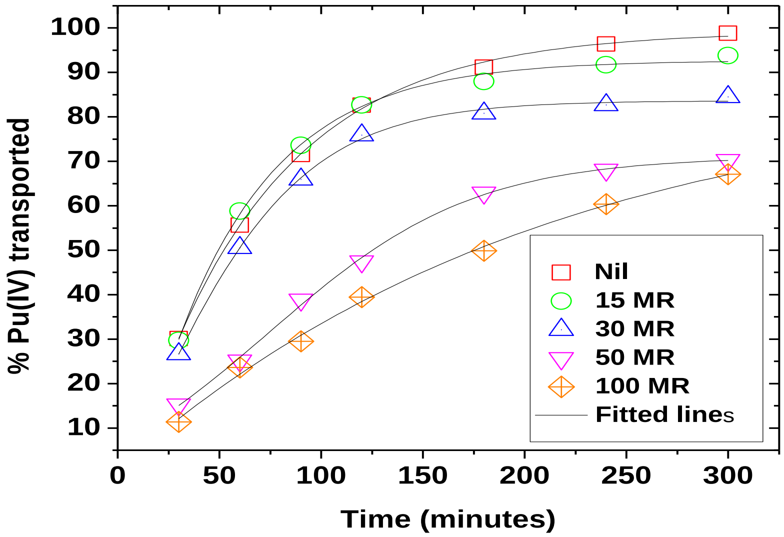

Fig. 3.18. Effect of absorbed dose on the Pu^{4+} transport rates. Feed: 3.0 M HNO_3; Receiver: 0.1 M oxalic acid. Carrier: 0.1 M TODGA in *n*-dodecane

play an important role [65]. It is required, therefore, to choose a suitable diluent for recycling the SLM carrier for a longer period.

3.3. Hexavalent Uranium Transport

Uranium is a major constituent of High Level Waste (HLW). Sometimes The concentration of U in HLW can be more than 10 g/L. Actinide partitioning strategists have proposed two different procedures: one is U removal prior to Actinide partitioning step and the other involves no prior removal of U. U removal is not a part of actinide partitioning using TODGA as it does not suffer the problem of third phase problem (as encountered with CMPO) when used along with phase modifier 0.5 M DHOA even in presence of 10-12 g/L of U [66]. Therefore, it is important to understand the transport behavior of U from HNO_3 medium using TODGA as the carrier. The present work, therefore, deals with the transport behavior of UO_2^{2+} from HNO_3 medium under varying experimental conditions.

3.3.1. Solvent Extraction Studies

The solvent extraction studies have indicated extraction of species of the type $UO_2(NO_3)_2 \cdot nTODGA$ conforming to the extraction equilibrium:

$$UO_2^{2+} + 2\,NO_3^- + nTODGA_{(o)} \rightleftharpoons UO_2(NO_3)_2 \cdot n(TODGA)_{(o)} \qquad (3.5)$$

where the species with the subscript '(o)' indicate those in the organic phase and those without any subscript indicate species in the aqueous phase. Sasaki et al., have reported the participation of 3 TODGA molecules in the extracted species while using *n*-dodecane as the diluent and 1 M HNO_3 as the feed [51]. On the other hand, Zhu et al., have reported the species of the type $UO_2(NO_3)_2 \cdot 2(TODGA)$ which has the involvement of two TODGA molecules while using the same diluent (*n*-dodecane) at a feed nitric acid concentration of 2.9 M [47]. In order to have a clear understanding about the nature of the extracted species, solvent extraction studies were carried out and the K_d values with varying TODGA and HNO_3 concentration are measured and listed in Table 3.11. The K_d data obtained as a function of equilibration time indicated that the equilibrium reached in less than 20 min (Fig. 3.19). It is reported that TODGA forms adducts such as $TODGA{\cdot}HNO_3$ and the equilibrium constant (K_H) is given as:

$$H^+ + NO_3^- + TODGA(o) \overset{K_H}{\rightleftarrows} TODGA \cdot HNO_3(o) \qquad (3.6)$$

The total TODGA concentration termed as $[TODGA]_t$ present in an experiment is presented as:

$$[TODGA]_t = n \times [UO_2(NO_3)_2 \cdot n(TODGA)]_{(o)} + [TODGA \cdot HNO_3]_{(o)} + [TODGA]_f \qquad (3.7)$$

where $[TODGA]_f$ represents the free TODGA concentration in the organic phase. Assuming that the TODGA tied up with the uranyl ion is negligible (as U-233 tracer was used whose concentration is $<10^{-5}$ M), the free TODGA concentration is calculated as follows:

$$(TODGA)_f = \frac{(TODGA)_t}{1 + K_H.[H^+][NO_3^-]} \qquad (3.8)$$

where $[H^+]$ and $[NO_3^-]$ are the equilibrium concentration of hydrogen and nitrate ion in the aqueous phase. The variation of the distribution ratio of U as a function of TODGA concentration was plotted at two different aqueous nitric acid concentrations using the $[\text{TODGA}]_f$ in the abscissa (Fig. 3.20). These data, which indicated TODGA concentration dependence (i.e., the number of TODGA molecules associated in the extracted species) of 1.18±0.08 and 1.74±0.08 for aqueous nitric acid concentration of 3 and 1 M, respectively, along with the distribution data as a function of nitric acid concentration have indicated the extraction of the species of the type $UO_2(NO_3)_2{\cdot}(TODGA)_{(o)}$ and $UO_2(NO_3)_2{\cdot}2(TODGA)_{(o)}$ at the respective nitric acid concentrations. These extracted species have suggested the reverse micellar mechanism of extraction, possibility of which increases with increasing acidity as suggested by Jensen et al. [46], is not valid for the extraction of UO_2^{2+}. Though surprising, it could be attributed to the structural limitations posed by the unusual conformation of the uranyl ion. The extraction constant (K_{ex}) is defined as:

$$K_{ex} = \frac{[UO_2(NO_3)_2.nTODGA]_O}{[UO_2^{2+}].[NO_3^-]^2.[TODGA]_o^n} \qquad (3.9)$$

The distribution ratio K_d is defined by the following equation:

$$K_d = \frac{[UO_2(NO_3)_2.nTODGA]_{(O)}}{\{[UO_2^{2+}] + \sum_i UO_2(NO_3)_i} \qquad (3.10)$$

Table 3.11. Distribution data of UO_2^{2+}–TODGA extraction system

$[HNO_3]$, M	D_U [a]	[TODGA], M	D_U [b]	[TODGA], M	D_U [c]
0.5	0.18 ± 0.01	0.02	0.05 ± 0.01	0.05	2.01 ± 0.04
1.0	1.01 ± 0.02	0.05	0.26 ± 0.01	0.1	4.99 ± 0.08
2.0	2.42 ± 0.01	0.1	1.01 ± 0.02	0.15	6.84 ± 0.21
3.0	4.99 ± 0.08	0.15	1.92 ± 0.06	0.2	10.9 ± 0.25
6.0	7.31 ± 0.11	0.2	2.51 ± 0.03	–	-

[a] :[TODGA] = 0.1 M. [b] :$[HNO_3]$=1.0M. [c] :$[HNO_3]$ = 3.0 M.

The log K_{ex} values were calculated from the above equations (using the distribution ratio values (D) at varying concentration of TODGA at a fixed nitric acid concentration) as 1.03±0.05 and 2.14±0.08 at 3.0 and 1.0 M HNO_3, respectively using the complex formation constants reported in the literature [67] and a reported method [68]. The log K_{ex} values are listed in Table 3.12. These extraction constant values are not in conformity with the value reported in the literature [49] which is obvious due to the difference in the nature of the extracted species reported in the present studies and those in the literature.

3.3.2. Transport studies

The transport studies were carried out using TODGA soaked PTFE filters as the SLM which separated the feed (usually 3.0 M HNO_3) and the receiver (0.1 M HNO_3) phases.

In a typical transport experiment, >75% U transport was possible in about 6 h. This is much lower than that observed for the trivalent actinides and lanthanides [41] and tetravalent actinides [54]. The transport profile of PuO_2^{2+} is also represented in Fig. 3.20 for comparison purpose. The transport rate for the latter metal ion was somewhat lower as compared to that for UO_2^{2+} ion. This may be due to either the higher complex formation and hence extraction constants for the uranyl

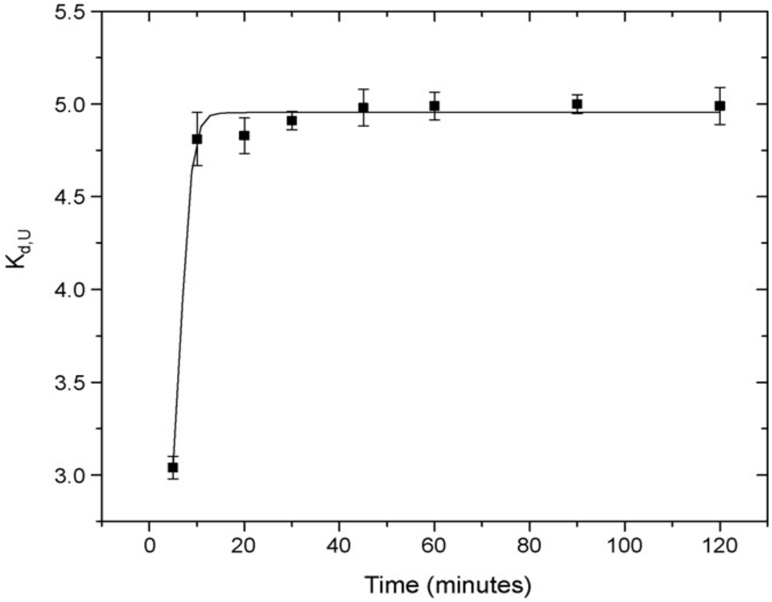

Fig. 3.19. Kinetics of U extraction using 0.1 M TODGA. Aqueous phase: 3 M HNO_3

Table 3.12. Slope and extraction constant (log K_{ex}) values for the system: UO_2^{2+}–TODGA/*n*-dodecane–HNO_3

$[HNO_3]$, M.	n	Major extracted species	Log K_{ex}
1.0	1.74±0.08	$UO_2(NO_3)_2·2(TODGA)$	2.14 ± 0.08
1.0	3.1±0.2	$UO_2(NO_3)_2·3(TODGA)$	2.9 ± 0.2 [2]
3.0	1.18±0.08	$UO_2(NO_3)_2·(TODGA)$	1.03 ± 0.05
2.9	2.0	$UO_2(NO_3)_2·2(TODGA)$	-

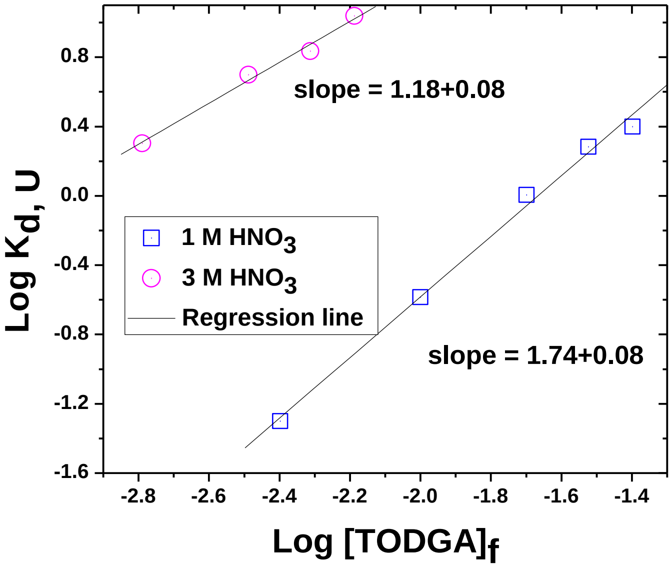

Fig. 3.20. Dependence of D_U on TODGA concentration. Aqueous phase acidity: 3 M HNO_3

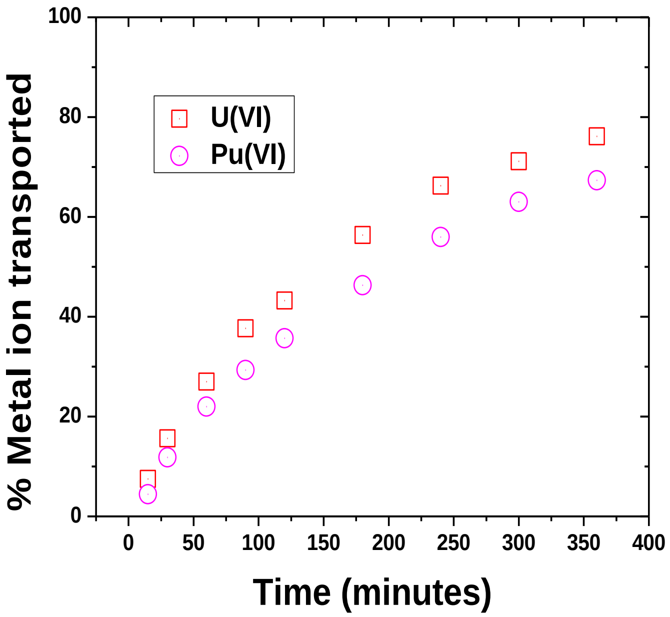

Fig. 3.21. Comparative transport profiles of UO_2^{2+} and PuO_2^{2+} ions. Feed: 3.0 M HNO_3; Receiver: 0.1 M HNO_3; Carrier extractant: 0.1 M TODGA; Support: 0.2 µm PTFE

ion compared to the plutonyl ion [46] or due to formation of extracted species with different stoichiometry than reported here for the uranyl ion. It may be noted that the valency of Pu was confirmed to be in the +6 state by carrying out TTA extraction studies at a fixed pH value. The concentration of U was around 10^{-5}M while that of Pu was about 10^{-6} M. A comparison of the permeability coefficients of different actinide ions is listed in Table 3.19. As indicated above, the permeability coefficient value for trivalent actinide ions such as Am^{3+} is much higher as compared to the tetra- or hexa-valent actinide ions.

Table 3.13. Permeability data of different actinide ions using TODGA as the carrier extractant

Metal ion	**P ×10^4(cm/s)**
Th^{4+}	0.12 ± 0.01
Pu^{4+}	15.2 ± 0.31
UO_2^{2+}	9.76 ± 0.15
PuO_2^{2+}	2.05 ± 0.06
Am^{3+}	36.7+ 0.62

3.3.2.1. Effect of feed nitric acid concentration

The extracted species contains two nitrate anions as the counter anion. It is, therefore, expected on the basis of the extraction equilibrium that the transport rates should increase with increasing nitrate ion concentration. We have reported earlier in analogous extraction/transport systems, strong influence of nitric acid with its increasing concentration [42,54]. Though an increase was observed from 0.5 to 3 M HNO_3, almost comparable transport rates were observed with 6 M HNO_3 as the feed (Fig. 3.22). This is in contrast to our observations with the tetra- and trivalent actinide ions, reported earlier in this chapter [42,54,69]. The permeability coefficients are listed in Table 3.14. The P values with HNO_3 concentration showed the trend: 6M~ 3M > 2M > 1M > 0.5M. This increase in the transport rate was attributed to the increasing tendency of the formation of the nitrate complexes with increase of feed acidity. Co-transport of acid (which was quite pronounced at 6 M HNO_3) due to the formation of TODGA·HNO_3 adduct is responsible for the comparable P values at 3 and 6 M HNO_3 [41]. It is reported in the literature that the basicity (K_H) of TODGA is 4.1±0.4 which is much higher as compared to extractants such as CMPO and this caused acid transport as reported in the present study [44]. This caused a decrease in the free ligand concentration and also reduced the stripping efficiency of the receiver phase. Higher transport efficiency of U(VI) with 6 M HNO_3 as compared to tri- and tetra-valent actinides is due to the ease of formation of the extractable species. This is due to the fact that two nitrate ions are required for the formation of the extractable complex in case of uranyl ion as compared to three and four nitrate ions required for the tri- and tetravalent ions, respectively. In fact, almost no transport of HNO_3 was detected in the receiver phase up to 90 and 60 min when the feed phase was 3 and 6 M HNO_3, respectively. This was indicated by higher transport efficiency with 6 M HNO_3 as compared to 3 M HNO_3 in the initial portion of the transport profiles (Fig. 3.22).

3.3.2.2. Effect of TODGA concentration

Similar to the solvent extraction studies, an increase in the concentration of TODGA in the membrane phase is expected to have a positive influence on the transport rate.

Table 3.14. Permeability data of UO_2^{2+} using TODGA as the carrier extractant

$[HNO_3]$, M[a]	P (cm/s)×10^4	[TODGA], M[b]	P (cm/s)×10^4
0.5M	0.59 ± 0.02	0.05	3.06 ± 0.13
1.0M	1.99 ± 0.08	0.10	9.76 ± 0.37
2.0M	3.78 ± 0.37	0.15	10.1 ± 0.02
3.0M	9.76 ± 0.15	0.20	11.0 ± 0.05
6.0M	9.36 ± 0.04	–	–

[a] :[TODGA] = 0.1 M., [b] : $[HNO_3]$=1 M.

In a blank experiment, no U transport was observed when the membrane was dipped in *n*-dodecane alone (without TODGA). On the other hand, increasing TODGA concentration resulted in the increase in U transport rate up to 0.1 M TODGA beyond which a near constancy in the transport rate was observed (Fig. 3.23). This was in sharp contrast to our studies on the transport of other actinide ions such as Th^{4+} , Pu^{4+}, Pu^{3+} and Am^{3+} where a decrease in the transport rate was reported beyond 0.1 M or 0.15 M TODGA [41,54,55,57]. With increasing TODGA concentration there was an increase in the D values resulting in high concentration of the complex at the feed–membrane interface (Table 3.11). On the other hand, the increase in the carrier viscosity may oppose the metal ion transport across the membrane. With the change in the nature of extractable species, the viscosity effect may vary from one metal ion to the other. Jensen et al., have reported mechanism for Nd^{3+} extraction which involved the

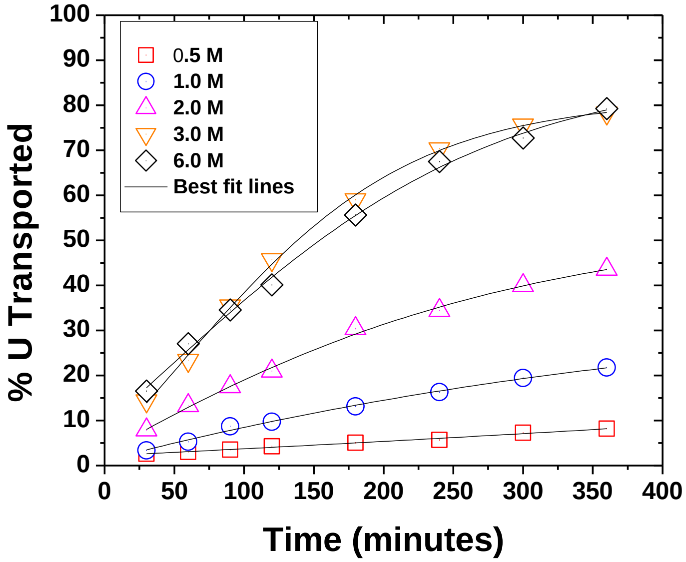

Fig. 3.22. Effect of the feed phase acid concentration on the transport of UO_2^{2+} ion. Receiver: 0.1 M HNO_3; Carrier extractant: 0.1 M TODGA; Support: 0.2 µm PTFE

formation of reverse micelles with 4 TODGA molecules at 0.1 M TODGA with a critical HNO_3 concentration of 0.7 M [46]. In the present extraction system involving mono-solvate TODGA complexes, mechanism appears to be different. Accordingly, a plateau was observed in the plot of P vs. TODGA concentration (Fig. 3.24) in which a limiting permeability coefficient value of 1.16×10^{-3} cm/s was obtained. Fig. 3.24 shows that D plays an important role up to 0.1 M, beyond which increase in the D value is countered by increasing viscosity resulting in a plateau.

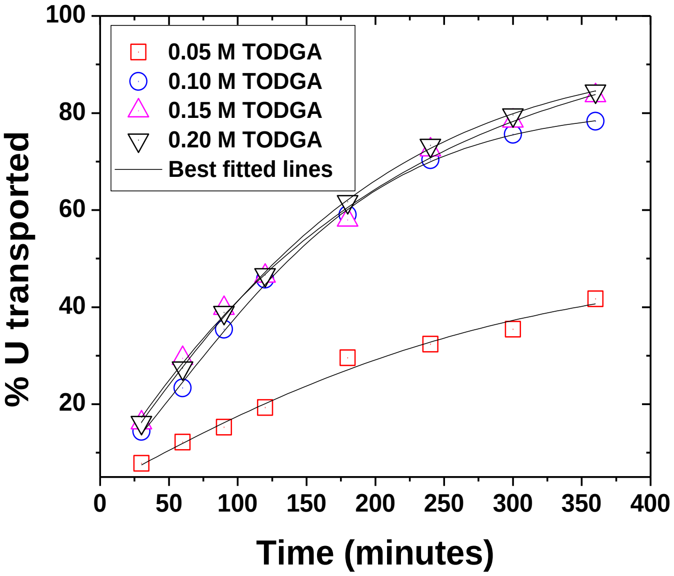

Fig. 3.23. Effect of TODGA concentration on the transport of UO_2^{2+} ion. Feed: 3.0 M HNO_3; Receiver: 0.1 M HNO_3; Support: 0.2 µm PTFE

3.3.2.3. Effect of membrane pore size

In case of diffusion controlled transport processes, membrane pore size should have a direct correlation with the permeation rates. In general, the permeability coefficient of a diffusing species in a porous polymeric matrix is correlated with the pore size (R is the effective pore radius) and tortuosity (τ) as per the following equation:

$$P = \frac{\varepsilon R^2}{\tau . 2d_o} \tag{3.11}$$

Where ε is the membrane porosity and d_o is the membrane thickness [70]. Therefore, higher the pore size, lower is the resistance experienced by the complex species. On the other hand, indefinite increase in the pore size can result in the release of the organic phase from the pores [56]. This is expressed by the Laplace's equation which correlates the minimum trans-membrane pressure (p) required to displace the extractant out of the membrane pores with the pore radius, R.

$$p=\frac{2\gamma}{R.\cos\theta} \tag{3.12}$$

Where p is the trans-membrane pressure required to displace the organic molecule from the pores having pore radius R and γ and θ are the interfacial tension and contact angle, respectively.

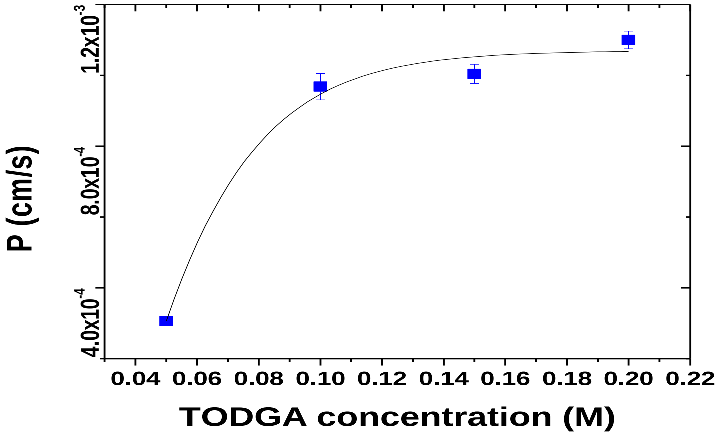

Fig. 3.24. Effect of TODGA concentration on UO_2^{2+} ion permeability coefficients. Feed: 3.0 M HNO_3; Receiver: 0.1 M HNO_3

To investigate the effect of membrane pore size, PTFE membrane filters of varying pore sizes viz. 0.2, 0.45, 1.2 and 5.0 μm were used for the transport studies. Literature reports have indicated a decrease in the permeability coefficient with increasing pore size. This is also expected from the Laplace's equation. Fig. 3.25 shows the comparative transport efficiencies of the four different membranes. From the transport data in Fig. 3.25, it is clearly seen that the transport efficiency decreased with increasing membrane pore size conforming to the general trend reported in the literature [71].

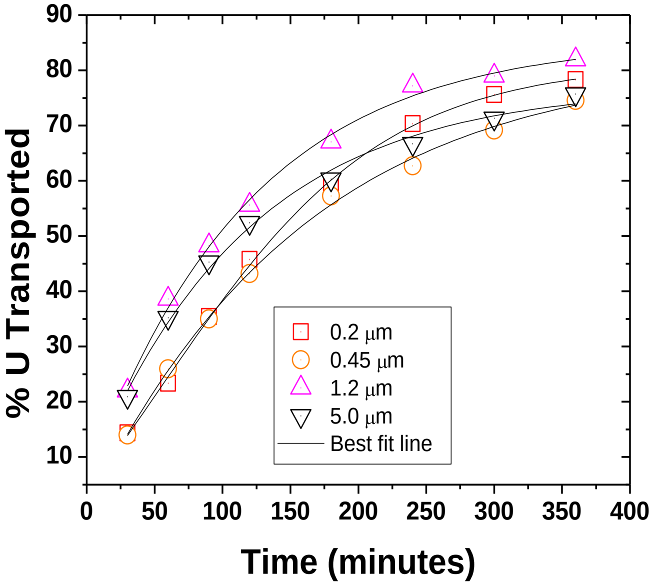

Fig. 3.25. Effect of membrane pore size on the transport of UO_2^{2+} ion. Feed: 3.0 M HNO_3; Receiver: 0.1 M HNO_3

3.3.2.4. Effect of U carrier concentration

The transport equations have indicated that the flux would increase with an increase in the metal ion concentration. However, there is a limitation posed by the ligand concentration in the membrane phase. Effect of U carrier concentration in the feed was investigated using the metal ion concentration in the range 0.1–15 g/L. Fig. 3.26 shows the transport rates as a function of feed phase U concentration. The saturation effect is clearly seen in the U concentration range of 10–15 g/L and the transport rates slowed down thereafter significantly. Due to loading of the membrane phase with U-TODGA extracted complex, the P values should eventually decrease as the effective TODGA concentration becomes lower. The permeability coefficients show a decreasing trend with increasing U concentration. The flux values were calculated and were found to increase from $(2.95\pm 0.13)\times10^{-7}$ mol cm^{-2} s^{-1} for U concentration of 0.1 g/L to $(1.73 \pm 0.06)\times10^{-5}$ mol cm^{-2} s^{-1} for U concentration of 15 g/L in the feed phase. This steady increase suggested an efficient transport system up to 10 g/L. Similar results were reported by Nakamura et al. [72] while studying the effect of metal ion loading for Eu(III) transport using a phosphinic acid extractant.

3.3.2.5. Calculation of diffusion parameters

The diffusion controlled transport process can be of significance when the distribution ratio values are not too large. Based on the Danesi's model [40], experiments were carried out by varying the membrane thickness by stacking 60 μm thick membranes. As expected, the transport rates decreased with increasing membrane thickness (Eq. (3.11)). A plot of 1/P vs. d_o should yield a slope of $1/D.D_o$ and an intercept of d_a/D_a. From a literature value of aqueous diffusion coefficient for UO_2^{2+}, calculated as 1.394×10^{-5} cm^2/s [73], the thickness of the aqueous diffusion layer (d_a) was calculated to be (8.12±0.72) $\times10^{-3}$ cm. The organic phase diffusion coefficient was calculated to be 2.98×10^{-6} cm^2/s. The effective diffusion coefficient (D_{eff}) can also be calculated from lag time (t_{lag}) measurements involving the metal

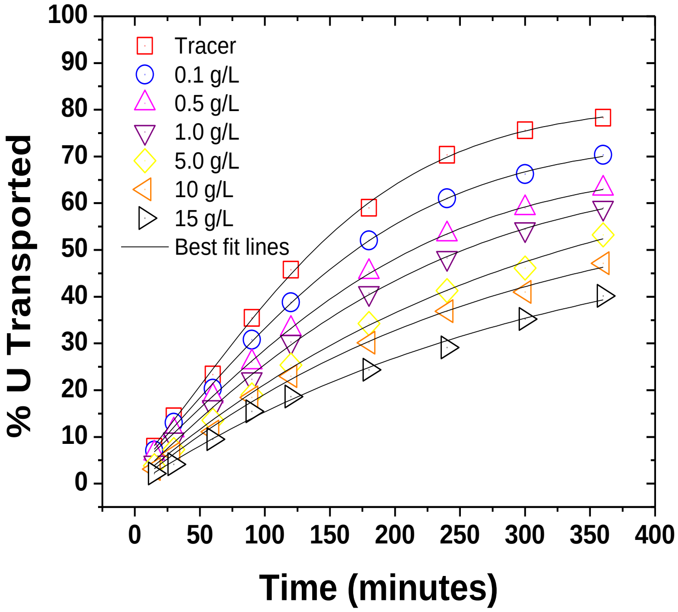

Fig. 3.26. Effect of U concentration on UO_2^{2+} ion permeability coefficients. Feed: 3.0 M HNO_3; Receiver: 0.1 M HNO_3; Carrier: 0.1 M TODGA

carrier complex from the following expression [74]:

$$D_{eff} = \frac{d_0^2 \varepsilon}{6t_{lag}} \tag{3.13}$$

where ε is the membrane porosity and do is the membrane thickness. For 0.1 M TODGA as the carrier and 240 μm as the membrane thickness (four 60 μm membranes were put together) the lag time was measured to be 20 s. Therefore, the D_{eff} value was calculated to be 2.48×10^{-6} cm^2/s. The D_{eff} value calculated here is somewhat lower than the value determined by the Danesi's method (vide supra).

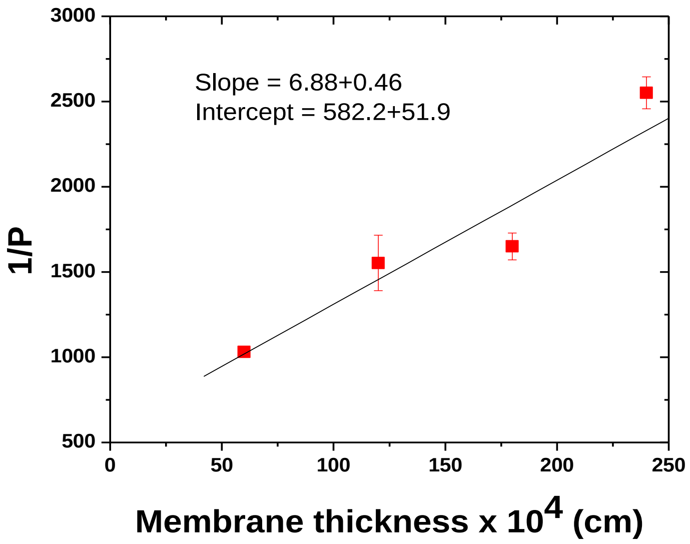

Fig. 3.27. Plot of 1/P vs. membrane thickness for calculation of diffusion coefficient for complexes of UO_2^{2+} ion. Feed: 3.0 M HNO_3; Receiver: 0.1 M HNO_3; Carrier: 0.1 M TODGA

This is possibly due to the fact that four membranes of 60 μm are used instead of a single membrane of a continuous thickness of 240 μm.

3.4. Tetravalent Thorium transport

While trivalent actinides such as Am^{3+} and Cm^{3+} are of particular relevance in ‘‘actinide partitioning,’’ it is also required to understand the extraction of Pu and Np which are invariably present in the High Level Waste (HLW) stream. While Pu is mainly present as Pu^{4+}, it can also simultaneously be present in the +3 as well as +6 oxidation states. The transport behavior of Pu^{3+} and Pu^{4+} using TODGA as the carrier are already discussed in this chapter. However, there is a possibility of partial conversion of Pu^{4+} to Pu^{3+} and vice versa. To understand the behavior of Pu^{4+} (without any possible interference from Pu^{3+} and PuO_2^{+2}) Th^{4+}, in view of its non-variable oxidation state, was used as a model tetravalent actinide ion. Moreover, it is also of interest to recover Th from various effluent streams (including THOREX (THORium EXtraction) process effluents) in nitric acid. The present work deals with the transport behavior of Th^{4+} from HNO_3 medium under varying experimental conditions such as, nitric acid concentration, TODGA concentration, and Th concentration. PTFE flat sheets containing 0.1 M TODGA in *n*-dodecane as the carrier solvent were used as the support while 0.1 M oxalic acid was used as the strippant solution.

3.4.1. Solvent extraction studies

The extraction of tetravalent Th from aqueous nitrate medium using TODGA is represented by the following extraction equilibrium:

$$Th^{4+} + 4\,NO_3^- + nTODGA_{(o)} \rightleftharpoons Th(NO_3)_4 \cdot nTODGA_{(o)} \qquad (3.14)$$

where, the species with subscript ‘(o)’ represent those in the organic phase while those without any subscript indicate species in the aqueous phase. Solvent extraction

studies were carried out as a function of TODGA concentration as well as aqueous HNO_3 concentration. As indicated in Table 3.15, Th^{4+} extraction increased with TODGA concentration as well as with HNO_3 concentration. The log-log plot of D_{Th} (distribution ratio) vs TODGA concentration (Fig. 3.28) with a slope of 3.82±0.10 indicated that the extracted species contained about 4 molecules of TODGA resulting in the extraction of species of the type $Th(NO_3)_4.4TODGA_{(o)}$, which was in sharp contrast to the results reported by Zhu, et al. (13), who had reported that the extracted species contained about 3 TODGA molecules in the extract. The extraction constant (log K_{ex}), represented as

$$K_{ex} = \frac{[Th(NO_3)_4.4TODGA]_O}{[Th^{4+}].[NO_3^-]^4.[TODGA]_o^4} \qquad (3.15)$$

was calculated to be 7.91±0.16 (after making corrections for the nitrate ion complexation (67)). This is in sharp contrast to the value reported by Sasaki et al. (23) (log K_{ex} = 5.55±0.04) and can be attributed to the difference in the nature of the extracted species as explained above.

For the stripping studies, dilute nitric acid was not used as the strippant. On the other hand, distilled water and oxalic acid were evaluated. Solvent extraction studies carried out for the stripping process using distilled water and 0.1 M oxalic acid indicated D_{Th} values to be 2.08 and 0.38, respectively. In view of efficient stripping by oxalic acid, for all subsequent studies, 0.1 M oxalic acid was used as the strippant in the receiver compartment. This is in view of the strong preference of tetravalent actinides for oxalate ions (43). The kinetics of the extraction and stripping steps were fast enough to consider that the transport process was controlled by the kinetics of diffusion of the extracted species.

3.4.2. Th Transport Studies

3.4.2.1. Effect of Nature of Strippant

As the distribution ratio at the membrane-receiver interface should be as low as possible, the strippants used in the receiver compartment should be low in acidity (<0.1M HNO_3) or should contain a complexing agent. Distilled water and oxalic acid were evaluated as strippants for the effective transport of Th from the membrane phase.

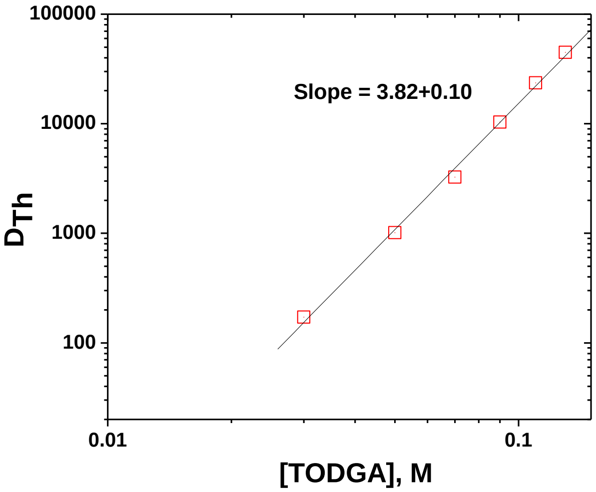

Fig. 3.28. Dependence of D-Th on TODGA concentration. Aqueous phase acidity: 3 M HNO_3

The transport data are presented in Fig. 3.29. It is clearly seen that 0.1 M oxalic acid, when used as the strippant, is quite effective as compared to

Table 3.15. Distribution data of Th^{4+} – TODGA extraction system

$[HNO_3]$, M	D_{Th} (0.1 M TODGA)	[TODGA],M	D_{Th} (3 M HNO_3)
0.5	12	0.03	341
1	198	0.05	675
2	5318	0.08	9812
3	15893	0.10	15893
6	95672	0.15	42892

distilled water. This is evident from the fact that for 60% transport of Th, about 107 minutes were required with 0.1 M oxalic acid as the strippant while >155 minutes was needed when distilled water was used as the strippant (Fig. 3.29). Higher concentration of oxalic acid was avoided as it could result in the precipitation of Th in the presence of large concentration of thorium carrier in the feed. Earlier studies on the non-dispersive extraction of Th have indicated similar results (75)

3.4.2.2. Effect of Feed Nitric Acid Concentration

The transport rates showed an interesting trend with the variation in the feed acid concentration. On the basis of Eq. (3.14) one would expect an increase in the transport rates with the feed acidity. Though an increase was indeed observed up to 3 M HNO_3, a decrease in the transport rate was observed when 6 M HNO_3 was used as the feed. Figure 3.30 shows the rate of Th transport from the feed to the receiver side as a function of the feed acidity. For comparison purpose, the time required for about 65% Th transport was 125 minutes with 3 M HNO_3, 145 minutes with both 2 M as well as 6 M HNO_3, 225 minutes with 1 M HNO_3, and 350 minutes with 0.5 M HNO_3. The permeability coefficients are listed in Table 3.16. This increase in the transport rate was attributed to the increasing tendency of the formation of the nitrate complexes at higher feed acidity while the decrease is ascribed to the formation of $TODGA\cdot HNO_3$ adduct formation (resulting in the decrease of the free ligand, TODGA). The interaction of TODGA with HNO_3 has been reported by Sasaki et al., in an earlier publication (50).

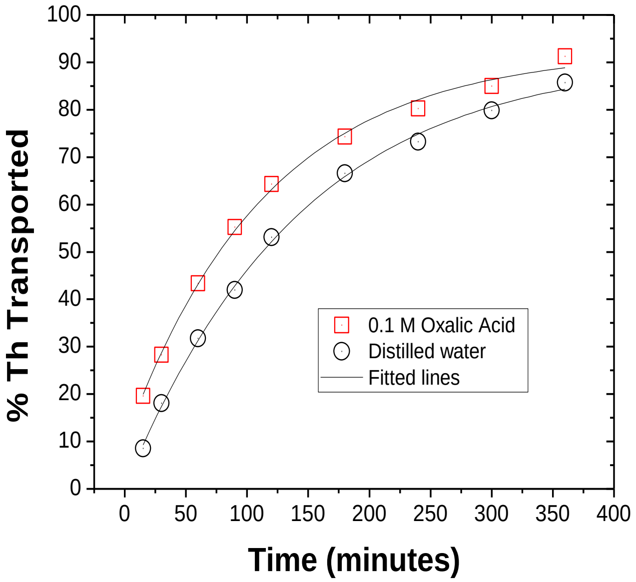

Fig. 3.29. Transport profiles of Th^{4+} with distilled water and 0.1 M oxalic acid as the strippant. Feed: 3 M HNO_3; Extractant: 0.1 M TODGA

Acid co-transport from the feed compartment to the receiver compartment is reported earlier in this Chapter, and the effect was pronounced especially at 6 M HNO_3 (41). As reported earlier, the enhanced acid co-transport at 6 M HNO_3 as the feed acidity reduced the stripping efficiency of the receiver phase. A similar observation on the co-transport of HNO_3 was also made in the present case.

3.4.2.3. Effect of Extractant Concentration

The extractant concentration in the organic phase has a significant effect on the metal ion transport across the membrane. The transport experiments carried out with

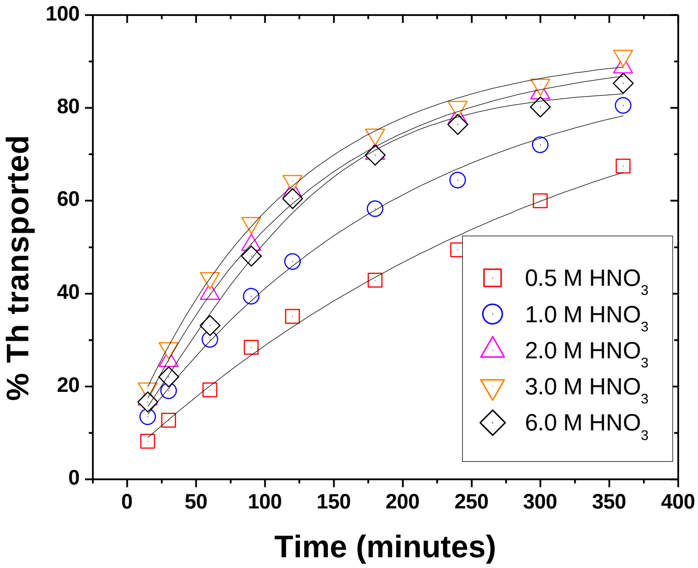

Fig. 3.30. Effect of feed acid concentration on the transport of Th^{4+}. Receiver: 0.1 M oxalic acid; Extractant: 0.1 M TODGA

membranes dipped in dodecane alone (without TODGA) have shown no transport of Th from the feed side to the receiver side. On the other hand presence of TODGA leads to Th transport and increasing TODGA concentration resulted in increase in Th transport rate (Fig. 3.31). Similar observation was made during the studies on Am(III) transport, though the transport studies were limited to 0.1 M TODGA (41). As the transport rates (on the basis of the %T vs time profiles) appear comparable in the TODGA concentration range of 0.1-0.2 M (Fig. 3.31), the permeability coefficients (P) were calculated to arrive at a trend. The increase in P with increasing TODGA concentration is ascribed to the increase in D_{Th} values at the feed-membrane interface (Table 3.16).

Table 3.16. Permeability data of Th^{4+} using TODGA as the extractant

$[HNO_3]$,M[a]	P × 10^4(cm/s)	[TODGA],M[b]	P × 10^3(cm/s)
0.5	(4.81±0.14)	0.05	(0.79±0.04)
1.0	(7.02±0.21)	0.10	(1.18±0.05)
2.0	(9.87±0.40)	0.15	(1.27±0.08)
3.0	(11.8±0.05)	0.20	(1.04±0.05)
6.0	(8.46±0.04)	–	–

Note. [a] [TODGA]=0.1 M; [b] 3 M HNO_3.

On the other hand, though an increase in the D_{Th} value on increasing TODGA concentration was observed during the solvent extraction studies, the decrease in the P values (Fig. 3.32) is ascribed to the viscosity effects as per the Stokes-Einstein equation (Eqn. 3.2).The viscosity and density data along with the permeability coefficient data are presented in Table 3.17. As the %T values were marginally higher in case of 0.15 M TODGA (56.8% 90 minutes and 93.5% after 360 minutes) as compared to 0.10 M TODGA (55.2% 90 minutes and 91.3% after 360 minutes), in all subsequent studies, 0.1 M TODGA in *n*-dodecane was chosen as the extractant solution.

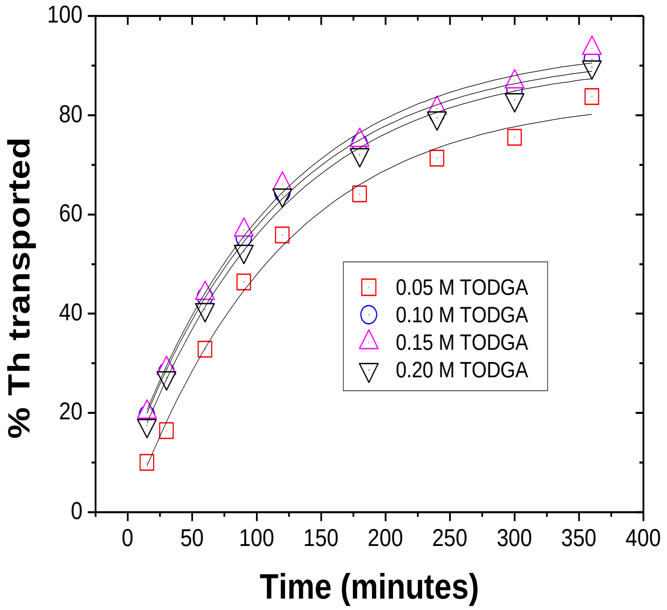

Fig. 3.31. Effect of TODGA concentration on the transport of Th^{4+}. Feed: 3.0 M HNO_3; Receiver: 0.1 M oxalic acid

3.4.2.4. Effect of Th concentration

The transport equations have indicated that the flux would increase with an increase in the metal ion concentration. However, there is a limitation posed by the ligand concentration in the membrane phase. The effect of Th carrier concentration in the feed was investigated using thorium concentration up to 5 g/L. Figure 3.33 shows the transport rates as a function of feed phase Th concentration. The saturation effect is clearly seen in the Th concentration range of 1-5g/L and the transport rates slowed down significantly at higher concentration of Th. Due to loading of the membrane phase with Th-TODGA extracted complex, the P values should effectively decrease as the

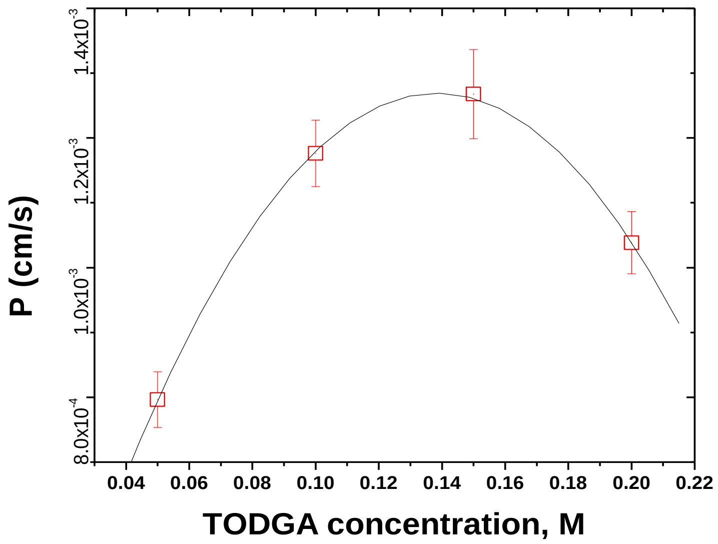

Fig. 3.32. Effect of TODGA concentration on Th^{4+} permeability coefficients. Feed: 3.0 M HNO$_3$; Receiver: 0.1 M oxalic acid

effective TODGA concentration becomes lower. The effect was reflected in the flux values with increasing concentration of Th. Fig. 3.34 represents the plot of flux vs Th concentration in the feed phase and a steady increase suggests an efficient transport system up to 5 g/L. As reported by Danesi et al. (19), when the carrier is completely converted to the metal-carrier complex, Th(NO$_3$)$_4$ ·4TODGA$_{(o)}$, the flux should remain constant with time. However, as this is not true, the flux changes with time as indicated in Fig. 3.34.

Table 3.17. Viscosity and density data for TODGA solutions used in the present studies along with the P (cm/s) values

[TODGA],M	Viscosity (mPa.S)	Density (g/cc)	P $\times 10^3$(cm/s)
0.05	1.539	0.754	(0.80±0.43)
0.1	1.641	0.758	(1.18±0.05)
0.15	1.860	0.764	(1.27±0.07)
0.2	2.012	0.771	(1.04±0.05)

3.5. Effect of gamma-irradiation of TODGA on the SLM transport behaviour of radio nuclides

3.5.1. Introduction

TODGA (N,N,N'N'-tetraoctyl diglycolamide) has been found to be a promising reagent for 'actinide partitioning' due to its excellent extraction ability of trivalent actinides such as Am^{3+} from nitric acid medium, complete incenaribility, innocuous degradation products, etc [23]. However for actual application of TODGA requires further insight into the problems associated with it, viz, i) third phase formation at higher metal loadings ii) radiation Stability of the solvent and iii) decontamination from Sr(II). Tachimori et al [2] have reported modification of TODGA-*n*-dodecane

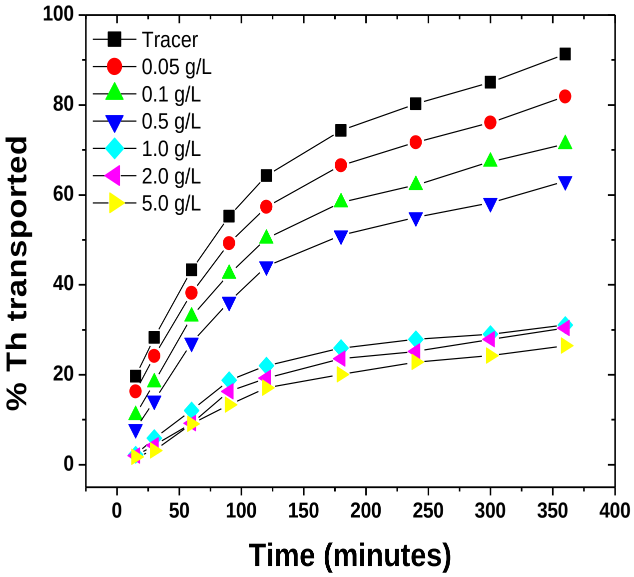

Fig. 3.33. Effect of the metal ion concentration on the transport of Th^{4+}. Feed: 3.0 M HNO_3; Receiver: 0.1 M oxalic acid; Extractant: 0.1 M TODGA

solvent with a monoamide, N,N-dihexyl octanamide (DHOA) to prevent formation of third phase. Radiation stability of TODGA has been systemically studied by Sugo et al [76]. They have found that gamma ray induced radiolysis of TODGA produced dioctylamine and various N,N-dioctylmonoamides as degradation products. Separation of trivalent actinides from Sr(II) using TODGA has been reported by Suzuki et al [77]. Advantages of supported liquid membrane based separation systems using TODGA have already been mentioned earlier in this Chapter. However, there is no literature report on the effect of gamma ray induced degradation of TODGA on the transport

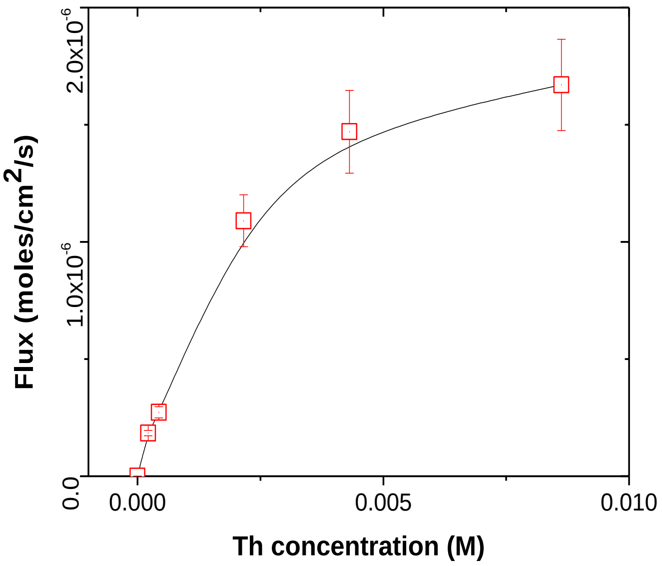

Fig. 3.34. Effect of the metal ion concentration on Th^{4+} flux. Feed: 3.0 M HNO_3; Receiver: 0.1 M oxalic acid; Extractant: 0.1 M TODGA

properties of different actinides. The present work deals with the transport behavior of several actinides and Sr(II) using TODGA at different irradiation dose. Effect of DHOA concentration on the permeability of actinides in their different oxidation states at different dose levels and its effect on the decontamination of the actinides with respect to Sr(II) have also been studied.

3.5.2. Transport of Am(III)

Trivalent actinides and lanthanides are the major constituents that are proposed to be separated from HLW in ‘Actinide Partitioning’. Extraction and transport of trivalent Am(III) using TODGA as the extractant have been reported in detail[41,44]. But the effect of irradiation or the effect of DHOA concentration on the transport of Am(III) have not been studied in detail. Understanding these effects is essential for the application of the TODGA based solvent system. Figs. 3.35, 3.36 and 3.37 represent

the transport profile of Am(III) using three different carrier concentrations viz, 0.1 M TODGA, 0.1 M TODGA+0.1 M DHOA and 0.1 M TODGA+0.5 M DHOA respectively against varying radiation dose. For unirradiated 0.1 M TODGA, >99% of Am(III) was found to be transported in ~4 h time whereas for 0.1 M TODGA+0.5 M DHOA only ~95% Am(III) got transported even after 5 h in unirradiated condition. In unirradiated condition, the presence of DHOA was found to decrease the transport rate of Am(III). This is due to two factors: i) lower distribution coefficients are obtained with 0.1 M TODGA + 0.5 M DHOA as compared to 0.1 M TODGA, and ii) higher viscosity of the 0.1 M TODGA + 0.5 M DHOA as compared to 0.1 M TODGA. Therefore, the transport rate decreases. Further, with increasing irradiation dose, less carrier molecules are available due to the radiation induced degradation of the carrier molecules. This causes a decrease in the transport rate of Am(III) at higher radiation dose level. The rate of decrease of transport was found to be lower for higher concentration of DHOA. This is due to the fact that DHOA inhibits the radiolysis of TODGA [65]. As a result when 0.1 M TODGA was irradiated at 100 MRad, ~79% Am(III) got transported in ~5 h time. On the other hand ~ 85% Am(III) got transported using 0.1 M TODGA +0.5 M DHOA exposed to 100 MRad dose. This fact is also reflected in Permeability co-efficient values. For 0.1 M TODGA, P value 3.04 × 10^{-3} cm/s obtained using unirradiated solvent decreased to 0.96 × 10^{-3} cm/s when the solvent was exposed to 100 MRad dose. For 0.1 M TODGA + 0.5 M DHOA, the P values were found to be 2.31 × 10^{-3} and 1.27 × 10^{-3} cm/s, respectively for unirradiated solvent and that exposed to 100 MRad absorbed dose.

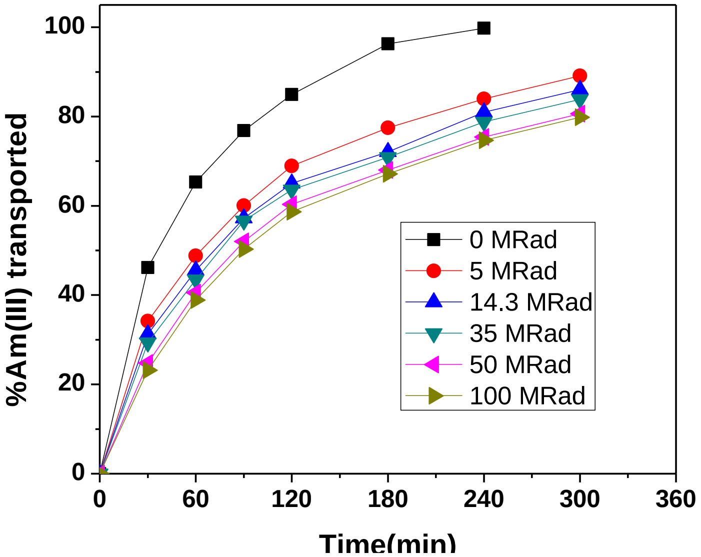

Fig. 3.35: Transport of Am(III) using 0.1 M TODGA irradiated at varying radiation doses. Feed: 3 M HNO_3; Receiver: 0.1 M HNO_3

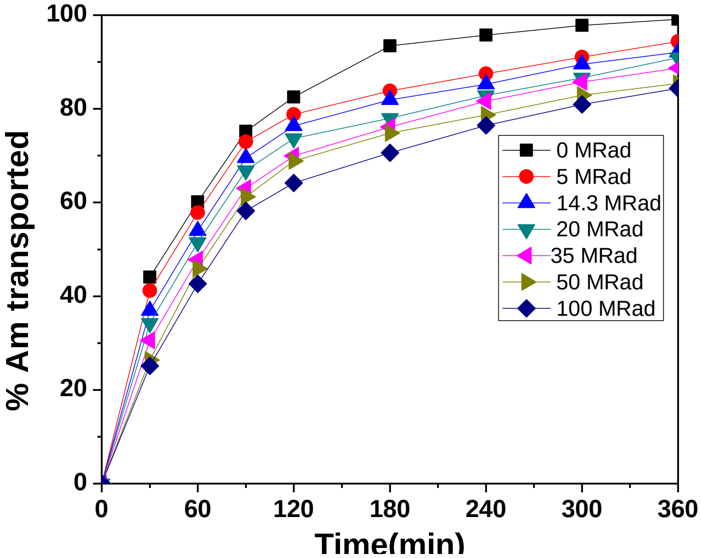

Fig. 3.36: Transport of Am(III) using 0.1 M TODGA + 0.1 M DHOA irradiated at varying radiation doses. Feed: 3 M HNO_3; Receiver: 0.1 M HNO_3

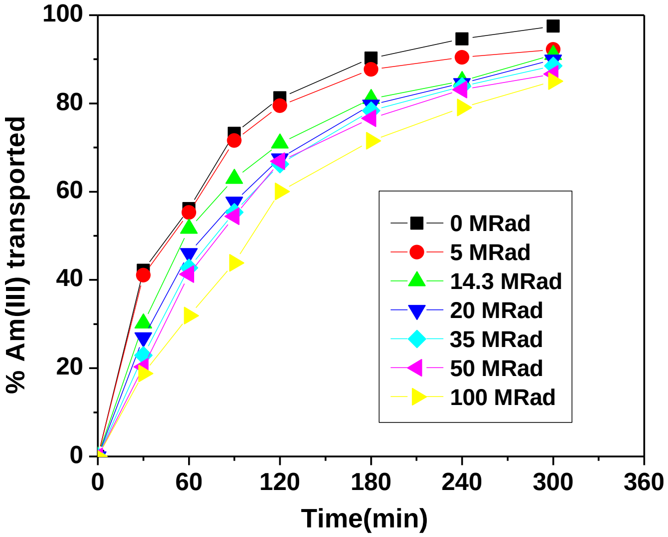

Fig. 3.37: Transport of Am(III) using 0.1 M TODGA + 0.5 M DHOA irradiated at varying radiation doses. Feed: 3 M HNO_3; Receiver: 0.1 M HNO_3

3.5.3. Transport of Pu(IV)

Pu is a major constituent of HLW and the major portion of Pu remains in tetravalent state at the acidity of the HLW. Thus, transport of Pu(IV) from nitric acid medium using TODGA in the absence and in the presence of DHOA as the carrier solvent as a function of radiation dose is needed to be understood for effective application of TODGA based membrane separation system. The transport rates for Pu(IV) against varying radiation dose for three different carrier concentrations viz, 0.1 M TODGA, 0.1 M TODGA +0.1 M DHOA and 0.1 M TODGA +0.5 M DHOA are presented in Fig. 3.38, 3.39 & 3.40 respectively. Using unirradiated solvents the percentage of transport for Pu(IV) in ~4 h was found to be ~90% for 0.1 M which increased to ~99.8% with 0.1 M TODGA + 0.5 M DHOA as the solvent system. Higher transport rate with the 0.1 M TODGA +0.5 M DHOA system as compared to 0.1 M

TODGA is attributed to significant extraction of Pu(IV) by DHOA alone. When the carrier molecules were irradiated with increasing gamma dose, the percentage transport of Pu(IV) got reduced to ~37% for 0.1 M TODGA in the same time period. On the other hand the percentage of transport after ~4h was found to be ~86% and ~60% after exposing 0.1 M TODGA +0.1 M DHOA and 0.1 M TODGA +0.5 M DHOA respectively to 100 MRad dose. This behaviour was unlike any other actinides where the percentage of transport was always higher for higher concentration of DHOA. Increasing absorbed dose caused increase in the degradation rate of TODGA and DHOA causing decrease in the carrier molecule concentration in the membrane phase which led to the lower transport rate at higher irradiation dose. With increasing concentration of DHOA at same irradiation dose, concentration of available carrier molecule in the membrane phase is also higher at any dose of irradiation. This caused higher transport for higher concentration of DHOA. However, for 0.5 M DHOA, the concentration of the degradation products of DHOA viz, carboxylic acids and amines are higher. These degradation products were found to cause retention of Pu(IV) in the degraded solvents which led to the in-effective stripping of Pu(IV) by 0.1 M HNO_3 at higher radiation dose. This fact was clearly proven by material balance between feed and strip phase. For 0.1 M TODGA and 0.1 M TODGA + 0.1 M DHOA the material balance was ~90% even after irradiation at 100 MRad. But for 0.1 M TODGA + 0.5 M DHOA, it was ~80% at 100 MRad dose. So it can be concluded that degradation products of DHOA play a negative role as far as stripping of Pu(IV) is concerned. Though 0.1 M HNO_3 was chosen as strippant for the actinides, it is reported that oxalic acid is a more effective stripping agent for Pu(IV). Therefore, use of oxalic acid in the stripping side might have changed the unusual behaviour of Pu(IV) transport using 0.1 M TODGA and 0.5 M DHOA. The behaviour can also be understood clearly from the permeability coefficient values of Pu(IV). Though the P values for unirradiated carrier molecules were: 2.1×10^{-3} cm/s, 3.7×10^{-3} cm/s and 4.06×10^{-3} cm/s for 0.1 M TODGA, 0.1 M TODGA+ 0.1 M DHOA and 0.1 M TODGA+ 0.5 M DHOA respectively, after exposing to 100 MRad dose, values decreased to 0.36×10^{-3}, 1.62×10^{-3} and 0.74×10^{-3} cm/s, respectively.

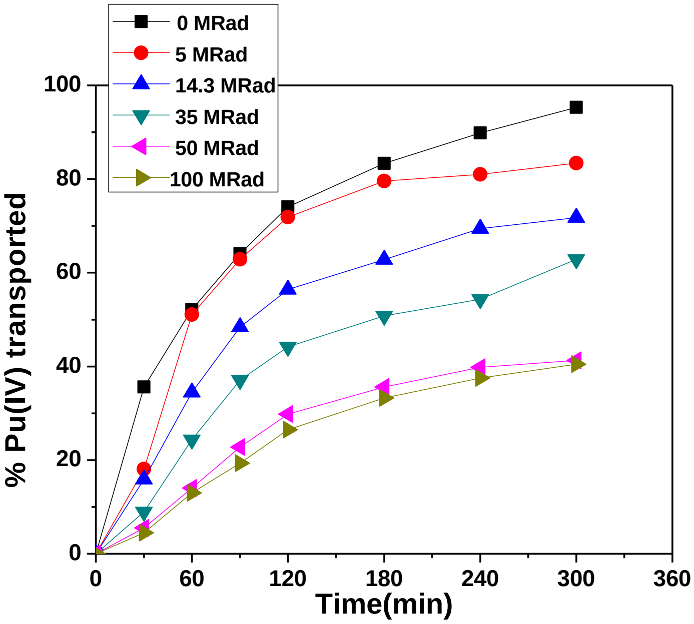

Fig. 3.38: Transport of Pu(IV) using 0.1 M TODGA irradiated at varying radiation doses. Feed: 3 M HNO_3; Receiver: 0.1 M HNO_3

3.5.4. Transport of U(VI)

The transport of U(VI) from nitric acid solution using a mixture of TODGA and DHOA as a function of radiation dose was also needed to be understood as it constitute a major portion of actinide concentration in HLW. The transport profile of U(VI) using three different composition of carriers viz, 0.1 M TODGA, 0.1 M TODGA + 0.1 M DHOA and 0.1 M TODGA + 0.5 M DHOA is presented in Figs. 3.41, 3.42 & 3.43, respectively. As can be seen from the figures, increasing concentration of DHOA causes increase in the U(VI) transport at all the absorbed dose levels. This suggested that like

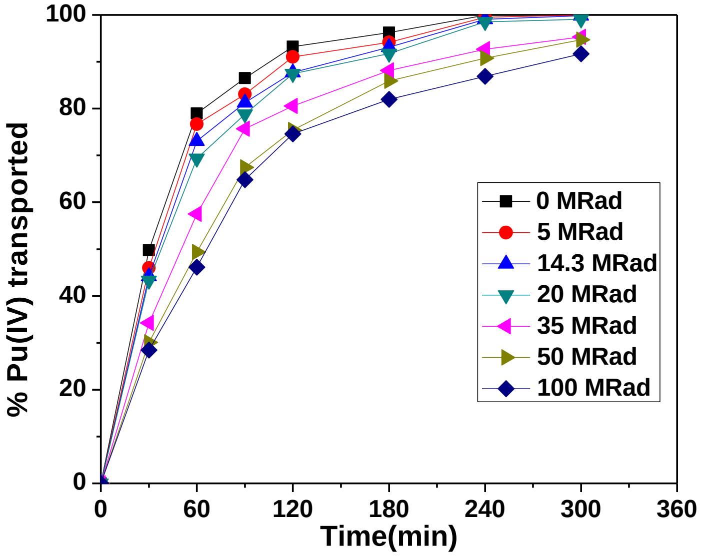

Fig. 3.39: Transport of Pu(IV) using 0.1 M TODGA + 0.1 M DHOA irradiated at varying radiation doses. Feed: 3 M HNO_3; Receiver: 0.1 M HNO_3

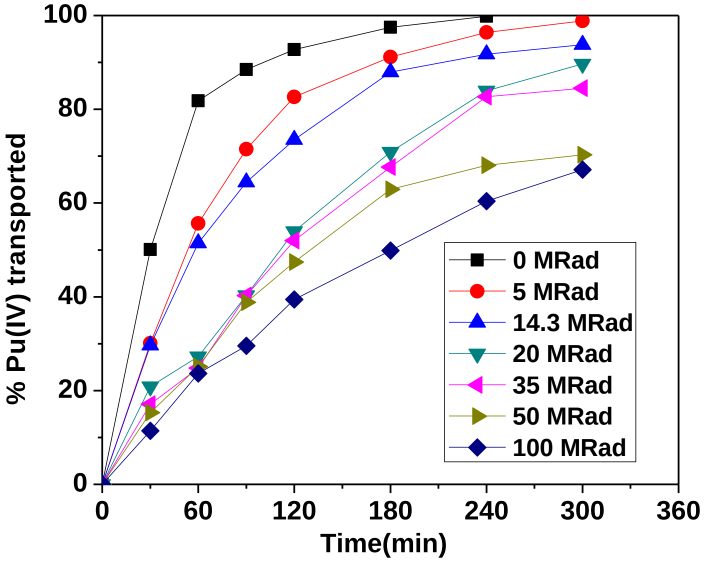

Fig. 3.40: Transport of Pu(IV) using 0.1 M TODGA + 0.5 M DHOA irradiated at varying radiation doses. Feed: 3 M HNO_3; Receiver: 0.1 M HNO_3

Pu(IV), DHOA is playing the role of a synergistic extractant for U(VI) as well, as it acts as an extractant for U(VI) [78]. With increasing radiation dose, the transport rate was found to decrease for all the three solvent systems. This is due to the less availability of carrier molecules in the membrane phase due to radiation induced degradation of the carrier molecules. For 0.1 M TODGA ~76% transport of U(VI) was seen in ~5 h using unirradiated carrier molecule which increased to ~ 90% when unirradiated 0.1 M TODGA +0.5 M DHOA was used. When the carrier molecules were irradiated to 100 MRad, the percentage of transport for 0.1 M TODGA was decreased to ~34% in the same duration of time. However for 0.1 M TODGA + 0.5 M DHOA, ~60% U transport was noticed. The difference in transport rate between 0.1 M TODGA and 0.1 M TODGA +0.1 M DHOA was insignificant for gamma irradiation dose upto 14.3 MRad. When the irradiation dose was increased further, significant difference in the transport rate was observed for the two carrier concentrations with higher transport rate for 0.1 M TODGA in presence of 0.1 M DHOA solvent system. Thus, the presence of DHOA not only helps in preventing the third phase formation for TODGA but also plays the role of carrier molecule for tetravalent and hexavalent actinides. The efficiency of stripping was also ~95% even for 100 MRad dose as calculated from the material balance between the feed and strip phase and there was no significant hold up of U(VI) in the membrane phase. Therefore, it can be concluded that the degradation products of DHOA do not play any negative role for U(VI) stripping unlike Pu(IV). The permeability coefficient value was found to increase from 1.0×10^{-3} cm/s for 0.1 M

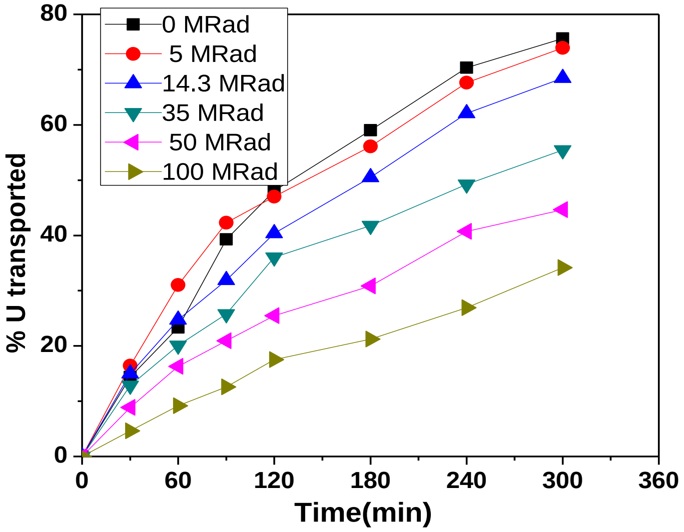

Fig. 3.41: Transport of U(VI) using 0.1 M TODGA irradiated at varying radiation doses, Feed: 3 M HNO_3; Receiver: 0.1 M HNO_3

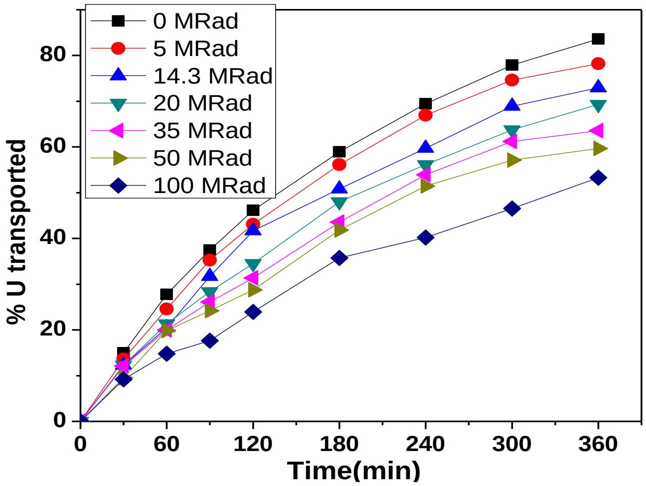

Fig. 3.42: Transport of U(VI) using 0.1 M TODGA + 0.1 M DHOA irradiated at varying radiation doses, Feed: 3 M HNO_3; Receiver: 0.1 M HNO_3

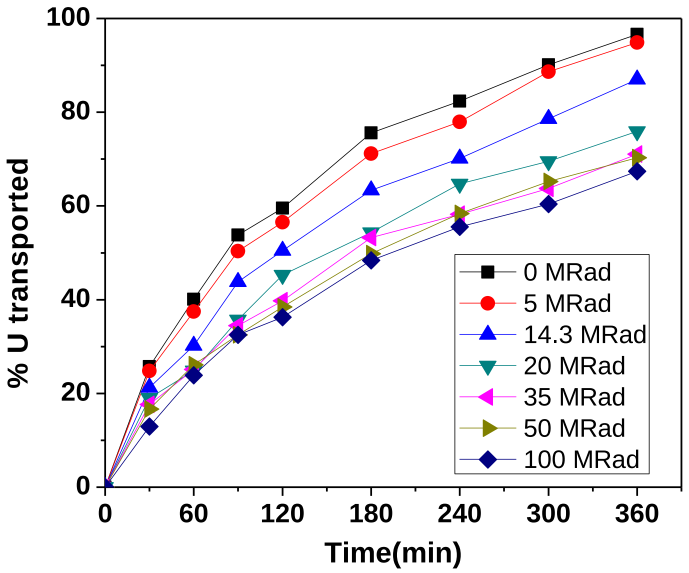

Fig. 3.43: Transport of U(VI) using 0.1 M TODGA + 0.5 M DHOA irradiated at varying radiation doses, Feed: 3 M HNO_3; Receiver: 0.1 M HNO_3

TODGA to 1.34 × 10^{-3} cm/s for 0.1 M TODGA + 0.5 M DHOA using unirradiated solvents. The values decreased to 0.29 ×10^{-3}cm/s and 0.6 × 10^{-3} cm/s for 0.1 M TODGA and 0.1 M TODGA + 0.5 M DHOA respectively when exposed to 100 MRad dose.

3.5.5. Transport of Sr(II)

In addition to actinides and lanthanides, TODGA also extracts divalent fission product, viz, Sr(II) from nitric acid medium [79]. In the presence of DHOA as the phase modifier, extractability of Sr(II) with TODGA decreases. This has been explained by Suzuki et al.,[79] due to high polarity of solvent and high reactivity between reactant and proton. Thus in order to understand the effect of DHOA concentration and irradiation dose on the transport of Sr(II), transport experiments were carried out using a mixture of TODGA and DHOA as carrier at different radiation dose. Transport profiles of Sr(II) using three different concentrations of carrier viz, 0.1 M TODGA, 0.1 M TODGA +0.1 M DHOA and 0.1 M TODGA +0.5 M DHOA are presented in Figs. 3.44,3.45 and 3.46, respectively. Significant transport of Sr(II) was seen from 3 M HNO_3 for 0.1 M TODGA as the carrier in unirradiated condition. It was observed that ~65% of Sr(II) got transported in ~6 h time. Increasing the DHOA concentration to 0.5 M caused significant decrease in the transport rate and ~24% Sr(II) got transported at the same time frame for the unirradiated carrier. This decrease in transport rate with increasing concentration of DHOA can be explained due to decreased extractability of Sr(II) at higher concentration of DHOA [79] as well as slower diffusion rates with higher viscosity of the medium. Increase in the irradiation dose caused the transport rate to decrease for all the carrier concentrations studied here. For 100 MRad dose level, there was only ~4-5% transport of Sr(II) at the same time interval in all the three carrier compositions. For both 0.1 M TODGA and 0.1 M TODGA+0.1 M DHOA, there was significant transport of Sr(II) even at 50 MRad dose. However for 0.1 M TODGA +0.5 M DHOA, the transport rate decreased much faster with increasing radiation dose and even at 35 MRad dose only ~6% Sr(II) got transported in ~6 h. The reason behind the decrease in transport rate with increasing irradiation dose is less availability of carrier molecules due to radiation induced degradation of them. It can also be concluded that degradation products of TODGA and DHOA do not lead to higher extraction of fission

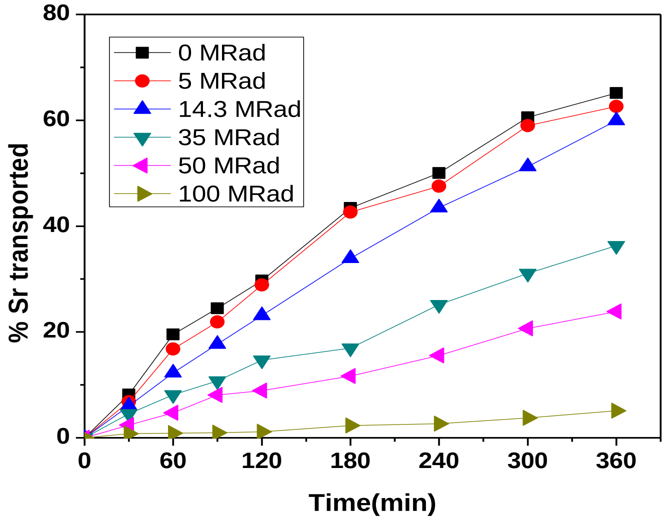

Fig. 3.44: Transport of Sr(II) using 0.1 M TODGA irradiated at varying radiation doses, Feed: 3 M HNO_3; Receiver: 0.1 M HNO_3

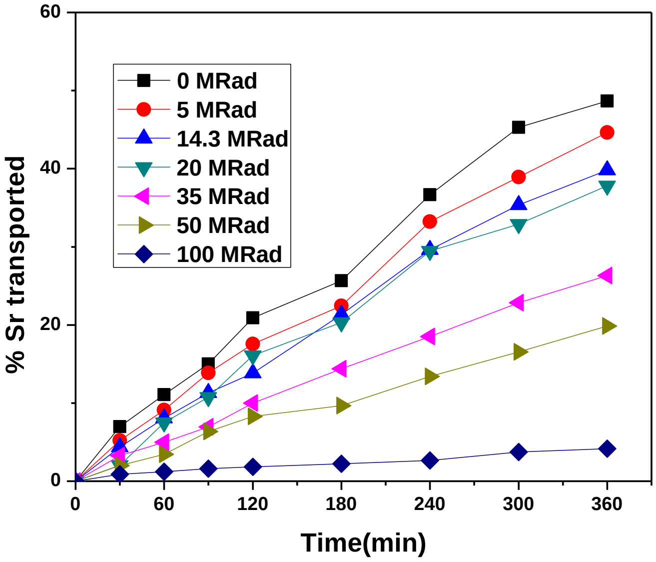

Fig. 3.45: Transport of Sr(II) using 0.1 M TODGA + 0.1 M DHOA irradiated at varying radiation doses, Feed: 3 M HNO_3; Receiver: 0.1 M HNO_3

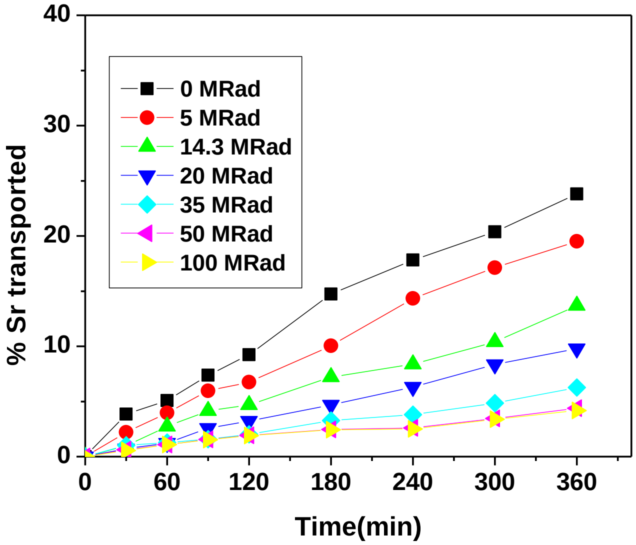

Fig. 3.46: Transport of Sr(II) using 0.1 M TODGA + 0.5 M DHOA irradiated at varying radiation doses, Feed: 3 M HNO_3; Receiver: 0.1 M HNO_3

products causing more contamination of separated actinides and lanthanides. These degradation products also do not lead to retention of Sr(II) in the membrane phase as evidenced by ~95% material balance between feed and strip phase.

3.5.6. Decontamination Factors with Respect to Sr(II)

Decontamination factors (D.F) for actinides over divalent fission product, Sr(II) in membrane transport experiments are calculated as a ratio of P values at different doses. The D.F values of the actinide ions are listed in Tables 3.18 and 3.19 for 0.1 M TODGA and 0.1 M TODGA+0.5 M DHOA, respectively at different absorbed dose. The values are higher for higher concentration of DHOA in all the irradiation doses. Also at the absorbed dose of 100 MRad, the D.F values are higher with respect to unirradiated carrier molecules. D.F values increased with increasing radiation dose level due to the fact that the decrease in transport rate of the actinides with increasing dose level is slower compared to that of Sr(II). Thus, though increasing irradiation dose causes a decrease in transport rate of the actinides, it also caused an increase in D.F of all the actinides with respect to Sr(II).

Table 3.18: Decontamination Factors of actinides over Sr(II) for 0.1 M TODGA

Dose	D.F$_{[Am(III)/Sr(II)]}$	D.F$_{[U(VI)/Sr(II)]}$	D.F $_{[Pu(IV)/Sr(II)]}$
0	5.06	1.66	3.50
5	2.92	1.57	2.82
14.3	2.66	1.50	2.29
35	4.30	2.38	2.70
50	6.55	2.93	3.51
100	16.27	4.95	6.10

3.6. Diluent Effect on the Transport of Am(III) across SLM using TODGA as a carrier

3.6.1. Introduction

Various properties of organic liquids that are responsible for their salvation behaviour(which effect the solvent extraction) have been described in detail by Marcus [80]. They

Table 3.19: Decontamination Factors of actinides over Sr(II) for 0.1 M TODGA + 0.5 M DHOA

Dose	**D.F$_{[Am(III)/Sr(II)]}$**	**D.F$_{[U(VI)/Sr(II)]}$**	**D.F $_{[Pu(IV)/Sr(II)]}$**
0	14.71	8.53	25.86
5	13.46	9.62	20.75
14.3	18.51	9.87	24.18
20	21.86	12.07	23.55
35	36.97	17.85	38.03
50	56.89	28.45	42.67
100	57.73	27.27	33.69

are polarity, hydrogen bonding ability, basity, acity and structured ness etc. Linear Free Energy Relationships (LFER) or Linear Solvation Energy Relationships (LSER) has been proposed that relates the above mentioned properties to various processes in solution: solubility, distribution between two liquids, free energy and enthalpy of equilibria, rates of reactions etc. Many research groups have reported the effect of organic diluents on the extraction and transport behaviour of various metal ions [81,82,83]. Nature of the organic diluent profoundly affects the nature of the extracted species as well as the extraction equilibrium for a particular metal ion [81]. Lakshmi et al have reported the dependency of Sr(II) transport on the organic diluents [83] . Bartsch etal have investigated the effect of solvent in competitive alkali metal cation transport across a Bulk Liquid Membrane [81].

The effect of organic diluent on the extraction and transport of Am(III) in SLM system has been investigated using 0.1 M TODGA as carrier. Effect of pore size for various diluents has also been investigated in detail. Diffusion coefficient values have been calculated for each diluent.

3.6.2. Solvent Extraction Studies

Solvent extraction of Am(III) from 1 M HNO_3 using 0.1 M TODGA in diluents like *n*-dodecane, nitrobenzene, chloroform, 1-octanol, CCl_4, kerosene, etc has been carried out. The respective $D_{Am(III)}$ values for different diluents have been reported in Table 3.20. It is quite evident that the diluents have profound effect on the extraction of Am(III). The values for D_{Am} varied from 0.7 to 195.14 in 1 M HNO_3 medium. Maximum value of 195.14 was observed for nitrobenzene whereas the lowest value of 0.7 was observed for chloroform. The distribution coefficient values are given in Table 3.20. The trend with respect to $D_{Am(III)}$ value is as follows: nitrobenzene > 1-octanol > *n*-dodecane > *tert*-butyl benzene > kerosene > 1,2-dichloro methane > toluene > CCl_4 > $CHCl_3$. We have also tried to investigate the nature of species formed by TODGA-Am(III) in different diluents. This was done by plotting log D vs log [TODGA] which is presented in Fig. 3.47 and the slope for each diluent is mentioned in Table 3.21. As evident from the Fig. 3.47 and the table the number of TODGA molecules attached varied from 2 to 4 depending on the nature of the diluent. Chloroform which was found to give lowest extractability had maximum four molecules of TODGA attached with Am(III). Nitrobenzene which showed maximum extractability had two molecules of TODGA attached with Am(III). These findings do not match with the observations of Sriram et al [82]. They have observed that 3 molecules of dimethyldibutyltetradecyl-1,3-malonamide (DMDBTDMA) attach with Am(III) in varying diluents. So both the extractability and nature of species of Am(III) were found to be dependent on the diluent used for TODGA as the extractant. When we tried to correlate the extraction strength of Am(III) by TODGA in different diluents, no single parameter correlation was found to be valid. Therefore, it is imperative to use multi parameter approach to explain the variations in extractability of Am(III) of 0.1 M TODGA in different diluents from HNO_3 medium. The eqn. describing the extraction equilibrium for nitrate ion assisted complexation of Am(III) is shown below:

$$\mathrm{Am}^{3+} + 3\,\mathrm{NO_3}^{-} + \mathrm{nTODGA}_{(o)} \rightleftharpoons \mathrm{Am(NO_3)_3.n(TODGA)}_{(o)} \tag{3.16}$$

Where the species with the subscript ‘(o)’ indicate those in the organic phase and those without any subscript indicate species in the aqueous phase.

3.6.3. Transport studies

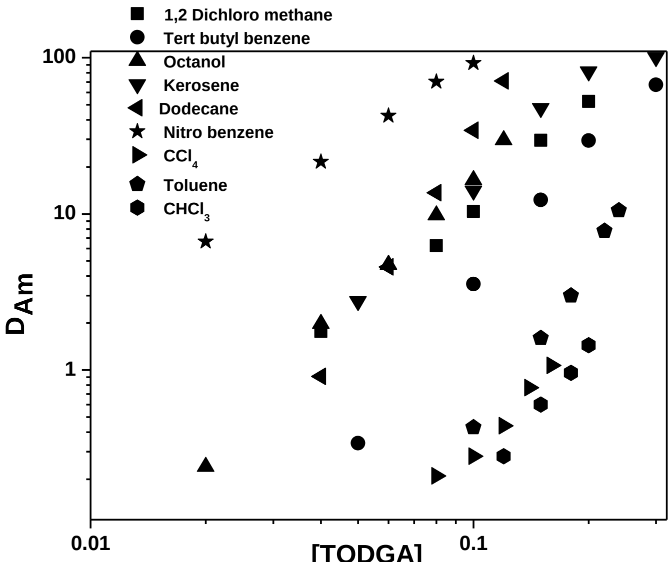

Fig. 3.47: Log-Log plot of D_{Am} vs. TODGA concentration at 1 M HNO_3 in different diluents

To understand the effect of the diluents on the transport of Am(III) for 0.1 M TODGA as the carrier extractant, experiments were carried out from 1 M HNO_3 using 0.1 M HNO_3 as the receiving phase. Fig. 3.48 shows the corresponding transport profiles of Am(III). Maximum transport was observed for toluene whereas $CHCl_3$ was found to give the minimum transport. The percentage transport in 300 minutes for different diluents using 0.1 M TODGA is given in Table 3.22. The trend with respect to transport of Am(III) is as follows: toluene ~ *n*-dodecane > kerosene > 1-octanol > *tert*- butyl benzene > CCl_4 > $CHCl_3$. Carrier facilitated transport of metal ion across SLM is dependent on various parameters out of which these factors are of utmost importance viz, extractability of the metal ion by the carrier at the membrane-feed interface, diffusion of the metal-carrier complex through the membrane phase, stripping of the metal ion from the metal-carrier complex at the membrane-strip interface. Stripping of Am(III) from Am(III)-TODGA complex was found to be independent of the diluents as 0.1 M TODGA showed $D_{Am(III)} < 10^{-3}$ at 0.1M HNO_3 for all the diluents studied in the present work. So transport rates are dependent on the first two factors as mentioned above. From the trends of $D_{Am(III)}$ values and transport rates of Am(III) it is seen that both of them are not same. Thus, the extractability of Am(III) by TODGA is not the deciding factor for the transport rates. The diffusion of the metal-carrier complex through membrane is dependent on various factors like, nature of species and viscosity of the medium. Among the diluents *n*-dodecane and $CHCl_3$ form a tetra solvate whereas kerosene forms a disolvate but the transport rate of *n*-dodecane was found to be greater than $CHCl_3$ and kerosene. So no single factor was found to be sufficient to explain the trend in transport rate for all the diluents and this requires a multi parameter approach. Permeability coefficient values are presented in Fig. 3.49.

3.6.4. Effect of Membrane Pore Size

Membrane pore size plays an important role in the transport of a particular metal ion across a SLM. In a diffusion controlled process across a polymeric matrix, the permeability co-efficient (P) value is directly proportional to the membrane pore size as can be seen from Eqn. 3.12. This suggests that with increasing pore size of the membrane the diffusing species experiences less hindrance and hence the transport rate

Table 3.20: Slopes of log-log plot of D_{Am} as a function of TODGA concentration in various diluents at 1 M HNO_3 along with respective $D_{Am(III)}$ values

Diluent	**Slope**	**$D_{Am(III)}$**
Nitrobenzene	1.66±0.03	195.14
Chloroform	3.80±0.36	0.7
CCl4	2.44±0.25	0.97
Toluene	3.28±0.14	1.57
n-Dodecane	3.87±0.04	30.29
Kerosene	2.15±0.24	14.1
1-Octanol	2.62±0.08	65.24
Tert- butyl benzene	2.99±0.15	10.37
1,2-Dichloro ethane	1.87 ± 0.11	3.55

should increase with increasing pore size. However it can not increase indefinitely as increasing the pore size can result in the release of the organic carriers from the membrane pores. This can be explained on the basis of Laplace's Eqn (Eqn.3.13). Hence increase in the pore radius results in enhanced release of the organic phase from the membrane causing the transport rates to decrease. These two factors thus show entirely opposite trends and the overall transport rate. The effect of membrane pore size on the transport rates of Am(III) for TODGA in different diluents are presented in Figs.

Table 3.21: % Transport of Am(III) from 1 M HNO_3 medium using 0.1 M TODGA in different diluents

Diluent	% Transport (300 min)
1-Octanol	78.88
Tert-butyl benzene	73.30
Toluene	90.93
n-dodecane	89.93
Carbon tetra chloride	69.95
Chloroform	49.01
Kerosene	86.24

3.50 and 3.51 which shows the plot of P vs membrane pore size for different diluents. As seen from the figures there is no particular trend as far as variation of membrane pore size is concerned. For *n*-dodecane, kerosene, 1-octanol and *tert*-butyl benzene the P values decrease with increasing membrane pore size. But for toluene, $CHCl_3$ and CCl_4 no particular trend was observed. Hence for *n*-dodecane, kerosene, 1-octanol and *tert*-butyl benzene, the effect of release of carrier molecules from the membrane pore size plays dominant role. Thus, for all the diluents no particular trend with a single parameter was observed and here also a multi parameter approach was found necessary.

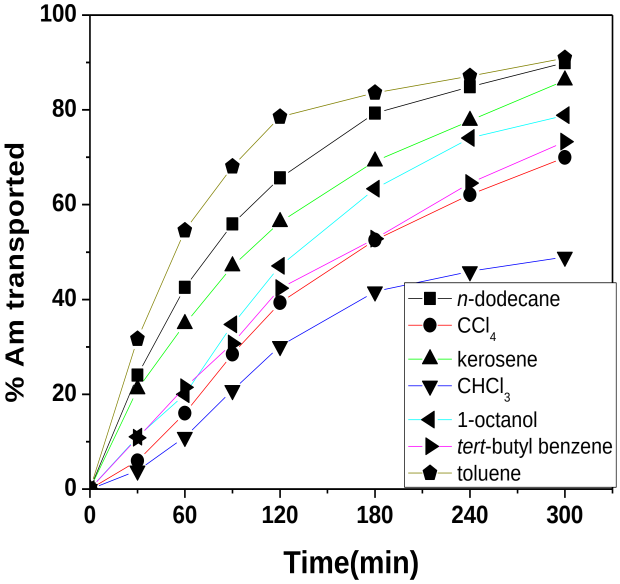

Fig. 3.48: Transport of Am(III) from 1 M HNO_3 using 0.1 M TODGA in varying diluents

3.6.5. Calculation of Diffusion Parameters

The diffusion coefficient D_{eff} can be calculated as per the empirical Wilke–Chang equation [84] for the bulk diffusion coefficient defined as:

$$D_{eff} = \frac{7.4\times10^{-8}(\chi^{0.5}M^{0.5}T)}{(\eta.V_m^{0.6})} \quad (3.17)$$

where M, χ and η are the molecular weight (M for TODGA is 580 and for $Am(NO_3)_3{\cdot}nTODGA$ varies from diluent to diluent), solvent association parameter and the viscosity of the solvent, respectively, V_m the molar volume of TODGA and T is the temperature. The association parameters for the diluents are taken as unity [84]. The

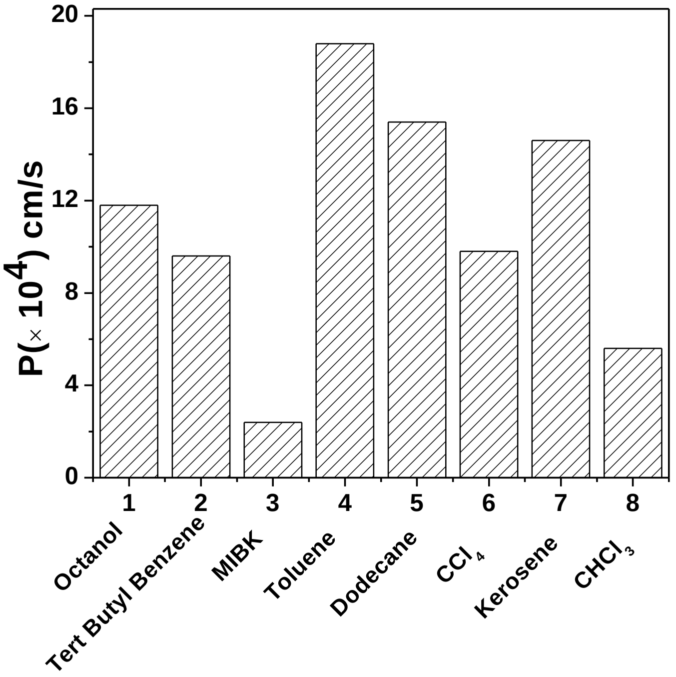

Fig. 3.49: Effect of diluent on the P values of Am(III) for 0.1 M TODGA, Feed: 1 M HNO_3, Receiver: 0.1 M HNO_3

molar volume of TODGA was calculated to be 834.06 $cm^3.mol^{-1}$. The calculated D_{eff} values are reported in Table 3.23. The effective diffusion coefficient (D_{eff}) can also be calculated from lag time (t_{lag}) measurements involving the metal carrier complex from Eqn. 3.13. For 0.1 M TODGA as the carrier and 180 µm as the membrane thickness (three 60 µm membranes were put together) the lag times for Am(III) were measured for varying diluents. Feed acidity was maintained at 1 M HNO_3. The D_{eff} values calculated by the procedure are also reported in Table 3.23 along with the respective t_{lag} values. The Deff value calculated here is somewhat lower than the value determined by

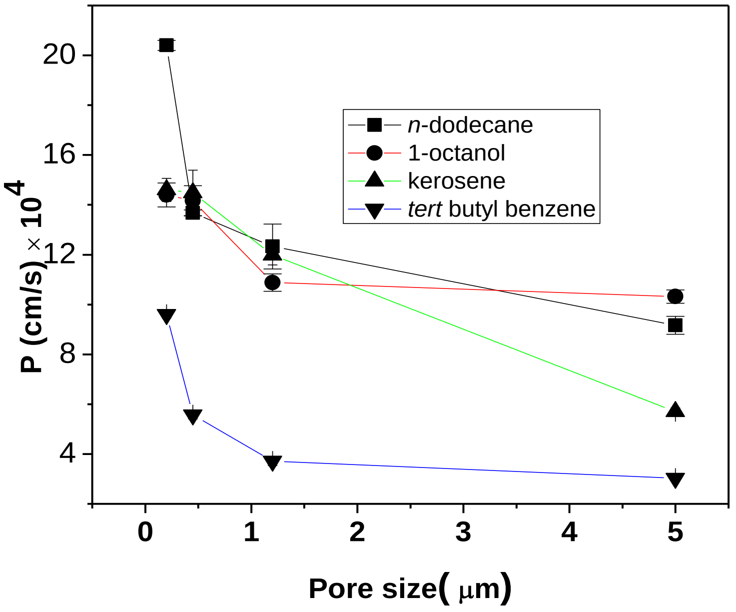

Fig. 3.50: Effect of membrane pore size on the P values of Am(III) for 0.1 M TODGA in varying diluents

Table 3.22: Viscosity and density of 0.1M TODGA in various diluents

Diluent	Viscosity(mPa.S)	Density(g/cc)
n-dodecane	1.6680	0.7596
Tert-Butyl benzene	2.0102	0.5723
$CHCl_3$	2.1501	1.5021
CCl_4	2.2010	1.5921
Toluene	1.7213	0.4218
Kerosene	1.9509	0.6321
1-Octanol	1.8561	0.6451

the Wilke-Chang eqn (*vide supra*). This is possibly due to the fact that three membranes of 60 µm are used instead of a single membrane of a continuous thickness of 180 µm.

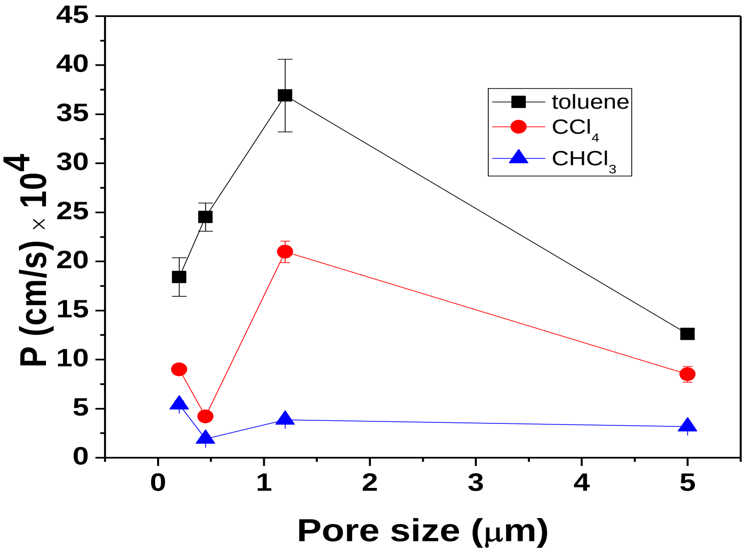

Fig. 3.51: Effect of membrane pore size on the P values of Am(III) for 0.1 M TODGA in varying diluents

3.7. Conclusions

The detail study presented in the Chapter can be concluded by commenting that TODGA based supported liquid membrane was found to be quite effective for transport of actinides in various oxidation states from nitric acid medium. Various factors affect the transport rates and have been evaluated in detail. Membrane transport was found to be diffusion controlled for the actinides. Effect of diluent and radiation on the extraction and transport of the actinides were also evaluated in detail.

Table 3.23: Diffusion coefficient values of Am(III)-TODGA complex obtained with 0.1 M TODGA in varying diluents, Feed: 1 M HNO_3, Strip: 0.1 M HNO_3, Membrane pore size: 0.2 µm

Diluent	t_{lag},s	$D_{eff} \times 10^6$ (cm^2/s)	Do (Wilke Chang) $\times 10^6$ (cm^2/s)
n-Dodecane	540	5.1	5.33
1-Octanol	600	4.59	4.75
Toluene	570	4.83	5.35
Kerosene	560	4.92	5.16
Tert-butyl benzene	630	4.37	4.67
$CHCl_3$	720	3.83	4.17
CCl_4	660	4.17	4.45

3.8. REFERENCES:

1. R.J.M. Konings and J.L. Kloosterman, *Progress in Nucl. Energy*, 38 (2001) 331.
2. Proceedings of the Seventh Information Exchange Meeting on Actinide and Fission Product Partitioning and Transmutation, Jeju, South Korea, October 14–16, 2002.
3. C. Madic, M.J. Hudson, J.O. Liljenzin, J.P. Glatz, R. Nannicini, A. Facchini, Z. Kolarik and R. Odoj, New Partitioning Techniques for Minor Actinides, European Commission Report, EUR 19149, European Union, Brussels, 2000.
4. C. Cuillerdier, C. Musikas and L. Nigond, *Sep. Sci. Technol.*, 28 (1993) 155.

5. V.K. Manchanda and P.N. Pathak, *Sep. Purif. Technol*., 35 (2004) 85.
6. T.H. Siddall, *J. Phys. Chem*., 64 (1960) 1863.
7. C. Musikas, *Inorg. Chim. Acta*, 140 (1987) 197.
8. C. Musikas, *Sep. Sci. Technol*., 23 (1988) 1211.
9. H. Stephan, K. Gloe, J. Bager and P. Muhl, *Solv. Extr. Ion Exch*., 9 (1991) 435.
10. H. Stephan, K. Gloe, J. Bager and P. Muhl, *Solv. Extr. Ion Exch*., 9 (1991) 459.
11. K. Matloka, A. Gelis, M. Regalbuto, G. Vandegrift and M.J. Scott, *Dalton Trans*. (2005) 3719.
12. M. Hirata, P. Guilbaud, M. Dobler and S. Tachimori, *Phys. Chem. Chem. Phys*., 5 (2005) 691.
13. Z. Zhu, Y. Sasaki, H. Suzuki and T. Kimura, *Anal. Chim. Acta*, 527 (2004) 163.
14. S.P. Kusumocahyo, T. Kanamori, T. Iwatsubo, K. Sumaru, T. Shinbo, H. Matsuyama and M. Teramoto, *J. Appl. Polym. Sci*., 102 (2006) 4372.
15. E.A. Mowafy and H.F. Aly, *Solv. Extr. Ion Exch*., 25 (2007) 205.
16. Y. Sasaki, H. Suzuki, Y. Sugo, T. Kimura and G.R. Choppin, *Chem. Lett*., 35 (2006) 256.
17. Y. Sasaki and G.R. Choppin, *Anal Sci.*, 12 (1996) 225.
18. Y. Sasaki and G.R. Choppin, *J. Radioanal. Nucl. Chem*., 207 (1997) 383.
19. Y. Sasaki, T. Adachi and G.R. Choppin, *J. Alloy comp*., 271-273 (1998) 799.
20. Y. Sasaki and G.R. Choppin, *Radiochim. Acta*, 80 (1998) 85.
21. Y. Sasaki and G.R. Choppin, *J. Radioanal. Nucl. Chem*., 246 (2000) 267.
22. H. Narita, T. Yaita, T. Kimura and S. Tachimori, *Radiochim. Acta*, 81 (1998) 223.

23. Y. Sasaki, Y. Sugo, S. Suzuki and S. Tachimori, *Solv. Extr. Ion Exch.*, 19 (2001) 91.

24. A. Pabby, S. H. S. Rizhi and A. M. S astre,Handbook of MembraneSeparations. Chemical, Pharmaceutical, Food and Biotechnological Applications. CRC Press, New York (2009).

25. A.M. Sastre, A. Kumar, J. P. Shukla and R. K. Singh, Improved techniques in liquid membrane separations: an overview. *Sep Purif Methods,* 27 (1998)213.

26. H.K. Lonsdale, *J. Membr. Sci.*, 10 (1982) 81.

27. E.L. Cussler (Ed.), Multicomponent Diffusion, Elsevier, Amsterdam (1976), Chap-8.

28. N.M. Kocherginsky, Q. Yang and L. Seelam, *Sep. Purif. Technol.*, 53 (2007) 171.

29. H.J, Fendler, *J. Membr. Sci.*, 30 (1987) 323.

30. R.D. Noble, *Sep. Sci. Technol.*, 22 (1987) 731.

31. E.L. Cussler and D.F. Evans, *Sep. Purif. Meth.*, 3 (1974) 399.

32. R. Marr and A. Kopp, *Int. Chem. Eng.*, 22 (1982) 44.

33. L.L. Tavlarides, J.H. Bae and C.K. Lee, *Sep. Sci. Technol.*, 22 (1987) 581.

34. R.M. Izatt, J.D. Lamb and R.L. Bruening, *Sep. Sci. Technol.*, 23 (1988) 1645.

35. J.D, Way, R.N. Noble, T.M. Flynn and E.D. Sloan, *J. Membr. Sci.*, 12 (1982) 239.

36. H.C. Visser, D.N. Reinhoudt and F. de Jong, *Chem. Soc. Rev.*, (1994) 75.

37. R.A. Bartsch, J.D. Way, L.A.J. Chrisstoffels, F. de Jong and D.N. Reinhoudt, "*Chemical Separations with Liquid Membranes*", R.A. Bartsch and J.D. Way (Eds.), ACS Symposium Series Number 642, ACS, Washington DC (1996),10.

38. L. Boyadzhiev and Z. Lazarova, “*Membrane Separations Technology. Principles and Applications*”, R.D. Noble and S.A. Stern (Eds.), Elsevier Science B.V. (1995)

39. G. Spach, Ed., "*Physical Chemistry of Transmembrane Ion Motions*", Elsevier: Amsterdam, (1983).

40. P.R. Danesi, *Sep. Sci. Technol*., 19 (1985) 857.

41. S.A. Ansari, P.K. Mohapatra, D.R. Prabhu, V.K. Manchanda, *J. Membr. Sci*. 282 (2006) 133.

42. S.A. Ansari, P.K. Mohapatra, D.R. Prabhu, V.K. Manchanda, *J. Membr. Sci*. 298 (2007) 169.

43. J.J.Katz, G.T. Seaborg, L.R. Morss, In: *The Chemistry of the Actinide Elements*, 2nd Ed.; Chapman and Hall, New York, (1986) 550.

44. S.A Ansari, P.N. Pathak, V.K. Manchanda, M. Husain, A.K. Prasad, V.S. Parmar, *Solv. Extr. Ion Exch*., 23 (2005) 463.

45. Cleveland, J.M. (1970) The Chemistry of Plutonium; Gordon and Breach Science Publishers: New York.

46. M. P. Jensen, T. Yaita, and R. Chiarizia; *Langmuir*, 23(2007)4765.

47. Zhu, Z.-X.; Sasaki, Y.; Suzuki, H.; Suzuki, S.; Kimura, T. *Anal. Chim. Acta*, 527(2004)163.

48. R.D. Shannon; *Acta Cryst. A*, 32 (1976) 751.

49. Y. Sasaki, Y. Sugo, S. Suzuki and S. Tachimori, *Solv. Extr. Ion Exch.*, 19 (2001) 91.

50.Y. Sasaki, P. Rapold, M. Arisaka, M. Hirata, and T. Kimura; *Solv. Extr. Ion Exch.*, 25 (2007) 187.

51. Y. Sasaki, Y. Sugo, S. Suzuki, T. Kimura; *Anal. Chim. Acta*, 543 (2005) 31.

52. S.K. Patil and D.D. Sood; *J. Radioanal. Nucl. Chem.*, 203 (1996) 547.

53. P.K. Mohapatra, L.B. Kumbhare, P.B. Ruikar, V.K Manchanda, *Solv. Ext. Ion Exch.*, 22 (2004) 267.

54. S. Panja, P.K. Mohapatra, S.C. Tripathi, V.K. Manchanda, *Sep. Sci. Technol.*, 45 (2010) 1112.

55. S. Panja, P.K. Mohapatra, S.C. Tripathi, V.K. Manchanda, *J. Membr. Sci.*, 337 (2009) 274.

56. A.J.B. Kemperman, D. Bargeman, T.V.D. Boomgaard, H. Strathmann, *Sep. Sci. Technol.*, 31 (1996) 2733.

57. S. Panja, P.K. Mohapatra, S.C. Tripathi, V.K. Manchanda, *Sep. Sci. Technol.*, 46 (2011) 94.

58. S. Sriram, P.K. Mohapatra, A.K. Pandey, V.K. Manchanda and L.P. Badheka; *J. Membr. Sci.*, 177(2000) 163.

59. C.R. Wilke and P. Chang; *AIChE J.*, 1(1955) 264.

60. P.K. Mohapatra, D.S. Lakshmi, D. Mohan and V.K. Manchanda; *Sep. Purif. Technol.*, 51 (2006) 24.

61. P.K. Mohapatra, D.S. Lakshmi, D. Mohan and V.K. Manchanda; *J. Membr. Sci.*, 232 (2004) 133.

62. A.Bhattacharyya, P.K. Mohapatra, A. Roy, T. Gadly, S.K. Ghosh and V.K. Manchanda; *Hydrometallurgy,* 99 (2009) 18.

63. S.A. Ansari, D.R. Prabhu, R.B. Gujar, A.S. Kanekar, B. Rajeshwari, M.J. Kulkarni, M.S. Murali, Y. Babu, V. Natarajan, S. Rajeswari, R. Manivannan, M.P. Antony, T.G. Srinivasan and V.K. Manchanda, *Sep. Purif. Technol*., 66 (2009) 118.

64. D. Magnusson, B. Christiansen, J. Glatz, R. Malmbeck, G. Modolo, D. Purroy and C. Sorel, *Solv. Extr. Ion Exch.*, 27 (2009) 26.

65. Y. Sugo, Y. Sasaki and S. Tachimori; *Radiochim. Acta*., 90 (2002) 161.

66. E.P. Horwitz, D.G. Kalina, G.F. Vandrift and W.W. Schulz, *Solv. Extr. Ion Exch*., 3 (1985) 75.

67. E. Hogefeldt (Ed.), Stability Constant of Metal ion Complexes, Part A: Inorganic Ligands, IUPAC Chemical Data Series No. 21, Pergamon, Oxford, 1982.

68. P.K. Mohapatra, V.K. Manchanda, *Sep. Sci. Technol*. 29 (1994) 1073.

69. S. Panja, P.K. Mohapatra, S.C. Tripathi, V.K. Manchanda, *Sep. Sci. Technol.*, 46 (2011) 94.

70. V.G.J. Rodgers, S.F. Oppenheim, R. Datta, *AIChE J.* 41 (1995) 1826.

71. D.S. Lakshmi, P.K. Mohapatra, D. Mohan, V.K. Manchanda, *Desalination*, 163 (2004) 13.

72. S. Nakamura, A. Sato, K. Akiba, *J. Radioanal.Nucl. Chem.*, Articles 178 (1) (1994) 63.

73. E. Mauerhofer, K. Zhernosekov, F. Roesch, *Radiochim. Acta,* 92 (2004) 5.

74. J. Crank, *The Mathematics of Diffusion*, 2nd Ed., Oxford University Press Inc., New York, (1975), p. 414.

75. C.B. Patil, P.K. Mohapatra, V.K. Manchanda, *Desalination*, 232 (2008) 272.

76. S. Tachimori, Y. Sasaki, S. Suzuki; *Solv. Extr. Ion Exch*., 20 (2002) 687.

77. Y. Sugo, Y. Sasaki and S. Tachimori, *Radiochim. Acta*, 90 (2002) 161.

78. V.K. Manchanda, P.N. Pathak, *Sepn. and Purif. Tech*. 35 (2004) 85.

79. H. Suzuki, Y. Sasaki, Y. Sugo, A. Apichaibukol and T. Kimura, *Radiochim. Acta* 92, (2004) 463.

80. Y.Marcus, Diluent effects in Solvent Extraction, *Solv. Extr. Ion Exch.* 7 (1989) 567.

81. R.A. Bartsch, E-G.Jeona, W.Walkowiaka, W. Apostoluk, *J. Membr. Sci.*, 159 (1999) 123.

82. S.Sriram, V.K.Manchanda, *Solv. Extr. Ion Exch.* 20 (2002) 97.

83. P.K. Mohapatra, D.S. Lakshmi, V.K. Manchanda, *Desalination,* 198 (2006) 166.

84. C.R. Wilke, P. Chang, Correlation of diffusion coefficients in dilute solutions. *AIChE J.,* 1 (1955) 264.

85. S. Panja, P.K. Mohapatra, A. Dakshinamoorthy and V.K. Manchanda; *Sep. Sci. and Technol.* 46(2011) 94.

Chapter IV

TRANSPORT OF ACTINIDES AND LANTHANIDES USING N,N,N’,N’-TETRA (2-ETHYL HEXYL) DIGLYCOLAMIDE (T2EHDGA)

4.1. Introduction

N,N,N’,N’-tetra (2-ethyl hexyl) diglycolamide (T2EHDGA, Fig. 4.1) is a branched chain homolog of TODGA having identical structure except for a branching on the alkyl substituent in the acyl nitrogen atom of the di-glycolamide. It is reported to favourably extract trivalent actinides similar to TODGA though higher decontamination factor values (with respect to the fission products) are expected due to stereochemical effects [1].

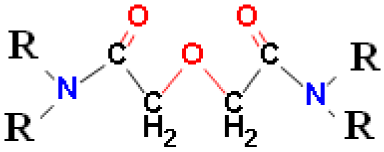

Fig. 4.1. Structure of T2EHDGA where R= (2-ethyl hexyl)

Solvent Extraction and Pilot scale Mixer-Settler studies with T2EHDGA for the separation of trivalent actinides and lanthanides have shown promising results [1]. Supported liquid membrane (SLM) transport studies of actinides and lanthanides using T2EHDGA as carrier have not been reported in literature. Present work was aimed at understanding the transport properties of actinides and lanthanides using T2EHDGA as the carrier across SLM.

4.2 Studies on the Transport of Trivalent Actinides

The current study was aimed at investigating the transport behavior of trivalent actinides, taking Am(III) as a representative element, from nitric acid medium. Various parameters were studied in detail to understand the different physicochemical factors responsible for Am(III) transport. Some of the parameters studied were feed acid concentration, concentration of T2EHDGA, membrane thickness etc. Understanding the mechanism of transport for Am(III) would help in applying T2EHDGA in Hollow Fiber module for remediation of large volumes of waste solution.

4.2.1. Solvent Extraction Studies

The extraction of Am(III) from nitrate medium with neutral T2EHDGA molecules is usually represented by the following expression:

$$Am^{3+}_{aq} + 3NO^{-}_{3(aq)} + n.T2EHDGA_{org} \overset{K_{ex}}{\Leftrightarrow} \hat{U}Am(NO_3)_3.nT2EHDGA_{org} \qquad (4.1)$$

The two-phase extraction constant (K_{ex}) can be expressed by the following equation:

$$K_{ex} = \frac{[Am(NO_3)_3.nT2EHDGA]_{org}}{[Am^{3+}]_{aq}.[NO^{-}_3]^{3}_{aq}.[T2EHDGA]^{n}_{org}} \qquad (4.2)$$

Since the distribution ratio of Am(III) ($D_{Am(III)}$)can be expressed by the ratio of total Am(III) concentration in the organic phase to that in the aqueous phase, Eqn. 4.2 can be modified as

$$D_{Am}=K_{ex}.[NO_3^-]^3_{(aq)}.[T2EHDGA]^n_{(org)} \qquad (4.3)$$

Taking log of both sides the eqn. becomes

$$\log D_{Am}=\log K_{ex}+3\log[NO_3]^-+n\log[T2EHDGA] \qquad (4.4)$$

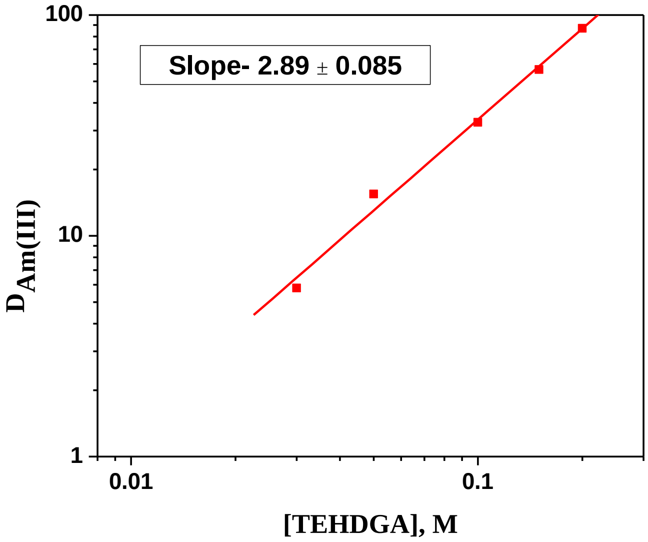

Fig. 4.2. Plot of D_{Am} vs T2EHDGA concentration in *n*-dodecane as diluent. Aqueous phase acidity: 3 M HNO_3

The value of 'n' has been determined to be close to 3 from the log-log plot of D_{Am} *vs* T2EHDGA concentration using *n*-dodecane as diluent at 3 M nitric acid concentration (Fig. 4.2). The value of 'n' for TODGA has been reported to be '4' [2]. The difference in number of carrier molecules being attached to Am(III) for TODGA and T2EHDGA may be due to the steric effect expected in the case of T2EHDGA due to its branched structure. From Eqn. (4.3) it is clear that nitric acid/nitrate concentration has a major role in the extraction of Am(III). To understand the effect of nitric acid concentration, solvent extraction studies were carried out at different acidities from 1 M to 6 M using 0.2 M T2EHDGA in *n*-dodecane.

As evident from Table (4.1), the D_{Am} values increased with increasing nitric acid concentration. This is due to the increase in nitrate ion concentration. Further, solvent extraction studies were carried out at a fixed nitrate ion concentration (using $NaNO_3$) but varying the nitric acid concentration. As evident from the Table (4.1), D_{Am} values increased with increasing nitric acid concentration. The increase in D_{Am} values with increasing nitrate concentration may be due to the nitrate ion facilitated extraction as evident from Eqn. (4.1) and also due to salting out effect. But by increasing the acidity at a fixed nitrate ion concentration, the same trend was observed which could not be explained as no significant H^+ ion extraction was observed.

4.2.2. Transport studies

4.2.2.1. Effect of Feed Nitric Acid/ Nitrate Concentration

Table4.1. Distribution data of Am(III) in T2EHDGA / *n*-dodecane, [T2EHDGA] = 0.2 M at varying acidity and nitrate ion concentration

$[NO_3^-]$ (HNO_3 +$NaNO_3$) in feed (M)	D_{Am}
(0.25 + 3.00)	12.8
(1.25 + 2.00)	41.5
(2.25 + 1.00)	69.5
(3.00 + 0.25)	95.7
(1.00 + 0.00)	3.40
(2.00 + 0.00)	32.2
(3.00 + 0.00)	87.1
(6.00 + 0.00)	141

A detailed study was carried out to understand the role of feed nitric acid concentration on the transport of Am(III). During the experiments, T2EHDGA concentration was kept at 0.2 M and 0.1 M HNO_3 was used as the strippant. Am(III) transport increased with the increase in nitric acid concentration in the feed up to 3 M and decreased thereafter. Near quantitative transport of Am(III) (99.62%) could be achieved in 3 h by using 3M nitric acid in the feed. Fig. (4.3) shows % transport of Am(III) transport at varying concentrations of HNO_3 in the feed. This is partly in agreement with the expected trend since the flux of a cation varies with NO_3^- ion concentration according to the relationship [3]:

$$J_M = \frac{(AT)[NO_3^-)_{aq}^n [Carrier]_{org}^n . C_{M,Feed}}{\eta} \qquad (4.5)$$

Where A is the area of the membrane (cm^2), T is absolute temperature (K), η is viscosity (1×10^{-3} Pa.s), $[Carrier]_{org}$ corresponds to concentration of T2EHDGA in the membrane phase and C_M is concentration of Am(III) in feed (mol/L).

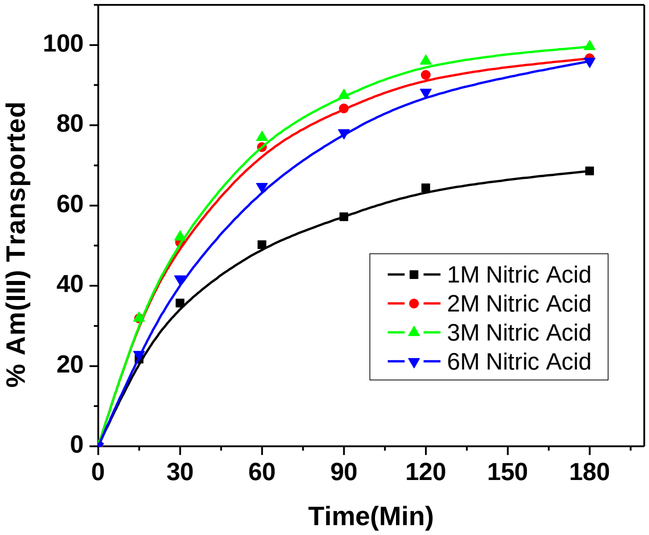

Fig. 4.3. Transport of Am(III) using 0.2 M T2EHDGA/*n*-dodecane as carrier from varying feed nitric acid concentration. Strippant- 0.1 M HNO_3 ; Membrane support: 0.45 µm PTFE

The increase in transport with increasing nitric acid concentration in THE feed from 1 M to 3 M is due to the increasing tendency of complex formation with increasing nitrate ion concentration while the reduction in transport from 3 M to 6 M is due to the formation of adduct between the extractant T2EHDGA and HNO_3 which decreases the concentration of free T2EHDGA available for complex formation. The strip phase acidity increased with increasing feed acidity (0.15 M for 1 M feed acidity to 0.35 M for 6 M feed acidity after 180 minutes). The increased strip phase acidity also reduced the stripping efficiency in the receiver phase and this could also be another reason for the lower transport rates in case of 6 M feed acidity. The same trend was also observed for the permeability coefficient values. The permeability coefficient value was found to be maximum (2.43×10^{-3} cm/s) at 3 M nitric acid as depicted in Table 4.2. In case of TODGA, maximum transport was found at 2 M HNO_3 [4]. In order to understand the role of H^+ ion on the transport of Am(III) through FSSLM containing T2EHDGA, experiments were carried out keeping the nitrate ion concentration fixed at 3.25 M and varying the HNO_3 concentration.

Table 4.2. Permeation coefficient data along with percentage transport of Am(III) using 0.2M T2EHDGA/n-dodecane as carrier at varying acidity and nitrate ion concentration of feed

$[NO_3^-]$ (HNO_3 +$NaNO_3$) in feed (M)	P ×10^3 (cm/s)	Transport after 180 min (%)
(0.25 + 3.00)	1.2	90.1
(1.25 + 2.00)	1.86	94.5
(2.25 + 1.00)	2.4	98.6
(3.00 + 0.25)	1.93	93.8
(1.00 + 0.00)	0.48	68.5
(2.00 + 0.00)	1.51	96.6
(3.00 + 0.00)	2.43	99.6
(6.00 + 0.00)	1.46	95.9

Table (4.2) shows the transport of Am(III) at a fixed nitrate ion concentration of 3.25 M but at different H^+ ion concentration varying from 0.25 M to 3 M. The maximum transport of 98.62% could be achieved when [$NaNO_3$] = 1 M and [HNO_3] = 2.25 M as can be seen from Table (4.2). The permeability coefficient value was found to be maximum in the above composition (2.4×10^{-3} cm/s, Table 4.2). The further decrease in permeability coefficient with increasing $NaNO_3$ concentration, is attributed to the competition of Na(I) ion with Am(III) [5].

4.2.2.2. Effect of Carrier Concentration

To understand the effect of T2EHDGA concentration in the membrane phase on the transport rate of Am(III), permeation experiments were carried out using varying concentrations of T2EHDGA (from 0.1 M to 0.3 M in n-dodecane as the diluent) supported on PTFE membranes (0.45 μm PTFE). Feed and strip phase acidities were maintained as 3 M HNO_3 and 0.1 M HNO_3, respectively. % Am(III) transported at varying concentration of carrier (Fig. 4.4) increased up to 0.2M of carrier concentration and decreased thereafter. The liquid membrane per traction of metal cations involves a heterogeneous chemical reaction between an organic carrier and the aqueous metal ion and so the metal flux (J_M) will be governed by the diffusion rates of the reactants in the presence of fast kinetics of interfacial reaction. The diffusion coefficient of a solute D, across the membrane is defined by the Stokes–Einstein equation (Eqn. 3.2). Generally, an increase in the carrier concentration will produce an increase in the cation flux. However, the concurrent increase in viscosity results in a steady decrease in the diffusivity of the carrier as well as of the metal-carrier complex. The transport of Am(III) should be a function of both the distribution coefficient and diffusion coefficient. In carrier-mediated transport of Am(III) with T2EHDGA, a more complex behavior was seen. Babcock et al. [6] have assigned the dominant effects that cause this "maximal phenomenon" to be due to: (i) the concentration gradient of the carrier-complex species (ii) the viscosity of the membrane phase and (iii) hindered diffusion of metal complex caused by aggregation of the complex.

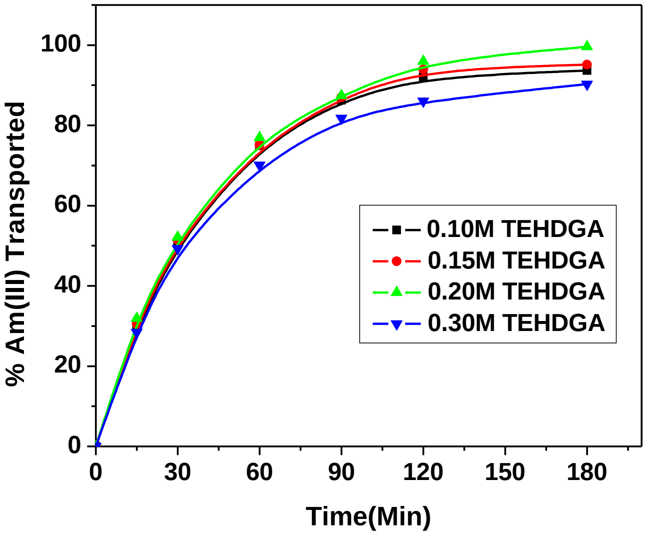

Fig. 4.4. Effect of carrier (T2EHDGA) concentration on the transport of Am(III). Feed: Am(III) in 3 M HNO$_3$; Strippant: 0.1 M HNO$_3$; Membrane support: PTFE (0.45 µm)

To understand the effect of carrier concentration on the transport of Am(III), various concentrations of T2EHDGA/ *n*-dodecane solutions, already equilibrated with the feed acidity, were used as carrier. From the results, it was quite clear that there was a significant increase in viscosity with increase in carrier concentration. From Fig. 4.5, it was evident that as the T2EHDGA concentration increased from 0.1 M to 0.3 M the viscosity increased from 1.62 to 2.35 mPa.s whereas the change in density was nominal from 0.758 to 0.779 g/cm^3. Since the flux is inversely proportional to the viscosity, an increase in the viscosity should reduce the flux, as was the case in the present study. Evidently, the organic phase viscosity proves to be a controlling parameter in the optimum carrier concentration for a liquid membrane system. Since an increase in the viscosity of T2EHDGA solutions may lead to decrease of the diffusion coefficient and hence permeability of the diffusing species, these opposing effects resulted in a maximum permeation at about 0.2 M T2EHDGA/ *n*-dodecane. With further increase in carrier concentration, the permeation decreased. The permeability coefficient was found to reach a maximum value (2.46×10^{-3} cm/s) for 0.2 M T2EHDGA/ *n*-dodecane as carrier at 3 M HNO_3. In case of TODGA, 0.1 M TODGA/ *n*-dodecane was found to be the optimum carrier concentration [4].

4.2.2.3. Effect of Nature of Strippant

Transport of metal ion across FSSLM is strongly dependent on the nature of the strippants used. Detailed experiments were carried out to understand the role played by stripping solution in the transport of Am(III) using T2EHDGA as the carrier. Different strippant mixtures such as distilled water, a buffer mixture (HFC consisting of 0.4 M hydrazine hydrate, 0.4 M formic acid and 0.1 M citric acid) [7], 0.1 M oxalic acid and 0.1 M nitric acid were studied for Am(III) transport. It was observed that among the strippants, 0.1M nitric acid proved to be the most efficient for stripping of Am(III) from membrane phase. Fig. (4.6) shows that near quantitative recovery of Am(III) was possible at ~3 h with 0.1M nitric acid as also observed in the case of TODGA [4].

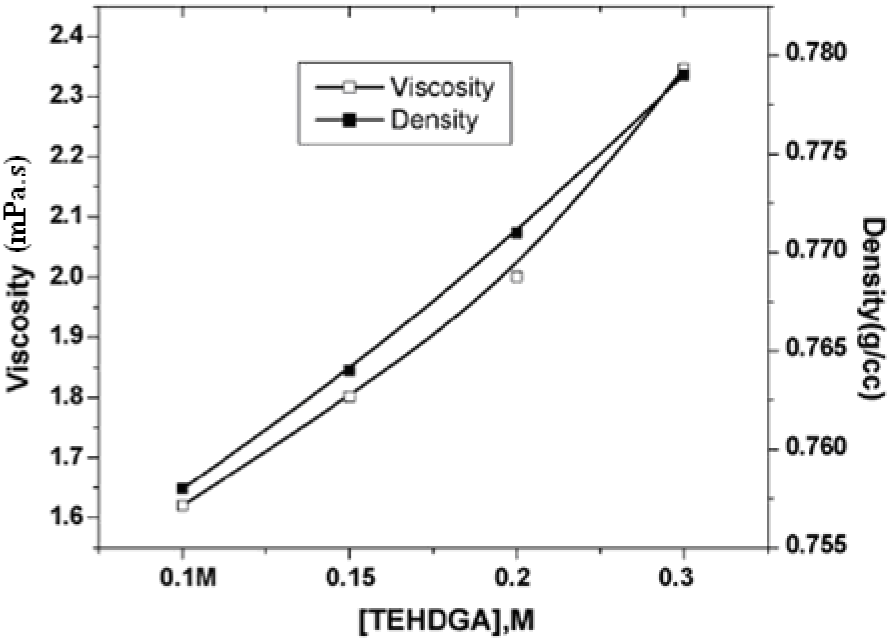

Fig. 4.5. Viscosity and density of varying concentration of T2EHDGA equilibrated with 3 M HNO_3

4.2.2.4. Effect of pore size of membrane support

The transport rate across an FSSLM depends on factors like the amount of carrier held in the pores of the filters, pore structure and pore size, the thickness, porosity and tortuosity of membrane, etc. [8,9]. In order to understand the effect of membrane pore size on the transport rates of Am(III) using T2EHDGA as the carrier, PTFE sheets with varying pore sizes, viz. 0.2, 0.45, 1.2 and 5.0µm were used. Membrane pore size has a very distinct role in the permeation rate of metal cation in the membrane studies. From

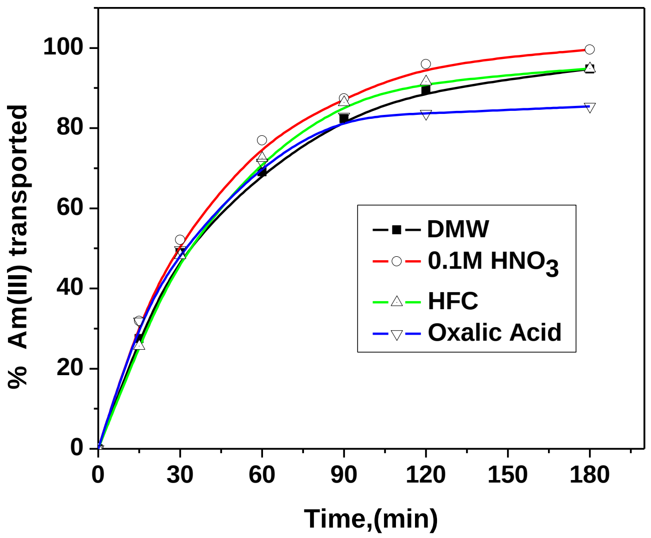

Fig. 4.6. Variation of transport rate of Am(III) using varying strippants. Feed: Am(III) in 3 M HNO_3; Carrier: 0.2 M T2EHDGA/ *n*-dodecane; Membrane support: PTFE (0.45 μm)

Stokes–Einstein law (Eqn. 4.5), the diffusion coefficient of the complex is inversely related to the radius of the diffusing complex. Therefore, higher the pore size, lower is the resistance experienced by the complex species which results in higher transport rate for higher pore size membranes. The effect of porosity and tortuosity can be expressed by the equation [10]:

$$D_m = \frac{D.\theta}{\tau} \tag{4.6}$$

Where D_m is the diffusion coefficient of the Am-T2EHDGA complex, θ and τ are the porosity and tortuosity of the membrane, respectively.

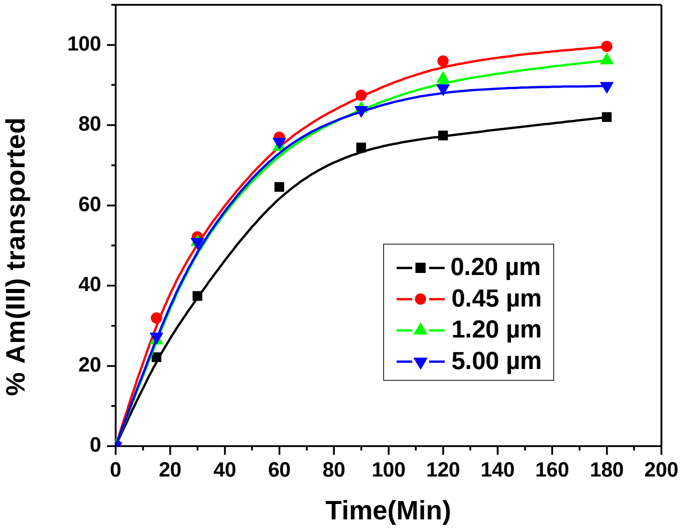

Fig. 4.7. Variation of transport rate of Am(III) against varying membrane pore size. Feed: 3 M HNO_3; strippant: 0.1 M HNO_3; Carrier: 0.2 M T2EHDGA/ *n*-dodecane; Membrane support: PTFE of varying pore size

With increasing membrane pore size, porosity of the membrane increases where as the tortuosity of the membrane decreases as shown in Table (4.3). So both these effects result an increase in the transport rate of Am with increasing membrane pore size. But for diffusion controlled transport process, transport rate also depends on the effective diffusion path length. This can be very well understood from Eqn. (4.7) which clearly indicates that P is inversely proportional to the thickness of the membrane support in diffusion controlled process [5].

$$P = \frac{D_0.D_M}{\tau.\ d_0} \tag{4.7}$$

As evident from Table 4.3, membrane thickness increases with increasing membrane pore size which causes an increase in the diffusion path length of Am-T2EHDGA complex. This results a decrease in the transport rate with increasing membrane pore size. Hence as an optimum condition of these effects mentioned, transport rate increases from 0.2 µm pore size to 0.45 µm pore size and then decreases thereafter up to 5 µm as shown in Fig. 4.7.

Table 4.3. Various physical parameters of the membrane

Pore size (µm)	**Thickness (µm)**[a]	**Porosity, θ** [b]	**Tortuosity, τ** [b]
0.20	65	0.51	2.15
0.45	80	0.64	1.44
1.20	90	0.74	1.22
5.00	100	0.84	1.00

[a]: Data from Catalogue of Sartorious AG Germany.[b]: From Ref. [5].

4.2.2.5. Selectivity over Fission Products

In order to determine the selectivity of T2EHDGA for actinides and lanthanides over different fission products, we carried out transport studies taking a feed solution containing different fission products, e.g., Ru(multivalent), Cs(I), Zr(IV), Nb(IV), Ce(III) at 3 M HNO_3 using 0.2 M T2EHDGA/n-dodecane taking 0.1 M HNO_3 as the strippant. As evident from Fig. (4.8) only Ce being a trivalent lanthanide got transported ~90% in 240min. Among the other fission products only Cs got transported ~8% and all other fission products got transported insignificantly (~1%). Ru inspite of being multivalent did not get transported in significant amount. Fe(III) too got transported to a much lower extent (~4%) though it existed in the trivalent state. This is probably because the rate constant for exchange of inner sphere water molecules of the hydrated Fe(III) ions is about five orders of magnitude lower as compared to trivalent lanthanides which may be taken as analogues of Am(III) [5]. Hence T2EHDGA can be used selectively to separate trivalent actinides and lanthanides from fission products with high selectivity.

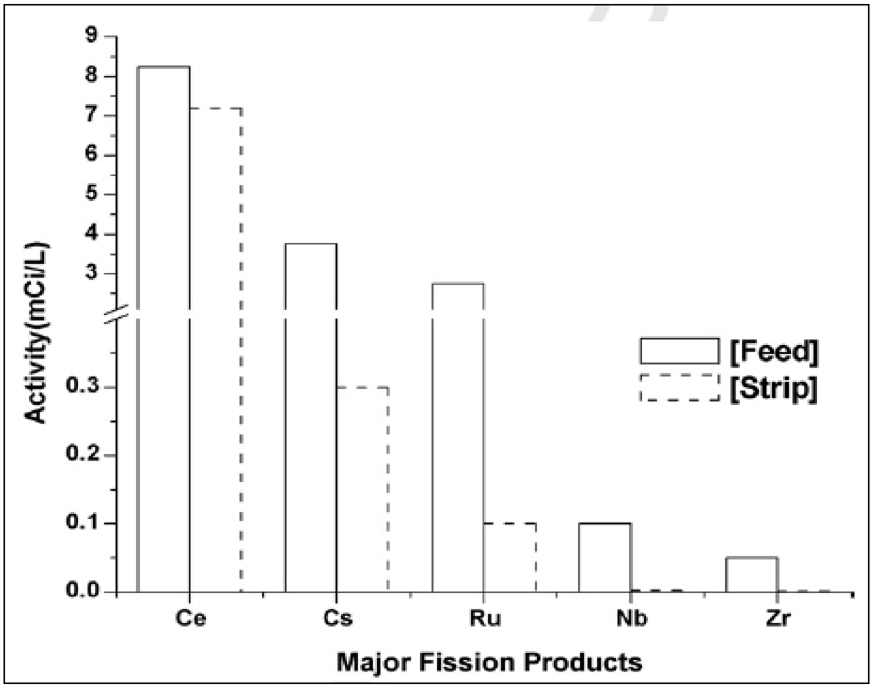

Fig. 4.8. Transport of various fission products across T2EHDGA/ *n*-dodecane FSSLM. Feed: Major F.Ps. in 3 M HNO_3; strippant: 0.1 M HNO_3; Carrier: 0.2 M T2EHDGA/dodecane; Membrane support: PTFE (0.45 μm)

4.2.2.6. Stability of Supported Liquid Membrane

The polymer supports used in supported liquid membranes are generally having pores which adsorb the organic solution or carrier within its moieties. This organic solution is held within its pores by the capillary forces of these pores. After prolong use, these membranes start to degrade. The degradation of the membranes can be because of the one or accumulative effect of chemical degradation, loss of carrier and/or solvent by dissolving in adjacent aqueous phases, leaching out of the membrane carrier by an osmotic or hydrostatic pressure gradient, formation of emulsion or reverse micelles, etc.

Sometimes stability of these membranes may be affected due to the chemical degradation of the support material. Hence studies were performed to see the stability of these membranes as a carrier leaching out of the support and integrity of the support material point of view. The chemical resistance of PTFE membranes against T2EHDGA/dodecane was periodically tested over a period of 30 days by keeping it dipped in 0.2 M carrier solution. Experiments carried out using 3 M HNO_3 as feed, 0.2 M T2EHDGA in n-dodecane as carrier and 0.1 M HNO_3 as the strippant showed that there was no significant change in the transport of Am(III) over a period of 30 days, thereby suggesting that the integrity of the support was not affected during this period. The stability of membrane, with respect to carrier leaching out, was checked by operating the same membrane over the period of 22 days continuously and it was found that there was no significant decrease in percentage transport of Am(III) over the first fourteen days of operations and then marginal decrease in percentage transport of Am(III) was observed (Fig. 4.9). Hence the stability of the membrane was found to be quite satisfactory over the time period studied.

4.3. Eu(III) Transport

Transport behavior of trivalent actinides using T2EHDGA as carrier across FSSLM has been described in detail in the previous section. However, in view of the large concentration of the trivalent lanthanides present in the high level waste (about 2-3 g/L in HLLW of fuel with a burn up of 33 GWD/te), it was required to understand the

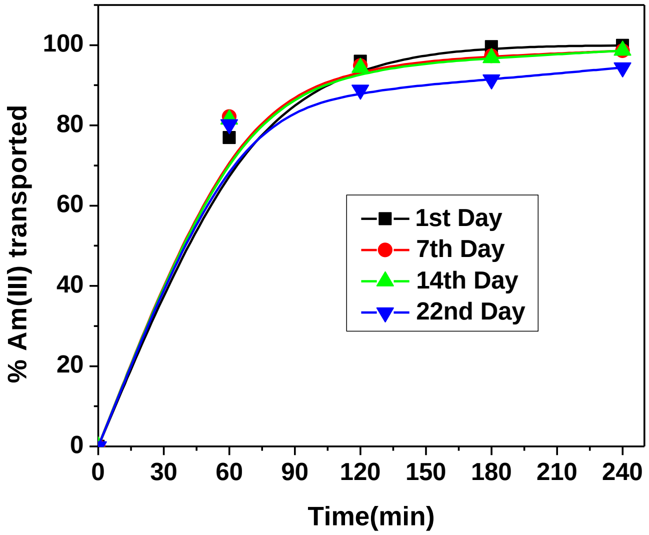

Fig. 4.9. Stability of PTFE membrane for Am(III)-T2EHDGA for carrier leaching. Feed: Am(III) in 3 M HNO_3; Strippant: 0.1 M HNO_3; Carrier: 0.2 M T2EHDGA/dodecane; Membrane support: PTFE (0.45 µm)

extraction and transport behavior of Eu^{3+} (surrogate for all the trivalent lanthanides) under acidic feed conditions similar to the HLLW.

The present study involves the extraction and transport studies involving Eu^{3+} using T2EHDGA in *n*-dodecane as the carrier solvent which also contained *iso*- decanol as the phase modifier. The SLM transport studies involved the effect of membrane pore size, feed acidity, Eu concentration in the feed, phase modifier composition etc on the transport rate of Eu^{3+}. Diffusion parameters have also been calculated and compared with the Am^{3+} - T2EHDGA transport system reported above.

4.3.1. Solvent Extraction Studies

4.3.1.1. Nature of the Extracted Species

Extraction of Eu(III) by T2EHDGA in *n*-dodecane can be represented by the following equilibrium reaction:

$$Eu^{3+} + 3NO_3^{-} + nT2EHDGA_{(o)} \rightleftharpoons Eu(NO_3)_3.n(T2EHDGA)_{(o)} \qquad (4.8)$$

Where the species with the subscript ‘(o)’ indicate those in the organic phase and those without any subscript indicate the species in the aqueous phase. The number of extractant molecules associated with the extracted species was reported to be 3 for the analogous Am(III)-T2EHDGA extraction system while n was reported to be 4 for the Am(III) – TODGA extraction system [4] which was ascribed to reverse micelle formation involving 4 TODGA molecules [10]. Eu(III) extraction studies carried out at varying T2EHDGA concentration indicated extraction of species of the type $Eu(NO_3)_3.3(T2EHDGA)_{(o)}$ (Fig. 4.10) suggesting participation of three T2EHDGA molecules similar to the Am(III)-T2EHDGA extraction studies reported above. It appears that the branched structure of T2EHDGA restricts the number of extractant molecules in the extracted species to 3 instead of 4 due to steric factors.

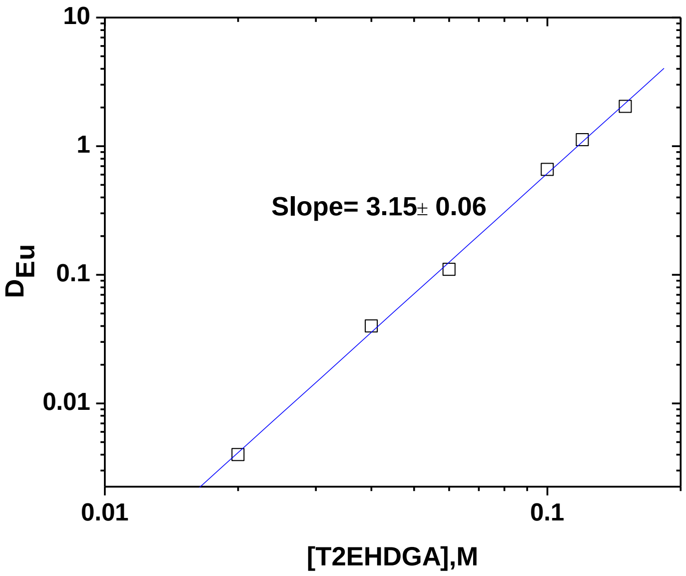

Fig. 4.10. Dependence of $K_{d,Eu}$ on T2EHDGA concentration. Aqueous phase acidity: 3 M HNO_3

4.3.1.2. Effect of the Feed Acidity

The extraction of Eu^{3+} by T2EHDGA takes place by nitrate ion assisted complexation as shown in Eqn. (4.8). With increasing nitric acid concentration in the aqueous phase, the D value of Eu increases from 0.76 at 0.5 M HNO_3 to 164 at 3 M HNO_3. On further increasing the aqueous phase acidity to 6 M HNO_3 third phase formation was observed. It was required, therefore, to use a phase modifier to prevent the formation of the third phase. The data on distribution ratio against different concentration of HNO_3 using 0.2 M T2EHDGA in the absence and the presence of *iso*-decanol is given in Table (4.4).

Table 4.4. Distribution data of Eu(III) using 0.2M T2EHDGA in the absence and the presence of 30% *iso*-decanol as extractant against varying concentration of HNO_3

$[HNO_3]$, M	$K_{d,Eu(III)}$ (0.2 M T2EHDGA)	$K_{d,Eu(III)}$ (0.2M T2EHDGA + 30% *iso*-decanol)	$P \times 10^4$(cm/s) (0.2M T2EHDGA)
0.5	0.76	0.64	0.76
1	4.36	4.15	3.54
2	67.87	36.1	10.02
3	164.75	114	6.19
6	Third phase	166	2.77

4.3.1.3. Effect of Phase Modifier

Earlier studies on the effect of phase modifier on the prevention of third phase with T2EHDGA have suggested *iso*-decanol as the most promising [11]. Therefore, 30% *iso-decanol* was chosen as the phase modifier for 0.2 M T2EHDGA and the distribution ratio data is presented in Table 4.4. Though the third phase problem was alleviated with the addition of the phase modifier, the D_{Eu} values were found to decrease in its presence which was attributed to the change in polarity of the solvent system. Studies were also carried out at varying percentage of the phase modifier. Table 4.5 shows that with increasing *iso*-decanol concentration from 0 to 40%, the D_{Eu} for Eu(III) value decreased which was ascribed to the increasing polarity of the organic phase which is not favorable for the extraction of the solvated species as given in Eqn. (4.8).

Table 4.5. Distribution data for Eu(III) at 3 M HNO_3 using 0.2 M T2EHDGA as extractant in presence of varying concentration of *iso*-decanol

% *iso*-Decanol (0.2 M T2EHDGA)	**$D_{Eu(III)}$ (3 M HNO_3)**	**P (cm/s) × 10^4 (3M HNO_3)**
0	164.75	6.19
10	149.52	4.72
20	135.45	2.89
30	113.95	2.65
40	91.77	2.60

4.3.2. Transport Studies

4.3.2.1. Effect of the Feed Acidity

As the metal ion pertraction is a consequence of its extraction at the feed– membrane interface, the transport of Eu(III) from nitric acid medium takes place via nitrate ion assisted extraction suggesting feed nitric acid concentration should play a major role in the transport rate of Eu(III). A continuous increase in the Eu pertraction with feed acidity was observed up to 3 M HNO_3 beyond which a significant decrease was seen for 6 M HNO_3. This observation was similar to our report on Am^{3+}-T2EHDGA supported liquid membrane work. On the other hand, maximum transport rate for the Am^{3+}-TODGA system was observed at 2 M HNO_3 which decreased considerably at 6 M HNO_3 [4]. In the present study, the transport rate was found to increase upto 2 M HNO_3 and then there was significant decrease at 6 M HNO_3 (Fig. 4.11). The permeability coefficient values are also calculated and are listed in Table (4.4). This trend was followed to be similar to that of Am^{3+}-T2EHDGA system except that maximum transport was observed at 3 M HNO_3.

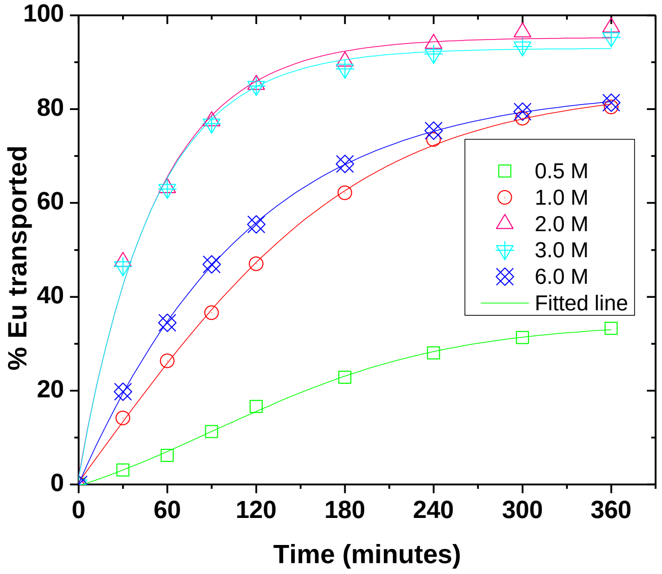

Fig. 4.11. Effect of feed acid concentration on the transport of Eu^{3+} ion. Receiver: 0.01 M HNO_3; Carrier: 0.2 M T2EHDGA; Membrane Support: 0.45 micron PTFE

The reason behind the increase in transport rate with increasing feed acidity is partly due to the increase in D with nitric acid concentration as indicated in Table (4.4). However, T2EHDGA being acidic in nature (K_H = 2.1) has tendency to form adduct with HNO_3 itself and this trend increases with increasing feed HNO_3 concentration. The formation of adduct with HNO_3 causes a decrease in the free T2EHDGA concentration in the membrane phase which can result in lower D of Eu^{3+} at higher acidities. This is the possible reason for the transport rate to decrease at higher feed acidity. Another reason behind the decrease in transport rate at higher acidity could be due to increasing acidity of the receiver phase which can lead to inefficient stripping of the metal ion. It may be mentioned here that the acidity of the receiver phase increases from 0.25 M at 1 M HNO_3 to 0.5 M at 6 M HNO_3 in ~5 h time.

4.3.2.2. Effect of T2EHDGA Concentration

Facilitated transport of a metal ion across a SLM takes place through complexation of metal ion with the carrier molecule at the feed – membrane interface followed by its release at the membrane – receiver interface. Therefore, the concentration of the carrier molecule in the membrane phase plays a very important role in the overall transport process. Generally, it is observed that there is a maximum concentration of carrier which gives highest transport rate of any metal ion. This “maximal phenomenon” has been assigned by Babcock et al., [6] due to factors such as: i) concentration gradient of the metal-carrier complex ii) viscosity of the complex iii) hindered diffusion of the metal complex due to the aggregation of the carrier. With increasing carrier concentration the first parameter becomes dominant causing transport rate to increase. But after a certain concentration of the carrier, viscosity and aggregation of the carrier molecule increase. Both these effects cause the transport to decrease. These facts have been investigated in detail in the experiments where concentration of T2EHDGA has been varied from 0.1 M to 0.3 M keeping all the other parameters fixed. As can be seen from Fig. (4.12), the transport rate increased up to 0.15 M T2EHDGA beyond which the transport rate was found to decrease. In about 360 minutes ~99.95% Eu(III) got transported to the receiver phase for 0.15 M T2EHDGA which got reduced to ~ 95.3% at the same time frame when 0.2 M T2EHDGA was used as the carrier solvent. As seen from Table (4.6), the permeability co-efficient value for 0.1 M T2EHDGA was 5.07×10^{-4} cm/s which increased to a maximum value of 11.2×10^{-4} cm/s for 0.15 M T2EHDGA. When Am(III) transport behavior using T2EHDGA as the carrier was compared, 0.2 M was found to be the optimum concentration where the permeability-coefficient value was 24.6×10^{-4} cm/s (Table 4.6). In view of this, 0.2 M T2EHDGA was chosen as the optimum carrier concentration for all other studies.

4.3.2.3. Effect of the Phase Modifier Concentration

The solvent extraction studies have indicated that 30% *iso*-decanol, when used as the phase modifier, prevented third phase at higher acidities and also in the presence of higher concentration of metal ion. Very few studies have been carried out to see the behavior of phase modifier on the transport rate of metal ions. We have investigated the effect of varying concentration of *iso*-decanol with 0.2 M T2EHDGA on the transport rate of U(VI) and found that the transport rate decreased with increasing concentration of the phase modifier [12]. Same trend was observed for Eu^{3+}-T2EHDGA system in the present studies. Transport rates for this system are shown in Fig. (4.13) while the permeability coefficient values are listed in Table 4.6.

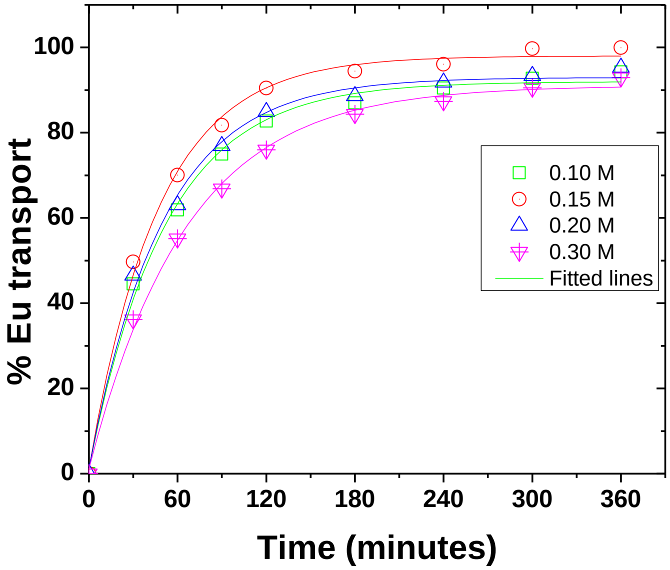

Fig. 4.12. Effect of T2EHDGA concentration on the transport of Eu^{3+} ion. Feed: 3.0 M HNO_3; Receiver: 0.01 M HNO_3; Support: 0.45 micron PTFE

It was observed that in the absence of any phase modifier about 95% Eu(III) got transported in 5 h when the feed acidity was 3 M HNO_3 while 0.01 M HNO_3 was used as the receiving phase. This rate was found to decrease continuously from 0 to 40% *iso*-

Table 4.6: Comparative permeability coefficient data for Eu(III) and Am(III) using different concentration of T2EHDGA/ *n*-dodecane from 3 M HNO_3

[T2EHDGA], M	$P_{Eu} \times 10^4$(cm/s)	$P_{Am} \times 10^4$(cm/s)
0.10	5.07	20.8
0.15	11.2	18.7
0.20	6.19	24.6
0.30	4.84	15.2

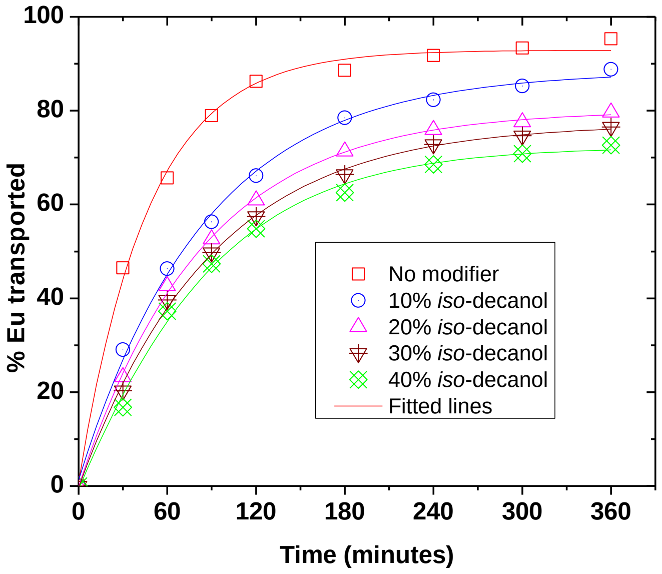

Fig. 4.13. Effect of phase modifier composition on the transport of Eu^{3+} ion. Feed: 3 M HNO_3, Receiver: 0.01 M HNO3, Support: 0.45 micron PTFE

decanol and about 72% Eu(III) got transported in the presence of 40% *iso*-decanol after 5 h and are attributed to the increased polarity of the medium.

4.3.2.4. Effect of Membrane Pore Size

The effect of membrane pore size in SLM on the transport of a metal ion for a particular carrier molecule is given by the Eqn. (3.12). This equation clearly shows that with increasing membrane pore size, the diffusing complex of metal-carrier faces less resistance and consequently the transport rate is higher. However, the Laplace's equation tells us that the pore size can not be increased infinitely to get higher transport as very high pore size means easy displacement of the carrier from the pores. This is shown by th Eqn. (3.13) based on which the transport rate should decrease with increasing pore size of the membrane. However for the Am(III)-T2EHDGA system, there was an initial increase in transport rate followed by a decrease. The plot of P vs membrane pore size for the present system is depicted in Fig. (4.14) and follows a decreasing trend with increasing membrane pore size. This signifies that for the system studied here increasing membrane pore size plays a destabilizing effect.

4.3.2.5. Effect of Eu Concentration

In actual HLW the concentration of lanthanides depends on the burn up of the fuel and can be as high as 3-4 g/L. Taking Eu as a surrogate of the rare earth elements the effect of Eu carrier concentration on the transport rate of Eu^{3+} was investigated using T2EHDGA as the carrier extractant. Eu carrier concentration was varied from 0.1 g/L to 10 g/L keeping 3 M HNO_3 as feed acidity while maintaining all other parameters identical. The transport rate against varying Eu carrier concentration is plotted in Fig. (4.15) which indicated that the transport rate decreased significantly

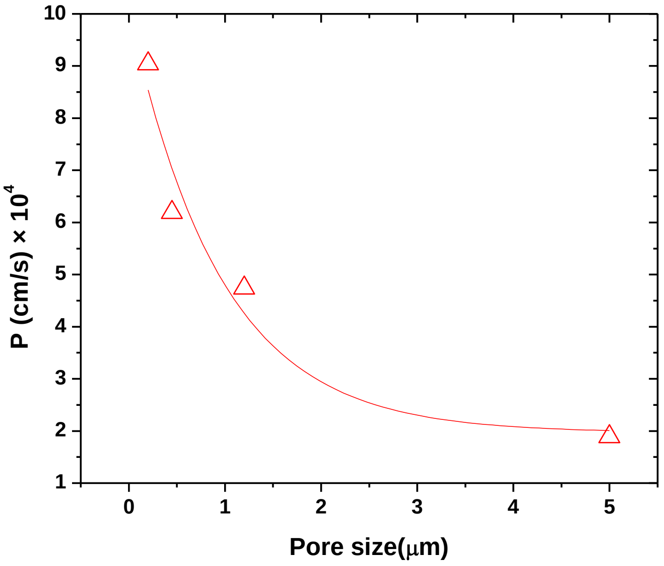

Fig. 4.14. Effect of membrane pore size on Eu^{3+} ion permeability coefficients. Feed phase: 3.0 M HNO_3; Carrier: 0.2 M T2EHDGA; Receiver: 0.01 M HNO_3

with increasing Eu concentration in the feed. This is in the expected line due to the limited availability of carrier molecule in the membrane phase for complexation. Similar trend was observed by Nakamura et al., [13] for Eu loading using a phosphinic acid extractant. The flux values were calculated to be 3.44 × 10^{-7} mol cm^{-2} s^{-1} for 0.1

g/L Eu which increased to 5.79 × 10^{-6} mol cm^{-2} s^{-1} for 10 g/L Eu (Fig. 4.16). For feed containing 3-4 g/L Eu carrier, the flux appears to be reasonable suggesting the feasibility of application of the supported liquid membrane system for the separation of rare earth element from acidic radioactive wastes such as the high level waste.

4.3.2.6. Thermodynamics study

Transport studies were carried out at varying temperatures to evaluate the activation energy of the transport of Eu^{3+} using T2EHDGA as the carrier extractant. Transport

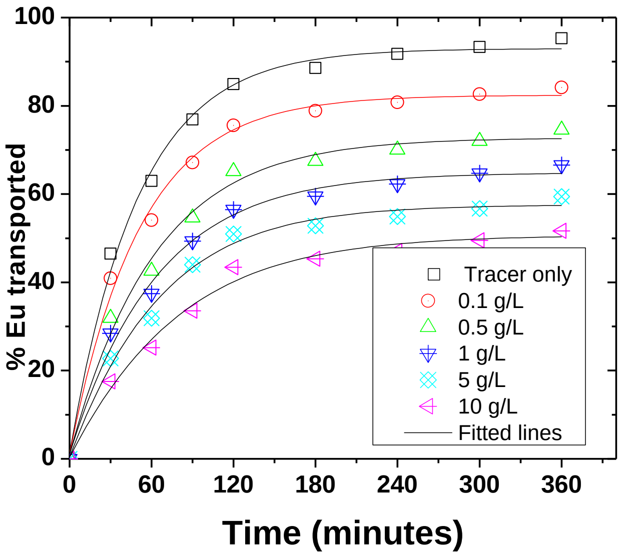

Fig. 4.15.Effect of Eu concentration on Eu^{3+} ion transport. Feed: 3.0 M HNO_3; Receiver : 0.01 M HNO_3; Carrier: 0.2 M T2EHDGA

rates measured at four different temperatures viz. 23, 30, 40 and 50^{o} C (Fig. 4.17) suggested that the transport becomes significantly faster at higher temperatures which are reasonable as the viscosity of the medium decreases with temperature thereby leading to more facile diffusion of the complex species as indicated from the Stokes – Einstein equation. The thermodynamic parameters were calculated from the

van't Hoff plots as well as the Gibbs – Helmholtz equation as follows. Free energy change for the extraction equilibria can be expressed as

$$\Delta G^{o} = -2.303 \text{ RT} \ln P \qquad (4.9)$$

$$\Delta G^{o} = \Delta H^{o} - T\Delta S^{o} \qquad (4.10)$$

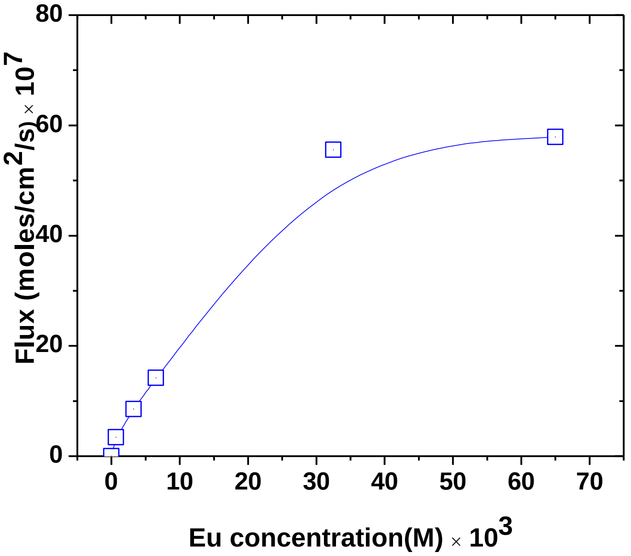

Fig. 4.16. Effect of Eu concentration on Eu^{3+} ion flux. Feed: 3.0 M HNO_3; Receiver: 0.01 M HNO_3; Carrier: 0.2 M T2EHDGA

From Eqns. (9) and (10),

$$\text{Ln } P = -(\Delta H^o/R)(1000/T) + (\Delta S^o/R) \qquad (4.11)$$

where R (8.314 $JK^{-1}mol^{-1}$) is the universal gas constant. ΔH^o (in $kJ.mol^{-1}$) and ΔS^o (in $J.K^{-1}.mol^{-1}$) were therefore calculated from the slope ($-\Delta H^o / R$) and intercept

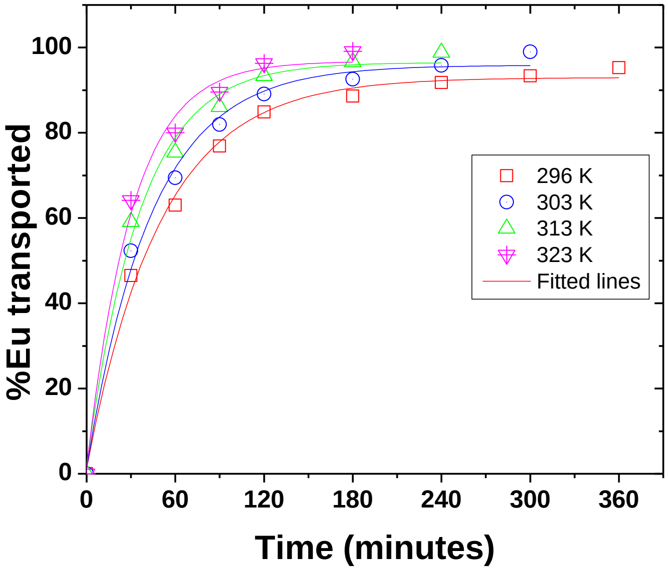

Fig. 4.17. Effect of temperature on Eu^{3+} ion transport. Feed: 3.0 M HNO_3; Receiver: 0.01 M HNO_3; Carrier: 0.2 M T2EHDGA

(ΔS^o / R) of the plot of ln P vs 1000/T (Fig. 4.18).The ΔH^o and ΔS^o values were calculated to be 26.5$\pm$2.4 kJ.mol^{-1} and 28.6$\pm$7.7 J.K^{-1}.mol^{-1}, respectively.

4.3.2.7. Calculation of diffusion parameters

The diffusion coefficient D_o can be calculated as per the empirical Wilke–Chang equation [14] (Eqn. 3.17). The association parameters for the diluents are taken as unity [14]. The molar volume of T2EHDGA was calculated to be 909.42 cm^3.mol^{-1} [15]. Using the dynamic viscosity value for 0.2 M T2EHDGA as 2.001 mPa.s, and assuming that the extracted species contained the diffusion coefficient (D_o) was calculated from eqn. (4.12) to be 4.25x10^{-6} cm^2/s which is higher than the value reported for Am^{3+} in an identical transport system for a feed containing 3 M HNO_3. The higher diffusion coefficient value is attributed to the approximations made in the Wilke – Chang model where the molar volume of the complex was calculated by taking three T2EHDGA molecules and three nitrate ions and the molar volume of Eu^{3+} ion has been ignored.

4.4. Hexavalent actinide [U(VI)] transport

4.4.1. Introduction

Uranium along with the trivalent actinides and lanthanides constitute a major part of High Level Waste (HLW). The concentration of U in HLW can be more than 10g/L. Actinide partitioning strategists have proposed two different procedures: one is U removal prior to Actinide partitioning step and in another there is no prior removal of U. U removal is not a part of actinide partitioning using T2EHDGA as it does not suffer

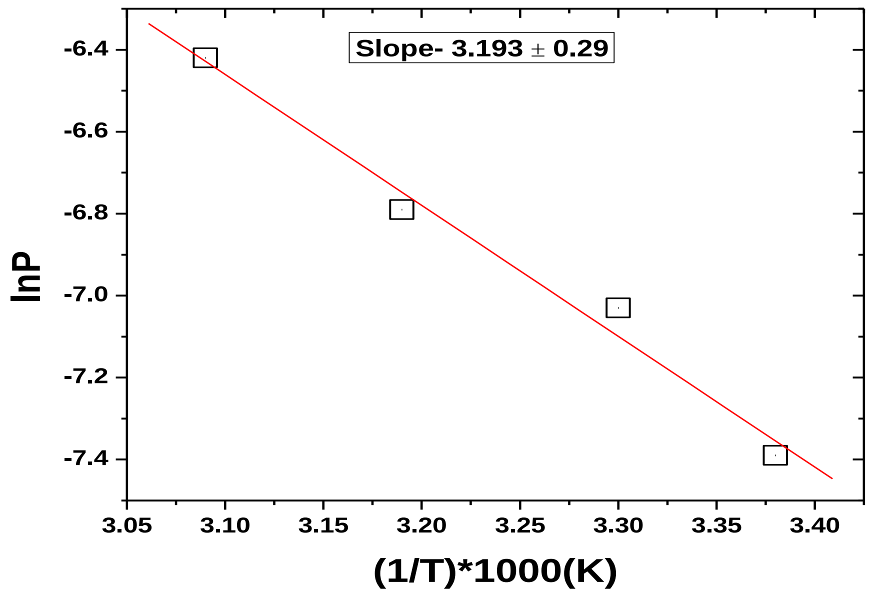

Fig. 4.18. Arrhenius plot of Eu^{3+} transport. Feed : 3.0 M HNO_3; Receiver: 0.01 M HNO_3; Carrier: 0.2 M T2EHDGA

the problem of third phase problem as encountered for the reagent N,N-isobutyl carbamoyl methyl phosphine oxide (CMPO) when used along with phase modifier(30% *iso*-decyl alcohol) even in presence of 10-12 g/L of U [16].

So it is very important to understand the transport behavior of U from HNO_3 medium using T2EHDGA as carrier prior to testing the reagent for actinide partitioning in Hollow Fiber module using actual HLW. Hence an attempt was made to carry out the transport behavior of U(VI) from HNO_3 medium and understand the effect of various parameters that effect the transport it using T2EHDGA as carrier in FSSLM mode. Feed acidity, carrier concentration, membrane pore size, membrane thickness, concentration of phase modifier, U concentration etc was varied and optimized for maximum permeation of the metal. Mechanism of membrane transport was established and membrane transport data like permeability coefficient, diffusion coefficient etc were calculated and compared with TODGA, a straight chain homologue of T2EHDGA.

4.4.2. Solvent Extraction studies

4.4.2.1. Effect of Phase Modifier Concentration

T2EHDGA was found to form third phase at higher acidities and under loading conditions and a phase modifier was required to mitigate this problem [1]. Out of the various reagents used as phase modifier, *iso*-decanol was found to be the most suitable due to its lower acid uptake [1]. The composition of the solvent, proposed for actinide partitioning, was 0.2 M T2EHDGA / *n*-dodecane with 30% *iso*-decanol [11]. In the present study, the distribution behaviour of U(VI) was investigated at varying concentrations of nitric acid with as well as without the phase modifier (30% *iso*-decanol). For comparison purpose, the solvent extraction data with 0.1 M TODGA in *n*-dodecane are also reported (Table 4.7). It is clear from the Table that the extraction efficiency of T2EHDGA decreased in the presence of 30% *iso*-decanol. This behavior is analogous to those obtained with other diglycolamide extractants, such as TODGA, which also show lower extraction efficiency in the presence of phase modifiers [17]. It is expected that the diglycolamides form reverse micelle aggregates in non-polar mediums such as *n*-dodecane [10]. By adding a polar phase modifier such as *iso*-decanol the aggregate formation is seriously affected. Though the polarity increase helps in increasing the limiting organic concentration (LOC) of the extracted complex (thereby suppressing the third phase formation), the D values show a decreasing trend, probably as a result of the deaggregation of the reverse micelles.

4.4.2.2. Effect of Feed HNO_3 Concentration

The solvent extraction data presented in Table 4.7 also show that increasing the nitric acid concentration increases the D value of U. This is expected as solvated species are extracted as will be discussed below. However, the D values of T2EHDGA increased more sharply with nitric acid concentration as compared to TODGA. When $NaNO_3$ was used in the feed in the absence of nitric acid, the D values were significantly enhanced and the enhancement was more prominent at lower $NaNO_3$ concentration. On the other hand, in TODGA system, an entirely opposite trend was observed, i.e., the D values were lower in the presence of $NaNO_3$ as compared to those in the presence of HNO_3. These results suggest that the presence of $NaNO_3$ may be responsible for breaking the TODGA aggregates thereby causing the drastic decrease in the D_U values. On the other hand, an entirely opposite trend was observed with T2EHDGA, i.e., the D_U values increased in the presence of $NaNO_3$, the reason for which is yet to be understood.

4.4.2.3. Nature of the Extracted Species

Extraction of U was also studied with varying concentration of T2EHDGA in *n*-dodecane and 30% *iso*-decanol as the phase modifier. In a previous report, Zhu et al. have suggested extraction of solvated species of the type $UO_2(NO_3)_2.nL$ where L represented the diglycolamide extractant [18]. The extracted species conform to the following extraction equilibrium:

$$UO_2^{2+} + 2(NO_3^-) + n\ L_{(o)} \ {}_{\backslash}{=}{=}^{\backslash}\ UO_2(NO_3)_2.nL_{(o)} \qquad (4.13)$$

where the species with the subscript ‘(o)’ indicate those in the organic phase and those without any subscript indicate species in the aqueous phase. The T2EHDGA concentration variation experiments indicated a dependence of ~ 1 when log D was plotted against log [T2EHDGA] (Fig. 4.19) suggesting that the extracted species is $UO_2(NO_3)_2.T2EHDGA_{(o)}$. Similar species was reported by us for the extraction studies involving TODGA [19]. However, Sharma et al., reported a species of the type $UO_2(NO_3)_2.T2EHDGA_{(o)}$ which is in sharp contrast to the species reported by us [20]. On the other hand, a recent structural analysis of a uranyl diglycolamide extract from nitrate medium conform to the presence of a single tridentate diglycolamide unit which is in conformity with our observation [21].

Table 4.7. D_U with varying feed nitrate concentration in the absence and presence of the phase modifier for T2EHDGA as extractant

[HNO_3/$NaNO_3$] in the feed	**$D_{U(VI)}$**	
	0.2 M T2EHDGA	**0.2 M T2EHDGA + 30% *iso*-decanol**
1 M $NaNO_3$	12.17	3.17
2 M $NaNO_3$	13.89	5.49
3 M $NaNO_3$	16.37	10.18
4 M $NaNO_3$	22.45	13.85
6 M $NaNO_3$	33.62	21.14
1 M HNO_3	0.82 (1.01)[a]	0.19
2 M HNO_3	2.74 (2.08)[a]	--
3 M HNO_3	7.63 (4.99)[a]	2.51
4 M HNO_3	12.25 (5.92)[a]	--
6 M HNO_3	--[b] (7.31)[a]	9.56

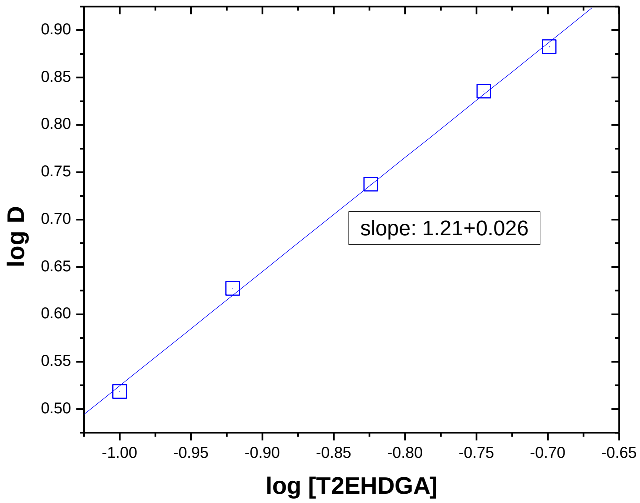

Fig. 4.19. Dependence of D_U on the concentration of [T2EHDGA]. Aqueous phase: 3 M HNO_3

4.4.3. Transport Studies

4.4.3.1. Effect of the Phase Modifier Concentration

The effect of the modifier (*iso*-decanol) concentration on the U extraction is already discussed above. However, the role of the modifier on the diffusion of the extracted complex across the membrane is not clearly known. Therefore, the transport behaviour of U(VI) was investigated for 0.2 M T2EHDGA as the carrier extractant in *n*-dodecane containing 0% to 40% *iso*-decanol as the phase modifier. Feed acidity was maintained at 3 M HNO_3 and 0.01 M HNO_3 was used as the strippant in the receiver compartment, in all the experiments. As shown in Fig. (4.20), the transport rates decreased with increasing concentration of *iso*-decanol. We found that after 300 minutes ~81% U was transported when 0.2 M T2EHDGA was used as carrier without any *iso*-decanol. This was found to decrease to ~ 64 % when 40% *iso*-decanol was used as the phase modifier after same transport time. The permeability coefficients are calculated and are listed in Table (4.8).

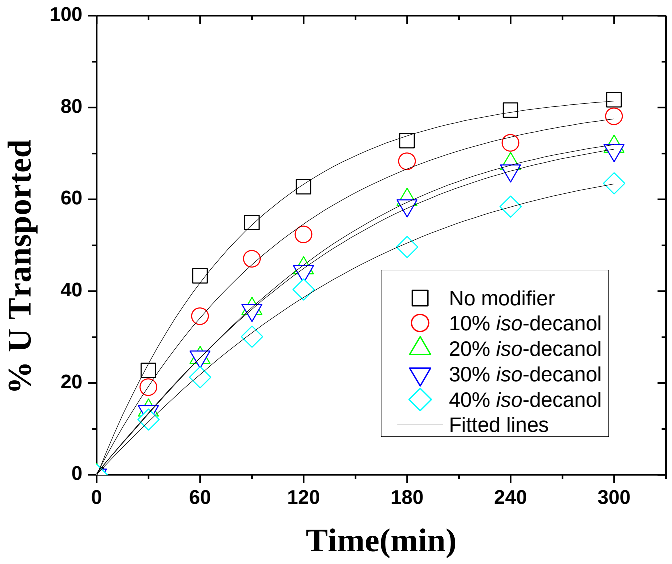

Fig. 4.20. Transport of U (VI) using 0.2 M T2EHDGA in *n*-dodecane with varying concentration of phase modifier. Feed: 3 M HNO_3; Receiver: 0.01 M HNO_3

The acid transport from the feed to the receiver side was estimated by volumetric method using standard alkali and phenolphthalein indicator. As indicated in Table 4.8, the acid transport was close to 6% in the absence of any phase modifier. On the other hand, in the presence of phase modifier the acid transport increased only marginally and was 7% even in the presence of 40% *iso*-decanol. This was probably beneficial in the transport of uranyl ion and in spite of significant decrease in the D_U values (about 4 times in the presence of 40% *iso*-decanol as compared to in the absence of the phase modifier) the decrease in the P was only by a factor of two. The dynamic viscosity, on the other hand, showed a significant increase with increasing *iso*-decanol fraction and might be responsible in the decrease in the transport rates. These results indicated that the diffusion of the metal – carrier complex is more important in deciding transport rates as compared to the D_U values. This also suggests that the transport is a diffusion controlled process similar to various SLM systems studied earlier [4,19].

Table 4.8.Transport data as a function of the phase modifier fraction in the carrier extractant. Support: 0.45 micron PTFE; Extractant: 0.2 M T2EHDGA; Feed: 3 M HNO_3; Receiver: 0.01 M HNO_3

Modifier concentration	P x 10^4(cm/s)	% T (5 h)	% Acid transport (5 h)	Dynamic viscosity (mPa.s)	D_U
Nil	(3.80$\pm$0.32)	81.7	5.67	2.0010	7.63
10%	(3.41$\pm$0.25)	78.1	6.33	2.3329	3.79
20%	(3.23$\pm$0.06)	71.5	6.67	2.9141	3.54
30%	(3.20$\pm$0.13)	70.7	6.33	3.8501	2.51
40%	(2.04$\pm$0.09)	63.5	7.00	4.8625	1.90

4.4.3.2. Effect of the Feed Acidity

Acidity of the feed solution plays an important role in the carrier facilitated metal ion transport by several factors. Firstly, the acid provides the counter anion in the solvated extraction mechanism, such as the present case. In such case, the transport rate should increase with increasing feed acidity. Secondly, if the acid interacts with the carrier extractant, then with increasing feed acid concentration, a decrease in the free ligand concentration is resulted leading to a decrease in U transport rate. Finally, if there is a co-transport of acid, then the receiver phase acidity can increase resulting in inefficient stripping. The transport profiles of U as a function of the feed nitric acid concentration are presented in Fig. 4.21. As indicated in the figure, the transport of U(VI) increased from 0.5 M HNO_3 to 3 M HNO_3 for 0.2 M T2EHDGA as the carrier. As per Eqn.(4.15), the transport of U(VI) takes place via nitrate assisted complexation of U(VI) with T2EHDGA. In other words, higher the feed acidity, higher will be the complexation and hence the transport rate. However, the possibility of the formation of T2EHDGA·HNO_3 complex can result in lower free T2EHDGA concentration which can lead to lower transport rates. T2EHDGA is expected to form adducts such as T2EHDGA·HNO_3 and the equilibrium constant (K_H) is given as:

$$H^+ + NO_3^- + \mathrm{T2EHDGA}_{(o)} \overset{K_H}{\rightleftharpoons} \mathrm{T2EHDGA}\cdot HNO_{3(o)} \qquad (4.14)$$

The value of K_H is reported as 1.8±0.3 as compared 4.1±0.4 for TODGA [22]. Therefore, though there is a decrease in the availability of free T2EHDGA for complex formation with U(VI), it is to a much lower extent as compared to TODGA, as reported earlier. This effect causes the transport rate to decrease after certain acidity similar to the transport studies involving TODGA. This is clear from Fig. 4.21 that when the feed acidity increases from 3 M to 6 M HNO_3, the transport rate is found to decrease. On the other hand, increasing the feed acidity to 8 M HNO_3, the transport rate is found to increase further. This unusual behaviour is probably due to a change in the extraction mechanism at higher acidities. It is clear from the above discussion that there is a possibility of higher transport of acid for higher feed acidity which may lead to an increase in the acidity of the receiving phase. It was observed that the acidity of the strip phase increased from 0.2 M for 1 M HNO_3 feed to 0.4 M for 6 M HNO_3 feed acidity after 5 h. As a consequence of increasing acidity in the receiving side stripping efficiency decreased and this led to lower transport rate at higher acidity. For trivalent and tetravalent ions we found that when the acidity of the feed phase increased from 3 M HNO_3 to 6 M HNO_3 transport rate decreased quite significantly for both T2EHDGA and TODGA. However, for the hexavalent ions, there is a consistency in the transport rate when feed acidity increased from 3 M HNO_3 to 6 M HNO_3 (Table 4.9). This is due to the fact that only two nitrate ions are required to form an extractable complex for hexavalent ions whereas for trivalent and tetravalent ions this number is three and four respectively. The transport of U with varying nitric acid concentration in the feed can be summarized as follows: 1) with increasing nitric acid concentration U extraction is expected to increase due to the availability of nitrate ion for complexation and formation of the extracted species (eqn. (4.15)); 2) with increasing nitric acid concentration (beyond 3 M) the T2EHDGA·HNO_3 adduct formation becomes predominant and this leads to a decrease in extraction and hence transport rates; 3) with increasing nitric acid concentration the extraction mechanism may change (beyond 6 M HNO_3) and this can result in higher extraction of U and hence higher transport rates. The net result of this three processes is an initial increase in transport up to 3 M HNO_3, slight decrease up to 6 M HNO_3 and further increase at 8 M HNO_3.

In order to discount the effect of nitric acid on the decrease in transport rates at higher acidities while trying to understand the effect of nitrate ion, transport experiments were carried out from feed solutions having varying nitrate ion concentration at a fixed H^+ ion concentration (0.1 M). The results, as shown in Fig. 4.22, clearly proved the effect of acid transport on the transport rate of U(VI). There was continuous increase in transport rate with increasing nitrate ion concentration from 1 M to 6 M. This is reflected in the permeability data (Table 4.9). Here neither was any adduct formation for T2EHDGA nor any transport of acid causing acidity of the receiver phase to increase. As a result, the transport rates increased with the nitrate ion concentration in the feed. However, though the transport rates were steep in the initial phase (up to 2 h) for 6 M $NaNO_3$ as the feed, a plateau was observed afterwards. On the other hand, a continuous increase in the transport rate was observed with 6 M HNO_3 and marginally higher transport (79%) as compared to 6 M $NaNO_3$ (74%) was observed after 5 h.

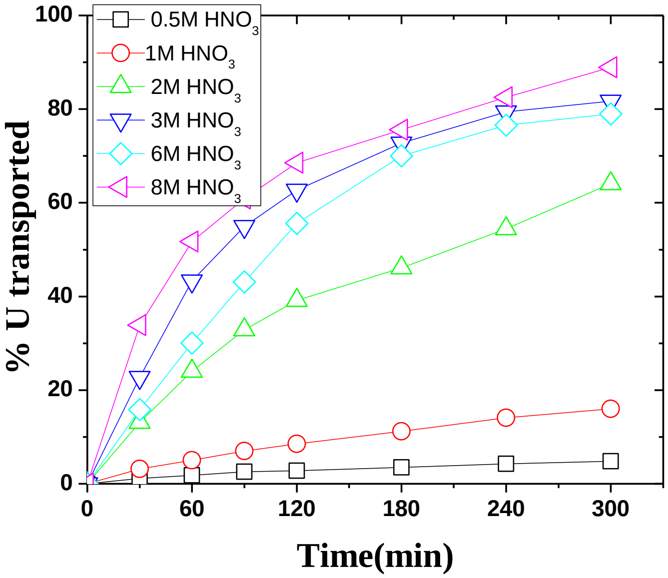

Fig. 4.21. Transport of U (VI) using varying concentration nitric acid in the feed. Carrier: 0.2 M T2EHDGA in *n*-dodecane containing 30% *iso*-decanol; Receiver: 0.01 M HNO_3

4.4.3.3. Nature of the Feed Acid

Table 4.9: Transport parameters as a function of the nitrate ion concentration in the feed. Support: 0.45 micron PTFE; Extractant: 0.2 M T2EHDGA; Receiver: 0.01 M HNO_3

$[HNO_3]$, M	P x10^4(cm/s)	$[NaNO_3]$, M	P x10^4(cm/s)
0.5	0.11±0.01	--	--
1.0	0.36±0.02	1.0	0.19±0.02
2.0	1.94±0.08	2.0	0.80±0.11
3.0	3.37±0.29	3.0	0.93±0.06
6.0	3.86±0.23	6.0	2.70±0.30
8.0	4.16±0.33	--	--

It was also required to investigate the effect of various mineral acid types such as HCl and $HClO_4$ on the U transport rates. Fig. 4.23 gives the transport profiles under these feed conditions at 3.0 M acidity. The transport rates followed the trend: HNO_3 >> HCl ~ $HClO_4$. This was in sharp contrast to the extraction of Am^{3+} reported with these acids which was explained on the basis of the reverse micelle formation abilityof these acids as indicated by the metal ion extraction ability which followed the trend $HClO_4$ > HNO_3 > HCl. Increasing the acid concentration from 3.0 M to 6.0 M indicated spectacular increase in the transport rate with HCl while there was no significant change in case of HNO_3. This is, of course, in line with the extraction behaviour of the metal ions observed with HCl and HNO_3 [2]. The permeability coefficient values are listed in

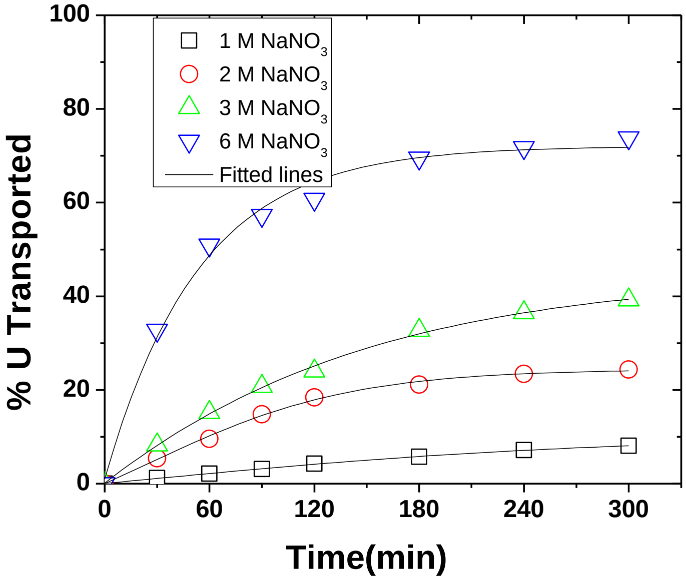

Fig. 4.22. Transport of U (VI) using varying concentration sodium nitrate in the feed. Carrier: 0.2 M T2EHDGA in *n*-dodecane containing 30% *iso*-decanol; Receiver: 0.01 M HNO_3

Table 4.10. In order to discount the effect of co-transport of hydrogen ion which adversely affected the transport of U, several experiments were carried out using the respective sodium salts in the feed. The results are presented in Fig. 4.23 while the permeability coefficients are listed in Table 4.10. The permeability data indicated that while the permeability coefficient for uranyl ion decreased significantly when the feed condition was changed from 3 M HNO_3 to 3 M $NaNO_3$ an entirely opposite effect was observed with 3 M HCl and 3 M NaCl. On the other hand, the transport rate became negligible when 3 M $NaClO_4$ was used as the feed. This behaviour is rather intriguing

and need a more detailed investigation. The significant increase in the P value, while changing the feed from 3 M $NaNO_3$ to 6 M $NaNO_3$, was ascribed to the increased tendency to form the extractable species with increased nitrate ion. On the other hand, a sharp decline in the transport rate and P vale was seen when the feed concentration of NaCl was increased from 3 M to 6 M which may be attributed to the formation of non-extractable anionic species such as $UO_2Cl_3^-$ and $UO_2Cl_4^{2-}$**.**

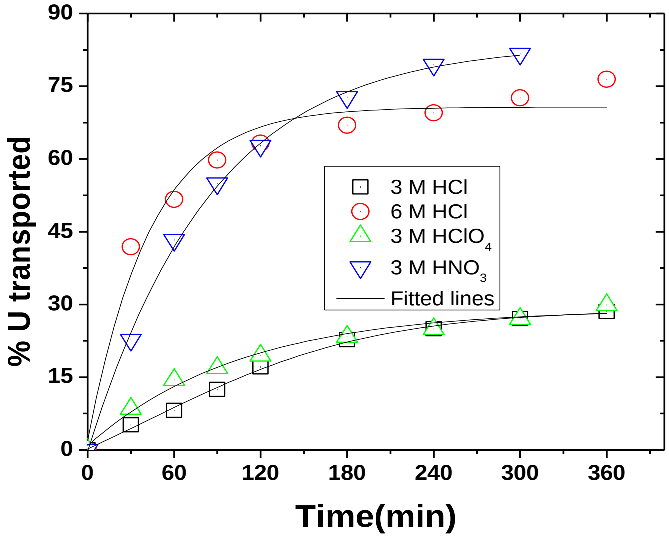

Fig. 4.23. Transport profile of U(VI) using different mineral acid types in the feed. Receiver: pH 2.0 solution; Carrier: 0.2 M T2EHDGA in *n*-dodecane. Pore size: 0.45 micron

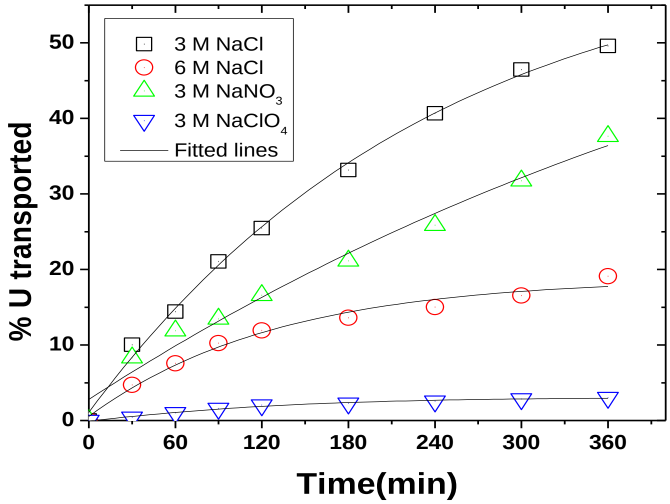

Fig. 4.24.Transport profile of U(VI) using different sodium salts of different mineralacids as the feed. Receiver: pH 2.0 solution; Carrier: 0.2 M T2EHDGA in *n*-dodecane. Pore size: 0.45 micron

Table 4.10: Permeability data of UO_2^{2+} under varying feed conditions using 0.2 M T2EHDGA in *n*-dodecane + 30% *iso*-decanol as the carrier solvent

Feed	**P x10^4(cm/s)**	**Feed**	**P x10^4(cm/s)**
3.0 M HNO_3	3.37±0.29	3.0 M $NaNO_3$	0.67±0.03
3.0 M HCl	0.86±0.12	3.0 M NaCl	1.12±0.03
3.0 M $HClO_4$	0.73±0.04	3.0 M $NaClO_4$	$(4.22\pm0.23)\times10^{-2}$
6.0 M HNO_3	3.86±0.23[a]	6.0 M $NaNO_3$	2.70±0.30[a]
6.0 M HCl	2.27±0.11	6.0 M NaCl	0.28±0.02

Note: [a]: Data taken from Ref [12]

4.4.3.4. Comparison with PuO_2^{2+} ion transport

As mentioned earlier HLW usually contains small amount of Pu due to the losses from the PUREX cycle. In view of the large number of metal ions present in the HLW and the oxidizing conditions prevailing, it was of interest to compare the transport behaviour of Pu in the +6 oxidation state. The transport profile of PuO_2^{2+} is presented in Fig. 4.25 along with that for UO_2^{2+} for comparison purpose. The transport rate for the PuO_2^{2+} ion was significantly lower as compared to that for UO_2^{2+} ion. This may be due to either the higher complex formation and hence extraction constants for the uranyl ion compared to the plutonyl ion [23] or due to formation of extracted species with different stoichiometry than that for the uranyl ion. Similar observation was made in the TODGA system reported earlier [19]. TODGA is found to be a far superior extractant as compared to T2EHDGA as the P values for both UO_2^{2+} and PuO_2^{2+} are significantly higher even with 0.1 M TODGA as compared that of 0.2 M T2EHDGA as the carrier extractant.

4.4.3.5. Effect of membrane pore size

Membrane pore size plays an important role in the transport of metal ions across an SLM. This has been shown by various workers for various metal ions and various extractants [24,25]. In diffusion controlled transport, as in the present case, the permeability coefficient of a diffusing species across a polymeric matrix is given by Eqn. (3.12).This equation clearly indicates that with increasing pore size, the resistance

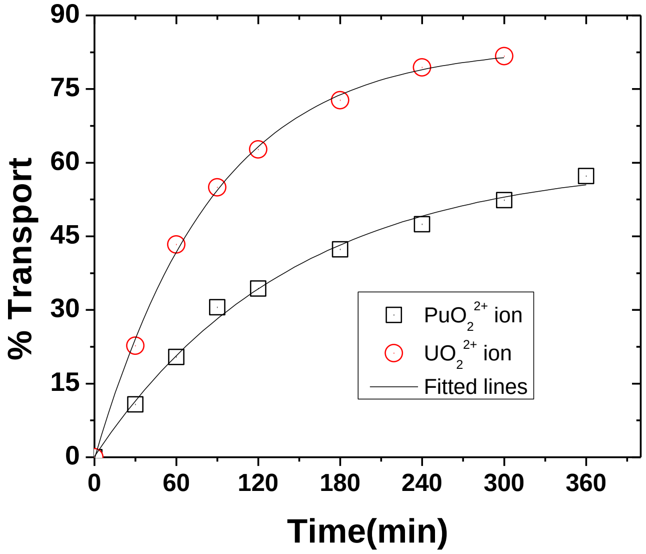

Fig. 4.25. Transport profile of U(VI) and Pu(VI) with 0.45 micron PTFE flat sheet membranes. Feed: 3 M HNO_3; Receiver: pH 2.0 solution; Carrier: 0.2 M T2EHDGA in *n*-dodecane

resistance felt by the diffusing complex decreases and as a result, the transport rate increases. But at the same time, from the Laplace's eqn.,(3.13) it is quite clear that the trans-membrane pressure (p) required to displace the carrier from the membrane pore is inversely proportional to the pore size (r_p) of the membrane. So when the pore size increases, the trans-membrane pressure also decreases and hence the stability of the membrane due to release of the organic carrier molecule from the pores also decreases. Both these factors play an opposing role on the transport of any metal ion across an SLM of varying pore size. Keeping these factors in consideration, the transport studies of U were carried out from 3 M HNO_3 feed using PTFE membranes of varying pore sizes, viz. 0.2 μm, 0.45 μm, 1.20 μm and 5.0 μm. As reported earlier, for different metal ions the variation in transport rate is affected differently with membrane pore size variation [24-26]. It is clear from Fig. (4.26) that for U(VI)-T2EHDGA system, transport rate increases up to 0.45μm and decreased there after similar to the Am(III)-T2EHDGA system reported earlier. This signifies that up to 0.45 μm the increase in transport due to less hindrance of U(VI)-T2EHDGA complex and thereafter the loss of carrier molecule due to lower trans-membrane pressure becomes dominant causing in decrease in transport rate. Due to this reason, 0.45 μm PTFE have been used as membrane filters throughout the present study.

4.4.3.6. Thermodynamics Study

As mentioned above, the transport process is a combination of extraction, diffusion and stripping steps. As diffusion is the rate determining step, the transport rates are decided by the diffusion coefficients or the permeability coefficients. It was decided to carry out transport studies as a function of temperature and the thermodynamic parameters were determined from the Van't Hoff equation and Gibb's Helmholtz equation given by Eqns. 4.9, 4.10 and 4.11.The plot of log P vs 1000/T is illustrated in Fig. 4.27 and from the slope and intercept the ΔH^o and ΔS^o values were calculated as 10.24±0.79 kJ/mol and – 31.82±2.55 J/oK/mol, respectively. Endothermicity of the transport process suggests that with increasing temperature the diffusion is facilitated by the decreasing viscosity of the membrane phase which favours the mobility of the complex and

T2EHDGA molecules alike. At the same time, the complexed molecules indicate a decrease in their entropy values resulting in a reasonably high negative entropy term.

4.4.3.7. Effect of U concentration

Concentration of U in the feed plays an important role in the transport rate of U(VI) ion. It is clear from eqn. (4.13) that the complexation and the transport rate increases with increasing U concentration in the feed. However, due to limitation in the carrier concentration in the membrane phase, the U transport rate may actually decrease. Transport studies were carried out using U concentration from 0.1g/L to 20g/L and the results are shown in Fig. 4.28. As expected, the transport rates decreased with increasing U concentration. The permeability coefficients also decreased with increasing U concentration (Table 4.12). On the other hand, analysis of the flux vs U concentration data indicates an initial increase was observed with a plateau approaching at higher U concentrations (Table 4.12). When the U concentration was

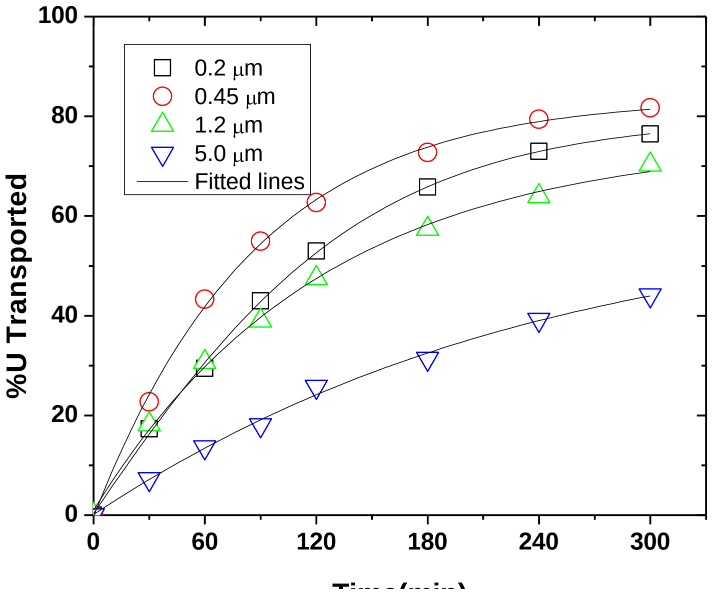

Fig. 4.26. Transport of U(VI) using 0.2 M T2EHDGA / n-dodecane from 3 M HNO_3 with varying membrane pore sizes

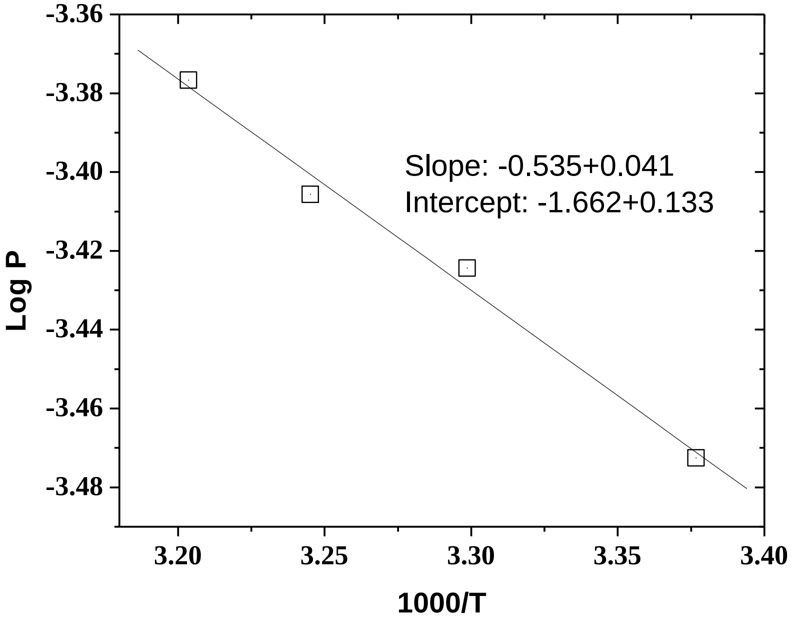

Fig. 4.27. Temperature dependence of permeability coefficient of U(VI) transport from 3 M HNO_3 using 0.2 M T2EHDGA as the carrier extractant

0.1g/L flux value was 2.09×10^{-7} mol cm^{-2}s^{-1} which increased to 80.3×10^{-7} mol cm^{-2}s^{-1} for 20g/L of U concentration.

4.4.3.8. Mathematical Modeling

The membrane transport was modeled using a computer software discussed in Chapter I. The membrane phase diffusivity (Δo) and aqueous phase diffusivity (Δa) were calculated by a plot of 1/P vs 1/Kd (Fig. 4.29) where the slope and the intercept values were found to be 8950 and 1105, respectively. Hence, the organic and aqueous phase mass transfer co-efficient were found out to be 9.04x10-4 and 1.12x10-4 cm/s, respectively. These values were used to predict the transport data. Based on the mathematical model and the known transport parameters, simulation of

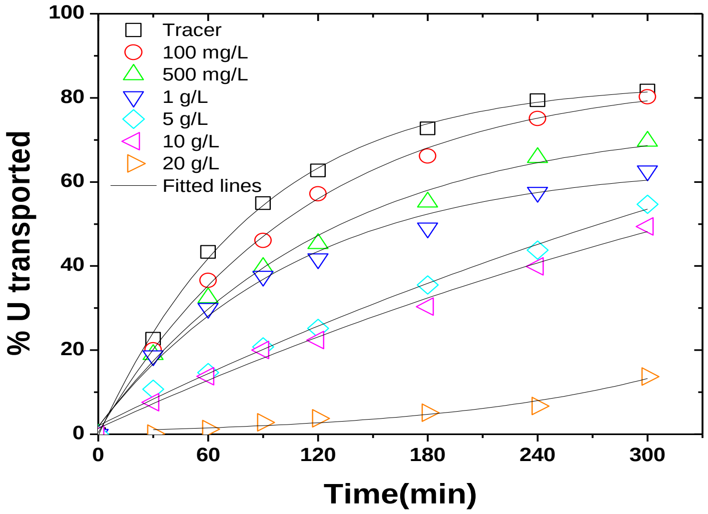

Fig. 4.28. Transport of U(VI) using 0.2 M T2EHDGA against different concentration of U from 3 M HNO_3. Feed: 3 M HNO_3; Receiver: pH 2.0 solution; Carrier: 0.2 M T2EHDGA in *n*-dodecane

Table 4.11: Permeability coefficients and flux values as a function of the U concentration in the feed

U Concentration (g/L)	P x10^4(cm/s)	Flux x10^9(mol.cm^{-2}.s^{-1})
0.1	3.27±0.19	0.14±0.01
0.5	2.21±0.17	0.47±0.03
1	1.88±0.08	0.79±0.02
5	1.61±0.12	3.38±0.21
10	1.45±0.06	6.01±0.23
20	0.69±0.05	5.81±0.03

the transport process was carried out for the three different feed acidity viz.; 2 M HNO_3, 3 M HNO_3 and 6 M HNO_3 for 0.2 M T2EHDGA as carrier and is presentedin Fig 4.30. In another fitting, simulation of the transport process was carried out for four different T2EHDGA concentration viz.; 0.05 M, 0.1 M, 0.15 M and 0.2 M at 3 M HNO_3 and is presented in Fig 4.31. The lines indicated the transport profile as predicted by the mathematical model (computed data) while symbols represented the experimental data in each figure. The predicted data found to be fitted with the 8% error limit to that obtained U(VI) transport rate. The data fitting was excellent up to 0.2 M T2EHDGA as the carrier concentration. The membrane parameters such as diffusivity and flux were optimized at this carrier concentration. However, at higher T2EHDGA concentration (0.3 M), the predicted transport profile was found to be in variance to the experimentally obtained transport profile. At higher T2EHDGA concentrations, the viscosity and aggregation of the carrier molecule causes the experimental data to differ greatly from that of predicted value as the factors mentioned above are not considered in the program.

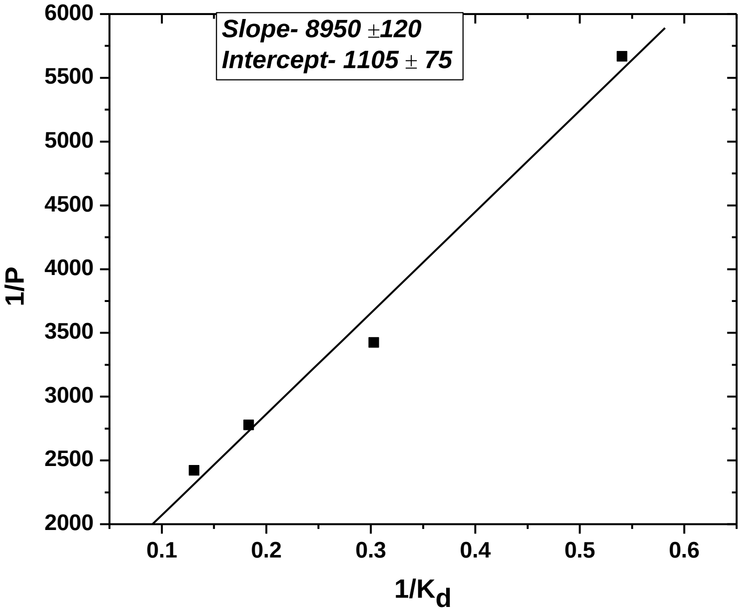

Fig. 4.29: Plot of 1/P vs 1/Kd for U(VI). Carrier: 0.2 M T2EHDGA in *n*-dodecane (30% *iso*-decanol as phase modifier). Feed: 3 M HNO_3; Receiver: 0.01 M HNO_3

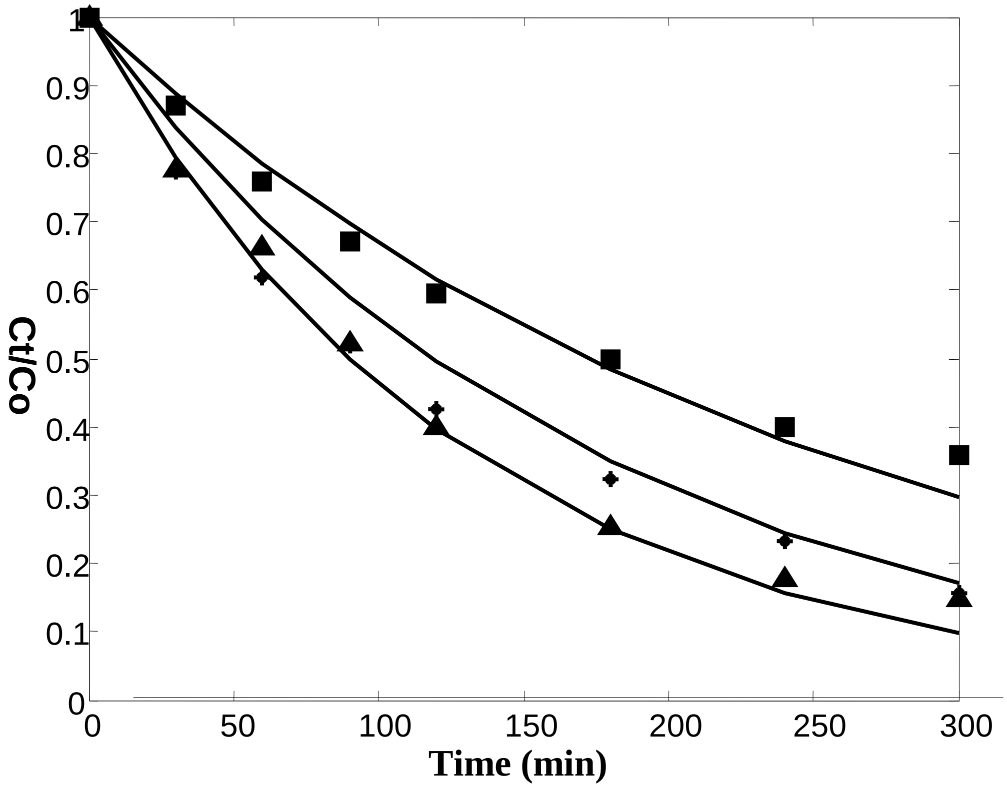

Fig. 4.30: Prediction of U(VI) transport rate (indicated by the lines in the fig.) for the varying feed acidity in SLM using 0.2 M T2EHDGA as carrier and actual (indicated by the symbols in the fig.) transport rate observed, ■ 2M HNO_3, ✦ 3M HNO_3, ▲ 6M HNO_3

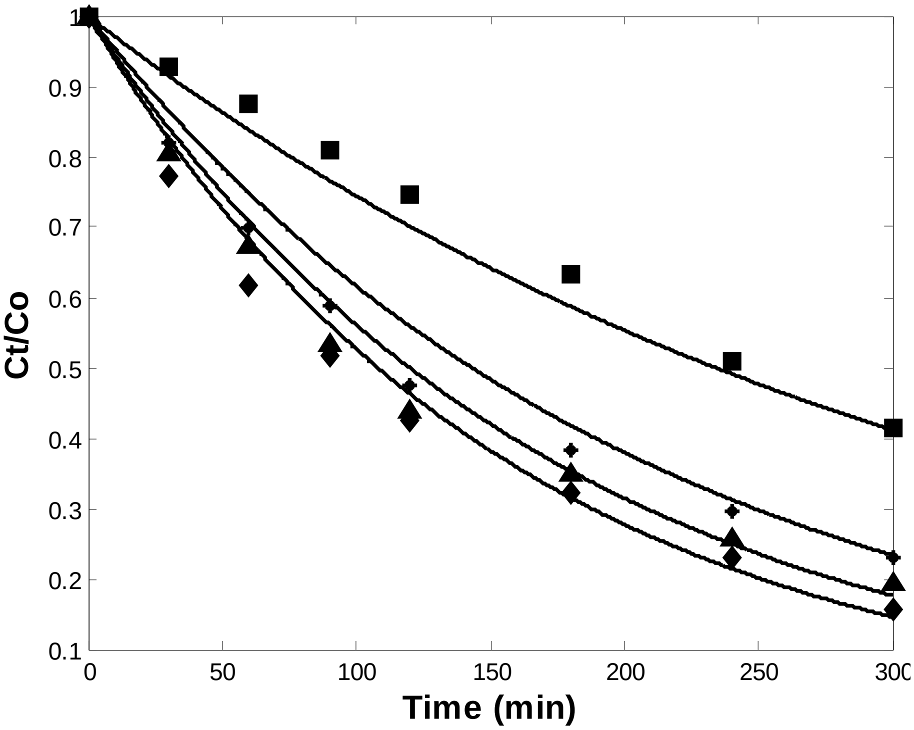

Fig. 4.31: Prediction of U(VI) transport rate (indicated by the lines in the fig.) in SLM at 3M HNO_3 using different concentration of T2EHDGA as carrier and actual (indicated by the symbols in the fig.) transport rate observed, ■ 0.05 M T2EHDGA, ✦ 0.1 M T2EHDGA, ▲ 0.15 M T2EHDGA, ◆ 0.2 M T2EHDGA

4.5. Conclusions

In conclusion T2EHDGA based support liquid membrane was found to be effective for transport of actinides and lanthanides from nitric acid medium. Various factors like feed acidity, membrane pore size, carrier concentration, phase modifier concentration were found to affect the transport rate significantly and were studied in detail.

4.4.5. REFERENCES

1. S. Manohar, J.N. Sharma, B.V. Shah, P.K. Wattal, *Nucl. Sci. Eng.* 156 (2007) 96.
2. S.A. Ansari, P.N. Pathak, M. Hussain, A.K. Prasad, V.S. Parmar, V.K. Manchanda, *Solv. Extr. Ion Exch*.23 (2005) 463.
3. J.P. Shukla and S.K. Misra, *J. Membr. Sci*. 64 (1991) 93.
4. S.A. Ansari, P.K. Mohapatra, D.R. Prabhu, V.K. Manchanda, *J. Membr. Sci.* 282 (2006) 133.
5. S. Sriram, P.K. Mohapatra, A.K. Pandey, V.K. Manchanda, L.P. Badheka, *J. Membr. Sci*. 177 (2000) 163.
6. W.C. Babcock, R.W. Baker, E.D. LaChapelle, K.L. Smith, *J.Membr. Sci*. 7 (1980) 89.
7. G.Cousinou, M.Ganivet, Method of selective stripping of Plutonium from an organic solvent containing Plutonium and in some cases Uranium by reduction of said Plutonium, US Patent, 3980750 (1976).
8. T.C. Huang, R.S. Juang, *J. Membr. Sci*. 31 (1987) 209.
9. A. Kiani, R.R. Bhave, K.K. Sirkar, *J. Membr. Sci*. 20 (1984) 125.
10. M.P. Jensen, T. Yaita, and R. Chiarizia, *Langmuir*, 2007, 23, 4765.
11. R.B. Gujar, S.A. Ansari, P.K. Mohapatra and V.K. Manchanda; *Solv. Extr. Ion Exch.*, 28 (2010) 350.

12. S.Panja, P.K. Mohapatra, S.C. Tripathi and V.K. Manchanda; *J. of Hazardous Materials***,** 188 (2011) 281.
13. S. Nakamura, A. Sato, K. Akiba; *J. Radioanal. Nucl. Chem., Articles* 178 (1) (1994) 63.
14. C.R. Wlike and P. Chang; *A.I.Ch.E. Journal*, 1(1955) 264.
15. W. Schotte; *Chem. Eng. J*, 48(1992)167.
16. J.N. Mathur, M.S. Murali and K.L. Nash; *Solv. Extr. Ion Exch.*, 19 (2001) 357.
17. Y. Sasaki, Y. Sugo, S. Suzuki, T. Kimura; *Anal. Chim. Acta* 543 (2005) 31.
18. Z. Zhu, Y. Sasaki, H. Suzuki, S. Suzuki and T. Kimura, *Anal. Chim. Acta* 527 (2004) 163.
19. S. Panja, P.K. Mohapatra, S.C. Tripathi, and V.K. Manchanda; *J. Membr. Sci.*, 337 (2009) 274.
20. J. N. Sharma, R. Ruhela, K. N. Harindaran, S. L. Mishra, S. K. Tangri, A. K. Suri;*J. Radioanal. Nucl. Chem*., 278 (2008) 173.
21. S. Kannan, M. A. Moody, C. L. Barnes, and P. B. Duval; I*norg. Chem*., 47 (2008) 4691.
22. R.B. Gujar, S.A. Ansari, M.S. Murali, P.K. Mohapatra and V.K. Manchanda; *Solv. Extr. Ion Exch*. 28(2010) 377.
23. E. Hogefeldt (Ed.), Stability Constant of Metal ion Complexes, Part A: Inorganic Ligands, IUPAC Chemical Data Series No. 21, Pergamon, Oxford, 1982.

24. D.S. Lakshmi, P.K. Mohapatra, D. Mohan and V.K. Manchanda; *Desalination*, 163 (2004)13.
25. S.K. Singh, S.K. Mishra, S.C. Tripathi and D.K. Singh; *Desalination*, 250(2010)19.
26. P.K. Mohapatra, D.S. Lakshmi, D. Mohan and V.K. Manchanda; *Sep. Purif. Technol.*, 51 (2006) 24.

Chapter V

EXTRACTION AND TRANSPORT BEHAVIOR OF TRIVALENT ACTINIDES AND LANTHANIDES USING SUBSTITUTED DIGLYCOL AMIDES

5.1. Introduction

Though N,N,N’,N’-tetraoctyl-3-oxapentanediamide (TODGA) was found to be the most promising [1] of the diglycolamides, it was required to investigate other homologus compounds. Recently, modifications of the diglycol amides by introducing a branching on the alkyl substituents of the acyl nitrogen and also by changing the carbon chain length of the same alkyl substituents have been attempted [2]. In this context, a series of substituted diglycolamides viz, N,N,N’N’-tetraoctyl diglycolamide (TODGA), Tetra(2-ethyl hexyl) diglycolamide (T2EHDGA), N,N,N’N’-tetrahexyl diglycolamide (THDGA), N,N,N’N’-tetrapentyl diglycolamide (TPDGA) and N,N,N’N’-tetradecyl diglycolamide (TDDGA) etc have been synthesized at Thermax India Ltd., Pune and evaluated in the present work. Extensive SLM transport studies in the separation of actinides, lanthanides and fission products have been carried out using a varied class of reagents [3-5]. Supported Liquid Membrane experiments are preliminary requirement to understand the feasibility of metal separations using membrane technology that can be subsequently scaled up by the hollow fiber contactors.

Chapter V

In this work, detailed solvent extraction studies of Am(III), Eu(III) and Sr(II) from nitric acid medium using the above mentioned substituted diglycolamides have been carried out. Effect of nitric acid concentration on the extractability of all the metal ions mentioned above, nature of the extracted species for Am(III) and Eu(III) for each extractant, effect of phase modifier on the extractability of each element and their acid dependency, were studied in detail. Extractability of these elements from Synthetic High Level Waste (SHLW) at different acidity were also studied. Simultaneously, the SLM experiments for the transport of Am(III), Eu(III) and Sr(II) have been carried out using various diglycolamides namely TODGA, T2EHDGA, THDGA, TDDGA and TPDGA. Effects of feed acidity and membrane pore size on the transport of each metal ion have been investigated in detail using each of these reagents. Effect of phase modifier, i.e, 30% *iso*-decanol on the transport of the metal ions has also been investigated.

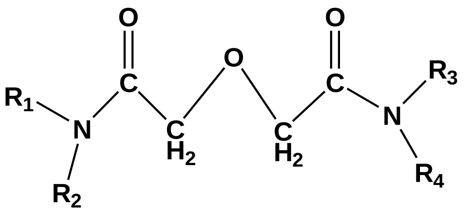

Fig. 5.1. Tetra alkyl diglycolamides; R= pentyl for TPDGA, hexyl for THDGA, octyl for TODGA, 2-ethyl hexyl for T2EHDGA and decyl for TDDGA

5.2. Solvent Extraction Studies

5.2.1. Kinetics of Extraction

The time required to attain equilibrium for the extraction of Am(III) was investigated using 0.1 M of the DGA based extractants both in the absence and in the presence of *iso*-decanol as phase modifier from 1 M HNO_3 feed solution. The plots of D_{Am} against time are shown in Figs. 5.2 and 5.3. It was observed that 5-10 minutes were sufficient for attaining equilibrium both in the presence and in the absence of *iso*-decanol. Thus the kinetics of extraction of Am(III) for all the DGAs was reasonably fast and the presence of *iso*-decanol does not significantly influence the kinetics. It was interesting to note that the branched alkyl diglycolamides(T2EHDGA) displayed poor extraction behaviour as compared to all the other DGA based extractants. Moreover, the presence of the phase modifier decreased the distribution coefficients significantly.

5.2.2. Composition of the Phase Modifier

Evaluation of a phase modifier was essential due to the fact that TPDGA formed third phase even in presence of 0.5 M HNO_3 even in the absence of the metal ion. It was also observed that TODGA formed third phase at acidity >6 M HNO_3, T2EHDGA does the same at 5 M HNO_3 whereas THDGA was found to do the same at acidity greater than 1 M HNO_3. Therefore, three different phase modifiers were evaluated as reported in literature such as TBP, DHOA and *iso*-decanol. Concentrations of TBP and DHOA

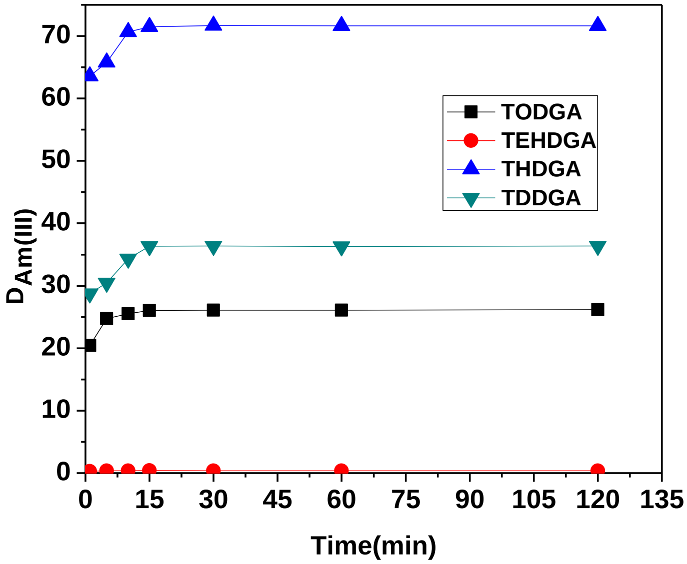

Fig. 5.2: Kinetics of extraction of Am(III) using 0.1 M DGAs under 1 M HNO_3 feed conditions

were kept at 1.2 M and 0.5 M, respectively [6] whereas *iso*-decanol concentration was kept at 30% [7]. We took TPDGA as the reference DGA as it was found to have maximum tendency for third phase formation. We investigated distribution coefficient value of Am(III) at three different acidity i.e., 1 M, 3 M and 6 M HNO_3 for 0.1 M TPDGA in the presence of the above mentioned concentration of the phase modifiers. It was found that though TBP and DHOA prevented third phase formation at 1 and 3 M HNO_3, they were not effective at 6 M HNO_3. On the other hand *iso*-decanol was found to be able to prevent third phase formation even at 6 M HNO_3. Therefore subsequent studies were carried out using 30% *iso*-decanol as the phase modifier for all the DGAs used in this work.

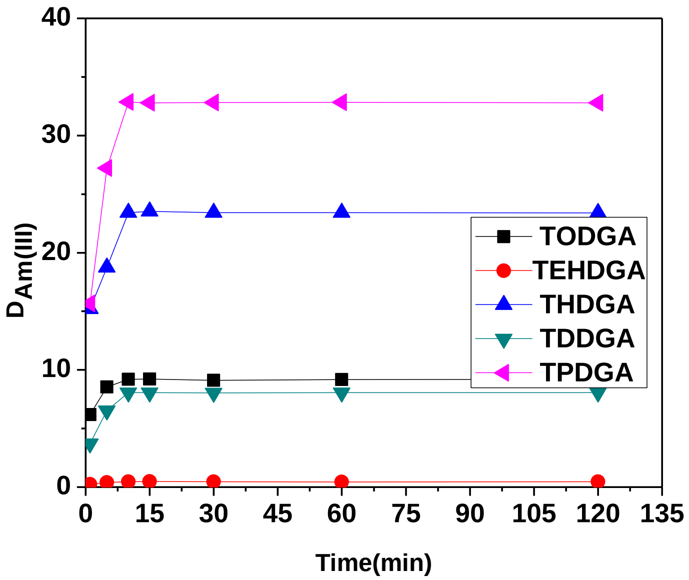

Fig. 5.3: Kinetics of extraction of Am(III) using 0.1 M DGAs in the presence of 30% *iso*-decanol under 1 M HNO_3 feed conditions

5.2.3. Effect of the Feed Acidity

The extraction of metal ions from nitric acid medium by DGAs can be epresented by the following eqn.

$$M^{n+} + mDGA_{(o)} + nNO_3^{-} \rightleftharpoons M(NO_3)_n.mDGA_{(o)} \qquad (5.1)$$

where, the subscript (o) represents the species in the organic phase, while those without any subscript refer to the species in the aqueous phase. It is clear from the Eqn. that with increasing feed nitric acid concentration the nitrate assisted complexation of the metal ion with DGA increases thus increasing the distribution coefficient. On the other hand, with increasing nitric acid concentration, the availability of free DGA also decreases due to the formation of DGA-HNO_3 adduct formation. This adduct formation depends on the basicity of the extractant. Thus, it is not the continuous increase of distribution coefficient with increasing feed nitric acid concentration for all the extractants. The dependency of distribution ratios of Am(III), Eu(III) and Sr(II) for 0.1 M DGAs both in the absence and in the presence of *iso*-decanol indicated an increasing trend with increasing feed acidity in each case. The plots are shown in Figs. 5.4 to 5.9. In the absence of *iso*-decanol, 0.1 M TPDGA formed third phase even in the presence of 0.5 M HNO_3 and hence the acid dependence studies were not carried out. For THDGA, third phase formation was seen above 1 M HNO_3 and hence the values of D_{Am} and D_{Eu} were evaluated up to1 M HNO_3 only. T2EHDGA showed third phase at 5 M HNO_3 and thus, the maximum acidity at which was the D value was measured was 3 M. The trend for D_{Am} as well as D_{Eu} is THDGA > TDDGA > TODGA >T2EHDGA upto 1 M HNO_3 and at higher acidity the trend is TDDGA > TODGA > T2EHDGA. When the distribution ratio measurements were carried out at different feed acidities in the presence of *iso*-decanol no third phase was observed for any of the DGAs upto 6 M HNO_3 in the presence of trace concentration of Am(III), Eu(III) and Sr(II). The values of distribution ratios for each of these elements were found to decrease than that obtained in the absence of *iso*-decanol up to 3 M HNO_3 beyond which an increase was notices at 6 M HNO_3. The reason behind this trend may be more availability of DGA

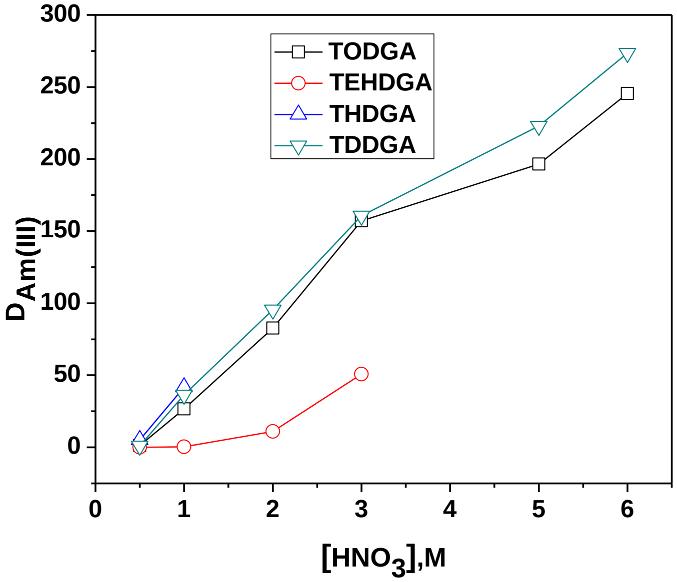

Fig. 5.4: Effect of feed nitric acid concentration on the extraction of Am(III) by 0.1 M concentration of DGA

molecules for complexation due to less complexation with HNO_3 in the presence of *iso*-decanol. The trend of D values for 0.1 M DGAs in presence of 30% *iso*-decanol was found to be TPDGA > THDGA > TODGA > TDDGA > T2EHDGA. This signifies that with increasing carbon chain length, extractability of the DGAs decreases. This trend was previously reported by Sasaki et al [8]. Why the trend is not followed in the absence of *iso*-decanol as phase modifier was not clear and needs further investigation. The values of D_{Am} and D_{Eu} were not only found to be highest for 0.1 M TPDGA, the same trend was also seen for Sr extraction.

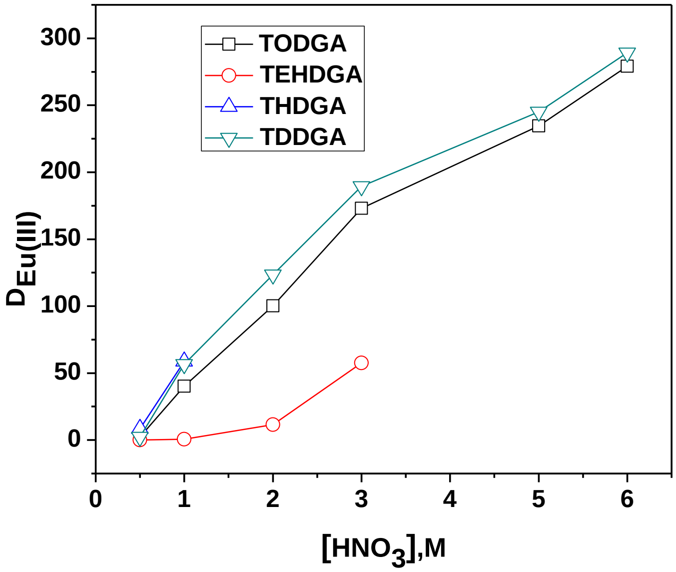

Fig. 5.5: Effect of feed nitric acid concentration on the extraction of Eu(III) by 0.1 M concentration of DGA

5.2.4. Nature of the extracted species

In order to understand the nature of the extracted species with Am(III) and Eu(III) by the DGA extractants, ligand concentration variation experiments were carried and the slopes of the log-log plot of D vs [TODGA] were calculated. Table 5.1 gives the slopes for Am(III) and Eu(III) for all the DGAs studied in the present work. It was found from the slopes that TODGA forms a tetra solvate, T2EHDGA forms a tri solvate and the remaining three DGAs form disolvate with both Am(III) and Eu(III) at 1 M HNO_3. It was reported that TODGA forms a reverse micelle with four TODGA molecules at acidities greater than 0.7 M HNO_3 [9]. Thus from these studies it can be concluded that

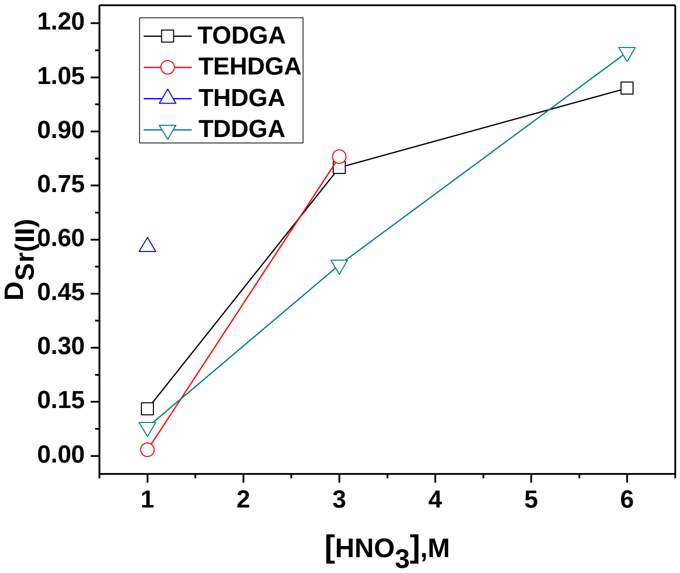

Fig. 5.6: Effect of feed nitric acid concentration on the extraction of Sr(II) by 0.1 M concentration of DGA

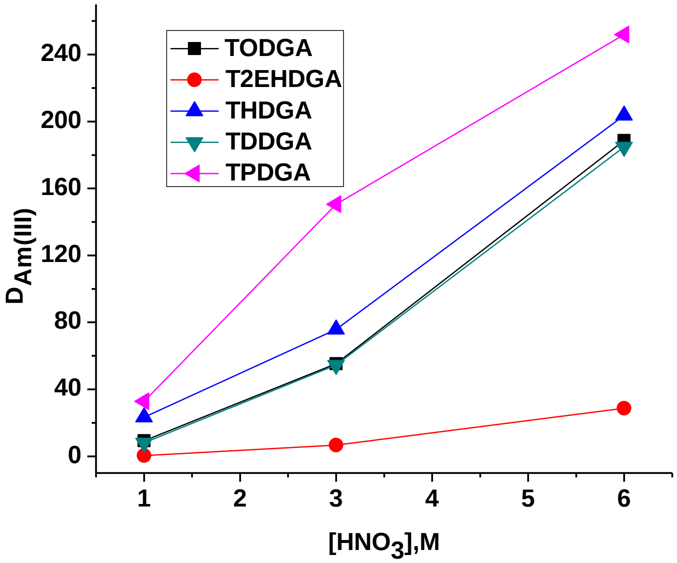

Fig. 5.7: Effect of feed nitric acid concentration on the extraction of Am(III) by 0.1 M concentration of DGA in the presence of 30% *iso*-decanol

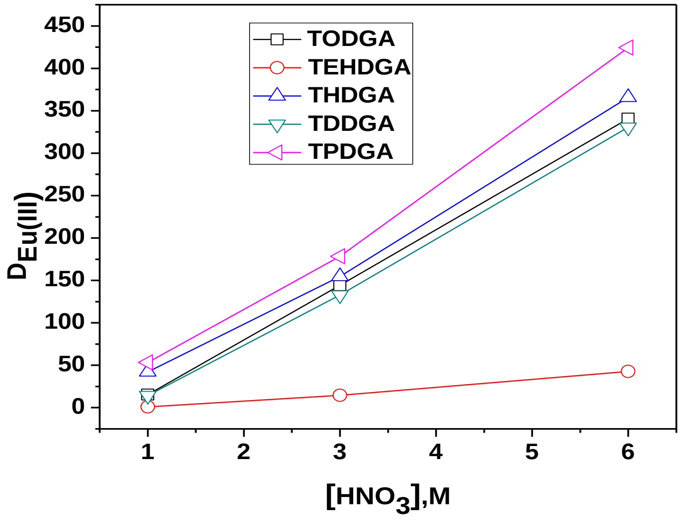

Fig. 5.8: Effect of feed nitric acid concentration on the extraction of Eu(III) by 0.1 M concentration of DGA in the presence of 30% *iso*-decanol

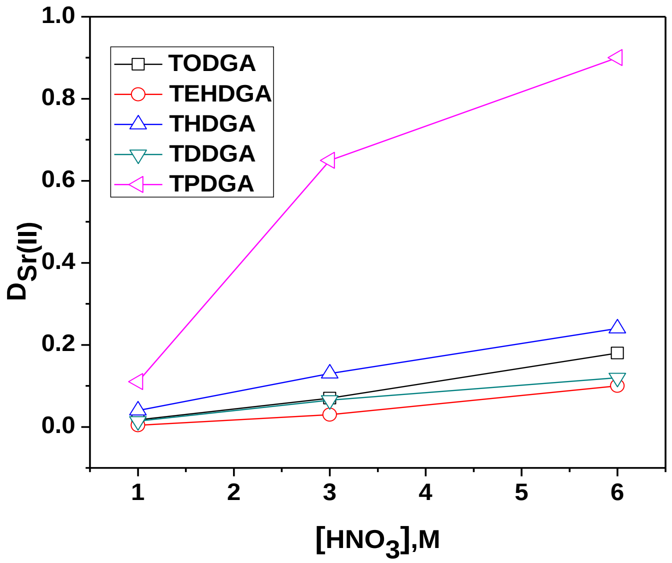

Fig. 5.9: Effect of feed nitric acid concentration on the extraction of Sr(II) by 0.1 M concentration of DGA in the presence of 30% *iso*-decanol

Table 5.1: Slope values of Am(III) and Eu(III) in the ligand concentration variation studies at 1 M HNO_3

DGA	**n**	
	[Am(III)]	**[Eu(III)]**
TODGA	3.78 ± 0.187	3.89 ± 0.256
T2EHDGA	2.86 ± 0.132	3.10 ± 0.061
TDDGA	2.08 ± 0.258	1.79 ± 0.103
THDGA	2.36 ± 0.117	2.42 ± 0.124
TPDGA*	1.68 ± 0.134	1.87 ± 0.112

*In the presence of 30% *iso*-decanol

increasing or decreasing the carbon chain length or introducing steric hindrance in the acyl nitrogen prevents the formation of tetrameric reverse micelle.

5.2.5. Extraction from Synthetic High Level Waste (SHLW)

Simulated PHWR waste as obtained from the raffinate of PUREX process was adjusted to different concentrations of nitric acid and spiked with ^{241}Am, $^{152+154}$ Eu and $^{85+89}$Sr. The composition of the SHLW is given in Table 2.3. Tables 5.2 and 5.3 show the distribution data of Am, Eu and Sr as a function of HNO_3 concentration from simulated waste solution for 0.1 M DGAs in the absence and in the presence of 30% *iso*-decanol as the phase modifier. In the absence of *iso*-decanol, THDGA and

TPDGA formed third phase at all the acidities, T2EHDGA at 3 M HNO_3 and TODGA at 6 M HNO_3 whereas no third phase formation was observed for TDDGA upto 6 M HNO_3. But no such third phase formation was observed for any of the DGAs at any of the acidity range in the presence of *iso*-decanol as the phase modifier. Though the D_M values were lower in the presence of SHLW, it was significantly higher for the quantitative and efficient extraction of actinides. Presence of uranium and lanthanides in the simulated waste solution competes with Am for the extractants leading to lower D_M values. On the other hand, alkali metals, alkaline earths and other non extractable ions contribute towards decrease in the water activity as well as increase in nitrate concentration and thereby enhance the D_M values. 0.1 M TPDGA showed highest value of D_{Am} and D_{Eu} at all the acidities in presence of *iso*-decanol, but at the same time it also showed highest D_{Sr} values. Decrease in the distribution ratio for the trivalent elements was much smaller compared to the decrease in the distribution ratio of Sr in the presence of *iso*-decanol at all the acidity range studied. Typical SF values for the metal ions observed at 3 M HNO_3 for the studied DGA extractants in presence of 30% *iso*-decanol were : 576 (Am/Sr) and 799 (Eu/Sr) for TODGA, 406(Am/Sr) and 811 (Eu/Sr) for T2EHDGA, 598(Am/Sr) and 817(Eu/Sr) for THDGA, 922(Am/Sr) and 1146(Eu/Sr) for TDDGA, 191(Am/Sr) and 212(Eu/Sr) for TPDGA, respectively.

Table 5.2: D_M from Simulated High Level Waste at varying acidities using 0.1 M DGAs

DGA	Am(III)			Eu(III)			Sr(II)		
	1 M HNO_3	3 M HNO_3	6 M HNO_3	1 M HNO_3	3 M HNO_3	6 M HNO_3	1 M HNO_3	3 M HNO_3	6 M HNO_3
0.1 M TODGA	27.8	56	TP	29.9	67	TP	0.08	0.66	TP
0.1 M T2EHDGA	0.64	TP	TP	0.77	TP	TP	0.002	TP	TP
0.1 M THDGA	TP	TP	TP	TP	TP	TP	TP	TP	TP
0.1 M TDDGA	25.4	51	160	27.6	65	185	0.07	0.47	0.87
0.1 M TPDGA	TP	TP	TP	TP	TP	TP	TP	TP	TP

Table 5.3:D_M from Simulated High Level Waste at varying acidities using 0.1 M DGAs+ 30 % *iso*-decanol

DGA	**Am(III)**			**Eu(III)**			**Sr(II)**		
	1 M HNO_3	3 M HNO_3	6 M HNO_3	1 M HNO_3	3 M HNO_3	6 M HNO_3	1 M HNO_3	3 M HNO_3	6 M HNO_3
0.1 M TODGA	6.83	46.1	173	24.4	63.99	189	0.02	0.08	0.10
0.1 M TEHDGA	0.38	5.15	20.5	0.64	20.3	39.3	0.004	0.025	0.06
0.1 M THDGA	20.1	56.9	104	30.4	78	121	0.024	0.095	0.12
0.1 M TDDGA	6.37	44.3	170	9.97	55	179	0.01	0.048	0.08
0.1 M TPDGA	24.4	88	161	31.9	98	174	0.08	0.46	0.87

5.3. Supported Liquid Membrane Transport Studies

5.3.1. Effect of the Feed Acidity

5.3.1.1. Am(III) Transport

The feed acidity plays an important role in the transport rate of the metal ion, especially for those reagents where the complexation takes place via solvation of the neutral metal-nitrate complex by the carrier molecule. In the present studies nitric acid was used as the feed medium. Am(III) forms a neutral nitrate complex with those nitrate ions followed by salvation by the diglycolamides leading to its extractants (Eqn. 5.1). When the feed acidity is increased, the complexation tendency of Am(III) increased resulting in an increase in the concentration of the Am(III)-DGA complexes in the feed-membrane interface. This increasing concentration causes an increase in the transport rate of Am(III). This behavior can be represented mathematically by the Eqn. (4.4). This increasing transport is observed up to an optimum acidity and then either there is saturation [10] or decrease in the transport rate [11]. The decrease in the transport in higher acidity can be due to: i) tendency of the DGAs to form adduct with nitric acid which causes a decrease in the availability of the carriers in the membrane phase; ii) with the increasing acidity of the feed phase, higher co-transport of acid is expected which causes the acidity of the receiving phase to increase. This increasing acidity in the receiver phase makes stripping of Am(III) from the membrane phase less efficient.

As is evident from the Figures (5.10-5.13) the effect of the feed acidity on the transport rates for Am(III) is different for the different diglycolamides. For TODGA, maximum transport was found at 2 M HNO_3 beyond which a decrease was seen. When T2EHDGA was used as the carrier, it was observed that maximum transport was

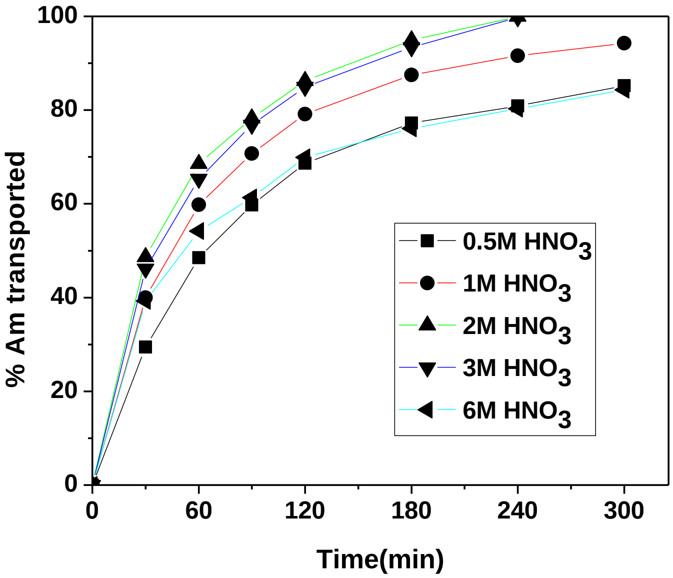

Fig. 5.10: Effect of feed acid concentration on the transport of Am(III) ion. Receiver: 0.1 M HNO_3; Carrier extractant: 0.1 M TODGA; Support: 0.2 micron PTFE

achieved for 3 M HNO_3 after which the transport rate decreased. But for THDGA in 1 M HNO_3 itself maximum transport of Am(III) was observed. The rate then decreased with increasing acidity upto 6 M HNO_3. The trend for TDDGA was same as that of T2EHDGA, maximum transport at 3 M HNO_3 and then it decreased with further increase in the feed acidity. TPDGA alone was not used in the transport experiments due to its tendency to form third phase even in the presence of 0.5 M HNO_3. On the other hand, it was used in combination

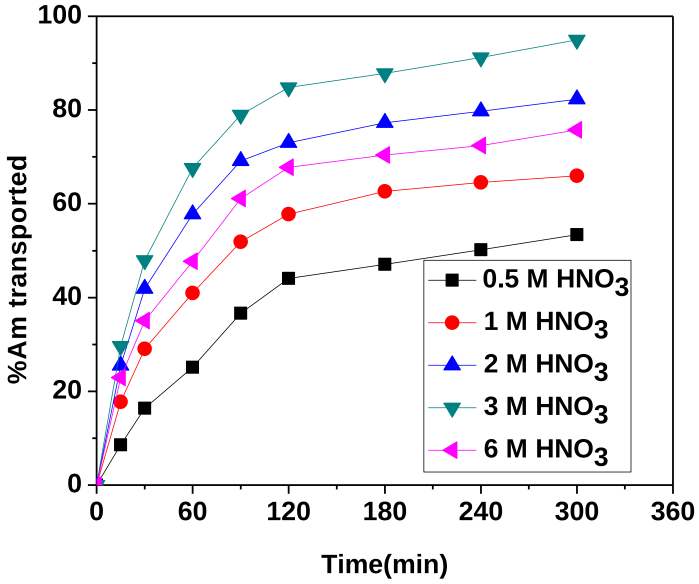

Fig. 5.11: Effect of feed acid concentration on the transport of Am(III) ion. Receiver: 0.1 M HNO$_3$; Carrier extractant: 0.1 M T2EHDGA; Support: 0.2 micron PTFE

with 30% *iso*-decanol to understand the acid dependency of Am(III) transport. In this case, the maximum transport was seen at 2 M HNO$_3$ which was found to decrease with further increase in the feed acidity (Fig. 5.14). Thus, it is quite evident that varying carbon chain length or branching of carbon chain does play a very important role in the diglycolamides behavior towards the feed acidity, but no particular trend was observed. This suggests that there is a complex dependency of increasing complexation, increasing viscosity, increasing acid transport, etc. on the transport rate of Am(III) for the series of diglycolamides studied here.

5.3.1.2. Eu(III) Transport

Eu(III) transport was also studied in detail for all the DGAs along with Am(III) as a representative lanthanide. Figs. 5.15-5.19 represent acid dependency transport of Eu(III) using 0.1 M DGAs. The Eqn. describing the extraction of Eu(III) is same as that describing the extraction of Am(III). Here also the value of ‘n’ varies from 2 to 4 for different DGA.

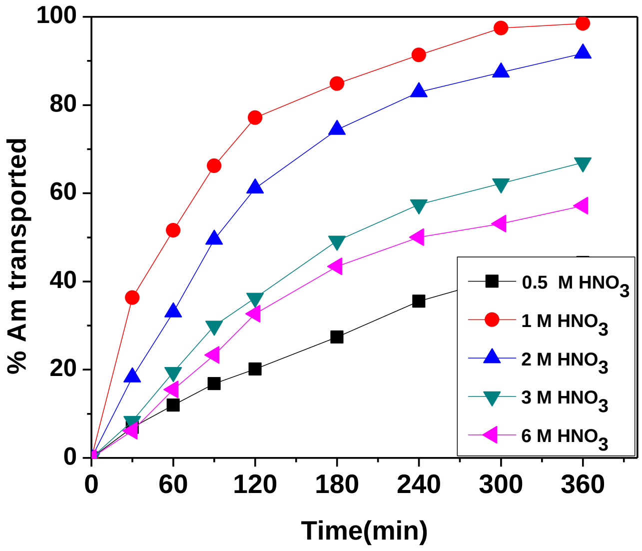

Fig. 5.12: Effect of feed acid concentration on the transport of Am(III) ion. Receiver: 0.1 M HNO_3; Carrier extractant: 0.1 M THDGA; Support: 0.2 micron PTFE

The reasons behind the variation of transport rate with varying feed acidity are also the same as that for Am(III). But the trend observed here is slightly different. For TODGA the maximum transport was observed at 1 M HNO_3 beyond which the transport decreased. This maximum was observed at 2 M HNO_3 for Am(III) as mentioned earlier. For T2EHDGA the same trend was observed as with Am(III), i.e., increasing transport rate upto 3 M HNO_3 where maximum transport was observed beyond which a decrease was seen. For THDGA maximum transport was observed at 2 M HNO_3 and then a decrease was observed. It was also marginally different than that of Am(III) where maximum transport was observed at 1 M HNO_3. For TDDGA 1 M HNO_3 was observed to give the maximum transport which was quite

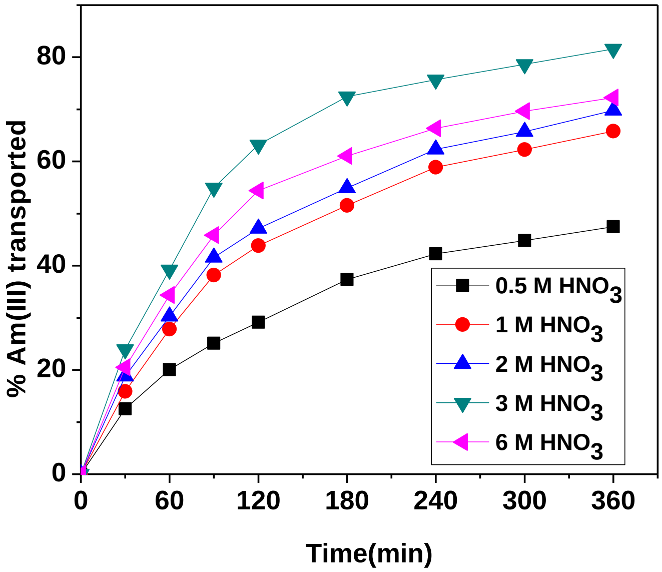

Fig. 5.13: Effect of feed acid concentration on the transport of Am(III) ion. Receiver: 0.1 M HNO_3; Carrier extractant: 0.1 M TDDGA; Support: 0.2 micron PTFE

different than that of Am(III) where maximum transport was observed at 3 M HNO_3. However, in the case of TPDGA + 30% *iso*-decanol, the same trend was observed for Am(III) and E(III), i.e., maximum transport at 2 M HNO_3 beyond which a decreasing transport behaviour was seen.

5.3.2. Effect of the Membrane Pore Size

Membrane pore size is one of the important factors deciding the transport rate across an SLM. In a diffusion controlled process across a polymeric matrix, the permeability co-efficient (P) value is directly proportional to the membrane pore size

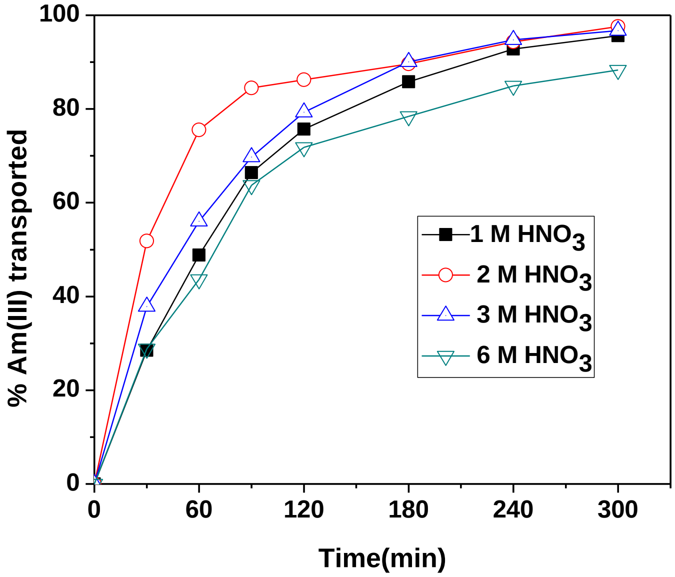

Fig. 5.14: Effect of feed acid concentration on the transport of Am(III) ion. Receiver: 0.1 M HNO_3; Carrier extractant: 0.1 M TPDGA with 30% *iso*-decanol; Support: 0.2 micron PTFE

as can be seen from Eqn. (3.11) and this suggests that with increasing pore size of the membrane the diffusing species experiences less hinderance and hence the transport rate increases with it. However, the transport rate can not increase indefinitely as increasing pore size results in release of the organic carrier molecules and diluent from the membrane. This can be explained on the basis of Laplace's Eqn. (Eqn. 3.12) which states that an increase in the pore radius results in enhanced release of the organic phase from the membrane causing the transport rate to decrease.

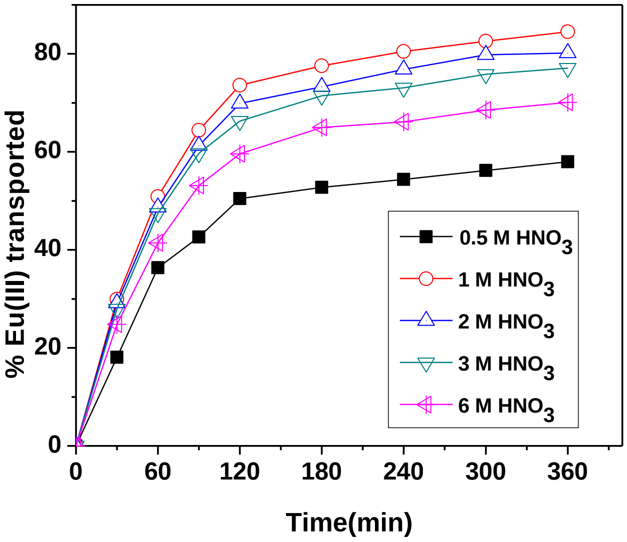

Fig. 5.15: Effect of feed acid concentration on the transport of Eu(III) ion. Receiver: 0.01 M HNO_3; Carrier extractant: 0.1 M TODGA; Support: 0.2 micron PTFE

5.3.2.1. Am(III) Transport

There are two different types of trends observed for all the DGAs when the membrane pore size was varied from 0.2 to 5.0 µm. The trends are shown in Figs. 5.20 and Fig 5.21. For TODGA, THDGA and TPDGA there is continuous decrease with increasing membrane pore-size. This trend is similar to that reported for the systems U(VI)-TODGA, Pu(III)-TODGA and Eu(III)-TODGA reported by us. Here, the effect of increase in carrier leaching rate and increase in membrane thickness plays the dominant role and causes the transport rate to decrease with increasing membrane pore size. On the other hand for T2EHDGA and TDDGA an initial increase from 0.2 to 0.45 µm and followed by a decrease upon further increase in

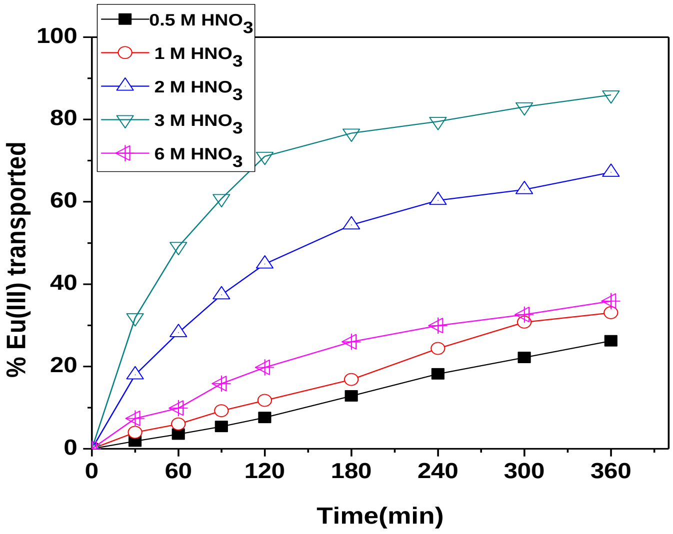

Fig. 5.16: Effect of feed acid concentration on the transport of Eu(III) ion. Receiver: 0.01 M HNO_3; Carrier extractant: 0.1 M T2EHDGA; Support: 0.2 micron PTFE

pore size was noticed. Here both the DGAs being bulky in nature, the Am(III)-DGA complex faces less hindrance for 0.45 µm compared to 0.2 µm. This factor plays major role in determining the transport rate which increases from 0.2 to 0.45 µm. However, beyond 0.45 µm the effect of carrier leaching and increasing membrane thickness becomes more dominant.

5.3.2.2.Eu(III) Transport

The trend of P vs membrane pore size in case of Eu(III) for the DGAs are similar to that of Am(III) discussed earlier and two types of plots are observed (Figs. 5.22 and

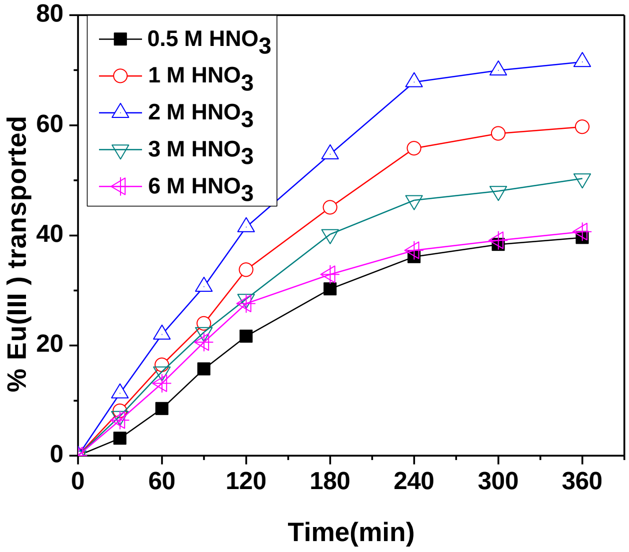

Fig. 5.17: Effect of feed acid concentration on the transport of Eu(III) ion. Receiver: 0.01 M HNO$_3$; Carrier extractant: 0.1 M THDGA; Support: 0.2 micron PTFE

5.23). For TODGA, THDGA and TPDGA (+ 30% *iso*-decanol) there is continuous decrease in permeability coefficient with increasing membrane pore size. This signifies that here the dominating effect is the increasing leaching of the carrier from the membrane and increasing membrane thickness. On the other hand, for T2EHDGA and TDDGA the trend is somewhat different though not similar to that reported with Am(III) transport. Initially, the P values decreased with increasing membrane pore size followed by an increase from 1.2 µm to 5.0 µm which appeared to be more pronounced for TDDGA. This signifies that initially the leaching of the carrier and increasing membrane thickness plays very significant role. It appears that

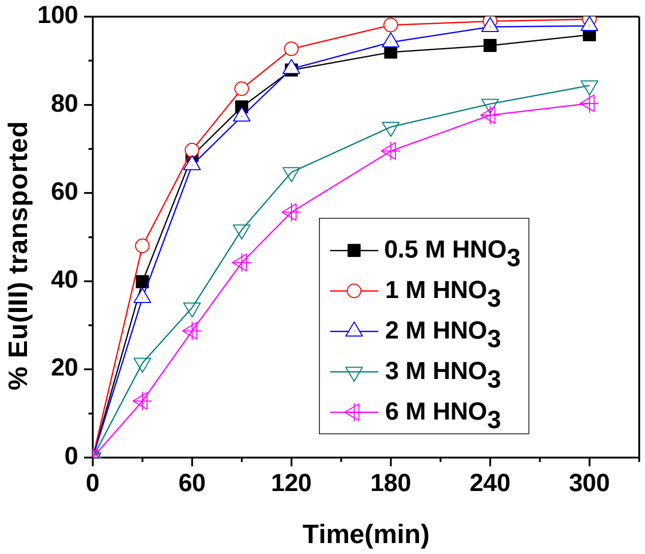

Fig. 5.18: Effect of feed acid concentration on the transport of Eu(III) ion. Receiver: 0.01 M HNO$_3$; Carrier extractant: 0.1 M TDDGA; Support: 0.2 micron PTFE

due to the bulky structure of the DGAs, the size of the extracted Eu(III)-DGA complex plays a significant role when the membrane pore size becomes 5.0 µm.

5.3.3. Effect of the Phase Modifier

Comparative studies were carried out to understand the effect of 30% *iso*-decanol on all the DGAs for the transport of Am(III) as well as Eu(III). Feed acidity was maintained at 3 M HNO_3 and 0.2 µm PTFE filters were used as the membrane support. The plots of percentage transport of Am(III) (Fig 5.24) vs time show that the order of transport is THDGA > TPDGA > TDDGA > TODGA > T2EHDGA.

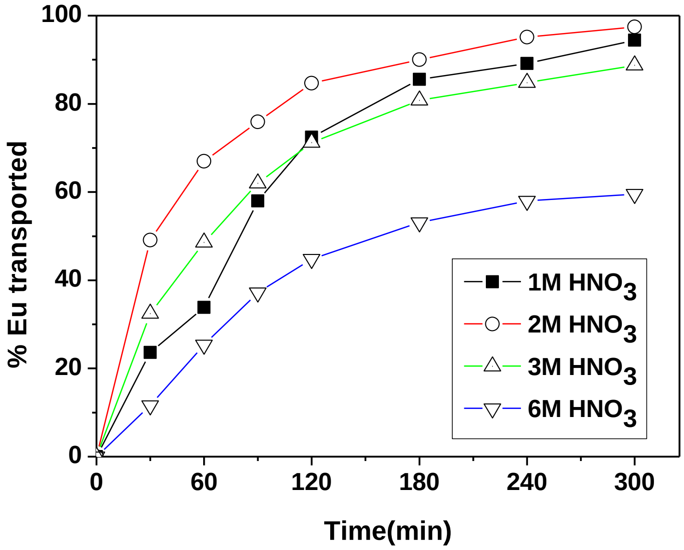

Fig. 5.19: Effect of feed acid concentration on the transport of Eu(III) ion. Receiver: 0.01 M HNO_3; Carrier extractant: 0.1 M TPDGA in presence of 30% *Iso*-decanol; Support: 0.2 micron PTFE

On the other hand, Eu(III) transport profiles follow the order T2EHDGA > TODGA > THDGA > TDDGA > TPDGA (Fig. 5.25). Thus, no particular trend was followed for the DGAs.

5.3.4. Sr(II) transport studies

To be effective actinide partitioning reagents, the DGAs must provide good decontamination factors from the fission products. In this regard, Sr(II) is significantly extracted with most DGAs and its transport behaviour needs to be investigated. Sr(II) transport studies were carried out using 0.1 M DGAs in the

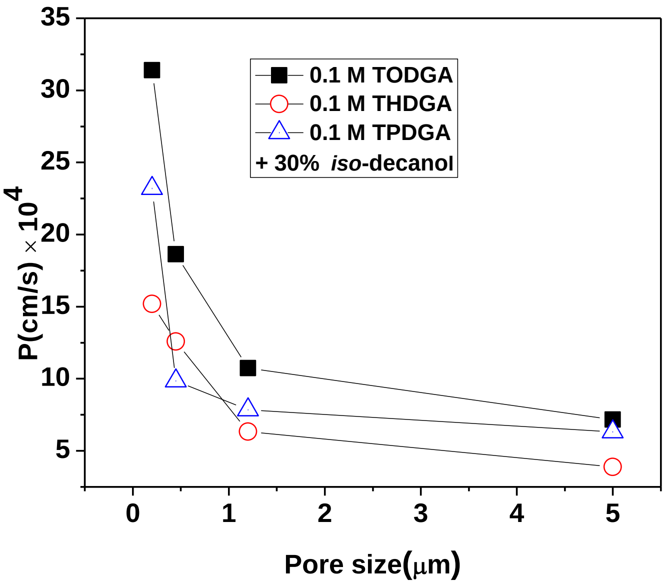

Fig. 5.20: Effect of membrane pore size on the transport of Am(III) ion. Feed: 3.0 M HNO_3 (2.0 M HNO_3 for THDGA); Receiver: 0.1 M HNO_3; Carrier: 0.1 M DGA (30% *iso*-decanol for TPDGA)

absence and the presence of 30% *iso*-decanol. Feed acidity was maintained at 3 M HNO_3 except for 0.1M THDGA where it was kept at 2 M HNO_3. Fig. 5.26 shows the transport profile of Sr(II) in presence of 0.1 M DGAs. Maximum transport was observed for 0.1 M THDGA and minimum was that for 0.1 M TDDGA. However, for each DGA, there was significant Sr(II) transport which signifies poor decontamination of the separated trivalent actinides and lanthanides from fission products particularly with respect to ^{90}Sr. In order to understand the role of phase modifier (i.e., 30% *iso*-decanol in this case), Sr(II) transport experiments were also carried out using 0.1 M DGA + 30% *iso*-decanol and the plots are shown in Fig. 5.27.

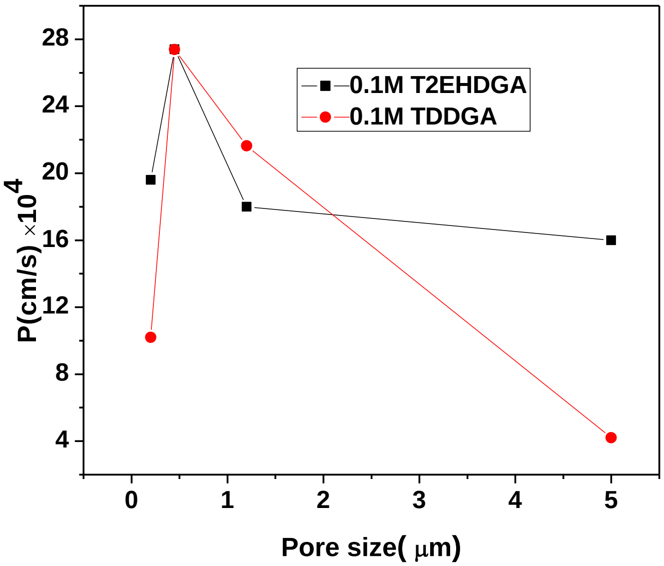

Fig. 5.21: Effect of membrane pore size on the transport of Am(III) ion. Feed: 3.0 M HNO_3; Receiver: 0.1 M HNO_3; Carrier: 0.1 M DGA

It was quite interesting to observe that the presence of *iso*-decanol drastically reduced the Sr(II) transport for TODGA, T2EHDGA and TDDGA. On the other hand, though decrease in Sr(II) transport was seen with THDGA, it was still quite significant (~38% in 6 h). TPDGA with 30% *iso*-decanol provided ~51% Sr(II) transport in 6 h. Thus 0.1 M T2EHDGA and 0.1 M TDDGA with 30% *iso*-decanol were found to be more suitable for decontamination with respect to Sr(II). It was quite interesting and intriguing to observe that 30% *iso*-decanol in addition to playing the role of the phase modifier to prevent third phase formation also helps in improving the decontamination factor with respect to Sr(II). The reason behind this phenomenon is not clearly understood and needs to be investigated in detail.

5.3.5. Thermodynamics study

Transport behaviour of Am(III) was studied at varying temperatures with all the DGAs to calculate the activation energy of transport for each DGA. Feed solution in each experiment was kept at 3 M HNO_3 except for THDGA where it was kept at 1 M due to the problem of third phase formation at 3 M HNO_3. Moreover, except for TPDGA, concentrations of all DGAs were kept at 0.1 M in *n*-dodecane. To prevent third phase formation 30% *iso*-decanol was used along with TPDGA during the transport experiments. From the plot of $\ln(C_o/C_t)$ vs time , permeability co-efficient values (P) were calculated. For the calculation of P, transport was followed for 2 h. After obtaining the P values at different temperatures, from the slopes of the plots of 1/T (K^{-1}) vs ln P

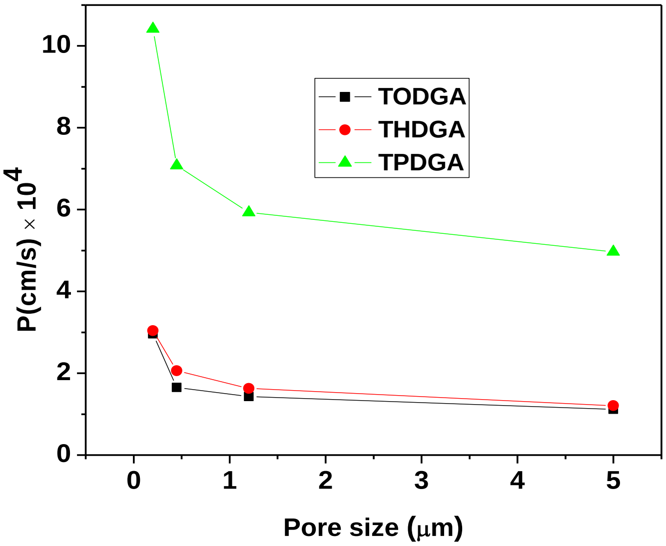

Fig. 5.22: Effect of membrane pore size on the transport of Eu(III) ion. Feed: 3.0 M HNO_3 (2.0 M HNO_3 for THDGA); Receiver: 0.1 M HNO_3; Carrier: 0.01 M DGA (30% *iso*-decanol for TPDGA)

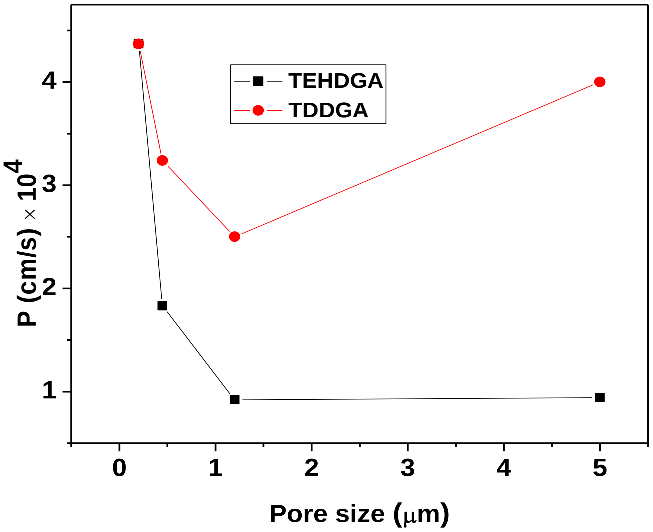

Fig. 5.23: Effect of membrane pore size on the transport of Eu(III) ion. Feed: 3.0 M HNO_3; Receiver: 0.01 M HNO_3; Carrier: 0.1 M DGA

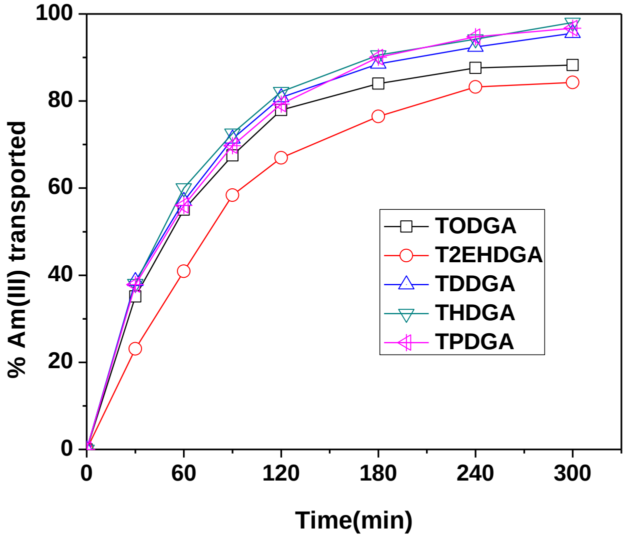

Fig. 5.24: Effect of phase modifier (30% *iso*-decanol) on the transport of Am(III) ion. Feed: 3.0 M HNO_3; Receiver: 0.1 M HNO_3; Carrier: 0.1 M DGA

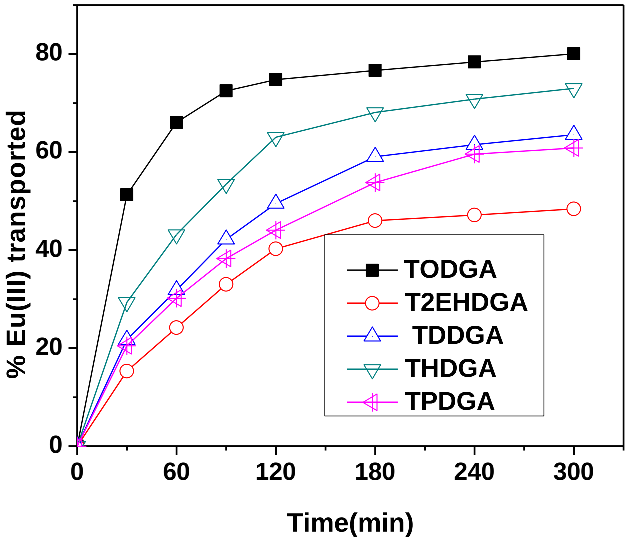

Fig. 5.25: Effect of phase modifier (30% *iso*-decanol) on the transport of Eu(III) ion. Feed: 3.0 M HNO_3; Receiver: 0.1 M HNO_3; Carrier: 0.1 M DGA

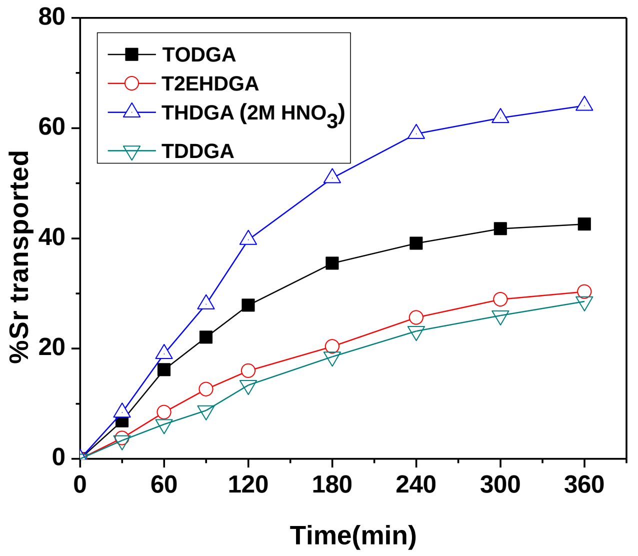

Fig. 5.26: Transport of Sr(II) using DGA as carrier. Feed: 3.0 M HNO_3; Receiver: 0.1 M HNO_3; Carrier: 0.1 M DGA

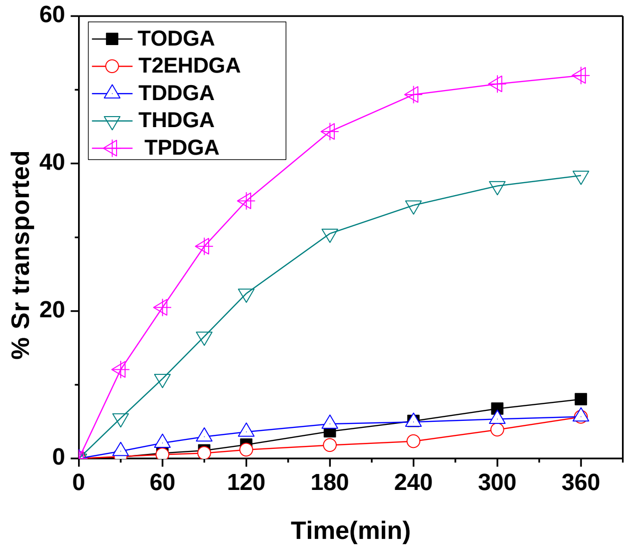

Fig. 5.27: Transport of Sr(II) using DGA with phase modifier as carrier. Feed: 3.0 M HNO_3; Receiver: 0.1 M HNO_3; Carrier: 0.1 M DGA + 30% *iso*-decanol

the activation energies of transport were calculated. Table 5.5 shows the activation energies of transport for the DGA extractants used in the present study. The order of activation energy is TDDGA > THDGA >TPDGA (with 30% *iso*-decanol) > TEHDGA > TODGA, which suggested that no particular trend was followed. This is due to the fact that transport of a metal ion across SLM is the sum total of various independent factors like: extractability of the carrier, size of the metal-carrier complex, acidity of the feed and strip phase, viscosity of the carrier, diffusion of the metal-carrier complex across the membrane, etc. Therefore, it is not possible to correlate the activation energies of transport of a metal ion across a SLM with any of the above mentioned parameters. It requires a multi-parameter approach which is being investigated in detail.

5.4. Conclusions

A series of substituted di-glycolamides have been studied for their solvent extraction and supported liquid membrane transport properties of different radionuclides. Different parameters like kinetics of extraction, effect of feed acidity on the extraction and transport, phase modifier concentration on the extraction, effect of membrane pore size on the transport have been investigated in detail

Table 5.4: Activation energy of transport of Am(III) using 0.1 M DGAs in 3 M HNO_3 medium

DGA	ΔH (kcal. $Mole^{-1}$)
TODGA	3.038
TEHDGA	3.416
THDGA[a]	4.165
TDDGA	7.798
TPDGA[b]	3.742

Note: [a]: Feed: 2M HNO_3, [b]: In the presence of 30% *iso*-decanol

5.5. REFERENCES:

[1] Y.Sasaki, Z-X Zhu, Y. Sugo and T. Kimura; *J. of Nucl. Sci. and Techn.*, 44 (2007) 405.

[2] E. A. Mowafy and H. F. Aly ; *Solv. Extr. Ion Exch.*, 25 (2007) 205

[3] L. Boyadzhiev and Z. Lazarova, in "*Membrane separations technology: principles and applications*". R.D. Noble and S.A. Stern (Eds), Elsevier Science B.V. (1995), pp. 283 - 300.

[4] R.A. Bartsch, J.D. Way, L.A.J. Chrisstoffels, F. de Jong and D.N. Reinhouldt, in "*Chemical separations with liquid membranes*", R.A. Bartsch and J.D. Way (Eds.), ACS symposium series number 642, ACS, Washington DC (1996).

[5] A.M. Sastre, A. Kumar, J.P. Shukla and R.K. Singh; *Sep. Purif. Methods*, 27 (1998) 213.

[6] S. Tachimori, Y. Sasaki, and S. Suzuki; *Solv. Extr. Ion Exch.* 20, (2002), 687.

[7] S. Manohar, J.N. Sharma, B.V. Shah, P.K. Wattal; *Nucl. Sci. Eng.* 156 (2007) 96.

[8] Y.Sasaki, Z.X.Zhu, Y.Sugo and T.Kimura; *J.of Nucl. Sci. and Techn*. 44 (2007) 405.

[9] M. P. Jensen, T. Yaita, and R. Chiarizia; *Langmuir*, 23(2007)4765.

[10] S. Panja, P.K. Mohapatra, S.C. Tripathi, V.K. Manchanda ; *J. Membr. Sci.* ,337 (2009) 274.

[11] S. Panja, R. Ruhela, S.K. Misra, J.N. Sharma, S.C. Tripathi , A. Dakshinamoorthy ; *J. Membr. Sci*, 325 (2008) 158.

Chapter VI

SUMMARY AND CONCLUSIONS

The challenge in the disposal of HLW is largely due to the radiotoxicity associated with the minor actinides. At present, the option for the management of HLW is to vitrify it in the glass matrix followed by burial in deep geological repositories. Since the half lives of minor actinides concerned range between a few hundred to millions of years, the surveillance of HLW for such a long period is economically as well as environmentally a daunting task. An alternative / complimentary concept is the partitioning and transmutation (P&T), which envisages the complete removal of minor actinides from HLW and their consequent burning in high flux reactors / accelerator driven subcritical systems (ADSS). After partitioning of the actinides along with the long lived fission products, the residual waste can be fixed in suitable matrices and buried in sub-surface repositories at a much reduced risk and cost. Among various techniques that can be applied for actinide partitioning, liquid membrane based methods appear most promising. The work reported in this Thesis has relevance to the application of Supported Liquid Membrane technique for the partitioning of minor actinides and long lived fission products from nuclear waste solutions.

The work reported in this thesis can be summarised as follows:

i) Plutonium recovery from various waste streams including high level waste is important due to its strategic importance. TODGA is used for the extraction of actinides in the +3, +4 and +6 oxidation states and the order of extraction is +3 > +4 > +6. TODGA loaded PTFE flat sheets were found to be effective for the transport of Pu^{3+} where phenyl hydrazine was used as the reductant and 0.1 M HNO_3 as the strippant. The species being extracted and diffusing inside the membrane were found to be $Pu(NO_3)_3\cdot$ 4TODGA from solvent extraction experiments. The transport of the complex increased with increasing TODGA concentration up to 0.1 M and decreased thereafter which was attributed to slow diffusion of the complex due to the increased carrier viscosity. The transport of the complex increased with increasing feed nitric acid concentration up to 3 M HNO_3 and decreased thereafter which was attributed to inefficient stripping in the receiver compartment due to the significant co-transport of nitric acid. Increasing Pu concentration increased the overall flux which tends to saturate at higher Pu concentration. The membrane stability was reasonably good for 0.2 micron filters which resulted in the highest P values.

ii) Though Pu^{3+} is extracted to a much larger extent, the predominant ionic species of plutonium is Pu^{4+} and it was required to investigate its extraction as well as transport behaviour. The transport studies carried out in the present work suggested that the transport rates increased monotonously with increasing nitric acid concentration up to 6 M. On the other hand, increasing the carrier concentration resulted in an increase in the transport rates up to 0.1 M and a decrease was seen thereafter which was ascribed to viscosity effects. The membrane stability was limited up to 5 days as compared to 20 days of continuous operation reported earlier for Am^{3+} transport. Radiation stability of TODGA was also limited up to an absorbed dose of 15 MRad. Though we had reported results from the Th^{4+} transport studies earlier, the transport behaviour of Pu^{4+} was significantly different due to difference in the extracted species.

iii) TODGA loaded PTFE flat sheets were also found to be effective for the transport of actinyl ions such as uranyl ion. Comparison with different metal ions indicated that the transport of hexavalent ions such as UO_2^{2+} and PuO_2^{2+} are relatively slower compared to the tri- and tetravalent actinide ions. Increase in the transport rates were observed with increasing HNO_3 as well as TODGA concentrations. The extracted species changed with increasing HNO_3 concentration and contrary to the reverse micelle model, non-aggregated form of TODGA appear to be forming the adducts. Eventually, this was responsible for the higher than expected transport rates at higher HNO_3 and TODGA concentrations. The diffusion coefficients for the extracted complexes were measured by two different experimental techniques. A decrease in the transport rates was observed with increasing U concentration in the feed though the flux increased up to 15 g/L and saturation can be seen at higher concentrations. The present studies have indicated that TODGA supported liquid membranes can be used for the recovery of U from nitric acid solutions.

iv) In a similar way, effective transport of $Th^{4+}$was also observed using TODGA based SLM. The transport rates are found to be lower than that of trivalent actinide ions. The results suggested that TODGA can be used for Pu recovery from the high level waste along with Am recovery during the ‘actinide partitioning’ stage with suitable adjustment of its oxidation to state to either +3 or +4 state. However, in case the separation method is applied to solutions containing large Pu concentrations, the flux would decrease. In such cases, hollow fiber SLM can be used to enhance the transport rates.

v) The effect of radiation induced degradation of TODGA and DHOA on the transport of actinides and fission products were also studied in detail. Presence of DHOA in the solvent system caused an increase in the transport of U(VI) and Pu(IV) but not for Am(III) and Sr(II). This was attributed to significant extraction of U(VI) and Pu(IV) by DHOA. Increasing radiation dose from 0 MRad to 100 MRad caused decrease in the transport rate for all the actinides and Sr(II) at all the three carrier compositions. The rate of decrease was much faster for Sr(II) compared to all the actinides. This caused an increase in the D.F with respect to Sr(II) for all the actinides at higher radiation dose.

vi) Effect of diluents on the extraction and transport of Am(III) using TODGA as extractant/ carrier molecule have also been investigated in detail. Nature of the diluent was found to be one of the major factors controlling the extraction and transport behaviour of Am(III). Maximum extraction was observed for nitrobenzene whereas most efficient transport was found for toluene. Diffusion co-efficient values for each of the studied diluent were calculated.

vii) T2EHDGA based Supported Liquid Membrane was also found to be effective for quantitative transport of Am(III) from nitric acid medium. Optimum feed acidity was found to be 3 M HNO_3 whereas 0.1 M HNO_3 was found to be optimal strippant. The pore size and thickness of the membrane played a major role in the transport of Am(III). Experiments with varying thickness of the membrane established that Am(III) transport was membrane diffusion controlled. It was also observed that the pore size of the membrane support was an important parameter in controlling the rate of permeation of Am(III). The mechanical stability of the membrane support and leachability of the extractant from the membrane support was found to be satisfactory over the time period investigated. Selectivity of Am(III) over fission products and other metal contaminants was found to be quite high.

ix) Along with trivalent actinides, T2EHDGA based SLM was also found to be similarly effective for the quantitative transport of trivalent lanthanides. Various parameters played major role in the transport process viz. feed acidity, T2EHDGA concentration, concentration of phase modifier etc. Diffusion coefficient values and thermodynamic parameters for transport were also calculated for Eu-T2EHDGA system.

ix) Present study also showed the possibility of application of T2EHDGA based membrane system for the effective transport of uranyl ion from nitric acid feed solution. Unlike the literature reports, the extracted species was found to contain one T2EHDGA molecule. The transport rate was found to depend on the type and concentration of acid in the feed. The lowering in the extraction and transport rates in the presence of the phase modifier is probably due to change in its aggregation behaviour due to a change in the polarity of the medium. The membrane transport mechanism is diffusion controlled similar to the literature report for an analogous system. The transport behavior was modeled by a computer programming and excellent matching of the predicated transport rate was observed with the experimental results. The transport rates of uranyl ion obtained in the present system with T2EHDGA as the carrier extractant matched very well with those reported earlier with the TODGA system and hold promise for application in the removal of U from acidic wastes including the PUREX raffinate and high level waste.

x) A series of substituted diglycolamides were evaluated for their solvent extraction and supported liquid membrane transport properties of trivalent actinides and lanthanides. 30% *Iso*-decanol was found to be optimum phase modifier for the DGAs.

The trend of D values for 0.1 M DGAs in presence of 30% *iso*-decanol was found to be TPDGA > THDGA > TODGA > TDDGA > T2EHDGA. Extraction from SHLW was also studied. Supported Liquid Membrane transport of the radionuclides for the DGAs was also investigated. Effects of feed acidity, membrane pore size and phase modifier concentrations were also investigated in detail. The order of activation energies of transport of Am(III) was found to be TDDGA > THDGA > TPDGA (with 30% *iso*-decanol) > T2EHDGA > TODGA.

The results obtained during the studies clearly demonstrated the feasibility of SLM technique for actinide partitioning purpose using diglycolamides as the carrier extractants. For large scale application at higher volume, hollow fiber supported liquid membrane technique is needed to be optimized in detail. Moreover, in view of radioactive dose emanating from the high level waste, radiation resistant polymeric membranes need to be developed.

Publications Included in the Thesis

1. Facilitated Transport of Am(III) through a Flat Sheet Supported Liquid Membrane(FSSLM) containing Tetra (2-Ethyl) Hexyl Diglycolamide (TEHDGA) as carrier; **S.Panja**, R.Ruhela, S.K.Misra, J.N.Sharma, S.C.Tripathi, A.D.Moorthy, *J. of Membr. Sci.*, 325 (**2008**) 158–165.
2. Studies on uranium(VI) pertraction across a N,N,N’,N’-tetraoctyldiglycolamide (TODGA) supported liquid membrane, **S. Panja**, P.K. Mohapatra, S.C.Tripathi,V.K. Manchanda, *J. of Memb. Sci*., 337 (**2009**) 274–281.
3. Transport of Thorium(IV) Across a Supported Liquid Membrane Containing N,N,N’,N’-Tetraoctyl-3-oxapentanediamide (TODGA) as the Extractant, **S. Panja**, P.K. Mohapatra, S.C. Tripathi, V.K. Manchanda, *Sep. Sci. and Technol*., 45 (**2010**)1112-1120.
4. Pertraction of plutonium in the +4 oxidation state through a supported liquid membrane containing TODGA as the carrier, **S. Panja**, P.K. Mohapatra, P. Kandwal, S.C. Tripathi, V.K. Manchand, *Desalination*, 262 (**2010**) 57–63.
5. Controlled Pertraction of Plutonium(III) Under Reducing Conditions From Acidic Feeds Using TODGA as the Carrier Extractant, **S. Panja**, P.K. Mohapatra, S.C. Tripathi, V.K. Manchanda, *Sep. Sci. and Technol*., 46 (**2011**)94–104.

---

6. Carrier Facilitated Transport of Europium(III) Across Supported Liquid Membranes Containing N,N,N’,N’-tetra-2-ethylhexyl-3-pentanediamide (T2EHDGA) as the Extractant, **S. Panja**, P.K. Mohapatra, S.K.Misra, S.C. Tripathi, *Sep. Sci. and Technol*., 46(12)(**2011**)1941-1949.

7. Facilitated transport of uranium(VI) across supported liquid membranes containing T2EHDGA as the carrier extractant; **S. Panja**, P.K. Mohapatra, S.C. Tripathi, V.K. Manchanda, *J. of Haz. Mater.*, 188 (**2011**) 281–287.

8. Permeation of Uranium(VI) Across Supported Liquid Membranes (SLM) Containing T2EHDGA as the Carrier Extractant, **S.Panja**, P.K. Mohapatra, S.C. Tripathi and V.K. Manchanda, *Desal. & Water Treatment* 38 (**2012**) 2017-214.

9. Uranium(VI) pertraction across a supported liquid membrane containing a branched diglycolamide carrier extractant: Mass transfer modeling, **S.Panja**, P.K.Mohapatra, P.Kandwal and S.C.Tripathi, *Desalination* 385(**2012**)213-218.

10. Role of organic diluents on Am(III) extraction and transport behaviour using N,N,N’N’-tetraoctyl-3-oxapentanediamide as the extractant, **S.Panja**, P.K. Mohapatra, S.C. Tripathi, P.M.Gandhi and P.Janardan, Journal of Membrane Science, 403-404(2012) 71-77

11. Liquid- liquid extraction and pertraction behavior of Am(III) and Sr(II) with diglycolamide carrier extractants, **S.Panja**, P.K. Mohapatra, S.C. Tripathi, G.D.Dekahne,P.M.Gandhi and P.Janardan, ***Journal of Membrane Sci*ence** ,399-400(**2012**) 28-36.
12. Effect of gamma-irradiation of TODGA on the SLM transport behaviour of radio nuclides, **S.Panja**, P.K.Mohapatra, S.C.Tripathi and P.M.Gandhi (Communicated).
13. Solvent Extraction and liquid membrane studies of Eu(III) using substituted di-glycolamide carrier extractants, **S.Panja**, P.K. Mohapatra, S.C. Tripathi, G.D.Dekahne and P.M.Gandhi (Communicated)

Conference / Symposia

1. Transport of Am3+ Using Supported Liquid Membrane Containing N,N,N',N'-Tetraoctyldiglycolamide (TODGA) as the carrier; **S. Panja**, P.K. Mohapatra, A. Dakshinamoorthy, S.K. Munshi, P.K. Dey and V.K. Manchanda, Indian Council Of Chemists, 26th Annual Conf. of the Indian Council of Chemists, Dr.Hari Singh Gaur University, Sagar (M.P.) 26th – 28th February, 2008.
2. Optimization and Stability Studies on Plutonium(III) Transport in Supported Liquid Membranes Containing TODGA as the Carrier Extractant; **S. Panja**,

---

P.K. Mohapatra, A. Dakshinamoorthy, S.K. Munshi, P.K. Dey and V.K. Manchanda, 333-334, *In proceedings of DAE-BRNS Theme meeting on Emerging Trends in Separation Science and Technology (SESTEC-2008), March 14-18, 2008,* University of Delhi, Delhi.

3. Transport of Thorium(IV) and Uranium (VI) in Supported Liquid Membranes Containing TODGA as the Carrier Extractant; **S. Panja**, P.K. Mohapatra, A. Dakshinamoorthy, S.K. Munshi, P.K. Dey and V.K. Manchanda, 335-336, *In proceedings of DAE-BRNS Theme meeting on Emerging Trends in Separation Science and Technology (SESTEC-2008), March 14-18, 2008,* University of Delhi, Delhi.
4. Carrier Mediated Transport of Actinide Ions Using Supported Liquid Membranes Containing TODGA as the Carrier Extractant; **S. Panja**, P.K. Mohapatra, A. Dakshinamoorthy, S.K. Munshi, P.K. Dey and V.K. Manchanda, *18th International Solvent Extraction Conference, ISEC-2008,* Tucson, Arizona, September 15 to 19, 2008 .
5. Effect of gamma-irradiation of TODGA on the SLM transport behaviour of radio nuclides, **S. Panja**, P.K. Mohapatra, S.C.Tripathi, S.K. Munshi, P.K. Dey and V.K. Manchanda, *In Proceedings of DAE-BRNS Symposium on Nuclear and Radiochemistry (NUCAR-2009)*, held at Bhabha Atomic Research Centre, Mumbai.
6. Transport of uranium(VI) complexes through supported liquid membranes containing N,N,N'N'-tetraoctyl diglycolamide as the carrier extractant; **S.**

Panja, P.K. Mohapatra, S.C. Tripathi, S.K. Munshi, P.K. Dey and V.K. Manchanda, *In Proceedings of DAE-BRNS Symposium on Nuclear and Radiochemistry (NUCAR-2009)*, held at Bhabha Atomic Research Centre, Mumbai.

7. Effect of organic diluents on the transport of Am(III) across TODGA based supported liquid membranes; **S. Panja**, P.K. Mohapatra, S.C. Tripathi, S.K. Munshi, P.K. Dey and V.K. Manchanda, *Indian Analytical Science Congress 2009,* Lonavala, Maharashtra.

8. Fcilitated transport of U(VI) across a supported liquid membrane(SLM) containing TEHDGA as carrier; **S.Panja**, P.K.Mohapatra, S.C.Tripathi, S.K.Munshi,P.K.Dey,V.K.Manchanda, *In proceedings of DAE-BRNS Theme meeting on Emerging Trends in Separation Science and Technology (SESTEC-2010)* held at Bhabha Atomic Research Centre.

9. Transport studies of Eu(III) across a Supported Liquid Membrane(SLM) using TEHDGA as carrier; **S. Panja**, S.K.Misra, P.K. Mohapatra, S.C. Tripathi, S.K. Munshi, P.K. Dey and V.K. Manchanda, *In proceedings of DAE-BRNS Theme meeting on Emerging Trends in Separation Science and Technology (SESTEC-2010)* held at Bhabha Atomic Research Centre.